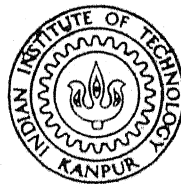


# SOUND TRANSMISSION THROUGH SANDWICH STRUCTURES

*By*

R. L. SHANBHAG

TH  
AE/1980/D  
Sh



A70495

AE

1980

D

SHA

SOU

DEPARTMENT OF AERONAUTICAL ENGINEERING

INDIAN INSTITUTE OF TECHNOLOGY KANPUR

1980

# SOUND TRANSMISSION THROUGH SANDWICH STRUCTURES

A Thesis Submitted  
in Partial Fulfilment of the Requirements  
for the Degree of

DOCTOR OF PHILOSOPHY

*By*

R. L. SHANBHAG

*to the*

DEPARTMENT OF AERONAUTICAL ENGINEERING  
INDIAN INSTITUTE OF TECHNOLOGY KANPUR

1980

AE-1980-D-SHA-SOU

I. I. T. KANPUR

CENTRAL LIBRARY

Acc. No. A 70495

16 APR 1982

TO

SUBRAOMAM

## CERTIFICATE

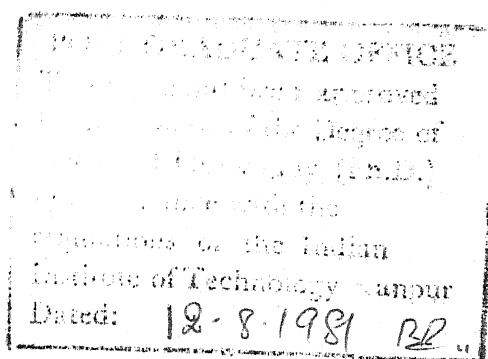
This is to certify that the work 'SOUND TRANSMISSION THROUGH SANDWICH STRUCTURES' has been carried out under my supervision and has not been submitted elsewhere for a degree.

  
(S. NARAYANAN)

Assistant Professor<sup>++</sup>  
Dept. of Applied Mechanics  
I.I.T., Madras - 36

<sup>++</sup>

Formerly, Assistant Professor, Department of Aero.Engg.,  
I.I.T., Kanpur.



## ACKNOWLEDGEMENTS

The author wishes to express his deep sense of gratitude and sincere appreciation to Dr.S.Narayanan for his invaluable guidance, critical supervision and constant encouragement throughout the course of this work.

The author is grateful to Professor N.C.Nigam for his encouragement. The author is also thankful to Dr.K.Ghosh and Dr.M.Krishnamurthy who helped him in sorting out many of the administrative problems, caused by the absence of his guide from Kanpur.

The author wishes to thank Mr.M.K.Patra for the timely help provided whenever necessary.

Thanks are due to all the members of the faculty of Machine Dynamics Laboratory, Department of Applied Mechanics, I.I.T. Madras, who helped the author in many ways during his tenure as a research scholar in the department.

Much gratitude is due to the author's wife, Tara, for her patience and willingness to make sacrifices during the course of the work.

The author is thankful to College of Engineering, Farmagudi, Goa, and the Ministry of Education, Government of India, who sponsored his candidature under the QIP scheme.

Thanks are also due to Mr.V.R.Ganesan who typed the manuscript at short notice with extreme care and to Mr.S. Ramanujam who drew the figures.

R.L. SHANBHAG

## CONTENTS

<u>Chapter</u>	<u>Page</u>
LIST OF TABLES	
LIST OF FIGURES	
LIST OF SYMBOLS	
SYNOPSIS	
1. INTRODUCTION	1
1.1 GENERAL INTRODUCTION	1
1.2 SCOPE AND ORGANISATION OF THESIS	4
1.3 LITERATURE REVIEW	9
1.3.1 Vibration of Damped Sandwich Structures	10
1.3.2 Sound Transmission Through Structures	15
2. DYNAMICS OF DAMPED SANDWICH PANEL	23
2.1 EQUATIONS OF MOTION	23
2.2 NATURAL FREQUENCIES, LOSS FACTORS AND DAMPED NORMAL MODES	30
2.3 BOUNDARY CONDITIONS ALONG y-WISE EDGES AT $x = \pm a/2$	32
2.3.1 Simply Supported Edges	32
2.3.2 Clamped Edges	34
2.3.3 Edges with Elastic Rotational Restraint and No Transverse Displacement	34
2.3.4 Edges with No Rotation But Transverse Elastic Restraint	36

2.4	SYMMETRIC MODES	37
2.5	DETERMINATION OF RESONANT FREQUENCIES AND LOSS FACTORS	38
2.6	FORCED DAMPED NORMAL MODE RESPONSE ANALYSIS	40
2.6.1	Harmonic Loading	40
2.6.2	Random Loading	41
3.	SOUND TRANSMISSION BY DAMPED SANDWICH PANELS OF INFINITE EXTENT	43
3.1	INTRODUCTION	43
3.2	SOUND TRANSMISSION LOSS	45
3.3	COINCIDENCE FREQUENCY AND COINCIDENCE NOISE TRANSMISSION	52
3.4	RESULTS AND DISCUSSION	56
3.5	CONCLUSIONS	75
4.	NOISE TRANSMISSION AND STRUCTURAL RESPONSE OF DAMPED SANDWICH PANELS BACKED BY RECTAN- GULAR CAVITY	77
4.1	INTRODUCTION	77
4.2	FORMULATION OF THE NOISE TRANSMISSION PROBLEM NEGLECTING THE EFFECT OF CAVITY ON STRUCTURAL MOTION	80
4.2.1	Acoustic Solution	80
4.2.2	Structural Response	86
4.2.3	Noise Transmission into Cavity	88
4.3	ACOUSTOELASTIC FORMULATION	90
4.3.1	Acoustic Solution	90
4.3.2	Coupled Acoustoelastic Equations	93
4.3.3	Solution of Acoustoelastic Problem	94
4.3.4	Inversion of [B] Matrix	101

4.4 APPROXIMATE FORMULATIONS	103
4.5 RESULTS AND DISCUSSION	106
4.5.1 Order of Modes in Summation	107
4.5.2 Resonant Frequencies and Loss Factors	109
4.5.3 Comparison of Results in the Two Formulations	119
4.5.4 Effect of Plate Boundary Conditions	124
4.5.5 Effect of Core Loss Factor	129
4.5.6 Effect of Shear Parameter	135
4.5.7 Effect of Geometric Parameter	141
4.5.8 Effect of Cavity Damping	144
4.5.9 Effect of Incidence Angle	151
4.5.10 Effect of Cavity Depth	153
4.6 CONCLUSIONS	153
5. NOISE TRANSMISSION AND STRUCTURAL RESPONSE OF LAYERED AND SANDWICH CYLINDRICAL SHELLS	158
5.1 INTRODUCTION	158
5.2 EQUATIONS OF MOTION FOR LAYERED SHELL WITH UNCONSTRAINED DAMPING LAYER TREATMENT	160
5.3 EQUATIONS OF MOTION OF DAMPED SANDWICH SHELL	165
5.4 ACOUSTOELASTIC FORMULATION	174
5.4.1 Acoustic Solution	174
5.4.2 Structural Solution	180
5.4.3 Modal Damping Coefficients and Other Modal Parameters	182
5.4.4 Acoustoelastic Problem Solution	184

5.5 RESULTS AND DISCUSSION	187
5.5.1 Natural Frequencies and Loss Factors	188
5.5.2 Noise Reduction and Structural Response	192
5.6 CONCLUSIONS	209
6. SUMMARY AND CONCLUSIONS	213
6.1 INFINITE SANDWICH PLATE	213
6.2 FINITE SANDWICH PLATE	216
6.3 FINITE LAYERED AND SANDWICH SHELLS	219
6.4 SCOPE FOR FURTHER RESEARCH	222
REFERENCES	225
APPENDIX A	234
APPENDIX B	239

## LIST OF TABLES

<u>Table</u>	<u>Page</u>
3.1 Coincidence Frequencies and Loss Factors for Different Values of $\bar{g}$	59
3.2 Coincidence Frequencies and Loss Factors for Different Values of $\beta$	61
3.3 Coincidence Frequencies and Loss Factor for Different Values of $\gamma$	62
4.1 Natural Frequencies and Loss Factors for Different Plate Boundary c Conditions	110
4.2 Natural Frequencies and Loss Factors for Different Shear Parameters	112
4.3 Natural Frequencies and Loss Factors for Different Shear Parameters	113
4.4 Natural Frequencies and Loss Factors for Different Core Loss Factors	115
4.5 Natural Frequencies and Loss Factors for Different Core Loss Factors	116
4.6 Natural Frequencies and Loss Factors for Different Geometric Parameters	117
4.7 Natural Frequencies and Loss Factors for Different Geometric Parameters	118
4.8 Acoustic Cavity Natural Frequencies	120
5.1 Resonant Frequencies and Loss Factors of Layered Shell	166
5.2 Resonant Frequencies and Loss Factors of Layered Shell	167

Tableix  
Page

5.3	Resonant Frequencies and Loss Factors of Layered Shell, O.C.	168
5.4	Resonant Frequencies and Loss Factors for Different Shear Parameters	175
5.5	Resonant Frequencies and Loss Factors for Different Core Loss Factors	176
5.6	Resonant Frequencies and Loss Factors for Different Geometric Parameters	177
5.7	Acoustic Resonant Frequencies of a Circular Cylindrical Cavity (Axi-symmetric Modes)	193

## LIST OF FIGURES

<u>Figure</u>	<u>Page</u>
2.1 Coordinate System Used for Damped Sandwich Plate	25
3.1 Components of Pressure Fields on Either Side of the Sandwich Panel	46
3.2 Variation of TL with Shear Parameter $\bar{g}$	64
3.3 Variation of TL with Shear Parameter $\bar{g}$	67
3.4 Variation of TL with Core Loss Factor $\beta$	68
3.5 Variation of TL with Geometric Parameter $\gamma$	70
3.6 Variation of TL with Incidence angle $\theta$	71
3.7 Variation of TL with Face Plate Thickness $h_1$	73
3.8 Comparison of TL of Sandwich Panel with Equivalent Homogeneous Panel	74
4.1 Sandwich Plate with Boundary Conditions	81
4.2 Rectangular Cavity-Sandwich Panel System	81
4.3 Comparison of Noise Reduction Between Vaicaitis and Acoustoelastic Formulation	121
4.4 Comparison of Displacement Spectral Densities Between Vaicaitis [2] and Acoustoelastic Formulation	123
4.5 Effect of Boundary Conditions on Noise Reduction	125
4.6 Effect of Boundary Conditions on Noise Reduction	127

FigurePage

4.7 Effect of Boundary Condition on Structural Response	128
4.8 Effect of Core Loss Factor on Noise Reduction	130
4.9 Effect of Core Loss Factor on Noise Reduction	131
4.10 Effect of Core Loss Factor on Structural Response	133
4.11 Effect of Core Loss Factor on Structural Response	134
4.12 Effect of Shear Parameter on Noise Reduction	136
4.13 Effect of Shear Parameter on Noise Reduction	137
4.14 Effect of Shear Parameter on Structural Response	139
4.15 Effect of Shear Parameter on Structural Response	140
4.16 Effect of Geometric Parameter on Noise Reduction	142
4.17 Effect of Geometric Parameter on Noise Reduction	143
4.18 Effect of Geometric Parameter on Structural Response	145
4.19 Effect of Geometric Parameter on Structural Response	146
4.20 Effect of Cavity Damping on Noise Reduction	147
4.21 Effect of Cavity Damping on Structural Response	148
4.22 Effect of Cavity Damping on Noise Reduction	149
4.23 Effect of Cavity Damping on Structural Response	150
4.24 Effect of Incidence Angle $\theta$ on Noise Reduction	152

<u>Figure</u>	<u>Page</u>
4.25 Effect of Cavity Depth on Noise Reduction	154
4.26 Effect of Cavity Depth on Structural Response	155
5.1 Dimensions and Coordinate System of Layered Shell (a) Outside Coating (OC); (b) Inside Coating (IC); (c) Two-side Coating (TC)	161
5.2 Dimensions and Coordinate System of Sandwich Shell	169
5.3 Equilibrium of Longitudinal Forces of Face Layer Element	169
5.4 Cylindrical Cavity-Shell System	178
5.5 Effect of Damping Layer Thickness on Noise Reduction	194
5.6 Effect of Damping Layer Thickness on Noise Reduction	196
5.7 Effect of Damping Layer Thickness on Structural Response	198
5.8 Effect of Damping Layer Thickness on Structural Response	199
5.9 Effect of Shear Parameter on Noise Reduction (Sandwich Shell)	201
5.10 Effect of Core Loss Factor on Noise Reduction (Sandwich Shell)	202
5.11 Effect of Geometric Parameter on Noise Reduction (Sandwich Shell)	203
5.12 Effect of Shear Parameter on Structural Response (Sandwich Shell)	205
5.13 Effect of Core Loss Factor on Structural Response (Sandwich Shell)	206

FigurePage

5.14	Effect of Geometric Parameter on Structural Response (Sandwich Shell)	207
5.15	Comparison of Noise Reduction Between Sandwich and Equivalent Layered Shell	208
5.16	Comparison of Structural Response Between Sandwich and Equivalent Layered Shell	211

## LIST OF SYMBOLS

$a$	panel dimension in $x$ direction, mean radius of shell
$[A]$	inverse of matrix $[B]$ in acoustoelastic formulation
$A_F$	area of flexible wall
$A_R$	surface area of rigid portion of cavity
$b$	panel dimension in $y$ direction
$[B]$	matrix in acoustoelastic formulation
$B_{ijk}$	coefficients in acoustic modal expansion
$c$	local acoustic velocity
$c_B$	flexural wave speed of panel
$C_{ij}$	pressure coefficients in acoustic modal expansion
$d$	depth of rectangular cavity
$D_t$	flexural rigidity of sandwich
$e_{ij}$	structural modal constants
$e_k$	cavity modal constants
$E$	Young's modulus of face layers
$E_2$	$E_2^*(1+i\beta)$ complex Young's modulus of damping layer
$E_2^*$	storage Young's modulus of damping layer
$E_s$	Young's modulus of stringer material
$(EI)_s$	flexural rigidity of stringer
$F_{ijk}$	generalized force corresponding to acoustic pressure

$F_n$	cavity mode
$g$	$g^*(1+i\beta)$ non-dimensional core shear parameter
$g'$	$\bar{g}(1+i\beta)$ core shear parameter $= g/a^2$
$\bar{g}$	real part of $g'$
$g^*$	real part of $g$
$G$	$G^*(1+i\beta)$ complex shear modulus of viscoelastic core layer
$G^*$	storage shear modulus of viscoelastic core layer
$G_s$	shear modulus of stiffener
$G_s J$	St.Venant torsional stiffness of the stringer
$h_i$	thickness of $i^{\text{th}}$ layer
$H_{mn}$	complex frequency response function of structure
$i$	$\sqrt{-1}$ unit imaginary number
$i, j, k, h, \emptyset$ $l, o$	acoustic modal numbers
$[I]$	identity matrix
$I_{mnrs}, I_{mr}$	acceptance functions
$I_s$	second moment of area of stringer cross section
$J$	St.Venant torsional constant of stringer
$J_j$	Bessel function of first kind of order $j$
$k, k'$	wave numbers
$K_{sv}, K_t, K$	torsional stiffness constants of stringer
$K_f$	flexural stiffness constant of stringer
$l$	length of shell
$L_{mnij}, L_{nm}$	acousto-structural modal coupling coefficients

$m, n, r, s$	structural modal numbers
$M_{n\Delta}$	$n^{\text{th}}$ cavity generalized mass
$M_{mS}$	$m^{\text{th}}$ structure generalized mass
$M_x$	bending moment per unit length
$M_{xy}$	twisting moment per unit width of sandwich
$m$	structural modal number in condensed form in acoustoelastic formulation
$n$	cavity modal number in condensed form in acoustoelastic formulation
$NR$	noise reduction inside enclosure
$p_c$	cavity pressure
$p_e$	external pressure
$p_i$	incident pressure
$p_s$	reflected pressure
$p_r$	radiated pressure
$p_t$	transmitted pressure
$p_o$	amplitude of harmonic pressure
$p_{mn}$	generalized force corresponding to $mn^{\text{th}}$ damped normal mode
$P_n$	pressure coefficients in acoustic modal expansion
$\{q\}$	generalized displacement vector
$Q_{mc}$	generalized force corresponding to cavity pressure
$Q_{me}$	generalized force corresponding to external pressure

$\{q\}$	generalized force vector
$r$	radius of the median surface of the shell, coordinate along radial direction
$r_{xy}$	spatial correlation spectrum of random external pressure
$R_T$	specific transmission resistance of infinite sandwich
$S_o$	constant spectral density of white noise pressure excitation
$S_{Q_m Q_r}, S_{Q Q'},$ $[S_{AS}], [S_{PP}],$ $[S_{Pq}], [S_{qq}]$	$\left\{ \begin{array}{l} \\ \\ \\ \end{array} \right\}$ spectral density functions and matrices
$S_{p_c p_c}$	power spectral density of cavity pressure
$S_{ww}$	power spectral density of deflection
$t$	time coordinate
$TL$	sound transmission loss of infinite sandwich
$u, v$	midplane displacements of face plate in x and y directions respectively
$u_i$	mid surface displacement of $i^{th}$ layer of shell
$w$	transverse displacement
$U, V, W$	forced damped normal modes along x, y and z directions
$V$	volume of acoustic enclosure
$x, y, z$	Cartesian coordinates
$X_T$	specific transmission reactance
$Y$	geometric parameter

$Z_{ms}$	complex structural modal impedance
$Z_{nA}$	complex cavity modal impedance
$Z_T$	specific transmission impedance of infinite sandwich
$\{\alpha\}$	normalized cavity modal vector
$\alpha_{jk}$	$k^{th}$ root of equation $dJ_j/dr = 0$
$\beta$	loss factor of viscoelastic damping layer
$\{\gamma\}$	structural modal vector
$\delta_{ijk}$	frequency response function corresponding to $ijk^{th}$ acoustic mode
$\epsilon_{ijk}$	cavity modal damping coefficient in $ijk^{th}$ cavity mode
$\eta$	loss factor
$\eta_{mn}$	modal loss factor in $mn^{th}$ mode
	incidence angle of pressure field
	root of bicubical equation
$\lambda_{jk}$	$\alpha_{jk}/a$
$\mu$	surface mass density of structure
$\mu_{mn}$	generalized mass in $mn^{th}$ forced damped normal mode
$\nu_i$	Poisson's ratio of $i^{th}$ layer
$\xi$	$x/a$ , non-dimensional coordinate in x direction
$\rho$	density of fluid (air)
$\rho_c$	density of damping layer
$\rho_p$	density of face layer

$\sigma_x$	direct stress in mid plane of face plate
$\tau$	transmission coefficient
$\phi$	$\frac{\partial w}{\partial x}$ bending slope
$\phi_m$	damped normal mode
$\psi$	$y/a$ non-dimensional coordinate in y direction shear strain in sandwich core
$\omega$	angular frequency of excitation
$\omega_{ijk}, \omega_{nA}$	cavity frequency
$\omega_{mn}^2$	$\omega_{mn}^{*2} (1+i\eta_{mn})$ square of complex structural frequency of the damped sandwich
$\omega_{mn}^{*2}$	real part of $\omega_{mn}^2$
$\omega_{ms}^2$	$\omega_{ms}^{*2} (1+i\eta_{ms})$ complex structural frequency
$\Omega_{mn}^2$	$\omega_{mn}^2 \mu a^4 / D_t$ , non dimensional complex structural frequency parameter

## SYNOPSIS

R.L. SHANBHAG  
Ph.D.  
INDIAN INSTITUTE OF TECHNOLOGY, KANPUR  
NOVEMBER, 1980

## SOUND TRANSMISSION THROUGH SANDWICH STRUCTURES

This thesis presents a theoretical analysis of the noise transmission characteristics of damped sandwich structures, with constrained damping layer treatment. The influence of the applied damping treatments on the structural response of the composite structure to harmonic and random excitation is also studied. The following problems are analysed in this work.

1. Sound transmission through an infinite sandwich plate.
2. Noise transmission and structural response of a finite damped sandwich panel backed by a rectangular cavity.
3. Noise transmission and structural response of a finite cylindrical sandwich shell backed by a cylindrical acoustical cavity.

In addition to these problems, the problem of the sound transmission of a layered shell with unconstrained damping treatment is also analysed in this work.

Firstly, the sound transmission through an infinite sandwich plate with constrained damping layer treatment is investigated on classical lines. The equation of motion of a finite three layered sandwich plate have been suitably reduced to represent the transverse vibration characteristics of the infinite sandwich plate. Closed form expressions for the sound transmission loss and the coincidence frequency are derived in terms of the sandwich core parameters, face layer properties and the incidence angle of the incident sound wave by using the dispersion relation between wave number and frequency. The interaction between the structure and the incident, reflected and radiated sound fields has been considered in the analysis. In the case of the sandwich panel, unlike the homogeneous panel the coincidence frequency is complex valued because, the structural wave motion is not a freely propagating wave, but a damped wave with a complex wave number.

It has been shown by the analysis that, significant improvements in the sound insulation characteristics of the sandwich panel as compared to the homogeneous panel can be achieved, due to the shift of coincidence frequencies to higher frequency ranges and due to positive transmission loss values corresponding to the coincidence frequency. It is also revealed by the analysis that the

core shear parameter is the most sensitive parameter with respect to sound transmission and that maximum transmission loss at coincidence can be obtained corresponding to an optimum value of the core shear parameter.

Noise transmission and structural response of a finite sandwich panel backed by a rectangular cavity is analysed next. The external pressure excitations include both harmonic and stationary random excitations. The short panel edges are assumed to be simply supported while the other two parallel edges are assumed to be elastically supported. These boundary conditions represent realistic boundary conditions typical of aircraft panels supported by orthogonal rows of stringers and frames. The frequency range of interest has been restricted to 1000 Hz.

An acoustoelastic formulation of the problem is made, where the coupling between the structural motion and the internal cavity pressure is fully taken into account. The resulting set of matrix differential equations in the pressure coefficients and the structural generalized coordinates is solved by a direct matrix inversion scheme which takes advantage of the diagonal nature of some of the matrices in the analysis. A 'forced damped normal mode' analysis is made for the structural response in view of arbitrary damping and arbitrary boundary conditions. The natural frequencies, the associated loss

factors and the damped normal modes are obtained by an iterative interpolation method. The results are compared with an approximate formulation which considers only a partial coupling between the internal sound field and the structural motion.

An exhaustive parametric study of the problem with respect to the sandwich core parameters is undertaken. It has been shown by the study, that,

- i) the boundary conditions of the panel influence the noise reduction inside the enclosure only in the low frequencies, mainly corresponding to the fundamental structural resonant frequency;
- ii) the applied damping treatment improves the noise transmission characteristics of the sandwich plate significantly in the lower order structural resonant frequencies;
- iii) the damping treatment has little effect on the noise reduction near the cavity resonant frequencies;
- iv) the structural response is reduced considerably due to the applied damping treatment.

The results which are presented as noise reduction and structural response curves with respect to frequency, indicate the coupling action between the cavity and the structure.

It appears from a literature survey that little or no work is available on the noise transmission through finite sandwich shells. In the thesis, the noise transmission and response characteristics of a layered shell with unconstrained damping treatment and a sandwich shell with constrained damping treatment are formulated similar to that of the sandwich plate taking into consideration the interaction of internal sound pressure field and the structural motion. Only the axi-symmetric modes of vibration of the shell and simply supported end conditions are considered in the analysis. The problem is solved by a similar approach adopted for the sandwich plate. It has been shown by the study that the damping treatment is not quite effective in controlling the noise transmission and the structural response of the sandwich shell, because of low modal loss factors.

In conclusion, it may be said, that the main contribution of the thesis is in formulating the problem of noise transmission and structural response of sandwich structures in a general coupled acoustoelastic frame work. The thesis proposes a simple matrix inversion procedure for the solution of the acoustoelastic problem and brings out clearly the use of forced damped normal modes in response analysis of highly damped structures.

## CHAPTER 1

### INTRODUCTION

#### 1.1 GENERAL INTRODUCTION

The interaction between sound fields and structural vibration is of considerable importance in many areas of engineering interest, especially in aerospace engineering, underwater acoustics, building acoustics, and machinery noise control. Damage to structural parts caused by acoustic fatigue, as a consequence of jet noise and boundary layer excitation, the transmission of noise into the interior of aircrafts causing annoyance to passengers, the vibration and malfunctioning of sensitive and sophisticated instrument packages in a vibro-acoustic environment are some of the problems to be considered in the design of aerospace structural systems. In such problems, an analysis of the vibro-acoustic response and the sound radiation characteristics of structures are of great value to the designer allowing him to select appropriate structural parameters, geometry, damping coatings and treatments to suppress structural vibration and control the associated radiation of sound.

Interior noise in many transportation vehicles is dominated by low and intermediate frequency components. Especially, in propeller driven aircrafts the cabin noise

has maximum intensities in the low frequency range (0 - 1000 Hz) corresponding to the blade passage frequencies. Acoustic absorption materials used in aircraft constructions are not quite effective in controlling interior noise at low frequencies [1]. Interior cabin noise at these frequencies, is strongly dependent on the structural resonances. Hence, noise attenuation in the low frequency ranges can best be achieved by controlling the dynamic and damping characteristics of structural components that radiate sound.

The vibration response of structural elements, can be reduced significantly at resonances, by improving their damping characteristics. Applied damping treatments, where a layer of a high damping material is added to the base structure, have been very popular in this respect. Both unconstrained and constrained viscoelastic layers are used for the purpose. In the unconstrained damping treatment, the damping of the composite is achieved by dissipation of the vibrational energy in the extensional deformations of the viscoelastic layer. In the constrained damping layer treatment, where the viscoelastic layer of relatively low rigidity is sandwiched between two layers of the base material, the damping is mainly due to the energy dissipation in the shear deformations of the viscoelastic core. Because of the reduction in vibration levels, consequent

reduction in the radiant acoustic energy should be possible with the applied damping treatments.

Available literature on noise transmitting characteristics of sandwich panels with constrained viscoelastic damping layer is very scant. Vaicaitis [2] has considered the sound transmission through a viscoelastic sandwich panel into a rectangular cavity, with simply supported panel edges. Recently, Reddy [3] considered the noise transmission characteristics of finite panels held in a rigid baffle, with both unconstrained and constrained damping treatments. But the emphasis of his work was on the determination of structural response to high intensity acoustic excitation and was mainly experimental. The noise transmission analysis was through an approximate formulation of sound power calculations which were compared with his experimental results. Moreover, in these works, the coupling between the acoustic field and the structural motion had not been treated adequately.

Aircraft panels are usually supported by orthogonal rows of stringers and frames. The edge conditions obtaining in such cases cannot be treated as simple supports. A realistic formulation of the structural response and noise transmission problems should consider appropriate boundary conditions in view of the shift in the structural resonant frequencies. In the case of panels with

additive damping treatment, and arbitrary boundary conditions at the edges, determining the resonant frequencies of the composite structure and the associated loss factors becomes a difficult proposition. Moreover in such cases, the classical normal mode analysis cannot be applied for response analysis.

Statistical energy analysis (SEA), which has been successfully employed in structural response prediction and noise transmission study of homogeneous elastic structures in the higher frequency ranges, cannot be of much use in analysing the low frequency noise transmission characteristics of viscoelastic sandwich structures. It is mainly because of two reasons. Firstly, in the low frequency ranges of interest, the modal density of the structure is small, making the response averages over frequency bands less accurate. Secondly, the assumption of weak coupling between modes in different frequency bands, which is widely adopted in SEA calculations is not quite valid for the sandwich panel, due to the large modal damping induced by the constrained damping layer, with significant intermodal coupling.

## 1.2 SCOPE AND ORGANISATION OF THESIS

This thesis presents a theoretical analysis of the noise transmission characteristics and structural response

of sandwich structures with constrained damping layer treatment. The frequency range of interest in the analysis is restricted upto 1000 Hz in the case of finite structural systems. However, in the study of noise transmission through sandwich panels of infinite extent, the restriction on frequency is governed by the orders of the thickness of the sandwich considered. The effect of the coupling between the sound pressure and structural motion has been considered in the analysis.

The analysis admits arbitrary boundary conditions at the edges of the sandwich panel. These are realistic boundary conditions, that would obtain in sheet-stringer constructions commonly found in aircraft structures. Since, classical normal mode analyses with sinusoidal modes is not applicable in the case of arbitrary boundary conditions and arbitrary damping, a 'forced damped normal mode' analysis is carried out for response and transmission loss calculations. Though the method has been outlined by Mead [4], perhaps, it is for the first time in this work, that a damped normal mode analyses is systematically made use of in solving a practical problem of the sound transmission through sandwich structures.

The transmission loss of an infinite sandwich panel is considered first on classical lines. Then, the noise transmission through the sandwich panel into a rectangular

cavity is analysed. The acoustic cavity-structure interaction analysis is presented in a general matrix format on the lines of Dowell [5]. It results in a matrix eigen value problem with gyroscoping coupling, characteristic of the dynamics of spinning structural systems. However, as the main interest of the present work is to determine the response and sound transmission characteristics of the sandwich panel, a direct matrix inversion scheme is adopted for the solution.

There seems to be relatively very few studies available in the literature on sound transmission through curved structures. Even the few works that are available are on sound transmission through homogeneous shells. There seems to be no literature on the sound transmission through sandwich shells. This thesis presents a study on the vibration response and noise transmission of cylindrical shells with both constrained and unconstrained viscoelastic damping treatments. However, the analysis is restricted to the axi-symmetric vibrations of the shell and to simply supported boundary conditions.

In this work, two basic assumptions have been made regarding the properties of the layers. They are:

- i) The variation of the core loss factor of the viscoelastic damping material with frequency is assumed

to be insignificant in the frequency range of interest and the viscoelastic nature of the material is expressed through the complex shear modulus  $G = G^*(1+i\beta)$ .

- ii) The base material to which the damping treatment is applied is elastic and nondissipative.

The organisation of the thesis is as follows. A literature review of the free and forced vibration response of sandwich structures with constrained damping layer treatment is presented in the next section of this chapter. The review also covers the noise transmission studies through flexible structures, pertinent to this work.

In Chapter 2, the equations of motion of a three layer sandwich panel is presented [6]. The method of determining the natural frequencies and associated modal loss factors for different boundary conditions is outlined. Expressions for forced damped normal modes, are derived for further analysis.

Chapter 3, considers the sound transmission through an infinite sandwich panel, for a travelling harmonic pressure wave excitation. The interaction between the sound wave and the structural motion is fully taken into account by considering the radiated sound on either sides

of the panel and the scattered sound field into the analysis. Reducing the equation of motion presented in Chapter 2 as applicable to the infinite sandwich, the dispersion relation and the expression for the complex coincidence frequency are derived. The transmission loss (TL) is obtained as a closed form expression in terms of the sandwich core parameters. The effects of the core parameters on the TL of the infinite sandwich are presented in the form of graphs, TL versus frequency.

In Chapter 4, the structural response and noise transmission characteristics through an elastically supported sandwich panel into a closed rectangular cavity are analysed. Initially, the analysis neglects the effect of cavity pressure on structural motion and solves the problem by converting a homogeneous differential equation with nonhomogeneous boundary conditions into a nonhomogeneous differential equation with homogeneous boundary conditions [2]. The solution is effected through a forced damped normal mode analysis. Subsequently, the coupling between the cavity sound pressure and the motion of the sandwich panel has been fully considered in an 'acoustoelastic' formulation of the problem [5]. As observed earlier, a direct matrix inversion scheme, which takes advantage of the diagonal nature of some of the matrices in the acoustoelastic formulation is adopted in a partition analysis for the

structural response and sound transmission calculations. This avoids the necessity of carrying out a complicated eigenvalue analysis of matrices, which have complex elements, due to the presence of the damping layer and makes the computational scheme much simpler. Both harmonic and stationary random external pressure excitations are considered in the analysis.

Chapter 5, deals with the noise transmission through finite, thin circular cylindrical shells with additive damping treatments. In this case, both unconstrained and constrained layer treatments are considered. The structural response including the effect of cavity is computed in the axisymmetric mode of vibration of the shell. Again, both harmonic and stationary random pressure excitations are considered.

General conclusions of the present work and scope for further extensions of this work are presented in Chapter 6.

### 1.3 LITERATURE REVIEW

In this section, a review, scanning almost three decades of research carried out in the areas of free and forced vibrations of sandwich structures with additive damping treatments and the noise transmission characteristics of flexible structural systems is presented.

### 1.3.1 Vibration of Damped Sandwich Structures

The free vibration characteristics of beams and plates with unconstrained and constrained damping treatments have been investigated extensively by research workers. Such studies include both theoretical analyses and experimental works and involve the derivation of the equations of motion of the composite structure and determination of the natural frequencies and the associated modal loss factors. The damping in these structures is obtained due to high energy losses mainly in the extensional mode of deformation of the viscoelastic layer in the case of unconstrained damping treatments, and in the shear deformation of the damping layer in the case of constrained sandwich constructions.

Oberst [7] was the first to consider the unconstrained damping treatment applied to a plate. He showed that the damping of the composite structure depends on the stiffness, thickness and loss factor of the damping layer. Kerwin [8], presented a general analysis of damping induced by the shear motion of a viscoelastic layer constrained between the plate to be damped and a constraining layer. He showed that the damping factor depends on the wavelength of bending waves in the damped plate, the damping layer and the constraining layer. Ross and Kerwin [9], developed an analysis considering both extensional and shear damping for two layers applied to a plate of infinite extent. Ross, Ungar and Kerwin [10]

presented a general analysis of damping mechanism due to a number of constraining layers. They showed that a multi-layer treatment having the same weight of viscoelastic material has almost equal amounts of damping as in the case of a single constrained layer. This theory is valid only for simply supported conditions for finite beams.

Using a variational approach and an energy formulation Yu [11] derived general equations of motion of sandwich plates and shells. Mead [6] analysed the forced flexural vibrations of a simply supported sandwich plate which vibrated in sinusoidal standing waves. He derived a general expression for the flexural stiffness.

Heretofore listed works have assumed sinusoidal modes of vibration, thus restricting the theory to simply supported conditions or infinite structures. A successful attempt to broaden Ungar-Kerwin's theory, for beams with finite length and arbitrary boundary conditions was made by DiTaranto [12]. He presented a general theory for free vibrations of sandwich beams with arbitrary boundary conditions. Complex natural frequencies  $\omega^*$  are obtained in the form  $\omega^{*2} = \omega^2(1+i\eta)$  where  $\eta$  is the modal loss factor. He showed that the modal loss factor bears a relationship with  $\omega^2$ , which is independent of the end conditions. However, the values of  $\omega^2$  depend on boundary conditions, and as such the numerical values of  $\eta$  need to

be determined separately for each boundary condition. He derived a sixth order differential equation in terms of the axial motion of the beam .

Mead and Markus [13], showed that the modes and frequencies discussed by DiTaranto constitute a special class of resonant frequencies and forced modes, which exist in the presence of an external transverse loading, proportional to the local inertia loading at all points along the beam. Mead [14] gave a general theory of the existence of 'forced damped normal modes' in structures having arbitrary damping. These modes can be used analogous to classical normal mode analysis, in steady state and stationary random response analysis of hysterically damped structures.

Yan and Dowell [15], derived a simplified equation of motion for the transverse displacement of sandwich beams and plates with constrained damping treatments. The analytical results of natural frequencies and loss factors obtained by them agreed closely with that of Mead and Markus [16]. Mead and Markus [17,18], in further extension of their earlier work determined the natural frequencies and modal loss factors of cantilever and encastered sandwich beams. Oravsky, Markus and Simkova [19] presented an approximate method of calculating the modal loss factors of damped sandwich structures by a perturbation analysis. The theories presented by Mead and Markus [13]

and Yan and Dowell [15], have been found to be in close agreement with experimental results [20,21,22].

The theory of vibration of sandwich beams was extended to the case of sandwich plates by DiTaranto and McGraw [23]. Mead [24] considered the damping properties of elastically supported sandwich panels with a viscoelastic core, in terms of symmetric and antisymmetric modes. He used a linear interpolation scheme in an iterative analysis to determine the complex natural frequencies. Rao and Nakra [25] included longitudinal, transverse and rotary inertia effects in their analysis of flexural vibrations of sandwich beams and plates. (Grootenhuis [26], analysed a multilayer damping treatment with viscoelastic materials and showed that unconstrained damping treatment could be as effective as constrained treatment compared on an equal weight basis.) Mead [27] analysed the damping characteristics of periodic damped sandwich plates by a wave propagation approach. Lu, Killian and Everstine [28,29] used a finite element method in the vibration analysis of three layered damped sandwich structures. They took into consideration the effect of frequency and temperature changes on the loss factor of the viscoelastic material. They also compared their theoretical results with experiment.

The vibration analysis of curved members with layered damping treatments is not as extensive as for beams or plates.

Initial research on vibration problems of sandwich cylindrical shells was done by Yu [30]. This work was confined to sandwich shells with elastic layer alone. Later, Yu[11] extended his work to include layers with viscoelastic property by modifying the equations of motion. The shear damping mechanism in sandwich cylindrical shells was investigated by Yu and Ren [31]. Jones and Salerno [32] also considered the effect of structural damping in the forced vibration of sandwich cylindrical shells. They showed that the shear damping in the core layer yields a much lower loss factor for the flexural modes of sandwich shells than for that of the corresponding sandwich plate. These works are again applicable only to the case of simply supported end conditions or shells of infinite length.

DiTaranto [33] analysed the free and forced vibrations of three layered sandwich rings. He used the variational method to derive the equations of motion and obtained analytical expressions for the structural response considering the circumferential bending modes. DiTaranto, Lu and Douglas [34] presented an approximate analysis for the free and forced vibrations of sandwich rings with segmented constrained damping treatment. Lu, Douglas and Thomas [35] obtained the forced response of damped sandwich rings by a mechanical impedance calculation. They included the temperature and frequency effects on the core loss factor

in their analysis, and found good agreement with experimental results.

Pan [36] investigated the vibrations of a damped sandwich cylindrical shell in the axisymmetric mode. He followed an analysis similar to DiTaranto [12] and outlined a procedure for calculating natural frequencies and loss factors for finite shells with arbitrary boundary conditions. Markus [37] derived the equations of motion in the axisymmetric modes of vibration of a cylindrical shell with unconstrained damping layer treatment in three configurations of inside, outside and two-side coatings.

### 1.3.2 Sound Transmission Through Structures

Structural response to acoustic excitation and sound radiation by vibrating structures and the general problem of sound structure interaction have been investigated by many authors. The different approaches to the problem can be found in the works of Cremer, Heckl and Ungar [38], Junger and Feit [39], Lyon and Smith [40] and Lyon [41]. The review, here will be mainly confined to the noise transmission characteristics of flexible structures.

Beranek [42], London [43], Feshback [44] and Cremer [45], investigated the sound transmission through flexible walls of infinite extent for plane harmonic wave incidence.

The phenomenon of coincidence transmission was presented, at which the wall became transparent to the incident sound for particular combinations of frequency and incidence angle. This is due to the matching of the trace wave length of the propagating sound with the free flexural wavelength of the plate. Subsequent works on noise transmission through infinite walls, divided the frequency ranges of transmission into three zones, namely below coincidence frequency, at or near coincidence and above coincidence frequency.

The transmission of sound through double wall constructions in the field of architectural acoustics was investigated by Beranek[46], London [47], Mullohand [48], essentially following the lines of Beranek [42].

Noise transmission and structural response of cavity backed finite panels have received the attention of many research workers. Pretlove [49], using a normal mode analysis determined the response of a cavity backed panel to harmonic excitation. Dowell [50], computed the response and noise transmission of cavity backed finite panels to boundary layer turbulence. He used a numerical integration procedure in the time domain after simulating the generalized forces. Dowell and Voss [51] analysed the response of a cavity backed finite panel clamped on all its edges, by a simplified modal approach, neglecting the

coupling between the structural modes and the structural acoustic coupling. Bhattacharya and Crocker [52], Guy and Bhattacharya [53] using a combination of Laplace transform in the time domain and Fourier transform in the space domain computed the response and noise transmission of a finite panel backed by a rectangular cavity. They found good agreement between their theoretical results and experimental results. They also gave a graphical procedure to determine the natural frequencies of the cavity structure system, and explained the negative transmission loss that occur at frequencies close to the cavity resonances. The existence of coincidence like phenomenon on a cavity backed finite panel system was shown by Guy, Bhattacharya and Crocker [54]. This happens at frequencies when the standing wave resonant wave length of the panel matches with the standing wave resonant wavelength of the cavity. Unlike in the case of the infinite panel they showed that the coincidence frequencies of the finite panel are independent of the incidence angle.

Dowell [5], and Dowell, Gorman and Smith [55] gave a general theory of the interaction between the internal sound pressure field and the elastic flexible wall of an enclosure and coined the term 'acoustoelasticity' for the study of such problems. They adopted a series expansion in terms of the structural normal modes and the cavity modes

and reduced the problem of determining the structural response and the sound pressure inside the enclosure to a matrix eigenvalue problem with gyroscopic coupling. They also gave approximate results for a sinusoidal excitation, corresponding to the exciting frequency being close to a structural or cavity frequency, or to both. Recently Guy [56] gave a general analysis of the response of a cavity backed panel to external excitation using a multimodal analysis.

The method of statistical energy analysis has also been used in the analysis of noise transmission through finite walls backed by a cavity. A balance of power flows into and away from the different modal systems was adopted in the statistical energy analysis models. Lyon [57], Eichler [58], White and Powell [59], Crocker and Price [60, 61], are some of the important contributors in this respect. They used the formulae derived by Maidanik [62,63], Lyon and Smith [40] for the important SEA parameters like radiation resistances, modal densities and coupling loss factors.

Pope [64], and Pope and Wilby [65] investigated the sound transmission into closed enclosures using structural and acoustic Green's functions and modal analysis. Conditions in terms of structural and cavity configurations

and structural and cavity damping are established for the resonant and non-resonant transmission of sound into the enclosure. They discussed the results in relation to the statistical energy analysis calculations.

McDonald, Vaicaitis and Myers [66] presented an analytical model for the noise transmission through rectangular plates into closed cavities using a normal mode analysis. Vaicaitis and Slazak [67] recently investigated the noise transmission through stiffened plates into rectangular enclosures by a similar analysis and using transfer matrix methods.

Craggs [68,69] considered a variational formulation for the structure-cavity system in the context of finite element representations for the coupled acoustoelastic problem.

The suitability of sandwich structures in improving the noise insulation characteristics of homogeneous panels was investigated by Kurtze and Watters [70]. A high transmission loss was sought to be achieved through a shift of the coincidence frequency towards higher frequency ranges by a choice of a thick core, whose elastic modulus is much less than that of the skin layers. Ford, Lord and Walker [71] investigated the sound transmission characteristics of sandwich constructions with a rigid polyurethane foam core.

They estimated the natural frequencies of the composite structure using an energy formulation. Their experiments revealed a low transmission loss due to resonance in the dilational mode. They suggested a scheme to increase the transmission loss corresponding to the 'mass law' by an optimal choice of the core stiffness.

Recently, Smolenski and Krokosky [72] investigated the sound transmission characteristics of soft core sandwich panels and stressed the importance of dilational mode sound transmission. They used a Rayleigh-Ritz procedure to calculate the natural frequencies and determined the transmission loss by an experimental procedure. Dym, Ventres and Lang [73], calculated the sound transmission loss of sandwich panels by a theoretical analysis. They included, shear deformation and rotary inertia of the thick core and dilational deformation in the core axial displacement. Using Hamilton's equations they derived the equations of motion of the sandwich in symmetric and antisymmetric modes and calculated the transmission loss by an impedance approach. They also compared their results with the experimental results of Smolenski and Krokosky [72]. Guyader and Leseueur [74] combined a statistical energy analysis and a normal mode approach in calculating the transmission loss of orthotropic multilayered plates. Madigosky and Fiorito [75] calculated the transmission loss as a function of

frequency, thickness and incident angle for single and multiple viscoelastic plates using a transfer matrix method modified to include complex wave velocities.

Reddy [3] calculated the transmission loss of three layered sandwich panels, with constrained viscoelastic damping treatment based on a simple transmission coefficient formula and by conversion of sound power radiated on the transmitting side of the panel into sound pressure levels.

In all the cases of sound transmission studies through sandwich panels, the panels were either of infinite extent or confined in an infinite baffle with simple support conditions. Vaicaitis [2], considered the noise transmission through a sandwich plate with a viscoelastic constrained layer into a closed rectangular cavity. He confined his analysis to the frequency range of 0 - 1000 Hz and reported significant noise reduction. A spatially uniform and stationary random pressure loading was considered in his analysis.

There seems relatively few studies on sound transmission through curved structures. Junger and Smith [76] gave a semiquantitative discussion of noise transmission through curved structures. Smith [77], improved upon his original work by calculating the ratio of the absorbed power to

incident power of a thin cylindrical shell. Cremer and Heckl [78], had also considered the transmission of an acoustic wave through an infinite, homogeneous, isotropic cylinder. Their results show that the transmission properties of the shell to an incoming single frequency wave depends on frequency and the angle between cylinder axis and wave normal. Furthermore, it was determined that the two most important characteristics of the problem were the ring frequency and the coincidence frequency.

White [79] considered the sound transmission through finite closed cylindrical shells using a statistical energy analysis. He used the radiation resistance calculations of Maidanik and Manning [80] and the modal density formulae derived by Heckl [81] in his analysis. Koval [82,83,84] in a series of papers extended the work of Smith [77] on sound transmission through cylindrical shells by including the effects of external flow, reflection and scattering of incident wave, internal cabin pressurization, internal cavity resonances and structural damping.

As observed earlier, there seems to be no work on sound transmission through sandwich shells. This thesis presents an investigation, on the sound transmission and structural response to both harmonic and random pressure excitation of circular cylindrical shells with unconstrained and constrained viscoelastic damping treatment vibrating in axisymmetric modes.

## CHAPTER 2

### DYNAMICS OF DAMPED SANDWICH PANEL

The response analysis and noise transmission studies of the damped sandwich panel require its vibration and damping characteristics. Different, but related analyses of the vibration of sandwich panels with constrained damping layer treatment are available in the literature [6,15,23]. Mead [6], derived the equations of motion of a three layered sandwich panel with a viscoelastic core, based on the shear damping mechanism of the core. [His theory has been found to be in excellent agreement with experimental results [20, 21,22] in the usual ranges of frequency interest and widely adopted.] In the present work the equations of motion derived by Mead are adopted in the study of structural response and noise transmission of sandwich panels. They are presented in this chapter for the sake of continuity and understanding of the subsequent chapters. The steps involved in the determination of the natural frequencies and the associated modal loss factors and the response analysis using damped normal modal analysis are also briefly outlined.

#### 2.1 EQUATIONS OF MOTION

The equations of motion of a uniform three layer sandwich panel under transverse pressure excitation was derived

by Mead [6], under the following assumptions.

- i) Direct stresses in the soft core are much smaller than the direct stresses in the face plates and hence neglected.
- ii) There is no significant direct strain in the core perpendicular to the plane of the plate. Therefore, the plate motion in the transverse direction  $w$  is the same for all the three layers.
- iii) There is no significant shear strain in either face-plate, in planes perpendicular to the plane of the plate.

The equations of motion, neglecting the inertia forces in the  $x$  and  $y$  direction are, (Refer to Figure 2.1)

$$\begin{aligned} \frac{E}{(1-\nu^2)} \frac{\partial^2 u}{\partial x^2} + \frac{E}{2(1+\nu)} \frac{\partial^2 u}{\partial y^2} - \frac{2G}{h_1 h_2} u \\ + \frac{E}{2(1-\nu)} \frac{\partial^2 v}{\partial x \partial y} + \frac{G(h_1+h_2)}{h_1 h_2} \frac{\partial w}{\partial x} = 0 \end{aligned} \quad (2.1)$$

$$\begin{aligned} \frac{E}{(1-\nu^2)} \frac{\partial^2 v}{\partial y^2} + \frac{E}{2(1+\nu)} \frac{\partial^2 v}{\partial x^2} - \frac{2G}{h_1 h_2} v \\ + \frac{E}{2(1-\nu)} \frac{\partial^2 u}{\partial x \partial y} + \frac{G(h_1+h_2)}{h_1 h_2} \frac{\partial w}{\partial y} = 0 \end{aligned} \quad (2.2)$$

$$\begin{aligned} D_t \nabla^4 w - \frac{G(h_1+h_2)}{h_2} [(h_1+h_2) \nabla^2 w - 2(\frac{\partial u}{\partial x} + \frac{\partial v}{\partial y})] + \mu \frac{\partial^2 w}{\partial t^2} \\ = p(x,y,t) \end{aligned} \quad (2.3)$$

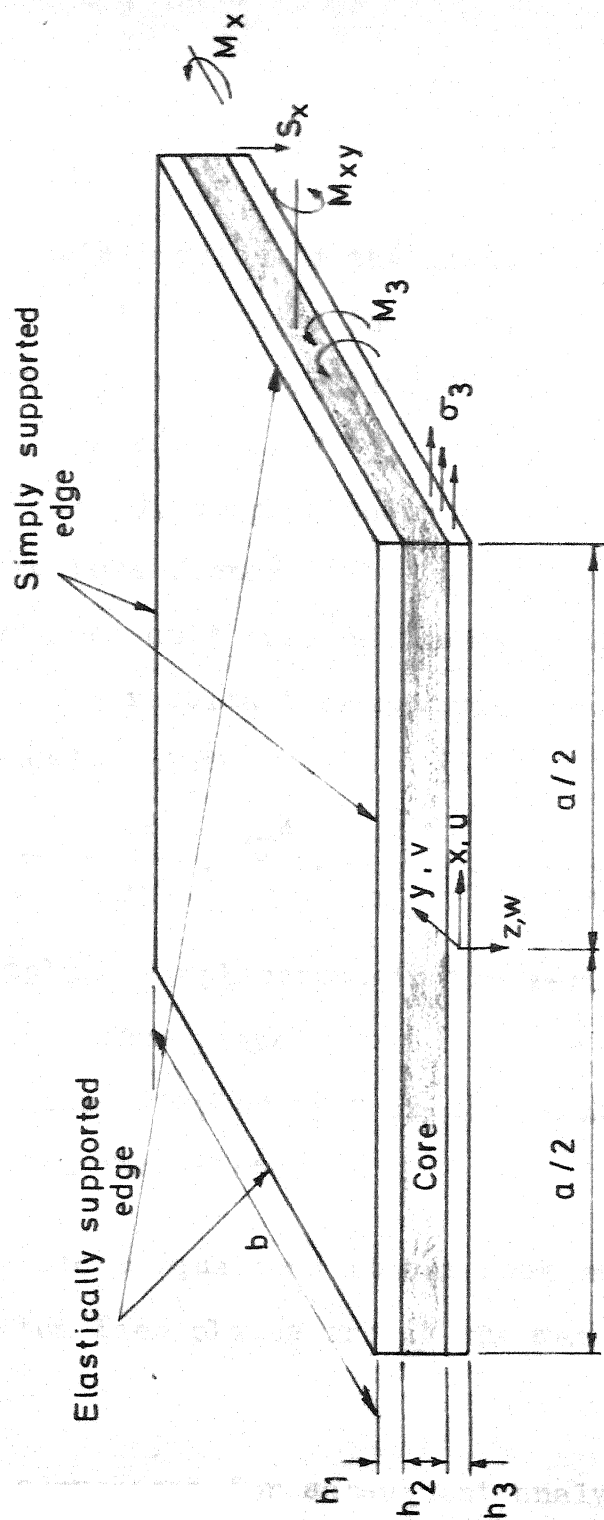


FIG. 2.1 COORDINATE SYSTEM USED FOR DAMPED SANDWICH PLATE

where,

$E$  = Young's modulus of the plate

$\nu$  = Poisson's ratio of the plate

$D_t$  = total flexural rigidity of both the face plates  
 $= [2Eh_1^3/12 (1-\nu^2)]$

$G$  =  $G^*(1+i\beta)$ , complex shear modulus of the core

$\beta$  = core loss factor

$\mu$  = mass per unit area of the whole sandwich panel

$p(x,y,t)$  = local resultant transverse loading on the sandwich plate

$$\nabla^2 = \frac{\partial^2}{\partial x^2} + \frac{\partial^2}{\partial y^2}, \quad \nabla^4 = \frac{\partial^4}{\partial x^4} + 2 \frac{\partial^4}{\partial x^2 \partial y^2} + \frac{\partial^4}{\partial y^4}$$

$u$  = midplane displacement in the x-direction of the bottom face plate

$v$  = midplane displacement in the y-direction of the bottom face plate.

In the above equations it has been assumed that the top and bottom face plates are of the same material and thickness.

It is convenient for subsequent analysis, to express the equations of motion in terms of the transverse displacement  $w$ , by eliminating  $u$  and  $v$  from equations (2.1) to (2.3). This is done in following manner.

Equations (2.1) to (2.3) can be rewritten as,

$$\frac{\partial^2 u}{\partial x^2} + \frac{1-v}{2} \frac{\partial^2 u}{\partial y^2} - g'u + \frac{1+v}{2} \frac{\partial^2 v}{\partial x \partial y} + \frac{g'}{2} (h_1 + h_2) \frac{\partial w}{\partial x} = 0 \quad (2.4)$$

$$\frac{1+v}{2} \frac{\partial^2 u}{\partial x \partial y} + \frac{\partial^2 v}{\partial y^2} + \frac{1-v}{2} \frac{\partial^2 v}{\partial x^2} - g'v + \frac{g'}{2} (h_1 + h_2) \frac{\partial w}{\partial y} = 0 \quad (2.5)$$

$$\begin{aligned} \nabla^4 w - g'Y \nabla^2 w + \frac{6g'(h_1 + h_2)}{h_1^2} \frac{\partial u}{\partial x} + \frac{6g'(h_1 + h_2)}{h_1^2} \frac{\partial v}{\partial y} \\ + \frac{\mu}{D_t} \frac{\partial^2 w}{\partial t^2} = \frac{p(x, y, t)}{D_t} \end{aligned} \quad (2.6)$$

where,

$Y = 3(1+h_2/h_1)^2$  is the geometric parameter

$g' = \frac{2G(1-v^2)}{Eh_1 h_2} = \bar{g}(1+i\beta)$  is the complex shear parameter.

Differentiating equation (2.4) and (2.5) with respect to  $x$  and  $y$  respectively, and adding the resulting equations one obtains,

$$\begin{aligned} \left( \frac{\partial^3 u}{\partial x^3} + \frac{\partial^3 v}{\partial y^3} \right) + \left( \frac{\partial^3 u}{\partial x \partial y^2} + \frac{\partial^3 v}{\partial x^2 \partial y} \right) - g' \left( \frac{\partial u}{\partial x} + \frac{\partial v}{\partial y} \right) \\ + \frac{g'}{2} (h_1 + h_2) \left( \frac{\partial^2 w}{\partial x^2} + \frac{\partial^2 w}{\partial y^2} \right) = 0 \end{aligned} \quad (2.7)$$

Differentiating equation (2.6) twice with respect to  $x$  and  $y$  separately, and adding the resulting equations, the following equation is obtained.

$$\nabla^6 w - g'Y \nabla^4 w + \frac{\mu}{D_t} \frac{\partial^2}{\partial t^2} (\nabla^2 w) + \frac{6g'(h_1+h_2)}{h_1^2} \left( \frac{\partial^3 u}{\partial x^3} + \frac{\partial^3 u}{\partial x \partial y^2} + \frac{\partial^3 v}{\partial x^2 \partial y} + \frac{\partial^3 v}{\partial y^3} \right) = \frac{1}{D_t} \nabla^2 p \quad (2.8)$$

where,

$$\nabla^6 \text{ is the differential operator}$$

$$\nabla^6 = \left( \frac{\partial^6}{\partial x^6} + 3 \frac{\partial^6}{\partial x^4 \partial y^2} + 3 \frac{\partial^6}{\partial x^2 \partial y^4} + \frac{\partial^6}{\partial y^6} \right)$$

Using equations (2.6) and (2.7) to eliminate the u and v terms from equation (2.8) one gets,

$$\nabla^6 w - g'(1+Y) \nabla^4 w + \frac{\mu}{D_t} \frac{\partial^2}{\partial t^2} [\nabla^2 w - g'w] = \frac{1}{D_t} (\nabla^2 p - g'p) \quad (2.9)$$

It has been shown by Mead [13,14], that separable harmonic motions for w with characteristic frequencies are possible, when the structure is excited by a particular form of forcing functions called the 'damped normal loading'. The corresponding modes in which the plate vibrates are called the forced damped normal modes. The damped normal loading for the sandwich panel is harmonic and is in phase with the local velocity but proportional in amplitude to the local inertia force. Hence the damped normal transverse loadings are of the form

$$p(x,y,t) = -i\eta\mu \frac{\partial^2 w}{\partial t^2} \quad (2.10)$$

where,

$\eta$  = the loss factor associated with a damped normal mode.

Under the damped normal loading, the plate motion can be expressed in the form,

$$w = W(x,y) e^{i\omega t} \quad (2.11)$$

where,

$W(x,y)$  represents the forced damped normal mode which is generally a complex function of  $x$  and  $y$ .

Substituting equations (2.10) and (2.11) into equation (2.9), one obtains

$$\nabla^6 W - g'(1+Y) \nabla^4 W - \omega^2 (1+i\eta) \frac{\mu}{D_t} [\nabla^2 W - g'W] = 0 \quad (2.12)$$

Equation (2.12) can be rewritten in non-dimensional form using non-dimensional coordinates  $\xi = x/a$  and  $\Psi = y/a$ , where  $a$  is the length of the plate in the  $x$ -direction. The result is

$$\nabla^6 W - g(1+Y) \nabla^4 W - \Omega^2 \nabla^2 W + g \Omega^2 W = 0 \quad (2.13)$$

In the above equation the differentiations are with respect to the nondimensional coordinates,  $\xi$  and  $\Psi$  in the operator  $\nabla$ .

$g = g'a^2 = g^*(1+i\beta)$  is the nondimensional shear parameter and

$\Omega^2 = \frac{\omega^2(1+i\eta) \mu a^4}{D_t} = \Omega^{*2}(1+i\eta)$  is the nondimensional frequency parameter.

## 2.2 NATURAL FREQUENCIES, LOSS FACTORS AND DAMPED NORMAL MODES

In the analysis, panel edges are assumed to be simply supported along the x-wise edges at  $y = 0, b$ . The y-wise edges at  $x = \pm a/2$  are assumed to be elastically supported. These assumptions are justified on the following grounds. The noise transmission studied in the present work, is in the context of interior cabin noise of aircrafts. Typical aircraft panels are supported by orthogonal rows of stringers and frames. It has been found that the boundary conditions at the x-wise edges have little effect on the natural frequencies of the plate, provided the width of the panel between the frames (in the y-direction) is more than two or three times the stiffener spacing (in the x-direction). Moreover, previous works on the vibration analysis of sheet stiffener combinations have consistently made these assumptions [85,86,87]. The analysis can as well include the admission of arbitrary boundary conditions along both x and y-wise edges, but in such a case the computational efforts in determining the complex eigenvalues and the damped normal modes would become enormous.

Under the above assumptions, the forced damped normal modes can be expressed as

$$W_{mn}(\xi, \Psi) = \sum_{r=1}^6 A_{rmn} \exp(\lambda_{rmn} \xi) \sin \frac{n\pi a \Psi}{b} \quad (2.14)$$

Substituting equation (2.14) in equation (2.13) a characteristic polynomial equation in  $\lambda_{rmn}$  is obtained.

$$(\lambda_{rmn}^2 - P_n^2)^3 - g(1+Y)(\lambda_{rmn}^2 - P_n^2)^2 - \Omega^2(\lambda_{rmn}^2 - P_n^2) + g\Omega^2 = 0 \quad (2.15)$$

where,

$$P_n = \frac{n\pi a}{b}.$$

Writing  $u$  and  $v$  analogous to equation (2.11) as,

$$u = U(x, y) \exp(i\omega t) \text{ and } v = V(x, y) \exp(i\omega t)$$

the damped normal modes corresponding to displacements  $u$  and  $v$  can be expressed as,

$$U_{mn}(\xi, \Psi) = \sum_{r=1}^6 B_{rmn} \exp(\lambda_{rmn} \xi) \sin P_n \Psi \quad (2.16)$$

$$V_{mn}(\xi, \Psi) = \sum_{r=1}^6 C_{rmn} \exp(\lambda_{rmn} \xi) \cos P_n \Psi \quad (2.17)$$

Substituting equations (2.14), (2.16) and (2.17) into the equations of motion (2.1) and (2.2), it can be shown that the coefficients  $B_{rmn}$  and  $C_{rmn}$  are related to  $A_{rmn}$  in the following form.

$$B_{rmn} = - \frac{\lambda_{rmn} g (h_1 + h_2)}{2a(\lambda_{rmn}^2 - P_n^2 - g)} A_{rmn} \quad (2.18)$$

$$C_{rmn} = - \frac{P_n g (h_1 + h_2)}{2a(\lambda_{rmn}^2 - P_n^2 - g)} A_{rmn} \quad (2.19)$$

The problem of determining the natural frequencies, modal loss factors and the damped normal modes reduces to finding the set of values  $\lambda_{rmn}$ ,  $P_n$  and  $\Omega^2$  that satisfy both equation (2.15) and the boundary conditions at  $x = \pm a/2$ .

### 2.3 BOUNDARY CONDITIONS ALONG Y-WISE EDGES AT $x = \pm a/2$

The following boundary conditions along the edges at  $x = \pm a/2$  are considered in the present analysis.

- i) Edges simply supported
- ii) Edges clamped
- iii) Edges with elastic rotational restraint and no transverse displacement, with and without rivets
- iv) Edges with no rotation but with transverse elastic restraint.

The nature of the boundary conditions in the above cases are given in reference [24].

#### 2.3.1 Simply Supported Edges

In this case the natural frequencies, the modal loss factors and the damped normal modes can be obtained

in closed form. The boundary conditions are,

$$w \Big|_{x = \pm a/2} = 0 \quad (\text{zero transverse displacement})$$

$$\left( \frac{\partial u}{\partial x} + \nu \frac{\partial v}{\partial y} \right) \Big|_{x = \pm a/2} = 0 \quad (\text{zero axial strain in entire face plate})$$

$$\begin{aligned} M_x &= 2M_1 + \sigma_1 h_1 (h_1 + h_2) && (\text{zero bending moment per} \\ &= D_t \left( \frac{\partial^2 w}{\partial x^2} + \nu \frac{\partial^2 w}{\partial y^2} \right) && \text{unit length along the} \\ &+ \frac{Eh_1}{1-\nu^2} (h_1 + h_2) \left( \frac{\partial u}{\partial x} \right. && \text{y-wise edges of the plate}) \\ &+ \nu \frac{\partial v}{\partial y} \Big|_{x = \pm a/2} = 0 \end{aligned} \quad (2.20)$$

Applying the boundary conditions (2.20) it can be shown that the damped normal modes in the case of simply supported conditions at  $x = \pm a/2$  are given by

$$W_{mn}(\xi, \Psi) = A_{mn} \sin m\pi \left( \xi + \frac{1}{2} \right) \sin P_n \Psi \quad (2.21)$$

Closed form expression for the nondimensional natural frequency parameter can be obtained by substitution of equation (2.21) in equation (2.13).

The result is

$$\Omega_{mn}^2 = \Omega_{mn}^{*2} (1 + i\eta_{mn}) = \frac{(m^2 \pi^2 + P_n^2)^3 + g(1+Y)(m^2 \pi^2 + P_n^2)^2}{m^2 \pi^2 + P_n^2 + g} \quad (2.22)$$

The real part of the above equation gives the natural frequency parameter and the ratio of the imaginary part to the real part gives the modal loss factor.

### 2.3.2 Clamped Edges

The boundary conditions in this case are:

$$w \Big|_{x=\pm a/2} = 0 \quad \text{(zero transverse displacement)}$$

$$\frac{\partial w}{\partial x} \Big|_{x=\pm a/2} = 0 \quad \text{(zero slope)}$$

$$\frac{1}{h_2} [-2u + (h_1 + h_2) \frac{\partial w}{\partial x}] \Big|_{x=\pm a/2} = 0 \quad \text{(zero shear strain in the core in x-z plane)}$$

Applying the above boundary conditions and using equations (2.14) and (2.16), the natural frequencies, loss factors, and the damped normal modes can be obtained, by solving the resulting determinantal equation in conjunction with equation (2.15). The natural frequencies are those which satisfy the equation (2.15) and make the determinant of the coefficient matrix of  $A_{rnm}$  zero.

### 2.3.3 Edges with Elastic Rotational Restraint and No Transverse Displacement

Such boundary conditions for the panel will arise when the edge stiffeners have finite rotational stiffness and very large transverse stiffness.

a) For the case of unriveted edges the boundary conditions become

$$w \Big|_{x = \pm a/2} = 0 \quad (\text{zero transverse displacement})$$

It will be assumed that at an unriveted edge there are no mid-plane direct stress  $\sigma_x$  in either face plate. This implies that

$$\left( \frac{\partial u}{\partial x} + \nu \frac{\partial v}{\partial y} \right) \Big|_{x = \pm a/2} = 0$$

The last two boundary conditions are due to the moment equilibrium between the stiffener and the plate and are expressed as,

$$G_s J \frac{\partial^3 w}{\partial x \partial y^2} - E_s \Gamma \frac{\partial^5 w}{\partial x \partial y^4} \Big|_{x = \pm a/2} = M_x \Big|_{x = \pm a/2}$$

where  $G_s J$  is the St. Venant torsional stiffness of the stiffener,  $\Gamma$  is the Wagner-Kappus torsion bending constant,  $E_s$  is the stiffener Young's modulus, and  $M_x$  is the moment per unit length along the y-wise edge of the plate to which the stiffener is attached.

b) For the case of riveted edges, the shear strain in the core is completely prevented. In this case the six boundary conditions are:

$$w \Big|_{x = \pm a/2} = 0 \quad (\text{zero transverse displacement})$$

$$\frac{1}{h_2} [-2u + (h_1 + h_2) \frac{\partial w}{\partial x}] \Big|_{x = \pm a/2} = 0 \quad (\text{zero shear strain in the core in the x-z plane})$$

and

$$G_s J \frac{\partial^3 w}{\partial x \partial y^2} - E_s \Gamma \frac{\partial^5 w}{\partial x \partial y^4} \Big|_{x = \pm a/2} = M_x \Big|_{x = \pm a/2} \quad (\text{moment equilibrium between plate and stiffener})$$

As for the clamped edges, the natural frequencies, loss factors and damped normal modes are obtained after solution of a determinantal equation in conjunction with the polynomial equation in  $\lambda s$ .

#### 2.3.4 Edges with No Rotation but Transverse Elastic Restraint

Such boundary conditions for the panel will arise, when the edge stiffeners have finite transverse stiffness and have large rotational stiffness.

Zero rotation at an edge is expressed as

$$\frac{\partial w}{\partial x} \Big|_{x = \pm a/2} = 0 \quad (\text{zero rotation})$$

Two more boundary conditions are due to equilibrium of the shear forces between the plate and the stiffener and are expressed as

$$\left. \frac{\partial M_x}{\partial x} - 2 \frac{\partial M_{xy}}{\partial y} \right|_{x = \pm a/2} = (EI)_s \left. \frac{\partial^4 w}{\partial y^4} \right|_{x = \pm a/2}$$

where,  $(EI)_s$  is the flexural rigidity of the stiffener

$$M_{xy} = -[D_t(1-\nu) \frac{\partial^2 w}{\partial x \partial y} + \frac{Eh_1}{2(1+\nu)} (h_1+h_2)(\frac{\partial u}{\partial y} + \frac{\partial v}{\partial x})]$$

where,  $M_{xy}$  is the twisting moment per unit length along the y-wise edge of the plate.

The last two boundary conditions corresponding to the riveted edge conditions are

$$\left. \frac{1}{h_2} [-2u + (h_1 + h_2) \frac{\partial w}{\partial x}] \right|_{x = \pm a/2} = 0, \text{ (zero shear strain in the core in } x\text{-}z \text{ plane)}$$

## 2.4 SYMMETRIC MODES

If the boundary conditions are identical at  $x = \pm a/2$  and if the loading is symmetric, the contributions to the total response will be mainly due to the symmetric modes and it is expedient in such cases to consider only the symmetric modes of vibration, which can be expressed in the form

$$W_{mn}(\xi, \Psi) = \sum_{r=1}^3 A_{rmn} \cos \lambda_{rmn} \xi \sin P_n \Psi \quad (2.23)$$

$$U_{mn}(\xi, \Psi) = \sum_{r=1}^3 B_{rmn} \sin \lambda_{rmn} \xi \sin P_n \Psi \quad (2.24)$$

$$V_{mn}(\xi, \Psi) = \sum_{r=1}^3 C_{rmn} \cos \lambda_{rmn} \xi \sin P_n \Psi \quad (2.25)$$

In this case the coefficients  $B_{rmn}$ ,  $C_{rmn}$  and  $A_{rmn}$  are related as,

$$B_{rmn} = - \frac{g \lambda_{rmn} (h_1 + h_2)}{2 a (g + \lambda_{rmn}^2 + P_n^2)} A_{rmn} \quad (2.26)$$

$$C_{rmn} = \frac{g P_n (h_1 + h_2)}{2 a (g + \lambda_{rmn}^2 + P_n^2)} A_{rmn} \quad (2.27)$$

and the polynomial equation in  $\lambda$ 's becomes

$$(\lambda_{rmn}^2 + P_n^2)^3 + g (1+Y)(\lambda_{rmn}^2 + P_n^2) - \Omega^2 (\lambda_{rmn}^2 + P_n^2 + g) = 0 \quad (2.28)$$

The effort of computing the natural frequencies is reduced considerably as the boundary conditions are to be applied only at one edge namely at  $x = + a/2$  and the frequency determinant reduces to the order  $3 \times 3$ .

The elements of the coefficient matrix for the different boundary conditions and the forced damped normal modes are given in Appendix A.

## 2.5 DETERMINATION OF RESONANT FREQUENCIES AND LOSS FACTORS

The solution of the determinantal equation is complicated because of the cumbersome complex arithmetic involved

and the inherent numerical problems associated with it. This difficulty can be overcome by splitting the determinant into its real and imaginary parts and setting these separately equal to zero. Considering the real part and the imaginary part of the determinant as two real functions in the two real variables  $\Omega^{*2}$  and  $\eta \Omega^{*2}$ , a two dimensional Newton-Raphson iteration scheme as reported by Narayanan and Mallik [88] can be adopted. But a direct iterative linear interpolation scheme as given by Mead [24] is used because of faster convergence. The steps in the procedure are as follows:

- i) A value of one of the  $\lambda_r$ 's is guessed, say  $\lambda_1$ . For a first approximation, the imaginary part may be neglected.
- ii) The first guessed value of  $\lambda_1$  was used to find  $\Omega^2$  from equation (2.15) or (2.28). Either of the corresponding two equations (2.15) or (2.28) is used to find the approximate values of the other two  $\lambda_r$ 's.
- iii) With the three approximate values of  $\lambda_{rmn}$ , the determinant of the coefficients for the approximate boundary conditions is evaluated.
- iv) The value of  $\lambda_1$  is slightly perturbed and steps(ii) and (iii) are repeated to find another value of the determinant. Linear interpolation is adopted to determine subsequent values of  $\lambda_1$  which brings

the determinant closer to zero. When the  $\lambda$  s converge sufficiently, the corresponding value of  $\Omega^2$  gives the frequency parameter and loss factor.

If the initial guess of  $\lambda$  is properly made then the convergence is obtained within four to five iterations. In some cases the number of iterations for convergence increased for higher order modes. In any case the number of iterations for convergence did not exceed twenty.

After getting the correct values of  $\lambda$  s, and substituting into equations (2.14) or equation (2.23) the damped normal modes are obtained. The form of the damped normal modes in the symmetric modes for the different boundary conditions, are given in Appendix A. The values of the natural frequencies and loss factors are given in Chapter 4, for the typical plate dimensions and layer properties adopted.

## 2.6 FORCED DAMPED NORMAL MODE RESPONSE ANALYSIS

### 2.6.1 Harmonic Loading

Considering a harmonic external pressure  $p(x,y,0,t) = p_0 \exp(i \omega t)$ , the damped normal modes can be made use of to obtain the response of the sandwich plate.

The forced response of the plate can be expanded in terms of the damped normal modes as

$$w(x,y,t) = \sum_{m=1}^{\infty} \sum_{n=1}^{\infty} W_{mn}(x,y) q_{mn}(t) \quad (2.29)$$

Substituting equation (2.29) into equation (2.9) and using orthogonality properties of the damped normal modes [14], it can be shown that

$$q_{mn}(t) = \frac{p_{mn}(t)}{\mu_{mn} [\omega_{mn}^2 (1 + i\eta_{mn}) - \omega^2]} \quad (2.30)$$

where,

$$p_{mn} = \int_0^b \int_{-a/2}^{a/2} p(x,y,0,t) W_{mn}(x,y) dx dy \quad (2.31)$$

and

$$\mu_{mn} = \int_0^b \int_{-a/2}^{a/2} \mu W_{mn}^2(x,y) dx dy \quad (2.32)$$

The  $p_{mn}$ 's and  $\mu_{mn}$ 's can be considered as the generalized force and generalized mass analogous to classical normal mode analysis. The expressions for  $p_{mn}$  and  $\mu_{mn}$  corresponding to the different boundary conditions are given in Appendix B.

### 2.6.2 Random Loading

Consider a random pressure excitation stationary with respect to time and homogeneous with respect to the spatial indexing parameters. Let the cross power spectral density of the pressures at two locations  $x_1, y_1$  and  $x_2, y_2$  on the panel be expressed as

$$S_{pp}(x_1, y_1; x_2, y_2; \omega) = S_{p_0 p_0}(\omega) r_{xy}(x_2 - x_1; y_2 - y_1; \omega) \quad (2.33)$$

where,  $r_{xy}(x_2 - x_1; y_2 - y_1; \omega)$  is in the form of a correlation function and being a function of  $\omega$  may be regarded as the spectrum of the correlation coefficient.

It can be shown that [89] the cross power spectral density of the displacement  $w$  is given by

$$S_{ww}(x_1, y_1; x_2, y_2; \omega) = \sum_{m=0}^{\infty} \sum_{n=0}^{\infty} \sum_{r=0}^{\infty} \sum_{s=0}^{\infty} W_{mn}(x_1, y_1) W_{rs}^*(x_2, y_2) H_{mn}(\omega) H_{rs}^*(\omega) I_{mnrs}(\omega) \quad (2.34)$$

where,

$$H_{mn}(\omega) = \frac{1}{\mu_{mn}[\omega_{mn}^{*2}(1 + i\eta_{mn}) - \omega^2]} \quad \text{is the complex}$$

frequency response function in the  $mn^{\text{th}}$  damped normal mode, the asterisk denotes the complex conjugate and

$$I_{mnrs}(\omega) = \int_{-a/2}^{b/2} \int_{-a/2}^{b/2} \int_{-a/2}^{b/2} \int_{-a/2}^{b/2} W_{mn}(x_1, y_1) W_{rs}^*(x_2, y_2) r_{xy}(x_1, y_1; x_2, y_2; \omega) dx_1 dy_1 dx_2 dy_2 \quad (2.35)$$

The auto power spectral density of the displacement corresponding to a point  $(x, y)$  in the panel is obtained from equation (2.35) by setting  $x_1 = x_2 = x$  and  $y_1 = y_2 = y$ . Expressions for  $I_{mnrs}(\omega)$  are also derived in Appendix B for different boundary conditions of the plate and for a uniform random pressure. ( $r_{xy}(x_1, y_1; x_2, y_2; \omega) = 1.0$ ).

## CHAPTER 3

### SOUND TRANSMISSION BY DAMPED SANDWICH PANELS OF INFINITE EXTENT

#### 3.1 INTRODUCTION

The interaction of an infinite homogeneous panel and an airborne sound wave incident on one side of the panel is a classical problem in acoustics. The phenomenon of coincidence, when the bending wavelength of the panel matches with the projected wavelength of the sound wave on to the panel, resulting in a high degree of coupling between the sound and structure is explained in the context of this problem. For grazing incidence, the frequency at which perfect matching of the free flexural wavelength and the sound wave length occurs is called the critical frequency and at this frequency for grazing incidence, the plate radiates sound of equal intensity as the incident sound in the transmission side of the panel. For other incident angles, the wave coincidence occurs at frequencies greater than the critical frequency depending on the incident angle.

In the present chapter, the sound transmission characteristics of a damped sandwich panel of infinite extent is investigated on classical lines. The sandwich panel consists

of two face plates of the same material and thickness, with a constrained viscoelastic damping layer in between. The expression for sound transmission loss in terms of the core parameters is derived, taking into account the incident, reflected and radiated waves from the panel. The condition for coincidence transmission is established in terms of core parameters and the incident angle of the exciting pressure, using the dispersion relation.

Parametric studies on transmission loss are carried out and the results are presented in the form of transmission loss curves. It is shown by the analysis that the core shear parameter has significant effect on the noise transmission characteristics of the sandwich panel, and the location of the coincidence frequencies. The core loss factor and the geometric parameter also influence the transmission characteristics of the sandwich panel. Results are compared with an equivalent homogeneous plate of face plate material having the same surface mass density as the sandwich. It is seen from the results that the sandwich panel has better sound transmission characteristics based on two counts. Firstly, the coincidence frequencies are shifted to higher frequency ranges for the case of the sandwich panel. Secondly, the coincidence transmission loss is considerably improved, due to the presence of the damping layer.

### 3.2 SOUND TRANSMISSION LOSS

Consider the sandwich panel of infinite extent, separating two semi-infinite air spaces as shown in Figure 3.1. Let a plane harmonic pressure wave be incident on the panel at an angle  $\theta$ .  $\theta$  is the angle between the normal to the plate and the normal to the wave fronts.

The incident pressure can be expressed as

$$p_i(x, z, t) = P_i \exp[ik(x \sin \theta - z \cos \theta)] e^{i\omega t} \quad (3.1)$$

where,  $k$  is the wave number of the incident wave and  $P_i$  is the amplitude of the incident pressure. In the analysis to follow, the harmonic term  $e^{i\omega t}$  is consistently dropped from all equations as a common term.

The resultant pressure on the incident side of the panel consists of the incident pressure  $p_i$ , the reflected pressure  $p_s$  and the radiated pressure denoted by  $p_r$ . The reflected pressure  $p_s$  corresponds to the scattered pressure from the panel when it is held rigid. The radiated pressure on the transmission side denoted by  $p_t$  is the transmitted pressure.

The reflected pressure  $p_s$  can be shown to be, [39]

$$p_s(x, z) = P_i \exp[ik(x \sin \theta + z \cos \theta)] \quad (3.2)$$

The difference between the expression for the reflected pressure and the incident pressure is only in the sign of

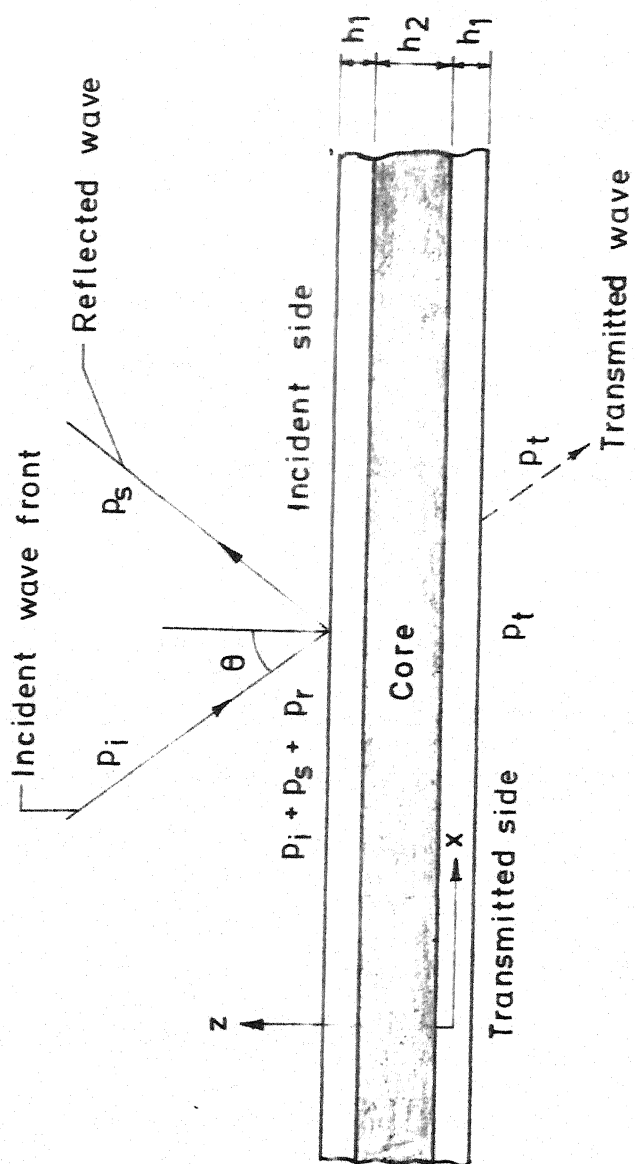


FIG.3.1 COMPONENTS OF PRESSURE FIELDS ON EITHER SIDE OF SANDWICH PANEL

the  $z$  coordinate which is reversed, implying thereby that the wave is specularly reflected.

As the external pressure excitation on the sandwich panel is independent of the  $y$  coordinate, the dynamic response of the plate must also be independent of  $y$ . This implies that the dynamic response consists of structure-borne waves propagating in the  $x$  direction, the wave fronts being parallel to the  $y$  axis.

The plate acceleration can be written as,

$$W(x) = \ddot{W} \exp (ikx \sin \theta) \quad (3.3)$$

The transmitted pressure  $p_t$  can be determined by solving the equation of motion to the resultant surface pressure loading on the panel. Since the radiated pressures on either side of the panel are dependent on the structural motion, which in turn depends on the resultant pressure loading, the problem of determining  $p_t$  represents a coupled structural-acoustic problem.

The radiated pressure  $p_r$  satisfies the two dimensional Helmholtz equation which for the acceleration distribution represented by equation (3.3) takes the form

$$\left( \frac{\partial^2}{\partial x^2} + \frac{\partial^2}{\partial z^2} + k^2 \right) p(x,z) = 0 \quad (3.4)$$

On the panel surface, the pressure satisfies the boundary condition

$$\frac{\partial p}{\partial z} = -\rho \ddot{w} \exp(ikx \sin \theta) \Big|_{z=0}$$

where  $\rho$  is the density of fluid medium (air). For waves propagating in the positive  $z$  direction, the pressure field satisfying the two dimensional Helmholtz equation and the boundary-condition at the surface is of the form,

$$p_r(x, z) = \frac{i \rho \ddot{w}}{k \cos \theta} \exp [ik(x \sin \theta + z \cos \theta)] \quad (3.6)$$

The above expression represents the radiated pressure on the incident side.

The transmitted pressure  $p_t$  associated with the elastic response of the plate is the pressure radiated by the plate into the half space  $z < 0$ . Since the two panel surfaces on the incident and transmitted sides have the same transverse motion, and the acoustic medium on either side of the plate being the same

$$|p_t| = |p_r| \quad (3.7)$$

On the plate surface, on the transmitted side, the transmitted pressure  $p_t$  takes the negative value of the radiated pressure on the plate surface on the incident side, since the plate acceleration  $w(x)$  producing a positive pressure on one plate surface generates a negative pressure on the

other surface. As the transmitted wave propagates in the negative  $z$  direction, it can be expressed as

$$\begin{aligned} p_t(x,z) &= |p_t| \exp [ik(x \sin \theta - z \cos \theta)] \\ &= -p_r(x,z) \exp (-i2kz \cos \theta) \end{aligned} \quad (3.7)$$

The resultant plate loading is now obtained as the sum of the incident, reflected and the radiated pressures on either side of the panel at the panel surface. The pressure loading on the plate surface is then,

$$p(x,0) = -p_i - p_s - p_r + p_t \Big|_{z=0} = -2p_i - 2p_r \quad (3.8)$$

The equation of motion for the sandwich panel considered in the analysis, is given by equation (2.9). For the  $y$  independent configuration it reduces to

$$\begin{aligned} \frac{\partial^6 w}{\partial x^6} - g'(1+Y) \frac{\partial^4 w}{\partial x^4} + \frac{\mu}{D_t} \left[ \frac{\partial^4 w}{\partial x^2 \partial t^2} - g' \frac{\partial^2 w}{\partial t^2} \right] \\ = \frac{1}{D_t} \left( \frac{\partial^2 p}{\partial x^2} - g' p \right) \end{aligned} \quad (3.9)$$

where the various terms representing the sandwich core parameters have been explained in the previous chapter. From equation (3.3), for harmonic motion, the displacement can be expressed as,

$$w(x) = - \frac{\ddot{W}}{\omega^2} \exp (ikx \sin \theta) \quad (3.10)$$

Substitution of equation (3.10) in equation (3.9), using equation (3.1) yields,

$$\begin{aligned}
 \ddot{W} & \left[ \frac{k^6 \sin^6 \theta}{\omega^2} + \frac{g'(1+Y)k^4 \sin^4 \theta}{\omega^2} - \frac{\mu}{D_t} k^2 \sin^2 \theta \right. \\
 & \left. - \frac{g'\mu}{D_t} + \frac{i\rho}{k \cos \theta D_t} (k^2 \sin^2 \theta + g') \right] \\
 & = - \frac{2P_i}{D_t} (k^2 \sin^2 \theta + g') \quad (3.11)
 \end{aligned}$$

Solving for  $\ddot{W}$ , we get,

$$\ddot{W} = - \frac{2 P_i \cos \theta}{\mu \left[ \frac{i\rho}{\mu k} + \left\{ \frac{D_t}{\mu} \frac{k^4 \sin^4 \theta}{\omega^2} \left( 1 + \frac{g'Y}{k^2 \sin^2 \theta + g'} \right) - 1 \right\} \cos \theta \right]} \quad (3.12)$$

Hence the radiated pressures on either side of the sandwich panel can be obtained from equations (3.6) and (3.7).

$$p_r(x,z) = \frac{2 P_i \exp [ik (x \sin \theta + z \cos \theta)]}{\frac{ik\mu}{\rho} \left\{ \frac{D_t}{\mu} \frac{k^4 \sin^4 \theta}{\omega^2} \left( 1 + \frac{g'Y}{k^2 \sin^2 \theta + g'} \right) - 1 \right\} \cos \theta - 2} \quad (3.13)$$

and

$$p_t(x,z) = - \frac{2 P_i \exp [ik (x \sin \theta - z \cos \theta)]}{\frac{ik\mu}{\rho} \left\{ \frac{D_t}{\mu} \frac{k^4 \sin^4 \theta}{\omega^2} \left( 1 + \frac{g'Y}{k^2 \sin^2 \theta + g'} \right) - 1 \right\} \cos \theta - 2} \quad (3.14)$$

From equations (3.14) and (3.1) the complex ratio of the incident and transmitted sound pressures for the sandwich panel can be written as,

$$\frac{p_i}{p_t} = 1 - \frac{ik\mu\cos\theta}{2\rho} \left[ \frac{D_t}{\mu} \frac{k^4 \sin^4\theta}{\omega^2} \left( 1 + \frac{g'Y}{k^2 \sin^2\theta + g'} \right) - 1 \right] \quad (3.15)$$

The above equation can be written in the form

$$\frac{p_i}{p_t} = 1 + \frac{Z_T \cos\theta}{2\rho c} \quad (3.16)$$

analogous to the case of a homogeneous panel, where  $Z_T$  can be considered as the specific transmission impedance of the damped sandwich panel. Unlike in the case of the homogeneous elastic panel, where the specific transmission impedance is always reactive, in the case of the sandwich panel with viscoelastic layer, the specific transmission impedance has both reactive and resistive parts.  $Z_T$  can be represented as

$$Z_T = R_T + i X_T \quad (3.17)$$

where  $R_T$  is the specific transmission resistance and  $X_T$  is the specific transmission reactance. The expressions for  $R_T$  and  $X_T$  can be expressed in terms of the sandwich core parameters and the properties of the elastic face plates and the incident angle

$$R_T = \frac{k^6 \sin^6\theta D_t \bar{g} \beta Y}{\omega (k^2 \sin^2\theta + \bar{g})^2 + g^2 \beta^2} \quad (3.18)$$

and

$$X_T = \omega \mu - \frac{D_t k^4 \sin^4 \theta}{\omega} \left[ 1 + \frac{\bar{g}'(k^2 \sin^2 \theta + \bar{g} + \bar{g} \beta^2)}{(k^2 \sin^2 \theta + \bar{g})^2 + \bar{g} \beta^2} \right] \quad (3.19)$$

where  $\bar{g}$  is the real part of  $g'$ .

Defining the sound transmission coefficient  $\tau$  of the sandwich panel as the ratio of the transmitted sound power to the incident sound power, one can express

$$\frac{1}{\tau} = \left( 1 + \frac{R_T}{2 \rho c} \cos \theta \right)^2 + \left( \frac{X_T}{2 \rho c} \cos \theta \right)^2 \quad (3.20)$$

and the sound transmission loss of the sandwich panel can be expressed as

$$TL = 10 \log \frac{1}{\tau} \quad (3.21)$$

It can be verified that equation (3.21) reduces to the transmission loss formula of single homogeneous panel, whose bending rigidity is twice the bending rigidity of either of the face plates as  $g'$  tends to zero, where the specific transmission impedance becomes wholly reactive. For an elastic core with  $\beta = 0$  also, the specific transmission impedance becomes reactive at all frequencies.

### 3.3 COINCIDENCE FREQUENCY AND COINCIDENCE NOISE TRANSMISSION

Unlike the case of the homogeneous elastic panel, for the damped sandwich panel, the coincidence frequency becomes

a complex number, as it depends on the core parameters. Because of the presence of the damping layer, propagation of free flexural waves in the sandwich panel is not possible. However, a damped wave motion decaying with respect to the spatial coordinate is possible. It can be thought of as a forced damped wave corresponding to the forced damped normal modes of finite sandwich panels discussed in Chapter 2. Hence, the structural wave number or the propagation constant becomes a complex number. Since coincidence is the condition of matching of the projected acoustic waves on to the panel and the structural wave forms, the coincidence frequency also becomes complex. The real part of the coincidence frequency represents the frequency of minimum transmission loss and the imaginary part indicates nonzero transmission loss at coincidence for the sandwich panel. The coincidence frequency can be derived for the sandwich panel by considering the dispersion relation between frequency and wave number.

Assuming a wave solution of the form

$$w = W \exp(ikx) \quad (3.22)$$

and substituting into the equation of motion (3.9) with the external loading terms zero, we get,

$$-k^6 - g'(1+Y) k^4 + \frac{\mu}{D_t} \omega^2 k^2 + \frac{\mu}{D_t} \omega^2 g' = 0 \quad (3.23)$$

In the foregoing equation, it should be noted that the wave number  $k$  is a complex quantity. Writing  $k = \omega / c_B$ , where  $c_B$  is the flexural wave speed in the panel, equation (3.23) represents a quadratic in  $\omega^2$ , the solution of which can be written as

$$\omega^2 = \frac{1}{2} \left[ \frac{c_B^4 \mu}{D_t} - c_B^2 g'(1+Y) \right] \pm \frac{1}{2} \sqrt{\left( \frac{c_B^4 \mu}{D_t} - c_B^2 g'(1+Y) \right)^2 + \frac{4g'\mu c_B^6}{D_t}} \quad (3.24)$$

Since the coincidence occurs when the trace acoustic velocity on the panel matches with the flexural wave speed, the coincidence condition is established by setting  $c_B = c / \sin \theta$  in equation (3.24) where  $c$  is the local acoustic velocity in the medium. Admitting only the positive real part for the complex root in equation (3.24), the coincidence frequency for different angles of incidence can be expressed as

$$\omega_c^2 = \frac{1}{2} \left[ \frac{c^4 \mu}{D_t \sin^4 \theta} - \frac{c^2}{\sin^2 \theta} g'(1+Y) \right] + \frac{1}{2} \sqrt{\left( \frac{c^4 \mu}{D_t \sin^4 \theta} - \frac{c^2}{\sin^2 \theta} g'(1+Y) \right)^2 + \frac{4g'\mu c^6}{D_t \sin^6 \theta}} \quad (3.25)$$

The real part of the above equation gives the coincidence frequency for the sandwich panel and the ratio of the imaginary part to the real part represents a measure of

the rate of decay of the damped wave in the structure, the modulus of which may be likened to the loss factor.

The same expression for the coincidence frequency equation (3.25) can also be obtained by requiring the amplitude of the transmitted pressure  $p_t$  to be equal to  $P_i$ .

The minimum value of coincidence frequency is obtained by letting  $\theta = \pi/2$  in equation (3.25), which is the critical frequency of the sandwich panel being the coincidence frequency for grazing incidence.

The phase velocity of bending waves of the sandwich plate is obtained from equation (3.23) as

$$c_B^2 = \frac{D}{\mu} \left[ \frac{k^2 + g'(1+Y)}{(g'/k^2 + 1)} \right] \quad (3.26)$$

which is the dispersion relation for the sandwich panel. The above relation reduces to the dispersion relation of a homogeneous panel having flexural rigidity equal to twice the flexural rigidity of either of the face plates as the shear parameter  $g'$  tends to zero, that is, with a very soft core. As the thickness of the core  $h_2$  becomes very small, ( $h_2 \rightarrow 0$ ) the flexural wave speed corresponds to the flexural wave speed of a homogeneous panel having twice the thickness of the face plate. For practical values of the shear parameter and geometric parameter and relatively

higher frequencies, equation (3.26) can be approximated by

$$c_B^2 \approx \frac{D_t}{\mu} k^2 \quad (3.27)$$

which is very similar in form as the flexural wave speed of homogeneous panels.

### 3.4 RESULTS AND DISCUSSION

The transmission loss for the infinite sandwich panel has been obtained from equation (3.21), for different values of the core parameters, viz, the core loss factor, the shear parameter and the geometric parameter. The face plate considered in the analysis is aluminium having Young's modulus  $E = 7.24 \times 10^{10} \text{ N/m}^2$  and density  $\rho_p = 2770 \text{ kgm/m}^3$ . The viscoelastic core considered corresponds to typical PVC materials, the variations in whose properties have been taken care of by the parametric study of the core shear parameter  $\bar{g}$  and the loss factor  $\beta$ . The storage shear modulus of the core and its loss factor have been assumed to be frequency independent. The face plate is assumed to be elastic and nondissipative.

The local acoustic velocity in air is taken as  $c = 330 \text{ m/sec.}$  and the density of air is taken as  $\rho = 1.225 \text{ kgm/m}^3$ .

The thickness of the face plate considered for parametric study is  $h_1 = 1$  mm. Variations in the sound transmission loss with changes in thickness of the face plate have also been studied. For a thin panel, such as considered in the analysis, equation (3.9) quite accurately predicts the behaviour of the sandwich panel as the flexural wavelengths are many times larger than the thickness of the face plates (about 30 to 40 times) in the frequency range of interest considered [16,21]. It obviates the necessity of including the effects of shear deflection and rotary inertia. Even for flexural wavelengths which are about twenty times the thickness of the face plate, the approximations implied in equation (3.9) by neglect of the shear deflection and rotary inertia effects will not significantly impair the accuracy of the results. The range of frequencies for which the equation of motion will be valid without much error can be determined from equation (3.26) for the face plate thickness adopted. For example,  $h_1 = 1$  mm the range of frequency, for a core of the same thickness as the face plate and  $\bar{g} = 100$  turns out to be 10440 Hz, for bending wavelengths thirty times the thickness of the face plate. The valid range of frequency will increase with increasing values of the core shear parameter  $\bar{g}$  as is evident from equation (3.26).

The density of the core material  $\rho_c$  is taken to be one-fifths of the density of the face plate material

(  $\rho_c = 554 \text{ kgm/m}^2$  ). in all calculations.

The coincidence frequencies and the loss factors calculated from equation (3.25) are shown in Table 3.1 for various incidence angles and the core shear parameters  $\bar{g}$ . From the table it is observed that the coincidence frequency decreases with increasing values of the core shear parameter  $\bar{g}$  for all angles of incidence. It is also seen that the coincidence frequencies decrease with increasing angles of incidence as it should be from equation (3.25), having minimum values for grazing incidence. In the practical ranges of frequency coincidence conditions exist only for incidence angles greater than about  $45^\circ$ .

This observation is also true for homogeneous elastic panels where the upper limit for the coincidence frequency is given by the condition for Rayleigh waves [90], which places a lower limit on the incidence angle  $\theta$  for which coincidence can occur. It is also seen from the table that the loss factor initially increases with increase in the core shear parameter  $\bar{g}$ , upto a certain value of  $\bar{g}$  and then decreases for further increase in  $\bar{g}$ . This is especially seen for incidence angles greater than  $45^\circ$ . Thus the value of  $\bar{g}$  at which the maximum loss factor is obtained also depends on the incidence angle  $\theta$ . The existence of an optimum value of the core shear parameter  $\bar{g}$

Table 3.1 - Coincidence Frequencies and Loss Factors for different values of  $g$ 
$$h_L = 0.001 \text{ m}, Y = 31.5 \text{ (} h_2 = 2.24 h_L \text{)}, \beta = 0.3$$

$\theta^\circ$	$f_c \times 10^{-5}$	$\eta_c \times 10^3$	$f_c \times 10^{-5}$	$\eta_c \times 10^3$	$f_c \times 10^{-5}$	$\eta_c \times 10^3$	$f_c \times 10^{-5}$	$\eta_c \times 10^3$
g	10	100	1000	10000				
15	1.8500	0.114	1.8467	1.141	1.8149	11.78	1.4703	173.00
30	0.4954	0.428	0.4922	4.298	0.4597	48.81	0.1291	393.20
45	0.2475	0.850	0.2444	8.713	0.2107	114.40	0.0517	126.70
60	0.1650	1.277	0.1617	13.250	0.1268	205.90	0.0324	75.02
75	0.1324	1.591	0.1292	16.650	0.0935	297.90	0.0254	57.75
90	0.1235	1.706	0.1203	17.910	0.0842	338.90	0.0236	53.25

$f_c$  - coincidence frequency Hz;  $\eta_c$  - loss factor corresponding to coincidence frequency.

for maximum damping effectiveness as revealed by the table is characteristic of the damping behaviour of sandwich beams and plates with constrained damping layer treatment [8,24,91].

Table 3.2 gives the coincidence frequencies and loss factors for different values of the core loss factor  $\beta$  and for typical values of the core shear and geometric parameters. It is observed that the loss factor varies linearly with respect to the core loss factor  $\beta$ , for the particular value of  $\bar{g}$  considered. There is practically no change in the coincidence frequency with  $\beta$ . But marginal changes in the coincidence frequencies with  $\beta$  can be observed for greater values of  $\bar{g}$  as will be discussed later in connection with transmission loss curves.

Table 3.3 gives the coincidence frequencies for different values of the core geometric parameter  $Y$ , for the particular value of the shear parameter  $g' = 30.97(1+0.3i)$ . The coincidence frequencies increase with increase in  $Y$  for all values of  $\theta$ . However, the loss factor does not increase monotonically with  $Y$ . Moreover, it is observed that the variation of the loss factor with  $\theta$ , for all values of  $Y$  considered is similar, in that the ratio of the loss factors for any two angles of incidence is very nearly a constant for all values of  $Y$ .

Table 3.2 - Coincidence Frequencies and Loss Factors for different values of  $\beta$

$h_1 = 0.001$  m,  $Y = 31.5$  ( $h_2 = 2.24$  h<sub>1</sub>),  $\bar{g} = \cancel{14.9} 30.97$

$\beta$	0.0					0.3					1.0				
$\theta_0$	$f_c \times 10^{-5}$	$\eta_c \times 10^3$	$f_c \times 10^3$	$f_c \times 10^{-5}$	$\eta_c \times 10^3$	$f_c \times 10^3$	$f_c \times 10^{-5}$	$\eta_c \times 10^3$	$f_c \times 10^3$	$f_c \times 10^{-5}$	$\eta_c \times 10^3$	$f_c \times 10^3$	$f_c \times 10^{-5}$	$\eta_c \times 10^3$	$\eta_c \times 10^3$
15	1.8491	0.0	1.8491	0.3524	1.8491	1.8491	1.8491	1.175							
30	0.4946	0.0	0.4946	1.3190	0.4946	0.4946	0.4946	4.397							
45	0.2468	0.0	0.2468	2.6490	0.2468	0.2468	0.2468	8.830							
60	0.1641	0.0	0.1641	3.9900	0.1641	0.1641	0.1641	13.300							
75	0.1317	0.0	0.1317	4.9790	0.1317	0.1317	0.1317	10.600							
90	0.1228	0.0	0.1228	5.3420	0.1228	0.1228	0.1228	17.810							
$f_c$ - coincidence frequency	· Hz, $\eta_c$ - loss factor corresponding to coincidence frequency														

Table 3.3 - Coincidence Frequencies and Loss Factors for Different values of Y

$$h_1 = 0.001, \bar{g} = \frac{119}{30.97}, \beta = 0.3$$

Y	6.75		12		75	
$\theta^\circ$	$f_o \times 10^{-5}$	$\eta_o \times 10^3$	$f_o \times 10^{-5}$	$\eta_o \times 10^3$	$f_o \times 10^{-5}$	$\eta_o \times 10^3$
15	1.7100	0.394	1.7530	0.3346	1.9774	0.4110
30	0.4580	1.476	0.4690	1.2520	0.5288	1.5390
45	0.2284	2.961	0.2340	2.5130	0.2637	3.0940
60	0.1519	4.457	0.1556	3.7820	0.1753	4.6650
75	0.1219	5.559	0.1249	4.7170	0.1407	5.8240
90	0.1136	5.963	0.1165	5.0610	0.1311	6.2510

$f_o$  - coincidence frequency Hz,  $\eta_o$  - loss factor corresponding to coincidence frequency

Figure 3.2 presents the variation of transmission loss with frequency for different values of the shear parameter and an incidence angle of  $\theta = 75^\circ$ . The other parameters which are kept constant are shown in the figure. For all values of  $\bar{g}$  the transmission loss curves have dips at the corresponding coincidence frequencies. As had been already observed from Table 3.1, the coincidence frequencies decrease with increasing  $\bar{g}$  which is also seen from the coincidence dips. For low values of  $\bar{g}$  the transmission loss curves follow the mass law almost uptill the coincidence frequency and have sharp dips at the coincidence frequency. For high values of  $\bar{g}$  too, the transmission loss curves follow the mass law at low frequencies, but start deviating from the mass law much earlier than the coincidence frequency. The sound transmission <sup>loss</sup> is significantly higher at intermediate frequency ranges (1000 - 4000 Hz) for the values of  $\bar{g} = 10$  and 100 as compared to those for  $\bar{g} = 5000$  and 10000. It is mainly due to the fact that the coincidence frequencies for the low values of  $\bar{g}$  are much higher than for the larger values of  $\bar{g}$  and the transmission loss curves for the latter tend to droop early, while for the former they continue to follow the mass law. But beyond the coincidence frequencies, the transmission loss increases rapidly with increase in frequency for the large values of the shear parameter  $\bar{g}$ , while for the smaller values of  $\bar{g}$  the

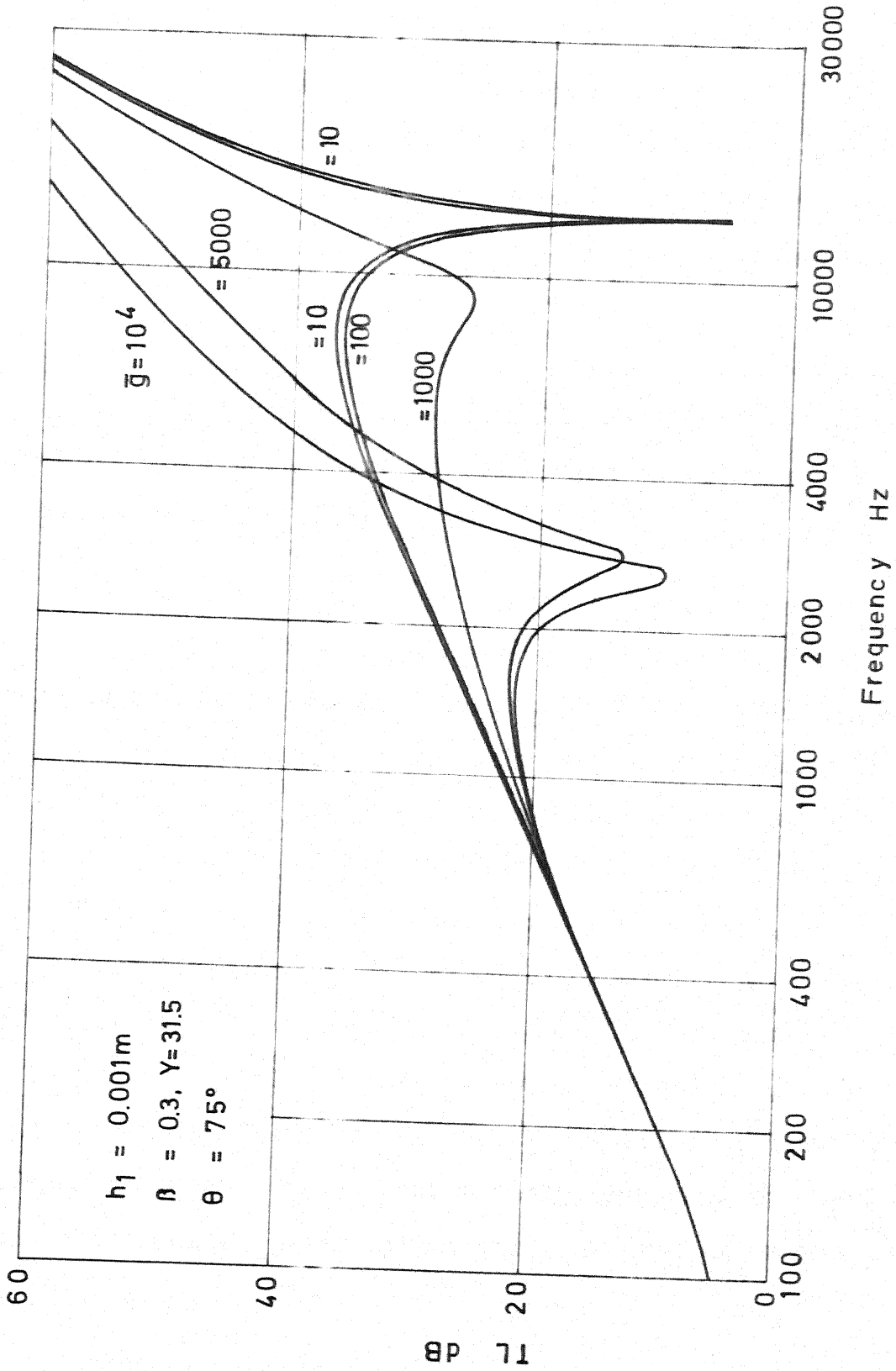


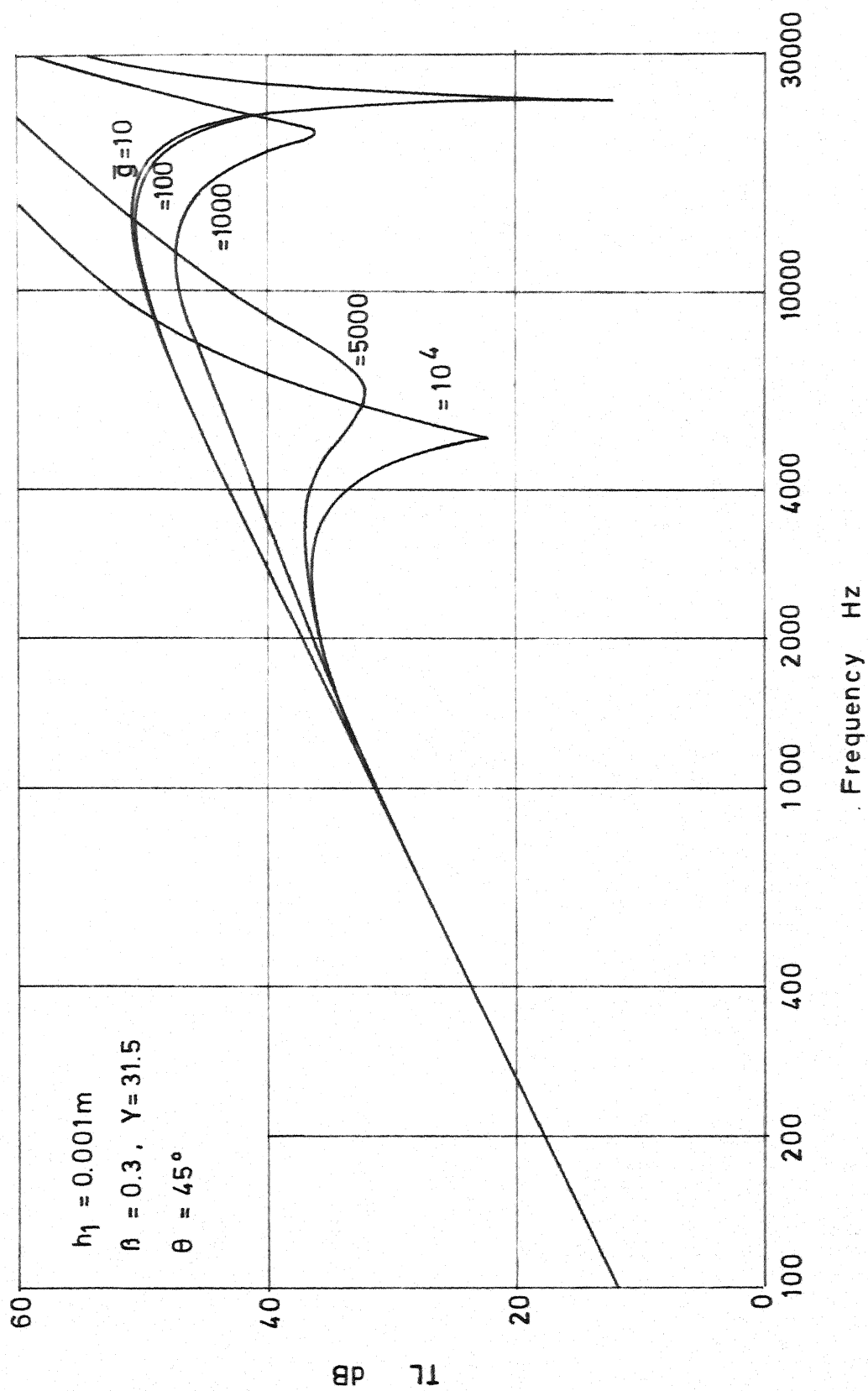
FIG. 3.2 VARIATION OF TL WITH SHEAR PARAMETER  $\bar{g}$

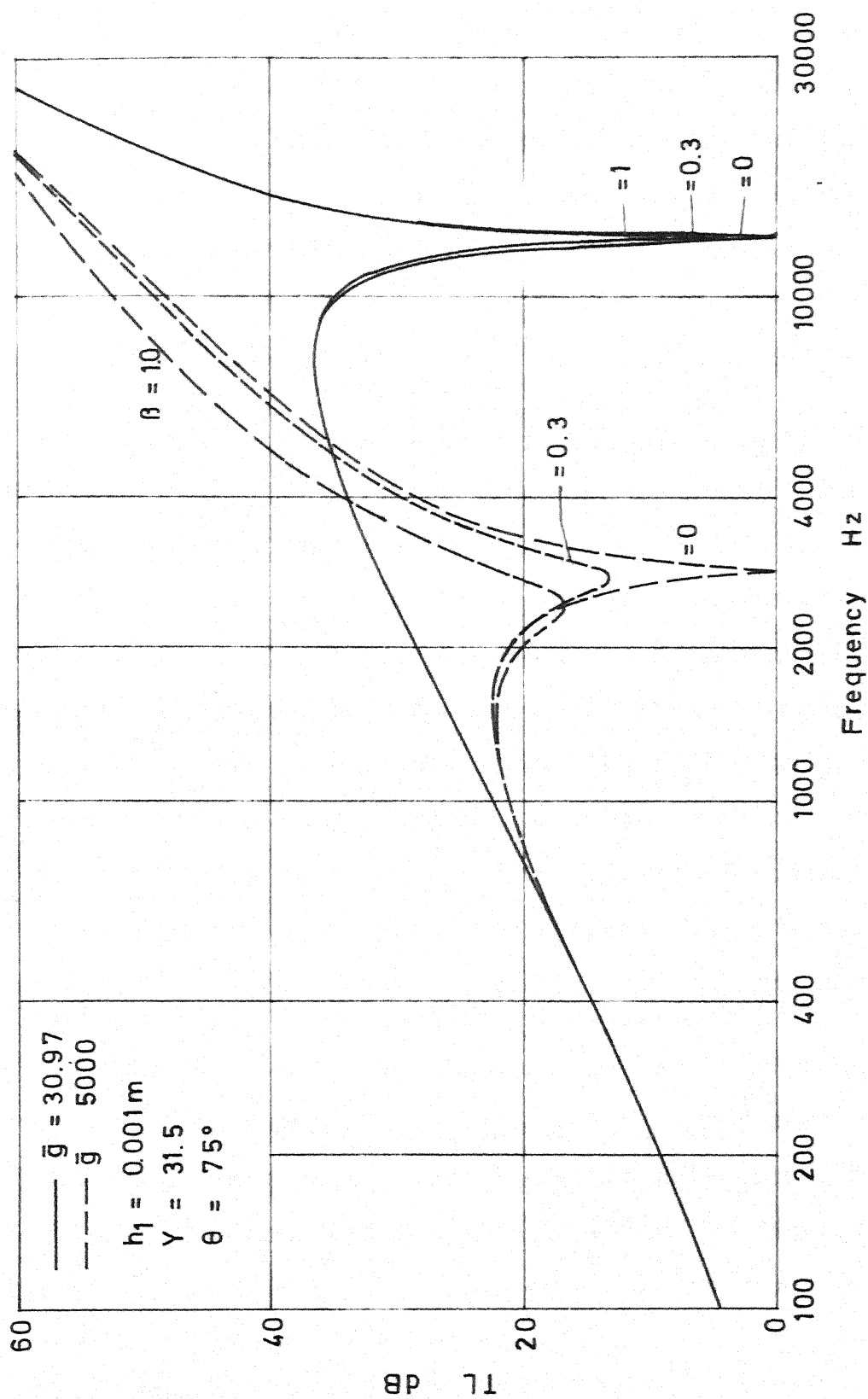
transmission loss decreases from the mass law as the corresponding coincidence frequencies are approached. Hence at these frequencies the transmission loss is very much greater for large values of  $\bar{g}$ , especially as the coincidence dips for small  $\bar{g}$ s are sharp and deep resulting in a very low transmission loss at coincidence. The low values of coincidence transmission loss for low values of the shear parameter can be attributed to the small values of the loss factors at coincidence corresponding to these shear parameters.

It is also seen from the graphs presented that the coincidence transmission loss can be considerably improved (about 20 dB) by an optimal choice of the core shear parameter  $\bar{g}$ . For example, for the case of  $\bar{g} = 1000$ , the transmission loss is the highest at coincidence, which is due to the fact that the coincidence loss factor for  $\bar{g} = 1000$  is the highest for the angle of incidence  $\theta = 75^\circ$ , as can be seen from Table 3.1. The transmission loss curve for this value of  $\bar{g}$  is very nearly flat and the coincidence dip is barely visible. Curves shown in Figure 3.2, thus clearly indicate that the transmission characteristics of the sandwich panel can be considerably improved, by a suitable choice of the shear parameter  $\bar{g}$ , depending on the frequency ranges of interest.

Figure 3.3 shows the transmission loss curves for various values of  $\bar{g}$  for an incidence angle of  $\theta = 45^\circ$ . The same observations are made as for  $\theta = 75^\circ$ , except that the transmission loss values are higher and the coincidence frequencies are also higher. Another observation that can be made from the figure is that the optimum value of the shear parameter  $\bar{g}$  for maximum transmission loss at coincidence for  $\theta = 45^\circ$  need not be the same as for  $\theta = 75^\circ$ .

Figure 3.4 shows the behaviour of the transmission loss curves with the core loss factor  $\beta$ , for two different values of the core shear parameter  $\bar{g}$ . ( $\bar{g} = 30.97$  and  $\bar{g} = 5000$ ). It is seen that for the low value of  $\bar{g}$ , the effect of  $\beta$  on the transmission loss is minimal except at the coincidence frequency, where with increasing  $\beta$ , increasing transmission loss is obtained. But the coincidence dips are steep. The effect of  $\beta$  on the transmission loss is more discernible in the case  $\bar{g} = 5000$ . Significant increase in the coincidence transmission loss (13 to 17 dB) of the sandwich panel is obtained with increase in  $\beta$ . It is because, the effect of increase in  $\beta$  is compounded by the effect of increase in the core shear parameter resulting in high loss factors at coincidence as can be seen from Table 3.1. The coincidence dips are also spread out and flattened for the same reason. Another observation that is made from

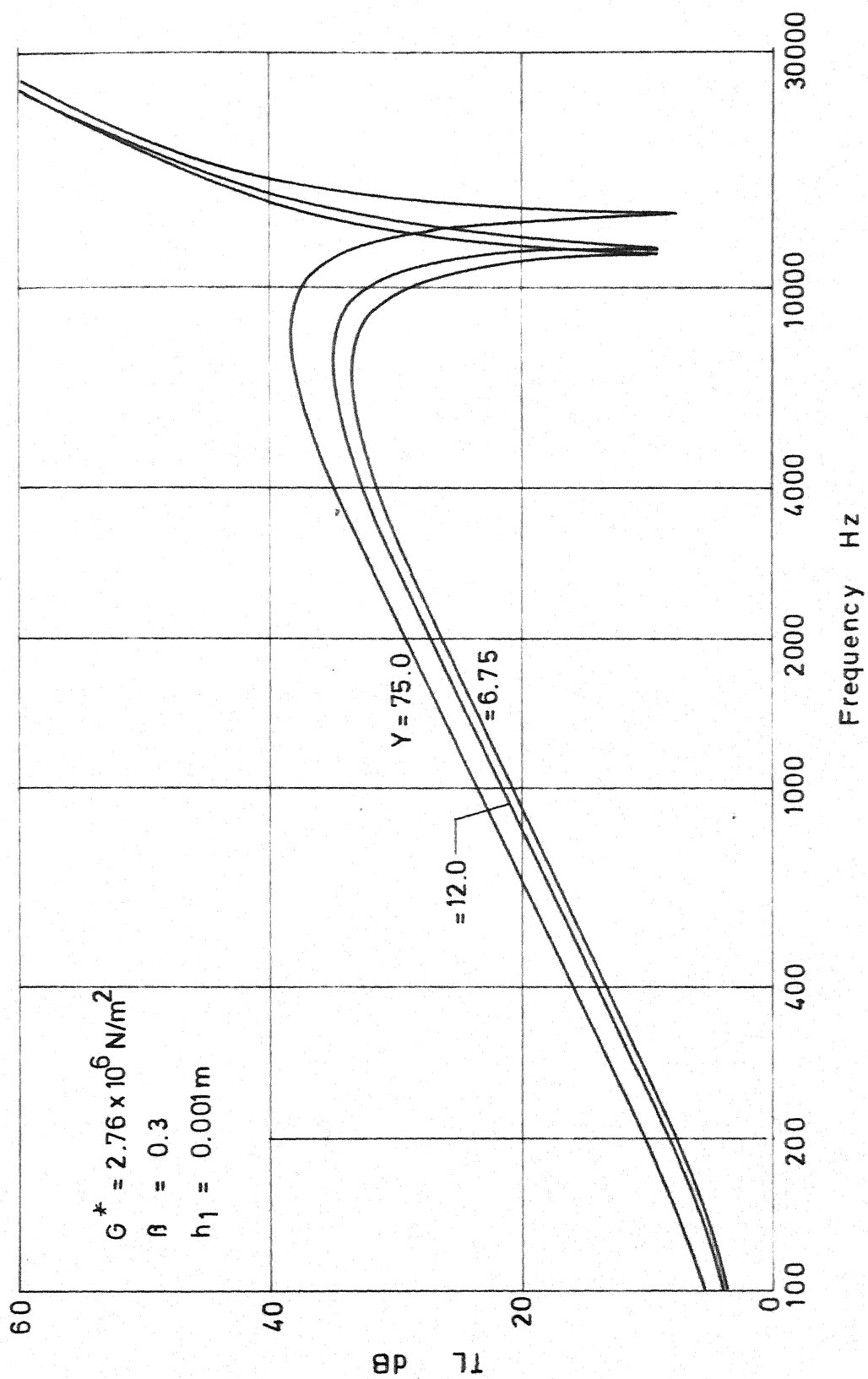

 FIG. 3.3 VARIATION OF TL WITH SHEAR PARAMETER  $\bar{g}$

FIG. 3.4 VARIATION OF TL WITH CORE LOSS FACTOR  $\beta$

the graphs is that, while increase in  $\beta$  has virtually no effect on the location of the coincidence frequencies for  $\bar{g} = 30.97$ , the coincidence frequencies are shifted to the left with increase in  $\beta$  for  $\bar{g} = 5000$ . Beyond the coincidence frequency also, higher values of  $\beta$  have a beneficial effect on the transmission characteristics of the sandwich panel for the higher value of  $\bar{g}$ . This is not so for  $\bar{g} = 30.97$ .

The transmission loss curves for different values of the geometric parameter is shown in Figure 3.5 for a constant value of the shear modulus of the core ( $G^* = 2.76 \times 10^6$  N/m<sup>2</sup>,  $\beta = 0.3$ ). The geometric parameters correspond to core thicknesses of one half, equal and four times the thickness of the face plate respectively. As can be seen from the graphs, till coincidence, increase in core thickness results in increasing transmission loss. As have been already observed from Table 3.3 the effect of increase in the geometric parameter is to increase the coincidence frequency which can also be observed from the graphs.

Figure 3.6 shows the variation of the transmission loss with incidence angle. As is obvious from equation (3.20), the transmission loss decreases with increasing angles of incidence and it is depicted in the figure. The coincidence frequency also decreases with increasing angles of incidence which is also seen from the coincidence dips.

FIG. 3.5 VARIATION OF TL WITH GEOMETRIC PARAMETER  $Y$

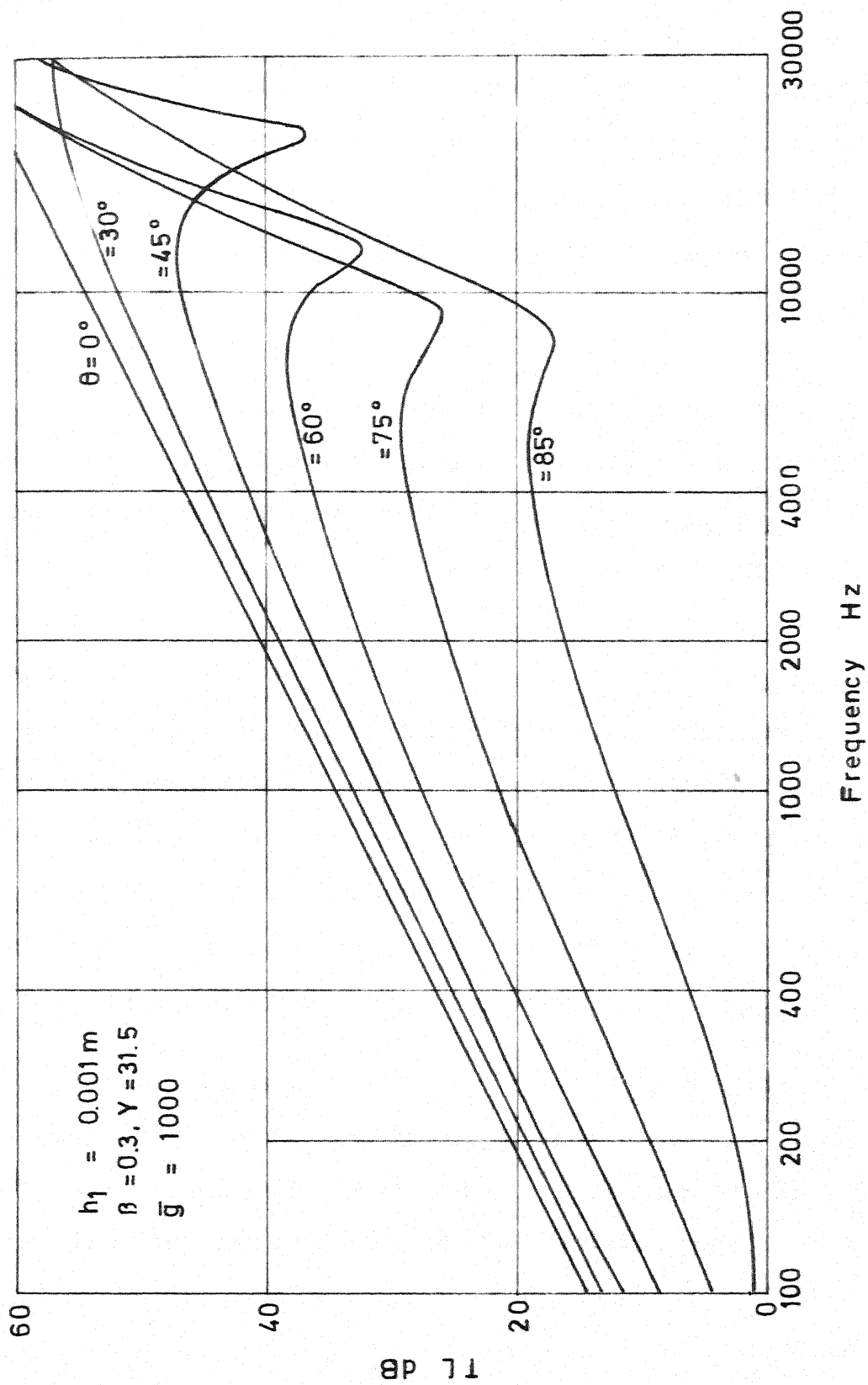
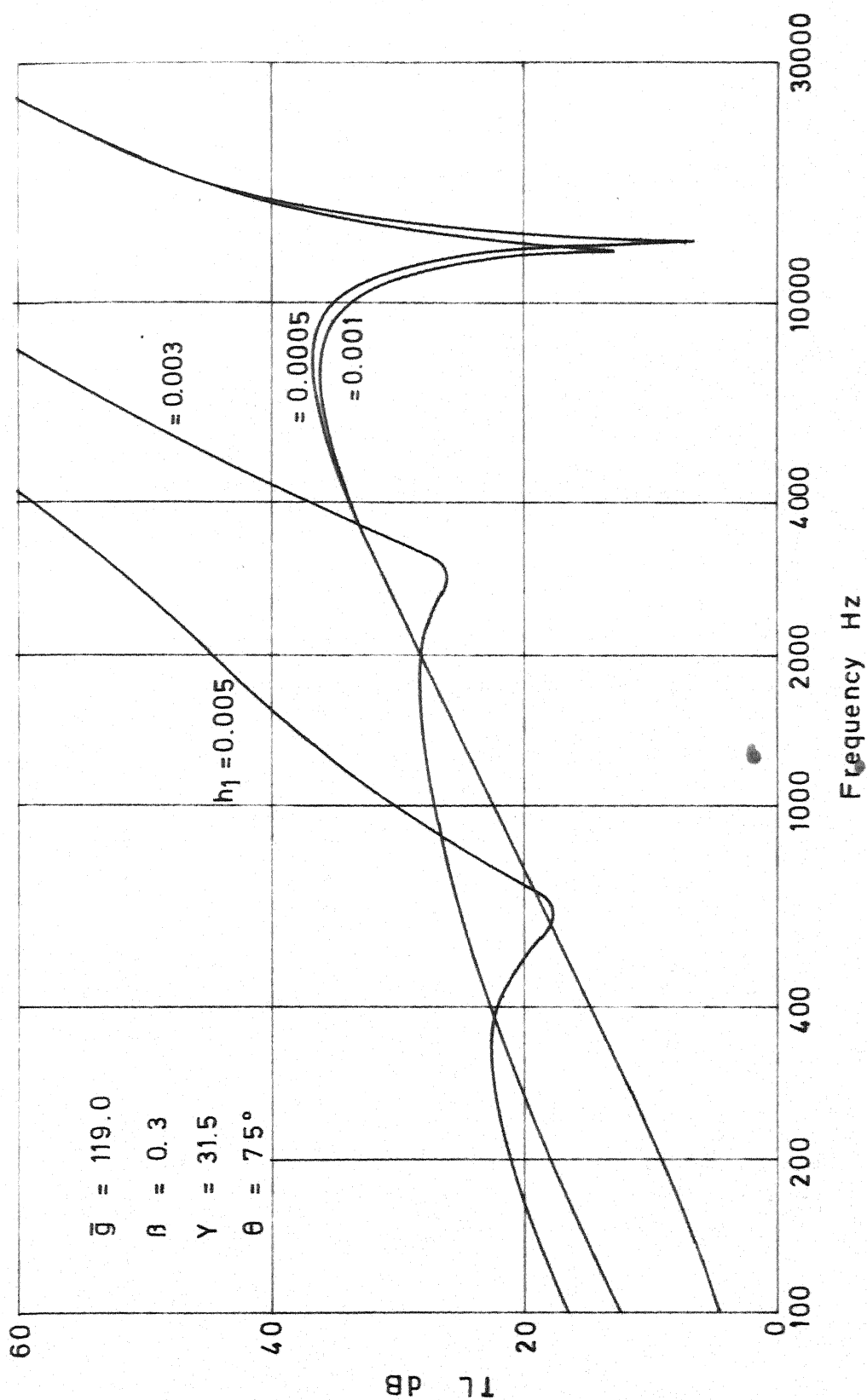


FIG.3.6 VARIATION OF TL WITH INCIDENCE ANGLE  $\theta$

In Figure 3.7, the effect of increasing the face plate thickness is shown. Simultaneously the core thickness is also increased in the same proportion, meaning thereby that the geometric parameter  $Y$  is kept constant. The shear parameter is also kept constant in these curves. With increasing thickness of the face plate the coincidence frequency is decreased. This is clear from equation (3.25). The coincidence frequency is proportional to the square root of the ratio of the surface mass density to the total bending rigidity of the sandwich panel. While  $D_t$  increases as the cube of the face plate thickness the surface mass density  $\mu$  varies only linearly with face plate thickness. Hence the decrease in coincidence frequency with increasing  $h_1$ . The transmission loss increases with increase in  $h_1$ , for in the mass law region the mass of the sandwich panel is considerably increased. The coincidence transmission loss is also higher for greater thickness of the face plate. This may be due to increased loss factors at coincidence with increase in face plate thickness.

Figure 3.8 compares the transmission loss of an equivalent homogeneous plate having the same surface mass density of the sandwich panel and of the face plate material with the transmission loss of the sandwich panel for two typical values of the core shear parameter  $\bar{g}$  and at an incidence angle of  $75^\circ$ . It is evident from the graphs


 FIG. 3.7 VARIATION OF TL WITH FACE PLATE THICKNESS  $h_1$

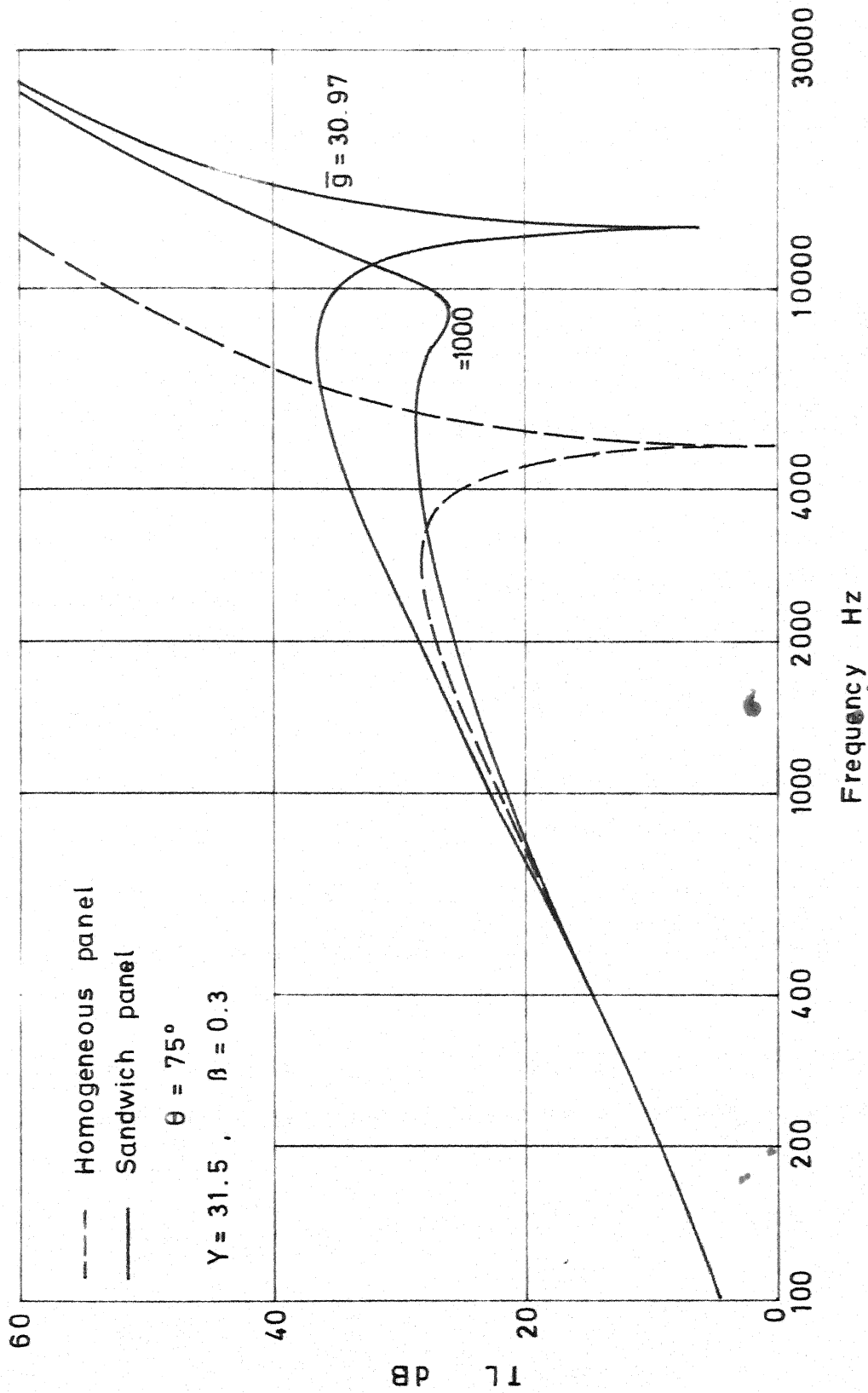


FIG. 3.8 COMPARISON OF TL OF SANDWICH PANEL WITH HOMOGENEOUS PANEL

that the sandwich helps in shifting the coincidence frequencies towards higher frequencies. Also, because of the damping layer the transmission loss at coincidence is increased to significant levels.

### 3.5 CONCLUSIONS

The problem of the sound transmission loss through an infinite sandwich panel with a constrained damping layer treatment is formulated in this chapter. Expressions for the sound transmission loss and the coincidence frequency are derived in terms of the sandwich core parameters and the incidence angle. From a parametric study of the transmission loss of the sandwich panel by the following conclusions can be drawn.

- i) The transmission loss is more sensitive to the variation of the core shear parameter  $\bar{g}$  than any other parameter.
- ii) High coincidence transmission loss is obtained by a suitable choice of  $\bar{g}$  and a high value of the core loss factor  $\beta$ .
- iii) The transmission loss of the sandwich panel increases with the thickness of the core below the coincidence frequency.
- iv) The coincidence frequency reduces significantly with increase in  $\bar{g}$ , while it increases with increase

in the geometric parameter  $Y$ .

- v) The sandwich panel has improved sound transmission characteristics as compared to a homogeneous panel of equivalent surface mass density.

## CHAPTER 4

# NOISE TRANSMISSION AND STRUCTURAL RESPONSE OF DAMPED FINITE SANDWICH PANELS BACKED BY RECTANGULAR CAVITY

### 4.1 INTRODUCTION

Several works have been presented in the past concerning the behaviour of cavity backed finite panels subjected to external airborne excitation. The evaluations of Pretlove [49], Dowell [50], Bhattacharya and Crocker [52], Guy and Bhattacharya [53], and Guy [56] have led to a progressively greater level of understanding of the phenomenon and improved accuracy of prediction. Dowell, et al [55] in a recent paper had considered the interaction between the internal sound pressure field and the elastic flexible wall of an enclosure in an 'acoustoelasticity' formulation. They adopted a series expansion in terms of the structural normal modes and the cavity acoustic modes and reduced the problem of determining the structural response and the sound pressure inside the enclosure to a matrix eigenvalue problem with gyroscoping coupling. All the works mentioned above dealt with elastic homogeneous panels and assumed simply supported panel edge conditions. Moreover, the analysis was mainly restricted to external harmonic excitation. These investigations led to interesting findings with respect to resonance location of the plate-cavity system and detailing the

mechanism of energy transfer. The problem was also investigated by use of statistical energy analysis by Lyon [57] and Eichler [58] in the high frequency ranges.

Recently, Vaicaitis [2] considered the noise transmission through a sandwich plate with a constrained viscoelastic damping layer treatment into a closed rectangular cavity, for a stationary random external excitation. He used a normal mode analysis, and showed that significant noise reduction can be achieved in the frequency range of 0 - 1000 Hz, by the additive damping treatment. In his analysis also the edges of the plate were assumed to be simply supported. Another assumption made in his analysis was that the plate motion was unaffected by the cavity pressure and could be determined by the in-vacuo flexural response of the plate. But the effect of the plate motion on the cavity pressure was taken into consideration. Thus only a partial coupling between the structure and the acoustic field was considered in his analysis.

This chapter concerns with the problem of noise transmission and structural response of elastically supported sandwich panels with constrained damping layer treatment backed by a cavity. Both harmonic and stationary external random pressure excitations are considered. Initially, an analysis based on Vaicaitis [2] is presented, where only a partial coupling of the structural motion and internal

cavity pressure is taken into account. Later, a more general analysis, allowing a full interaction between the internal sound field and the structural motion is made in an acoustoelastic formulation.

The y-wise edges at  $x = \pm a/2$  (Figure 4.1) are assumed to be elastically supported and the x-wise edges are assumed to be simply supported. These boundary conditions represent realistic boundary conditions that would obtain in aircraft skin-stringer constructions. The justification for the above assumption have been explained earlier in Chapter 2.

Interior cabin noise in propeller driven aircrafts, has maximum intensities in the low frequency range (0 - 1000 Hz) corresponding to the blade passing frequencies. In this analysis the noise transmission studies are restricted to this frequency range.

The response and noise transmission calculations in both the formulations use the forced damped normal mode analysis in view of the arbitrary boundary conditions at the panel edges and arbitrary damping.

In the acoustoelastic formulation the problem can be reduced to a matrix eigenvalue problem with gyroscopic coupling. Determining the eigenvalues and the eigenvectors for the combined natural frequencies of the cavity-panel

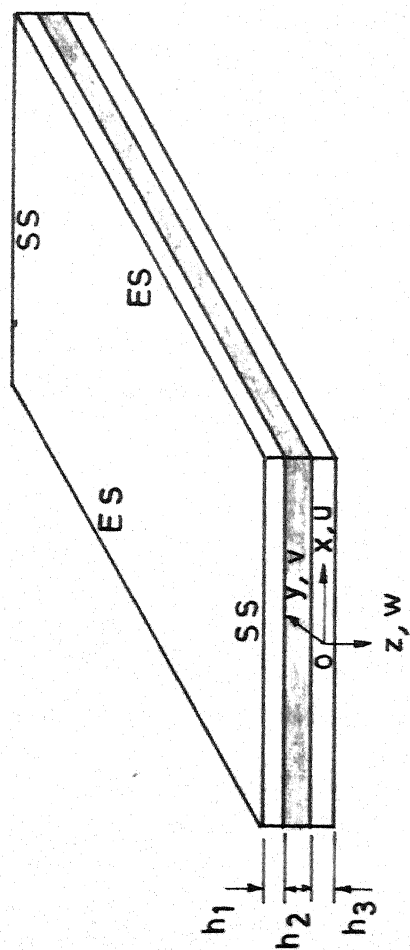
system involves cumbersome complex arithmetic due to the presence of the damping layer, whose shear modulus is represented by a complex number. However, since the concern here is mainly with response and noise transmission characteristics, the eigenvalue problem is not solved directly. The response and noise transmission are obtained by a direct matrix inversion scheme, taking advantage of the diagonal nature of certain matrices in a partition matrix analysis.

Parametric studies are made with respect to the sandwich core parameters and computer investigations show that the damping layer improves the noise reduction corresponding to structural resonances, especially near the first fundamental natural frequency of the panel. The damping layer significantly reduces the structural response levels near the structural resonant frequencies.

#### 4.2 FORMULATION OF THE NOISE TRANSMISSION PROBLEM NEGLECTING THE EFFECT OF CAVITY ON STRUCTURAL MOTION

##### 4.2.1 Acoustic Solution

Consider the rectangular enclosure shown in Figure 4.2. The wall at  $z = 0$  is flexible being the damped sandwich panel of concern. The other walls of the enclosure are assumed to be acoustically rigid.



ES - Elastically supported  
 SS - Simply supported

FIG. 4.1 SANDWICH PLATE WITH  
 BOUNDARY CONDITIONS

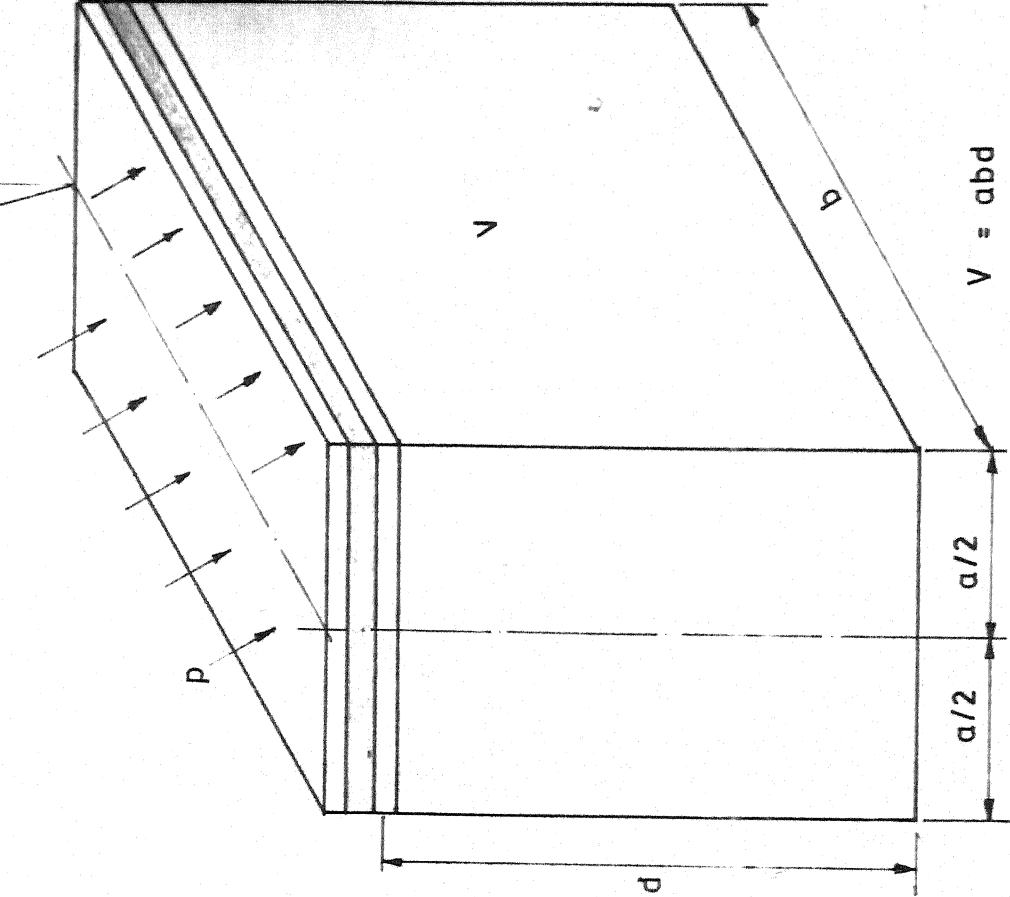


FIG. 4.2 RECTANGULAR CAVITY - SANDWICH PANEL

The acoustic pressure  $p_c$  inside the cavity is governed by the wave equation

$$\nabla^2 p_c = \frac{1}{c^2} \frac{\partial^2 p_c}{\partial t^2} = 0 \quad (4.1)$$

$$\text{with} \quad \frac{\partial p_c}{\partial n} = -\rho \frac{\partial^2 w}{\partial t^2} \quad \text{on } A_F \quad (4.2)$$

$$= 0 \quad \text{on } A_R$$

where,  $\nabla^2 = \frac{\partial^2}{\partial x^2} + \frac{\partial^2}{\partial y^2} + \frac{\partial^2}{\partial z^2}$ ,  $\rho$  and  $c$  are the fluid density and the local acoustic velocity in the medium respectively.  $w$  is the displacement of the flexible wall in the normal direction  $n$  ( $z$  direction).  $A_F$  and  $A_R$  indicate the flexible and rigid portions of the enclosure respectively and  $t$  represents time.

It is assumed in this particular analysis, that the cavity pressure does not affect the wall motion and the radiation loading on the plate surface, external to the cavity is negligible.

The solution of equation (4.1) can be written as

$$p_c(x,y,z,t) = \sum_{i=0}^{\infty} \sum_{j=0}^{\infty} C_{ij}(z,t) f_{ij}(x,y) \quad (4.3)$$

where,  $f_{ij}$  are the cavity modes with rigid walls at

$x = \pm a/2$  and  $y = 0, b$  (Figure 4.2) given by  $f_{ij} = \cos \frac{i\pi}{a}(x + \frac{a}{2}) \cos \frac{j\pi y}{b}$ .

The boundary conditions for the pressure coefficients  $C_{ij}$  in equation (4.3) are non-homogeneous. The solution for  $C_{ij}$  can be effected by transformation of the homogeneous differential equation with non-homogeneous boundary conditions into a non-homogeneous differential equation with homogeneous boundary conditions [92].

Then one can express,

$$C_{ij} = \alpha_{ij} + Z_{ij}(z, t) \quad (4.4)$$

where,  $\alpha_{ij}$  is the solution of the associated homogeneous problem and  $Z_{ij}$  is chosen to satisfy the given boundary conditions.

Substitution of equation (4.4) into equation (4.3) and (4.1) gives

$$\frac{\partial^2 \alpha_{ij}}{\partial z^2} - \frac{1}{c^2} \ddot{\alpha}_{ij} - A_{ij} \alpha_{ij} = \frac{1}{c^2} \ddot{Z}_{ij} - \frac{\partial^2 Z_{ij}}{\partial z^2} + A_{ij} Z_{ij} \quad (4.5)$$

where the number of dots represents the order of differentiation with respect to  $t$  and  $A_{ij} = \pi^2(i^2/a^2 + j^2/b^2)$ .

Since  $Z_{ij}$  is the solution satisfying the boundary conditions,

$$\left. \frac{\partial Z_{ij}}{\partial z} \right|_{z=0} = G_{ij}(t) \quad (4.6)$$

$$\text{where, } \sum_{i=0}^{\infty} \sum_{j=0}^{\infty} G_{ij}(t) f_{ij}(x,y) = -\rho w(x,y,0,t)$$

Using the orthogonality property of the cavity modes  $f_{ij}(x,y)$ , it can be shown that

$$G_{ij}(t) = - \frac{e_{ij}}{ab} \int_{-a/2}^{a/2} \int_0^b \rho \ddot{w} f_{ij}(x,y) dx dy \quad (4.7)$$

where,

$$e_{ij} = \begin{cases} 1 & \text{for } i = 0 \text{ and } j = 0 \\ 2 & i \neq 0 \text{ or } j \neq 0 \\ 4 & i \neq 0 \text{ and } j \neq 0 \end{cases}$$

$Z_{ij}$  can now be chosen as,

$$Z_{ij} = (z - z^2/2d) G_{ij} \quad (4.8)$$

where,  $d$  is the cavity depth. It can be seen that the form of equation (4.8) satisfies the boundary conditions of equation (4.6).

From equation (4.5), the solution for  $\alpha_{ij}(z,t)$  can be obtained as,

$$\alpha_{ij}(z,t) = \sum_{k=0}^{\infty} B_{ijk}(t) \cos \frac{k\pi z}{d} \quad (4.9)$$

where the  $B_{ijk}$ 's are governed by a single degree of freedom system equation of the form

$$\ddot{B}_{ijk} + 2 \varepsilon_{ijk} \omega_{ijk} \dot{B}_{ijk} + \omega_{ijk}^2 B_{ijk} = F_{ijk} \quad (4.10)$$

where  $\varepsilon_{ijk}$  is an equivalent viscous modal damping coefficient which accounts for the absorption losses in the wall and air damping in the cavity. The modal damping coefficient in the analysis is taken to be,

$$\varepsilon_{ijk} = \varepsilon_{ool} (\omega_{ool} / \omega_{ijk})^2 \quad (4.11)$$

based on the works of references [2,5].

$F_{ijk}$  in equation (4.10) is the generalized force corresponding to the  $ijk^{\text{th}}$  cavity mode, given by

$$F_{ijk} = - \frac{c^2 e_k}{d} \int_0^d \left( \frac{1}{c^2} \ddot{z}_{ij} + A_{ij} z_{ij} - \frac{\partial^2 z_{ij}}{\partial z^2} \right) \cos \frac{k\pi z}{d} dz \quad (4.12)$$

where,  $e_k = \begin{matrix} 1 & \text{for } k = 0 \\ 2 & \text{for } k \neq 0 \end{matrix}$

and  $\omega_{ijk}^2$  are the square of the cavity resonant frequencies given by

$$\omega_{ijk}^2 = c^2 (A_{ij} + k^2 \pi^2 / d^2) \quad (4.13)$$

From equations (4.9), (4.4) and (4.3), the cavity pressure is given by

$$\begin{aligned}
 p_c(x,y,z,t) = & \sum_{i=0}^{\infty} \sum_{j=0}^{\infty} \sum_{k=0}^{\infty} B_{ijk}(t) f_{ij}(x,y) \cos \frac{k\pi z}{d} \\
 & + \sum_{i=0}^{\infty} \sum_{j=0}^{\infty} Z_{ij}(z,t) f_{ij}(x,y)
 \end{aligned} \tag{4.14}$$

#### 4.2.2 Structural Response

a) Harmonic loading: Consider a plane harmonic pressure wave incident on the plate at an angle  $\theta$  to the normal. The external pressure field can be expressed as

$$p_e(x,y,0,t) = p_0 \exp [i(\omega t - k' x \sin \theta)] \tag{4.15}$$

where  $k' = \omega / c$  is the acoustic wave number. The pressure distribution is assumed to be uniform along the  $y$  direction. As it has been assumed in the analysis that the plate motion is not affected by the cavity pressure and the radiation loading on the plate external to the cavity is negligible, the structural response can be directly obtained as the in-vacuo structural motion. A forced damped normal mode analysis outlined in Chapter 2 is used for the same.

$$\text{Expressing } w(x,y,t) = \sum_{m=1}^{\infty} \sum_{n=1}^{\infty} W_{mn}(x,y) q_{mn}(t) \tag{4.16}$$

where  $W_{mn}(x,y)$  are the forced damped normal modes, the damped normal coordinates  $q_{mn}$  are given by

$$q_{mn}(t) = \frac{p_{mn}(t)}{\mu_{mn} [\omega_{mn}^{*2} (1 + i\eta_{mn}) - \omega^2]} \quad (4.17)$$

where,  $p_{mn}$  and  $\mu_{mn}$  are given by equations (2.31) and (2.32) respectively.

The particular forms of  $p_{mn}$  and  $\mu_{mn}$  for the different boundary conditions are given in Appendix B.  $\omega_{mn}^{*2} (1 + i\eta_{mn})$  is the complex natural frequency in the  $mn^{\text{th}}$  damped mode and  $\eta_{mn}$  is the corresponding modal loss factor.

b) Random loading: Consider a random pressure excitation on the plate. The pressure field is assumed to be stationary with respect to time and homogeneous with respect to the spatial indexing parameters. The power spectral density of the external pressure can be expressed as in equation (2.33).

$$S_{pp}(x_1, y_1; x_2, y_2; \omega) = S_{p_0 p_0}(\omega) r_{xy}(x_2 - x_1; y_2 - y_1; \omega) \quad (4.18)$$

In further analysis, the external excitation is assumed to be white noise with  $S_{p_0 p_0}(\omega) = S_0$ , and uniform with respect to the spatial co-ordinates, that is,  $r_{xy}(x_1, y_1; x_2, y_2; \omega) = 1.0$ . Then the power spectral density of the response is given by

$$S_{ww}(x_1, y_1; x_2, y_2; \omega) = \sum_{m=1}^{\infty} \sum_{n=1}^{\infty} \sum_{r=1}^{\infty} \sum_{s=1}^{\infty} W_{mn}(x_1, y_1) W_{rs}^*(x_2, y_2) \cdot H_{mn}(\omega) H_{rs}^*(\omega) S_0 I_{mnrs}(\omega) \quad (4.19)$$

The various quantities in equation (4.19) are defined by equation (2.35) and (2.36) and for the different plate boundary conditions are given in Appendix B.

#### 4.2.3 Noise Transmission into Cavity

a) Harmonic loading: Having determined the structural response, the pressure inside the cavity can be calculated in the following way. Substituting equation (4.16) into equation (4.8), one gets,

$$G_{ij}(t) = - \frac{\rho e_{ij}}{ab} \sum_{m=1}^{\infty} \sum_{n=1}^{\infty} L_{mnij} \ddot{q}_{mn} \quad (4.20)$$

where,

$$L_{mnij} = \int_{-a/2}^{a/2} \int_0^b W_{mn}(x,y) f_{ij}(x,y) dy dx \quad (4.21)$$

From equations (4.9), (4.11), (4.12) and (4.20) it follows that,

$$B_{ijk} = - \frac{\rho c^2 d e_{ij}}{ab} \delta_{ijk} \sum_{m=1}^{\infty} \sum_{n=1}^{\infty} L_{mnij} \ddot{q}_{mn} \quad (4.22)$$

where,

$$\begin{aligned} \delta_{ijk} &= e_k \left[ \frac{\left( \frac{\omega^2}{c^2} - A_{ij} \right) / 3 - 1/d^2}{\omega_{ijk}^2 - \omega^2 + 2i\epsilon_{ijk} \omega_{ijk} \omega} \right] \text{ for } k = 0 \\ &= \frac{e_k}{k^2 \pi^2} \frac{(A_{ij} - \omega^2/c^2)}{(\omega_{ijk}^2 - \omega^2 + 2i\epsilon_{ijk} \omega_{ijk} \omega)} \text{ for } k \neq 0 \end{aligned} \quad (4.23)$$

The pressure inside the cavity can now be obtained from equation (4.14) as

$$p_c(x,y,z,t) = - \frac{c^2 d}{ab} \sum_{i=0}^{\infty} \sum_{j=0}^{\infty} \sum_{k=0}^{\infty} e_{ij} \delta_{ijk} \sum_{m=1}^{\infty} \sum_{n=1}^{\infty} L_{mnij} \ddot{q}_{mn} \cdot$$

$$f_{ij}(x,y) \cos \frac{k\pi z}{d} - (z-z^2/2d) \frac{\rho}{ab} \sum_{i=0}^{\infty} \sum_{j=0}^{\infty} e_{ij}$$

$$\sum_{m=1}^{\infty} \sum_{n=1}^{\infty} L_{mnij} \ddot{q}_{mn} f_{ij}(x,y) \quad (4.24)$$

The noise reduction (NR) through the sandwich panel can be calculated by computing the cavity pressure at the panel at  $z = 0$ . The noise reduction through the centre of the panel ( $x = 0$ ,  $y = b/2$ ,  $z = 0$ ) is then expressed as,

$$NR = 20 \log \frac{p_0}{|p_c(0, \frac{b}{2}, 0)|} \quad (4.25)$$

b) Random loading: From equations (4.8) and (4.19) the cross power spectral density between the functions  $G_{ij}$  and  $G_{l0}$  is given by

$$S_{G_{ijl0}}(\omega) = \frac{\rho^2 e_{ij} e_{l0} \omega^4}{a^2 b^2} S_0 \left[ \sum_{m=1}^{\infty} \sum_{n=1}^{\infty} \sum_{r=1}^{\infty} \sum_{s=1}^{\infty} H_{mn} L_{mnij} H_{rs}^* L_{rslo}^* \right] \quad (4.26)$$

From equations (4.14) and (4.22) the cross spectral density of the cavity pressures at  $(x = x_1, y = y_1, z = 0)$  and at  $(x = x_2, y = y_2, z = 0)$  can be expressed as,

$$S_{p_c p_c}(x_1, y_1; x_2, y_2; \omega) = c_d^2 \left[ \sum_i \sum_j \sum_k \sum_l \sum_o \sum_h \delta_{ijk} \delta_{loh} f_{ij}(x_1, y_1) f_{lo}(x_2, y_2) S_{G_{ijlo}}(\omega) \right] \quad (4.27)$$

The auto power spectral density of the cavity pressure at a point  $(x, y, 0)$  in the sandwich panel can be obtained from equation (4.27) by setting  $x_1 = x_2 = x$  and  $y_1 = y_2 = y$ .

The noise reduction at the centre of the plate is calculated according to the formula

$$NR = 10 \log \frac{S_o}{S_{p_c p_c}(0, b/2, 0, \omega)} \quad (4.28)$$

### 4.3 ACOUSTOELASTIC FORMULATION

#### 4.3.1 Acoustic solution

Consider again the cavity shown in Fig.(4.2) occupying a volume  $V = abd$ . As before, it is assumed that the wall formed by the damped sandwich panel at  $z = 0$  is flexible and the other walls are acoustically rigid.

The cavity pressure  $p_c$  is governed by the following equations

$$\nabla^2 p_c - \frac{1}{c^2} \frac{\partial^2 p_c}{\partial t^2} = 0 \quad (4.1)$$

$$\begin{aligned}
 \frac{\partial p_c}{\partial n} &= -\rho \frac{\partial^2 w}{\partial t^2} && \text{on } A_F \\
 &= 0 && \text{on } A_R
 \end{aligned}
 \tag{4.2}$$

Equation (4.1) for homogeneous boundary conditions

$\frac{\partial p_c}{\partial n} = 0$ , has normal mode solutions  $F_n e^{i\omega t}$  which satisfy the equations

$$\nabla^2 F_n = -(\omega_{nA}/c)^2 F_n \tag{4.29}$$

$$\frac{\partial F_n}{\partial n} = 0 \text{ on } A \tag{4.30}$$

where,  $\omega_{nA}$  is the  $n^{\text{th}}$  acoustic natural frequency,  $F_n$  is the corresponding cavity mode,  $A$  is the total surface area of the enclosure. Note that the index  $n$  contains the indices  $i, j, k$  of the previous section in a compressed form which represent the modal shapes in the  $x, y$  and  $z$  directions. ( $F_n$  corresponds to  $f_{ijk}(x, y, z)$  of the previous section).

The orthogonality condition of the acoustic normal modes can be expressed as,

$$\frac{1}{V} \int_V F_r F_n dV = M_{nA} \delta_{rn} \tag{4.31}$$

where  $\delta_{rn}$  represents the Kronecker delta.

The wave equation (4.1) can be transformed into a set of ordinary differential equations by using Green's theorem in the form,

$$\int_V (p \nabla^2 F_n - F_n \nabla^2 p) dV = \int_A (p \frac{\partial F_n}{\partial n} - F_n \frac{\partial p}{\partial n}) dA \quad (4.32)$$

The acoustic pressure inside the cavity can be expanded in terms of the acoustic normal modes  $F_n$  as

$$p_c = \rho c^2 \sum \frac{P_n F_n}{M_{nA}} \quad (4.33)$$

The pressure coefficients  $P_n$  in the acoustic normal mode expansion are governed by the set of ordinary differential equations

$$\ddot{P}_n + \omega_{nA}^2 P_n = - \frac{A_F}{V} \ddot{W}_n \quad (4.34)$$

where,

$$P_n = \frac{1}{\rho c^2 V} \int_V p_c F_n dV \quad (4.35)$$

and

$$W_n = \frac{1}{A_F} \int_{A_F} w F_n dA_F \quad (4.36)$$

Wall absorption and air damping in the cavity can be expressed in terms of an equivalent viscous modal damping in which case equation (4.34) can be written in the form

$$\ddot{P}_n + 2\varepsilon_{nA} \omega_{nA} \dot{P}_n + \omega_{nA}^2 P_n = - \frac{A_F}{V} \ddot{W}_n \quad (4.37)$$

where,  $\varepsilon_{nA}$  is the modal damping coefficient in the  $n^{\text{th}}$  acoustic mode.

### 4.3.2 Coupled Acoustoelastic Equations

The equation of motion for the flexible sandwich panel with a constrained viscoelastic damping layer is given by equation (2.9)

$$\nabla^6 w - g'(1+Y) \nabla^4 w + \frac{\mu}{D_t} \frac{\partial^2}{\partial t^2} [\nabla^2 w - g'w] = \frac{1}{D_t} (\nabla^2 p - g'p) \quad (4.38)$$

In the above equation  $p$  is the net pressure excitation on the plate given by  $p = p_c - p_e$ , where  $p_c$  is the internal cavity pressure and  $p_e$  is the external pressure loading on the plate. The radiation loading on the plate surface external to the cavity is neglected.

As before, the response of the damped sandwich plate for a harmonic or stationary random pressure excitation can be expanded in terms of forced damped normal modes in the form,

$$w = \sum_m q_m \varphi_m \quad (4.39)$$

Here, in the index  $m$  are contained the indices of both  $m, n$  corresponding to the mode shapes in the  $x$  and  $y$  directions. In the terminology of equation (4.16),  $q_m$  corresponds to  $q_{mn}$  and  $\varphi_m$  the damped normal mode corresponds to  $W_{mn}(x, y)$ . Using the method of damped normal mode analysis outlined in Chapter 2, the damped normal co-ordinates  $q_m$ s are governed by the ordinary differential equations

$$M_{ms}[\ddot{q}_m + \omega_{ms}^2 (1 + i\eta_{ms})q_m] = Q_{mc} + Q_{me} \quad (4.40)$$

where  $M_{ms}$  is the generalized mass corresponding to the damped normal mode given by,

$$M_{ms} = \int_{A_F} \mu \varphi_m^2 dA \quad (4.41)$$

$Q_{mc} = \int_{A_F} p_c \varphi_m dA$  and  $Q_{me} = \int_{A_F} p_e \varphi_m dA$  are the generalized forces corresponding to the cavity and external pressures respectively. It should be noted that in general,  $M_{ms}$ ,  $Q_{mc}$  and  $Q_{me}$  are complex values. Using equations (4.33) to (4.36) and equations (4.39) to (4.41) the coupled acousto-structural equations can be expressed as

$$\ddot{P}_n + 2\varepsilon_{nA} \omega_{nA} \dot{P}_n + \omega_{nA}^2 P_n = - \sum_m \frac{A_F}{V} L_{nm} \ddot{q}_m \quad (4.42)$$

$$M_{ms}[\ddot{q}_m + \omega_{ms}^2 (1 + i\eta_{ms})q_m] = \rho c^2 A_F \sum_n \frac{P_n L_{nm}}{M_{nA}} + Q_m^E \quad (4.43)$$

where,

$$L_{nm} = \frac{1}{A_F} \int_{A_F} F_n \varphi_m dA \quad (4.44)$$

Note that,  $L_{nm}$  corresponds to  $L_{mni}$  of equation (4.21) divided by the area of the panel.

### 4.3.3 Solution of Acoustoelastic Problem

It is shown by Dowell [5], that expressing equations (4.42) and (4.43) in terms of the acoustic potential and in matrix notation, and limiting the summation in the

equations to a finite number of acoustic and structural normal modes, the problem reduces to a matrix eigenvalue problem with gyroscopic coupling, as would arise in the dynamics of spinning structural systems. The solution of the eigenvalue problem will give the coupled natural frequencies of the structure-cavity system. The eigenvectors can be used to obtain the pressure coefficients  $P_n$ 's and the structural coordinates  $q_m$ 's.

The solution of the eigenvalue problem for gyroscopic systems can be obtained by expressing the coupled acousto-elastic equations in state space form, in terms of displacements and velocity coordinates. Then one has to deal with  $2(m+n)$  first order ordinary differential equations defined by two matrices one symmetric and the other skew symmetric. Meirovitch [93] has proposed a new method of solution of such problems by taking advantage of the special nature of the problem. But his method is applicable only if the elements in the symmetric and skew symmetric matrices are real.

However, in the present work, many of the matrix elements are complex valued, due to the presence of the additive damping layer. Hence an eigenvalue analysis of the problem is a difficult proposition, because of the cumbersome complex arithmetic and the size of the

matrices involved. Moreover, the main interest in this analysis is to obtain the noise reduction inside the cavity and the structural response. They can be determined directly by a matrix inversion procedure, which takes advantage of the diagonal nature of some of the matrices in the analysis. Equations (4.42) and (4.43) can be expressed in matrix form as,

$$\begin{aligned}
 & \begin{bmatrix} [I] & [B_1] \\ (nxn) & (nxm) \end{bmatrix} \begin{Bmatrix} \ddot{P} \\ (n \times 1) \end{Bmatrix} + \begin{bmatrix} [-2\epsilon_{nA} \omega_{nA}] & [0] \\ (nxn) & (nxm) \end{bmatrix} \begin{Bmatrix} \dot{P} \\ (n \times 1) \end{Bmatrix} \\
 & - \begin{bmatrix} [0] & [I] \\ (mxn) & (mxm) \end{bmatrix} \begin{Bmatrix} \ddot{q} \\ (m \times 1) \end{Bmatrix} + \begin{bmatrix} [0] & [0] \\ (mxn) & (mxm) \end{bmatrix} \begin{Bmatrix} \dot{q} \\ (m \times 1) \end{Bmatrix} \\
 & + \begin{bmatrix} [-\omega_{nA}^2] & [0] \\ (nxn) & (nxm) \end{bmatrix} \begin{Bmatrix} P \\ (n \times 1) \end{Bmatrix} + \begin{bmatrix} [B_2] & [-\omega_{ms}^2 (1+i\eta_{ms})] \\ (mxn) & (mxm) \end{bmatrix} \begin{Bmatrix} q \\ (m \times 1) \end{Bmatrix} = \begin{Bmatrix} 0 \\ (n \times 1) \end{Bmatrix} + \begin{Bmatrix} Q \\ (m \times 1) \end{Bmatrix} \quad (4.45)
 \end{aligned}$$

where,  $[I]$  and  $[0]$  are identity and null matrices of appropriate orders indicated. Typical elements of the matrices  $[B_1]$  and  $[B_2]$  are given by,

$$b_{1ij} = \frac{A_F}{V} L_{ij} \quad \text{and} \quad b_{2ij} = - \frac{\rho c^2 A_F}{M_{jA} M_{is}} L_{ji}.$$

$\{P\}$  and  $\{q\}$  are the vectors of the pressure coefficients  $P_n$ s and generalized coordinates  $q_m$ s and  $\{Q\}$  is the external force vector whose  $m^{\text{th}}$  element is given by  $Q_m = Q_{me}/M_{ms}$ .

The letters inside the brackets indicate the order of the matrices,  $n$  being the number of acoustic cavity modes,  $m$ , the number of structural damped normal modes considered in the modal summations.

a) Harmonic loading: Consider an external pressure excitation with a harmonic component  $e^{i\omega t}$ . Matrix equations (4.45) are similar to equations of motion of linear multi-degree of freedom vibrating systems with both inertial and elastic coupling. The steady state solutions of such a system are harmonic with the same frequency  $\omega$ . Hence assuming

$\{P\} = \{\bar{P}\} e^{i\omega t}$  and  $\{q\} = \{\bar{q}\} e^{i\omega t}$  and  $\{Q\} = \{\bar{Q}\} e^{i\omega t}$  equation (4.45) can be written as

$$[B] \begin{Bmatrix} \{\bar{P}\} \\ \{\bar{q}\} \end{Bmatrix} = \begin{Bmatrix} \{0\} \\ \{\bar{Q}\} \end{Bmatrix} \quad (4.46)$$

where, the matrix  $[B]$  is given by,

$$[B] = \begin{bmatrix} [-Z_{nA}(\omega)] & | & -\omega^2[B_1] \\ \hline & & \\ [B_2] & | & [-Z_{mS}(\omega)] \end{bmatrix} \quad (4.47)$$

In equation (4.47)  $[-Z_{nA}(\omega)]$  and  $[-Z_{mS}(\omega)]$  are diagonal matrices having diagonal elements

$$Z_{nA}(\omega) = \omega_{nA}^2 + 2i \epsilon_{nA} \omega_{nA} - \omega^2 \quad (4.48)$$

$$Z_{mS}(\omega) = \omega_{mS}^2 (1 + i\eta_{mS}) - \omega^2 \quad (4.49)$$

$Z_{nA}(\omega)$ , and  $Z_{ms}(\omega)$  can be respectively regarded as the complex cavity impedance function in the  $n^{\text{th}}$  cavity mode and the structural impedance function in the  $m^{\text{th}}$  damped normal mode.

The complex amplitudes  $\{\bar{P}\}$  and  $\{\bar{q}\}$  can be obtained as,

$$\begin{Bmatrix} \{\bar{P}\} \\ \{\bar{q}\} \end{Bmatrix} = [A] \begin{Bmatrix} \{0\} \\ \{\bar{Q}\} \end{Bmatrix} \quad (4.50)$$

where  $[A] = [B]^{-1}$ .

The pressure inside the cavity can be obtained from equation (4.33) as,

$$p_c = \rho c^2 e^{i\omega t} \sum_n \bar{P}_n F_n / M_{nA} \quad (4.51)$$

and the structural response at a point  $(x,y)$  on the surface of the plate as,

$$w(x,y) = e^{i\omega t} \sum_m \bar{q}_m \varphi_m(x,y) \quad (4.52)$$

The noise reduction inside the cavity from equation (4.28) is

$$NR = 20 \log \frac{p_0}{|c^2 \sum_n \bar{P}_n F_n / M_{nA}|} \quad (4.53)$$

where,  $p_0$  is the amplitude of the external harmonic pressure excitation.

b. Random loading: Consider the external excitation to be a stationary random process with power spectral density function, given by equation (4.18). The cross spectral density between the generalized forces  $Q_m$  and  $Q_r$  is then given by,

$$S_{Q_m Q_r^*}(\omega) = \frac{S_{p_o p_o}(\omega) I_{mr}(\omega)}{M_{ms} M_{rs}} \quad (4.54)$$

where,

$$I_{mr}(\omega) = \int_{A_F} \int_{A_F} r(x_1, y_1; x_2, y_2; \omega) \varphi_m(x_1, y_1) \varphi_r^*(x_2, y_2) dA_1 dA_2 \quad (4.55)$$

Note that  $I_{mr}(\omega)$  in the foregoing equation corresponds to the acceptance functions  $I_{mnrs}$  defined in equation (4.19), the index  $m$  including both the indices  $m$  and  $n$  and the index  $r$  including both the indices  $r$  and  $s$  in a compressed form. The asterisk indicates complex conjugation.

The cross spectral density matrix of the generalized forces can be constructed from equations (4.54) and (4.55) as

$$[S_{QQ}(\omega)] = S_{p_o p_o}(\omega) [\bar{I}(\omega)] \quad (4.56)$$

where a typical element of the acceptance matrix  $[\bar{I}]$  is given by

$$\bar{I}_{mr}(\omega) = \frac{I_{mr}(\omega)}{M_{ms} M_{rs}} \quad (4.57)$$

The cross spectral density matrix of the pressure coefficients  $P_n$  s and the structural generalized coordinates  $q_m$  s can be shown to be

$$[S_{AS}(\omega)]_{(n+m) \times (n+m)} = \begin{bmatrix} [S_{PP}(\omega)]_{(n \times n)} & [S_{Pq}(\omega)]_{(n \times m)} \\ [S_{qP}(\omega)]_{(m \times n)} & [S_{qq}(\omega)]_{(m \times m)} \end{bmatrix} = [A] \begin{bmatrix} [0] & [0] \\ [0] & [S_{QQ}(\omega)] \end{bmatrix} [A^*]^T \quad (4.58)$$

where the superscript T refers to transpose and the asterisk again represents complex conjugation.

From equations (4.33) and (4.58) the power spectral density of the cavity pressure at any point in the cavity is,

$$S_{p_c p_c}(x, y, z, \omega) = \rho^2 c^4 \{\alpha\}^T [S_{PP}(\omega)] \{\alpha^*\} \quad (4.59)$$

where,  $\{\alpha\}$  is a n-dimensional vector whose  $n^{th}$  element is  $F_n(x, y, z)/M_{nA}$ .

Similarly using equations (4.16) and (4.58) the power spectral density of the displacement  $w$  of the panel at a point  $(x, y)$  is given by

$$S_{ww}(x, y, \omega) = \{\gamma\}^T [S_{qq}(\omega)] \{\gamma^*\} \quad (4.60)$$

where,  $\{\gamma\}$  is a m-dimensional vector whose  $m^{th}$  element is  $\varphi_m(x, y)$ .

The noise transmission characteristic of the sandwich panel can be expressed in terms of the noise reduction

$$NR = 10 \log [S_{p_o p_o}(x, y, 0, \omega) / S_{p_c p_c}(x, y, 0, \omega)] \quad (4.61)$$

#### 4.3.4 Inversion of [B] Matrix

Thus both for harmonic and random external acoustic excitation, the structural response, the cavity pressure and the noise transmission characteristics of the sandwich panel can be obtained by the inversion of the matrix [B].

It is not necessary to invert the whole matrix [B] which is of order  $(n+m) \times (n+m)$ . Advantage can be taken of the presence of the diagonal matrices  $[-Z_{nA}(\omega)-]$  and  $[-Z_{ms}(\omega)-]$ . Writing  $[B]^{-1} = [A]$  in partitioned form,

$$[A] = \begin{bmatrix} [A_1] & | & [A_2] \\ (nxn) & | & (nxm) \\ \hline [A_3] & | & [A_4] \\ (mxn) & | & (mxm) \end{bmatrix} \quad (4.62)$$

it can be shown that,

$$\begin{aligned} [A_1] &= [-Z_{nA}-] - \omega^2 [B_1] [-Z_{ms}-]^{-1} [B_2]^{-1} \\ [A_4] &= [-Z_{ms}-] - \omega^2 [B_2] [-Z_{nA}-]^{-1} [B_1]^{-1} \\ [A_2] &= -\omega^2 [-Z_{nA}-]^{-1} [B_1] [A_4] \\ [A_3] &= -[-Z_{ms}-]^{-1} [B_2] [A_1] \end{aligned} \quad (4.63)$$

$[-Z_{n\Lambda}]^{-1}$  and  $[-Z_{ms}]^{-1}$  are just the reciprocals of the diagonal matrices  $[-Z_{n\Lambda}]$  and  $[-Z_{ms}]$  respectively.

Hence, the problem of determining the inverse of matrix  $[B]$  of order  $(n+m) \times (n+m)$  reduces to finding the inverses of two matrices of order  $(n \times n)$  and  $(m \times m)$  respectively.

It is further shown here, that it is sufficient to find only the matrix  $[A_4]$  which is the inverse of a matrix of order  $(mxm)$ , for the determination of the cavity pressure and the structural response and not the inverses of two matrices as indicated above. It is so because, from equation (4.58), it is seen that the spectral density matrices are given by,

$$\begin{aligned}
 [S_{PP}(\omega)] &= [A_2] [S_{QQ}] [A_2^*]^T \\
 [S_{qq}(\omega)] &= [A_4] [S_{QQ}] [A_4^*]^T \\
 [S_{Pq}(\omega)] &= [A_2] [S_{QQ}] [A_4^*]^T \\
 [S_{qP}(\omega)] &= [A_4] [S_{QQ}] [A_2^*]^T
 \end{aligned}
 \tag{4.64}$$

Only the matrices  $[A_2]$  and  $[A_4]$  are needed for a complete solution of the problem. From equation (4.63)  $[A_2]$  is obtained from  $[A_4]$  by a simple transformation and so the solution of the acoustoelastic problem requires the inversion of the matrix of order  $(mxm)$ .

#### 4.4 APPROXIMATE FORMULATIONS

Before the discussion of the results obtained for a typical cavity-sandwich panel system, it is purposeful to consider certain simplified models as considered by Dowell[5], that would lead to a better understanding of the results.

If the exciting frequency  $\omega$ , say  $\omega_E$ , is very nearly equal to a structural resonant frequency  $\omega_{ms}^*$ , the coupled acoustoelastic equation in the structural coordinates can be decoupled by assuming that the main contribution to the structural response will arise due to  $q_m$  alone. Hence from equations (4.42) for harmonic loading

$$P_n = - \frac{A_F}{V} \frac{L_{nm} \ddot{q}_m}{(-\omega_{ms}^{*2} + \omega_{nA}^2 + 2i\epsilon_{nA} \omega_{nA} \omega_{ms}^*)} \quad (4.65)$$

and from equation (4.43),

$$M_{ms} [\ddot{q}_m + \omega_{ms}^{*2} (1 + i\eta_{ms}) q_m] = - \frac{\rho c^2 A_F^2}{V} .$$

$$\left[ \sum_n \frac{L_{nm}^2 \ddot{q}_m}{M_{nA} (-\omega_{ms}^{*2} + \omega_{nA}^2 + 2i\epsilon_{nA} \omega_{nA} \omega_{ms}^*)} \right] + Q_m^E e^{i\omega_E t} \quad (4.66)$$

From equation (4.66), it is seen that cavity modes having frequencies greater than  $\omega_{ms}^{*2}$  add to the inertia of the panel and cavity modes having frequencies less than

$\omega_{ms}^*$  add to the stiffness of the plate. The  $n = 0$  mode  $\omega_{oA} = 0$  always adds to the stiffness of the plate.

If the structural resonant frequency  $\omega_{ms}^*$  and the cavity resonant frequencies are well separated, then the structural resonant frequencies will not be influenced by the cavity. Then in equation (4.66), the sum on the right hand side can be neglected as small compared to the external excitation term. Then the response to harmonic excitation will be governed by the modal loss factor of the structure

$$q_m = \frac{Q_m^E e^{i\omega_E t}}{i M_{ms} \eta_{ms} \omega_{ms}^*} \quad (4.67)$$

From equations (4.33), (4.65) and (4.67), the pressure inside the cavity may be computed as,

$$p_c = \frac{\rho c^2 A_F}{i \eta_{ms} V} \sum_n \frac{F_n L_{nm} Q_{mE}}{M_{ms} M_{nA} (-\omega_{ms}^{*2} + \omega_{nA}^2 + 2i\epsilon_{nA} \omega_{nA} \omega_{ms}^*)} \quad (4.68)$$

If  $\omega_{ms}^*$  is very much less than the lowest nonzero acoustic resonance, only the  $n = 0$  acoustic mode will be dominant and the cavity pressure  $p_c$  can be approximated as

$$p_c \approx - \frac{\rho c^2 A_F F_o L_{om} Q_{mE}}{i \eta_{ms} V \omega_{ms}^{*2} M_{oA} M_{ms}} \quad (4.69)$$

Thus from equation (4.69), under the conditions mentioned above, the cavity pressure is inversely proportional to

$\eta_{ms} \omega_{ms}^2$  which can be likened to the energy dissipation parameter described by Mead [24]. The cavity pressure can at times exceed the external pressure giving rise to negative noise reduction for low values of  $\eta_{ms} \omega_{ms}^2$ . It can also be observed that the noise transmission characteristics of the panel at structural resonances can be improved by increasing modal loss factors, especially for the fundamental structural mode and other low order modes.

Significant changes in structural resonant frequencies will occur, mainly if a structural mode couples effectively with the  $n = 0$  acoustic cavity mode. Equation (4.66) can then be approximated by

$$M_{ms} [\ddot{q}_m + \omega_{ms}^2 (1 + i\eta_{ms})] = - \frac{\rho c^2 A_F^2}{V} L_{om}^2 q_m + Q_m^E e^{i\omega_E t} \quad (4.70)$$

From equation (4.70) it can be seen that the coupled structure-cavity frequency can be expressed as

$$\omega_{cs}^2 \approx \omega_{ms}^2 + \frac{\rho c^2 A_F^2 L_{om}^2}{M_{ms} V} \quad (4.71)$$

Another case where the structural frequency may be changed due to the effects of cavity is when a structural resonant frequency and a cavity modal frequency coincide. In this case, there is a strong coupling between the structure and the cavity and large sound pressure levels in the

cavity and large structural response corresponding to the coupled natural frequency of the cavity-structure system result. The phenomenon is described as multiple resonances or double resonance in literature [53,55,90]. The resonant condition arises mainly because of an impedance matching between the cavity and structural impedances. Large pressures inside the cavity will also arise when two cavity frequencies are in close proximity.

#### 4.5 RESULTS AND DISCUSSION

The following geometrical and material properties for the sandwich panel-cavity system are adopted in the computer investigations. The parameters which remain constant in most of the computations are,

Thickness of face plate	$h_1 = 0.0005 \text{ m}$
Length of panel along x direction	$a = 0.25 \text{ m}$
Length of panel along y direction	$b = 0.5 \text{ m}$
Youngs modulus of the face plate material E (aluminium)	$= 7.2 \times 10^{10} \text{ N/m}^2$
Density of face plate material (aluminium)	$\rho_p = 2770 \text{ kgm/m}^3$
Local velocity of sound in air	$c = 330 \text{ m/sec.}$
Density of air	$\rho = 1.225 \text{ kgm/m}^3$
Density of viscoelastic damping layer	$\rho_c = 0.2 \rho_p$

For most of the studies, the depth of the cavity is taken to be  $d = 0.762$  m. However, the effect of the cavity depth on the structural response and noise reduction inside the cavity are investigated by varying the cavity depths. As remarked earlier, in all cases the x-wise edges at  $y = 0, b$  are assumed to be simply supported (Figure 4.1).

#### 4.5.1 Order of Modes in Summation

The boundary conditions at  $x = \pm a/2$ , are assumed to be identical and elastically supported. The external pressure excitation in the case of harmonic loading is assumed to be uniform. In the case of random loading the pressure excitation is assumed to be white noise with respect to the temporal parameter and spatially uniform with  $r(x_1, y_1; x_2, y_2; \omega) = 1.0$ . Under these assumptions, the contribution to the generalized force in the case of harmonic loading or to the power spectrum of the generalized force in the case of random loading will arise only due to the symmetric structural modes. Hence only the symmetric structural modes are considered in the summation. From equation (B.5) of Appendix B it is seen that the structural acoustic coupling terms represented by  $L_{mni j}$  have nonzero values only for the combinations of  $(m+i)$  and  $(n+j)$  being odd integers, for the simply supported boundary conditions. The following

combinations,  $(i = \text{even}, j = \text{even}, m = \text{odd}, n = \text{odd})$ ,  $(i = \text{even}, j = \text{odd}, m = \text{odd}, n = \text{even})$ ,  $(i = \text{odd}, j = \text{even}, m = \text{even}, n = \text{odd})$ ,  $(i = \text{odd}, j = \text{odd}, m = \text{even}, n = \text{even})$  are then admissible. But from the earlier observation, that the generalized forces have nonzero values only for the symmetrical structural modes, the response and noise transmission are computed by considering only the combinations  $(i = \text{even}, j = \text{even}, m = \text{odd (symmetric)}, n = \text{odd})$  of acoustic and structural modes. This entails no error in the formulation where the effect of the cavity on the structural motion is neglected. In the acoustoelastic formulation, it amounts to neglecting the contributions from the coupling between the odd order cavity modes and the even order structural modes. The contributions from these terms will anyway be negligible compared to the terms considered in the summation because of the vanishing of the generalized forces corresponding to the even order structural modes represented on the right side of the equation (4.45). Since the frequency range of interest in this study has been restricted to 1000 Hz, the modal summations and the acoustic cavity modes include admissible combinations in them upto a frequency of 1000 Hz. Nine structural modes  $(m=1,3,5, n=1,3,5)$  and sixteen cavity modes  $(i=0,2, j=0,2, k=0,1,2,3)$  are included in the results presented.

#### 4.5.2 Resonant Frequencies and Loss Factors

The natural frequencies and the corresponding loss factors in the symmetrical modes, for different elastic support conditions at the edges  $x = \pm a/2$  are presented in Table 4.1. It can be observed that the lowest natural frequency for transversely restrained edges could be less than the fundamental frequency for simply supported edges at  $x = \pm a/2$ , depending on the relative value of the stringer flexural stiffness parameter  $K_f$ . It has been noticed during the computer investigations, that increasing the value of  $K_f$  to the order of  $10^4$ , results in natural frequencies and loss factors for the transversely restrained edges approaching the values of fixed edges. The natural frequencies and loss factors for the rotationally restrained edges with and without rivets do not differ very much for the particular values of the torsional stiffness parameters  $K$  and  $K_{sv}$  chosen and for the low value of the shear parameter  $g^* = 7.44$  and for the geometric parameter  $Y=31.5$  chosen. Such a behaviour has also been observed by Mead[24] for the fundamental mode. Again, apart from the first resonant frequency, little change is observed in the natural frequencies and loss factors between the fixed edge conditions and rotationally restrained edge conditions. The effect of the boundary conditions is felt significantly only in the fundamental structural mode.

Table 4.1 - Natural Frequencies and Loss Factors for Different Plate Boundary Conditions

$$g^* = 7.443, \quad Y = 31.5 \quad \text{and} \quad \beta = 0.3$$

SMN	n	SS		FF		RRWTR		RRWR		TR	
		f	$\eta$	f	$\eta$	f	$\eta$	f	$\eta$	f	$\eta$
1	1	81	.167	103	.195	94	.146	96	.165	52	.006
1	3	155	.205	162	.196	161	.192	162	.195	160	.187
1	5	261	.202	262	.197	262	.197	262	.197	262	.197
2	1	307	.194	352	.164	345	.164	346	.162	204	.167
2	3	351	.186	390	.161	389	.160	390	.161	381	.154
2	5	433	.171	465	.153	465	.153	465	.153	464	.152
3	1	628	.139	707	.116	694	.118	698	.117	461	.160
3	3	666	.134	741	.114	741	.114	741	.114	712	.107
3	5	742	.125	809	.109	810	.108	810	.109	806	.108

f - Natural frequency, Hz;  $\eta$  - Loss factor; SS - Simply supported at  $x = \pm a/2$ ;

FF - Fixed at  $x = \pm a/2$ ; RRWTR - Rotationally Restrained without rivets at  $x = \pm a/2$ ;

TR - Transversally Restrained at  $x = \pm a/2$ ; SMN - Symmetric Model Number along x;

RRWR - Rotationally Restrained with rivets at  $x = \pm a/2$ .

Table 4.2 gives the variation of the natural frequencies and loss factors with the core shear parameter  $g^*$  for simply supported edge conditions at  $x = \pm a/2$ . The other core parameters are kept constant. It is seen that it has the most significant effect on the natural frequencies and loss factors. The resonant frequencies increase with increase in  $g^*$  in all the modes, the increase in frequency becoming less for high values of  $g^*$ . It is so because, the core becomes stiff with increasing values of  $g^*$ . The loss factor decreases with the modal number for  $g^* = 1.0$ , while it increases with modal number for  $g^* = 100.0$  and  $1000.0$ . For  $g^* = 7.443$ , the loss factor increases upto a certain modal number and then decreases. It is also observed from the table that for a particular mode, there is an optimum value of  $g^*$  for maximum loss factor. This optimum value increases for higher modes. Since the modal loss factor depends on a complex fashion on the modal number and the shear parameter as can be seen from the expression for the simply supported edge conditions (equation (2.22)) no special reason can be attributed to such a behaviour. All that can be said is that damping of a sandwich plate is known to be mode dependent. Evidently when  $g^*$  is changed the modes of the sandwich plate are changed and hence the variation of the loss factor with  $g^*$ .

Table 4.3 shows the variation of the natural frequencies and the associated loss factors of the sandwich panel in the

Table 4.2 - Natural Frequencies and Loss Factors for Different Shear Parameters  
 $(x = \pm a/2, SS, Y = 31.5, \beta = 0.3)$

SMN		g*		1.0		7.443		100		1000	
n		f	$\eta$	f	$\eta$	f	$\eta$	f	$\eta$	f	$\eta$
1	1	41.35	.194	81	.167	121.2	.0294	127.02	.00325		
1	3	81.64	.141	155	.205	292.7	.0655	327.42	.008304		
1	5	155.8	.0895	261	.202	578.3	.1128	718.20	.017876		
2	1	192.17	.0754	307	.194	701.4	.1290	908.82	.022413		
2	3	228.38	.0652	351	.186	814.93	.1420	1096.4	.026796		
2	5	300.52	.0512	433	.171	1020.1	.1614	1462.9	.035128		
3	1	480.3	.0334	628	.139	1450.6	.1882	2333.0	.053723		
3	3	516.21	.0312	666	.134	1527.1	.1914	2499.7	.057104		
3	5	588.01	.0276	742	.125	1673.2	.1965	2826.6	.063565		

f - Natural frequency, Hz;  $\eta$  - loss factor; SMN - Symmetric modal no.along x.

Table 4.3 - Natural Frequencies and Loss Factors for Different Shear Parameters

(x =  $\pm a/2$ , Fixed, Y = 31.5,  $\beta = 0.3$ )

		g*		1.0		7.443		100	
SMN	n	f	$\eta$	f	$\eta$	f	$\eta$	f	$\eta$
1	1	57	.122	103	.195	204	.088		
1	3	91	.118	162	.196	323	.092		
1	5	159	.085	262	.197	579	.118		
2	1	245	.051	352	.164	800	.161		
2	3	276	.048	390	.161	886	.163		
2	5	340	.042	465	.153	1062	.170		
3	1	571	.025	707	.116	1543	.193		
3	3	602	.024	741	.114	1609	.194		
3	5	670	.022	809	.109	1739	.196		

f - natural frequency, Hz; SMN - Symmetric modal no. along x;  $\eta$  - loss factor

symmetric modes for the edges  $x = \pm a/2$  fixed. The variation of the natural frequencies is very similar to that for the edges  $x = \pm a/2$  simply supported. The loss factor is less in the fixed edges case than simply supported case for  $g^* = 1.0$ , but they are greater for  $g^* = 100$ . For the value of  $g^* = 7.443$ , the loss factor for fixed end conditions is more than the corresponding value for simply supported conditions in the first fundamental mode, but for other modes the loss factors are less. Again it is very difficult to offer a physical argument for such a behaviour, except to conclude that the modal loss factor is sensitive to the variations in  $g^*$  and the form of the damped normal modes.

Tables 4.4 and 4.5 show the variation of the resonant frequencies and loss factors with core loss factor, for the y wise edges simply supported and fixed respectively. In both the cases, increasing  $\beta$  has only a marginal effect on the resonant frequencies, but the modal loss factors increase almost linearly with  $\beta a z$  as is the case with the infinite sandwich panel.

Tables 4.6 and 4.7 show the variation of the resonant frequencies of the sandwich panel and the associated modal loss factors with the core geometric parameter  $Y$ , for

Table 4.4 - Natural Frequencies and Loss Factors for Different Core Loss Factors

(  $x = \pm a/2$ , SS,  $g^* = 7.443$ ,  $Y = 31.5$  )

		$\beta$		0.0		0.1		0.3		1.0	
SMN	n	f	$\eta$	f	$\eta$	f	$\eta$	f	$\eta$	f	$\eta$
1	1	80.31	0.0	80.4	.0573	81	.167	89.46	.4235		
1	3	153.36	0.0	153.5	.0693	155	.205	169.3	.5955		
1	5	258.88	0.0	259.0	.0677	261	.202	278.8	.6315		
2	1	304.54	0.0	304.8	.0650	307	.194	325.2	.6168		
2	3	348.00	0.0	348.2	.0622	351	.186	369.0	.5968		
2	5	430.80	0.0	431.0	.0569	433	.171	452.0	.5539		
3	1	626.02	0.0	626.2	.0463	628	.139	645.7	.4569		
3	2	663.99	0.0	664.2	.0446	666	.131	683.3	.4409		
3	5	739.3	0.0	739.4	.0415	742	.125	757.8	.4116		

f - natural frequency, Hz; SMN - Symmetric modal no. along x;  $\eta$  - loss factor

Table 4.5 - Natural Frequencies and Loss Factors for Different Core Loss Factors

( $x = \pm a/2$ , Fixed,  $g^* = 7.443$ ,  $Y = 31.5$ )

		0.0			0.1			0.3			1.0		
SMN	n	f	$\eta$	f	$\eta$	f	$\eta$	f	$\eta$	f	$\eta$		
1	1	101	0.0	101	.0659	103	.195	110	.581				
1	3	160	0.0	161	.0662	162	.196	175	.578				
1	5	260	0.0	260	.0661	262	.197	279	.616				
2	1	349.8	0.0	350	.0551	352	.164	367	.528				
2	3	387.8	0.0	388	.0530	390	.161	406	.519				
2	5	462.9	0.0	463	.0512	465	.153	482	.498				
3	1	705.8	0.0	706	.039	707	.116	722	.385				
3	3	739.9	0.0	740	.0381	741	.114	756	.376				
3	5	808.0	0.0	808	.0363	809	.109	824	.360				

f - natural frequency, Hz; SMN - Symmetric modal no. along x,  $\eta$  - loss factor.

Table 4.6 - Natural Frequencies and Loss Factors for Different Geometric Parameters  
 (  $x = \pm a/2$ ,  $SS, g = 7.443$ ,  $\beta = 0.3$  )

Y		3.63		12		31.5	
SMN	N	f	$\eta$	f	$\eta$	f	$\eta$
1	1	38.21	.1054	56.13	0.1487	81	.167
1	3	83.54	.098	111.80	0.1666	155	.205
1	5	165.98	.069	201.0	0.1435	261	.202
2	1	206.21	.0594	242.2	0.1312	307	.194
2	3	246.20	.0521	282.5	0.1205	351	.186
2	5	325.8	.0417	361.5	0.1030	433	.171
3	1	523.91	.0277	554.8	0.0751	628	.139
3	3	563.4	.0259	593.2	0.0712	666	.134
3	5	642.54	.023	669.7	0.0645	742	.125
f - Natural frequency, Hz; $\eta$ - loss factor; SMN - Symmetrical modal no. along x.							

Table 4.7 - Natural Frequencies and Loss Factors for Different Geometric Parameters  
 (x =  $\pm a/2$ , Fixed,  $g^* = 7.443$ ,  $\beta = 0.3$ )

		3.63		12		31.5	
y		f		$\eta$		f	
SMN	n						
1	1	59	.086	76	.153	103	.195
1	3	94	.082	121	.151	162	.196
1	5	170	.065	204	.138	262	.197
2	1	266	.041	295	.100	352	.164
2	3	299	.038	329	.096	390	.161
2	5	369	.034	399	.088	465	.153
3	1	624	.021	646	.059	707	.116
3	3	658	.020	680	.057	741	.114
3	5	728	.019	748	.054	809	.109
f -- natural frequency, Hz; $\eta$ -- loss factor; SMN -- Symmetric modal no.along x.							

the edges at  $x = \pm a/2$  simply supported and fixed respectively. It is seen that both the resonant frequencies and the modal loss factors increase with increasing value of  $Y$  in both the cases. The modal loss factors also increase with  $Y$ , which is expected because of the increased thickness of the damping layer.

The cavity modal frequencies for the dimensions of the cavity are shown in Table 4.8.

#### 4.5.3 Comparison of Results in the Two Formulation

The acoustoelastic formulation of the noise transmission and structural response problem represents a more exact analysis of the coupled cavity-structural system. Hence, only a few results following the approximate formulation given in section 4.2 are presented for purposes of comparison.

Figure 4.3 shows the variation of noise reduction at the centre of the plate, with respect to frequency in both the Vaicaitis (approximate) and the acoustoelastic formulations for the edges at  $x = \pm a/2$  simply supported, and for an external white noise excitation. The same number of cavity modes and structural modes are included in both the analyses. It is observed that neglecting the effect of the cavity pressure on the panel motion does not alter

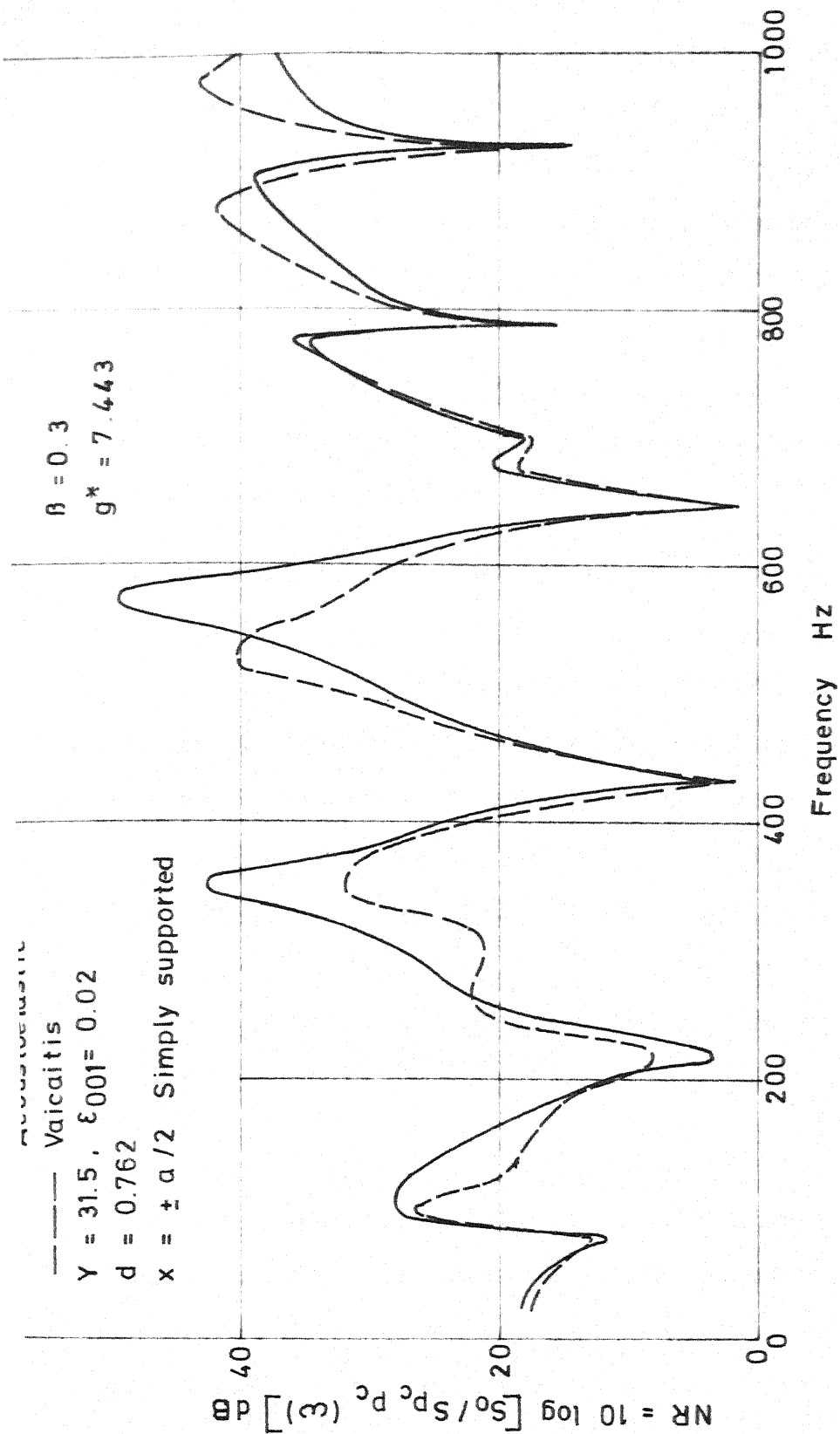


FIG. 4.3 COMPARISON OF NOISE REDUCTION BETWEEN VAICAITIS [2] AND ACOUSTOELASTIC FORMULATION

significantly the location of the dips in the noise reduction curves which occur very nearly at the cavity resonant frequencies. At low frequencies, the approximate formulation overestimates the noise reduction values by 1 to 3 dB at the cavity resonances, while at higher frequencies it underestimates the noise reduction values by the same order. However, there is significant difference in the non-resonant noise transmission characteristics of the plate in the two formulations.

The structural response for the same conditions as above is shown in Figure 4.4. In the low frequency ranges (0 - 200 Hz) there is practically no difference in the structural response in the two formulations. In the higher frequency regions, the in-vacuo structural response obtained by neglecting the cavity pressure on the plate motion is more than the structural response obtained when the full acoustic-structural coupling is taken into account. This may be attributed to the fact that the cavity modes in certain frequency bands act as dynamic absorbers for the structural motion.

The computational efforts involved in the coupled acoustoelastic formulation turned out to be even less than for the approximate formulation for the total number of modal summations considered. For the simply supported case the

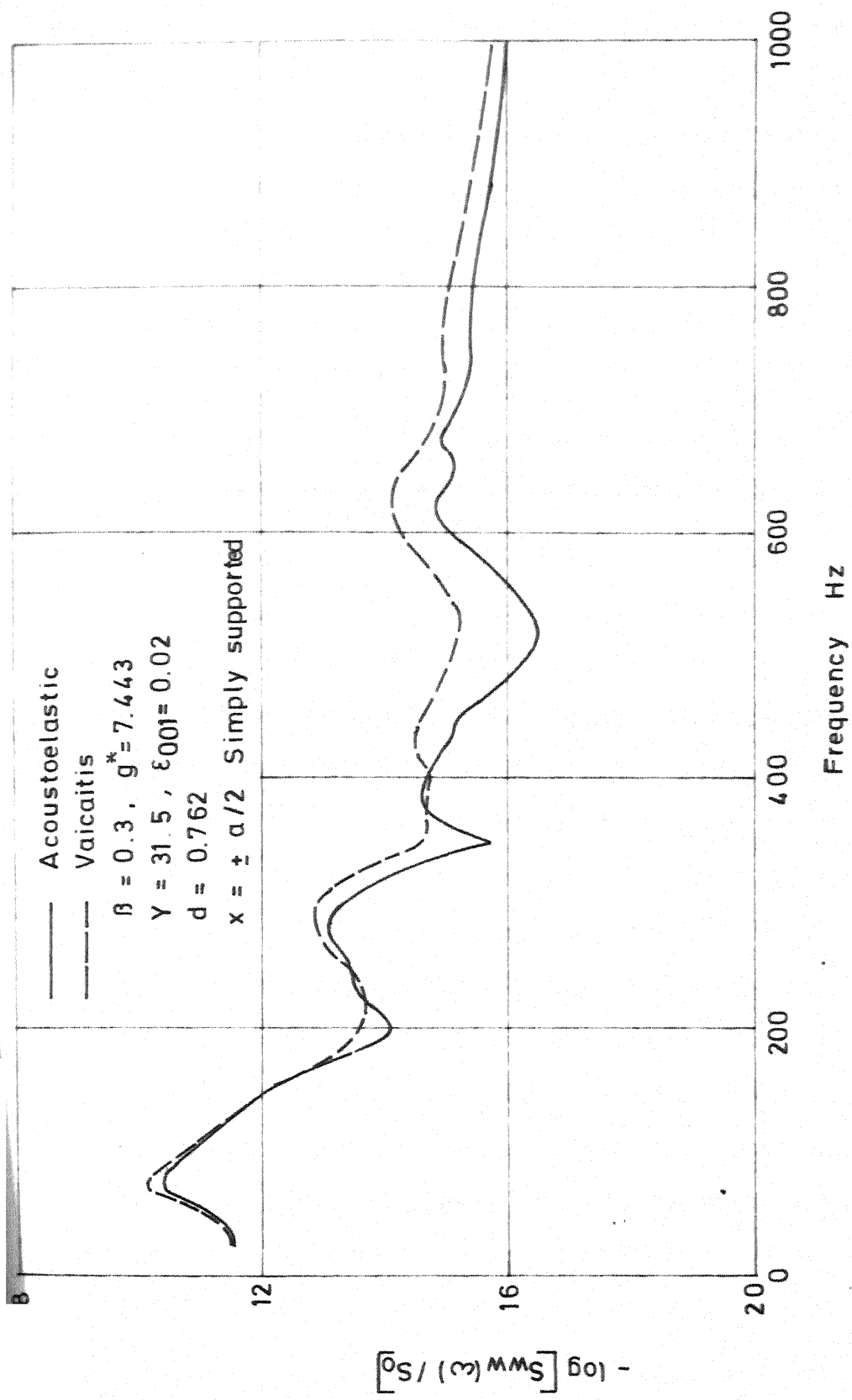


FIG. 4.4 COMPARISON OF DISPLACEMENT SPECTRAL DENSITIES BETWEEN VAICAITIS [3] AND ACOUSTOELASTIC FORMULATION

CPU time on a DEC10 computer for the acoustoelastic formulation considering a total number of 25 structural and cavity modes turned out to be 30 sec. for 40 frequency calculations. In the approximate formulation it turned out to be of the order of 1 minute.

Henceforth, the results obtained by the acoustoelastic formulation are presented.

#### 4.5.4 Effect of Plate Boundary Conditions

Figure 4.5 shows the variation of the noise reduction at the centre of the plate for different panel boundary conditions at  $x = \pm a/2$  and for a harmonic external pressure excitation with normal incidence. The trend of variation is the same for all the boundary conditions and beyond the fundamental structural resonant frequency, the noise reduction values do not differ by more than 4 dB at any frequency for the different boundary conditions. Below the first cavity resonance, (nonzero frequency) dips in the noise reduction curves occur at the first fundamental structural resonant frequency. The dip is most predominant in the case of transversely restrained edges and least noticeable for the case of fixed edges. The difference in the noise reduction values corresponding to these two curves is as high as 20 dB around these frequencies. The low noise reduction

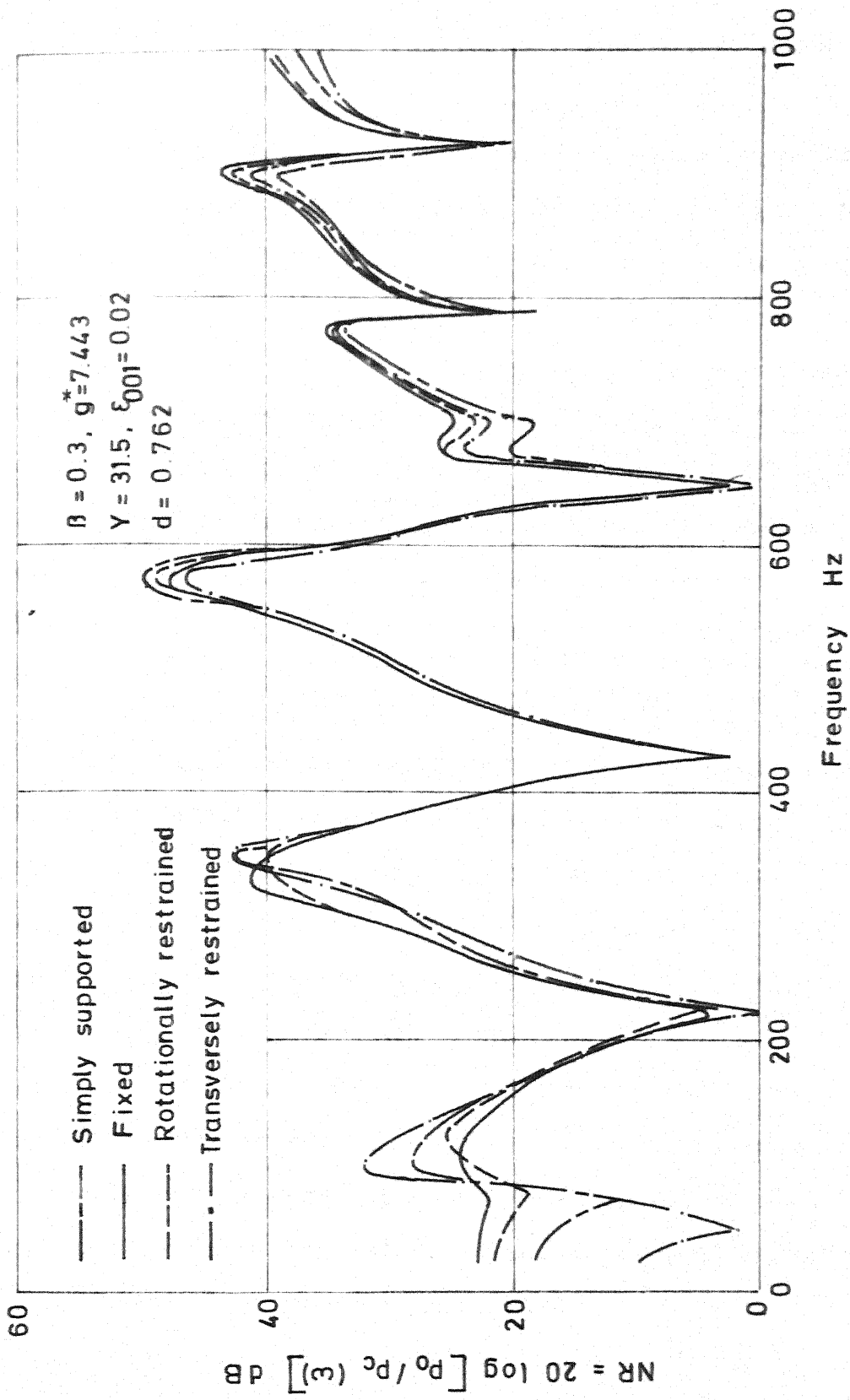


FIG. 4.5 EFFECT OF BOUNDARY CONDITIONS ON NOISE REDUCTION

value for the case of transversely restrained edges can be attributed to the low value of the modal loss factor as seen from Table 4.1. For the case of fixed edge conditions the high noise reduction value can likewise be related to the high modal loss factor corresponding to the first resonant frequency. For the case of rotationally restrained edges, there is virtually no change in the noise reduction curves between riveted and unriveted edges for the torsional stiffness parameter  $K_t$  chosen. Hence they are indistinguishable in the curves. The reason for such a behaviour can be found again in Table 4.1, where practically no difference is discernible in the natural frequencies' and loss factors' values for the two cases.

The noise reduction curves for a random external pressure excitation and for different y wise edge conditions are shown in Figure 4.6. The nature of the curves is very similar to that obtained in the case of harmonic excitation, as the random pressure field is weighted uniformly in all the frequency ranges being a white noise excitation, and spatially uniform. The deflection power spectral densities at the centre of the panel for these boundary conditions and external random excitation are shown in Figure 4.7. For all the boundary conditions, the displacement spectral density peaks nearly at the first structural resonant frequency, indicating that for the cavity depth adopted, the structural

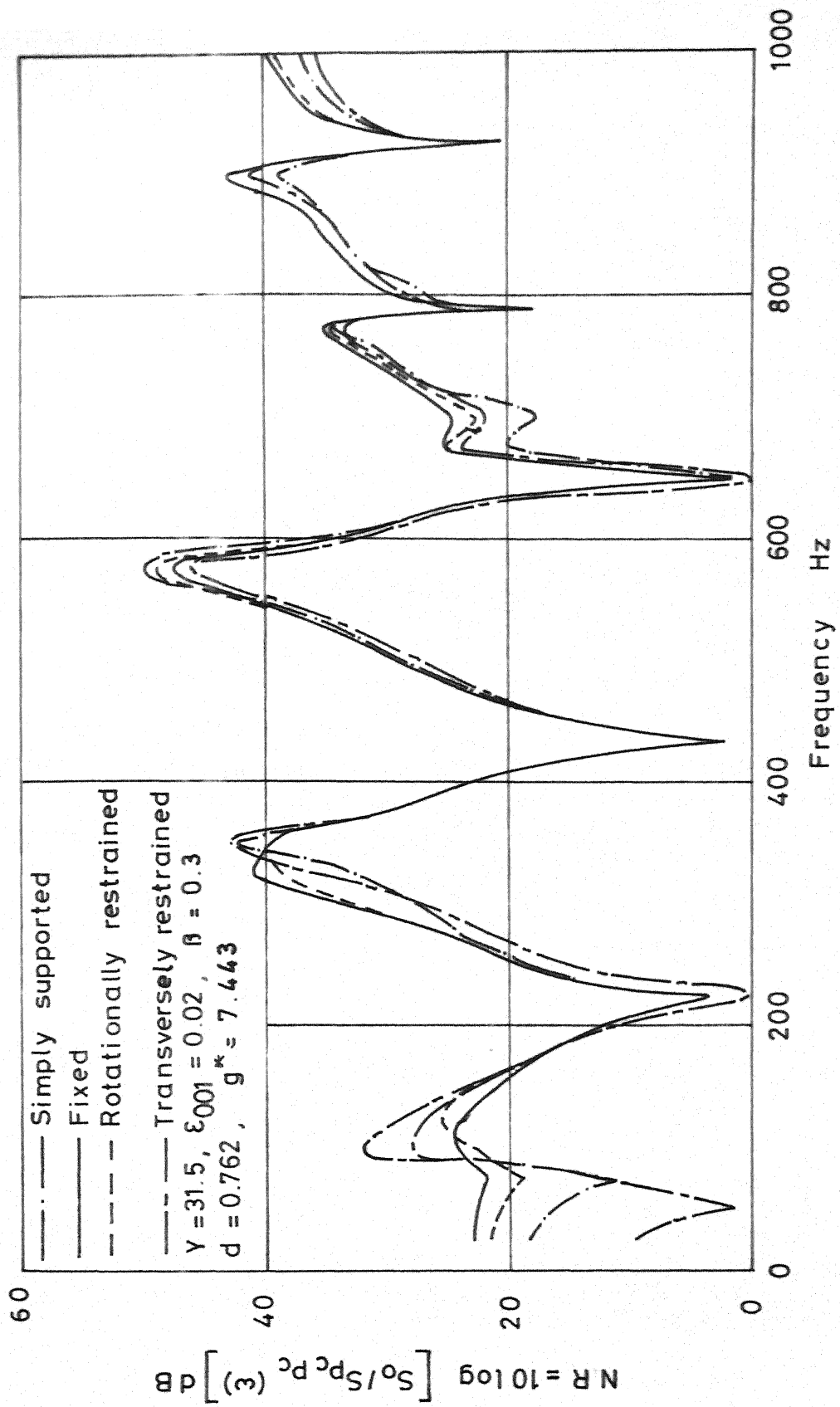


FIG. 4.6 EFFECT OF BOUNDARY CONDITIONS ON NOISE REDUCTION

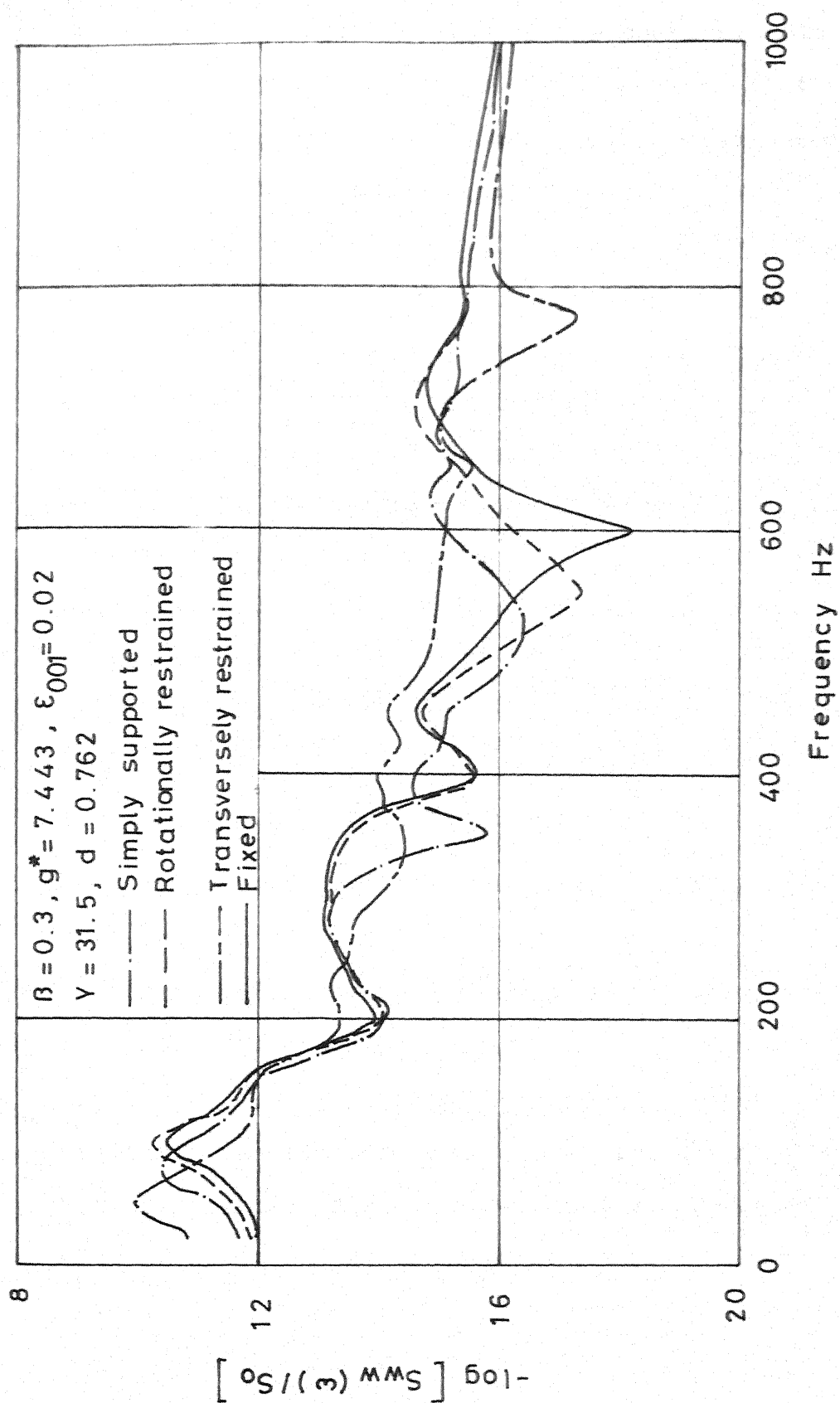


FIG. 4.7 EFFECT OF BOUNDARY CONDITIONS ON STRUCTURAL RESPONSE

resonances are not affected by the coupling action. The damping induced by the viscoelastic layer, flattens the peaks corresponding to other structural resonances. A careful scrutiny of the results reveals that the displacement maxima occur very nearly at the in-vacuo structural resonant frequencies and if there have been shifts in these peaks due to coupling action, they are not noticeable. The displacement response for the transversely restrained conditions is generally more than for other boundary conditions upto a frequency range of about 600 Hz, persumably because of the low modal loss factors associated with this boundary condition. For high frequencies above 800 Hz the response spectral density becomes almost independent of the nature of boundary conditions.

#### 4.5.5 Effect of Core Loss Factor

The change in noise transmission characteristics of the sandwich panel with respect to the core loss factor  $\beta$  is shown in Figures 4.8 and 4.9, respectively for simply supported and fixed edge conditions at the y wise edges and for external white noise excitation. For  $\beta = 0$  representing an elastic core, apart from the dips at the cavity resonances, dips corresponding to structural resonances also occur in the noise reduction curves. These dips are not present for  $\beta = 0.3$  and 1.0, except for the first structural

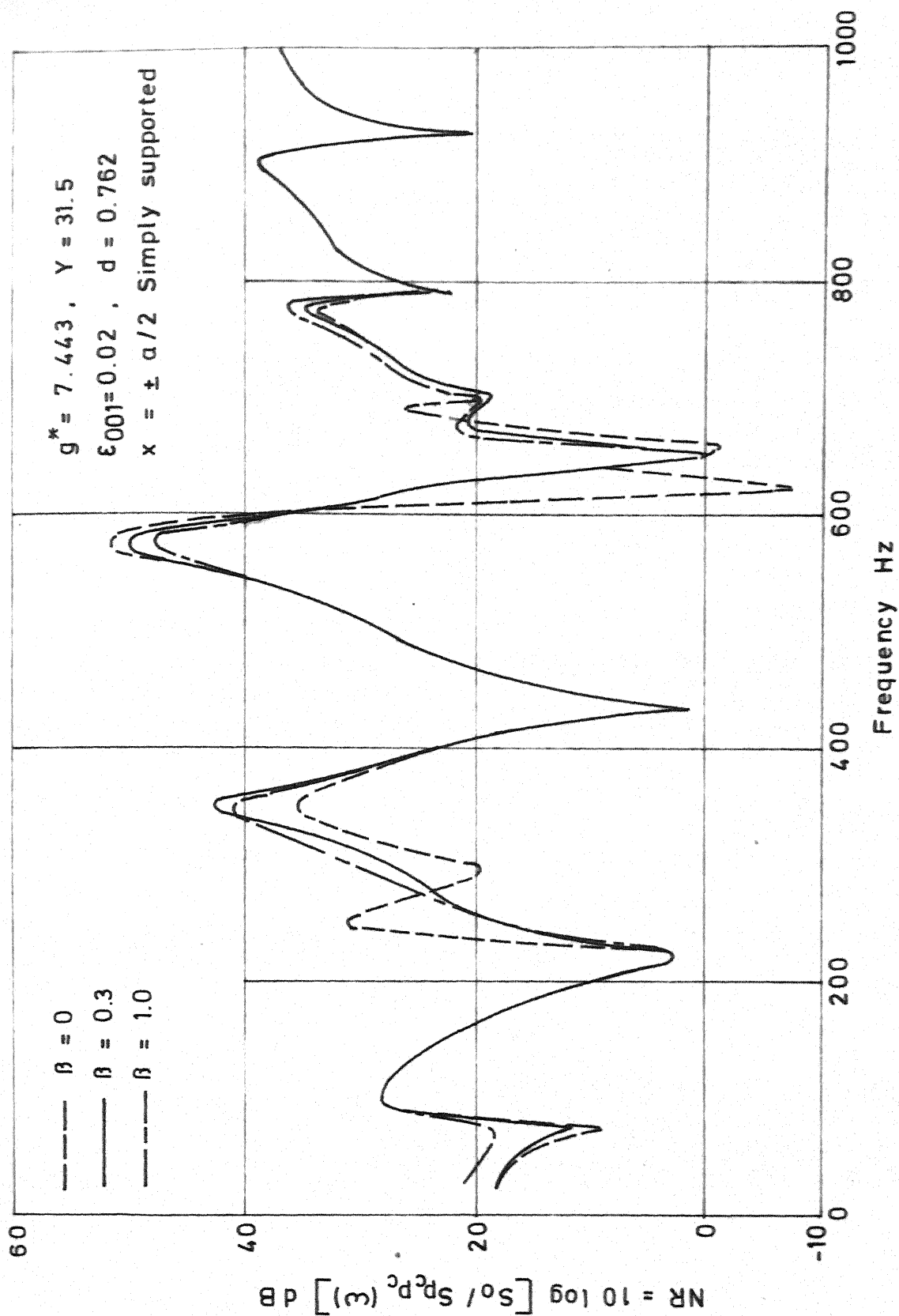
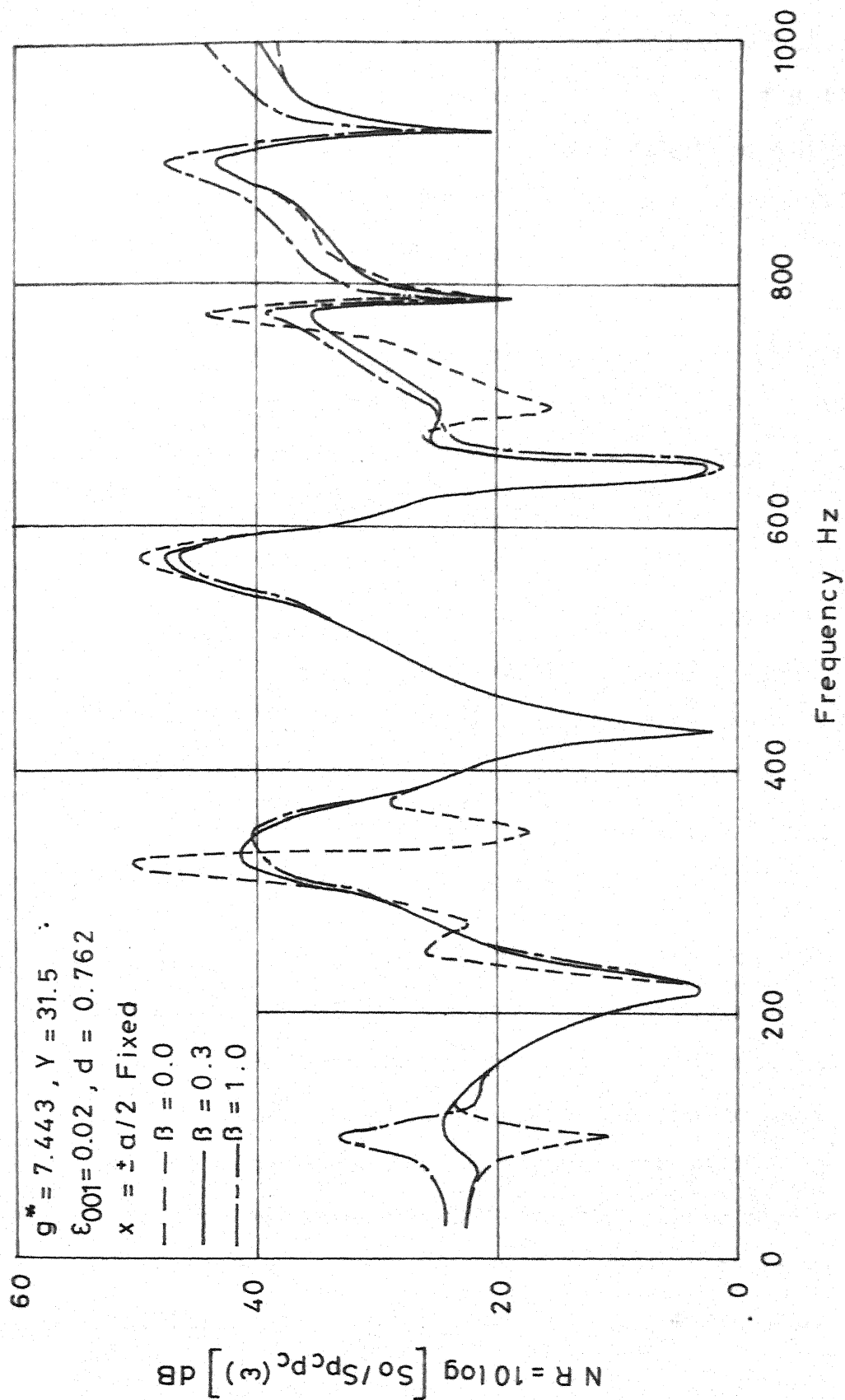


FIG. 4.8 EFFECT OF CORE LOSS FACTOR ON NOISE REDUCTION



CORE LOSS FACTOR ON NOISE REDUCTION

resonance. Even in that case, the noise reduction values are considerably higher for higher values of  $\beta$  than for  $\beta = 0$ . Increasing  $\beta$  has little effect on noise reduction values at cavity resonances. This observation agrees with that of Guy and Bhattacharya [53], who in their analysis of sound transmission through a cavity backed finite panel showed that the noise reduction at cavity resonances is independent of panel impedance. Figure 4.8 shows negative noise reduction values for  $\beta = 0$  around frequencies of 630 Hz and 650 Hz. It is so, because of the strong coupling of the ( $m = 5, n = 1$ ) structural mode which has a natural frequency of 628 Hz with the cavity mode ( $i=0, j=0, k=3$ ) which has a frequency of 649 Hz. Negative noise reductions have also been reported by Guy and Bhattacharya [53], and Mead [90] in connection with noise transmission studies of finite homogeneous panels. With increased  $\beta$  the noise reduction is slightly improved.

The displacement spectral density functions corresponding to the above two cases are shown in Figures 4.10 and 4.11. Increase in core loss factor significantly reduces the structural resonant responses as can be seen from the figures. Corresponding to a frequency of 630 Hz a large structural response results for the simply supported conditions because of the strong coupling between the structural mode and cavity modes earlier referred to, for an

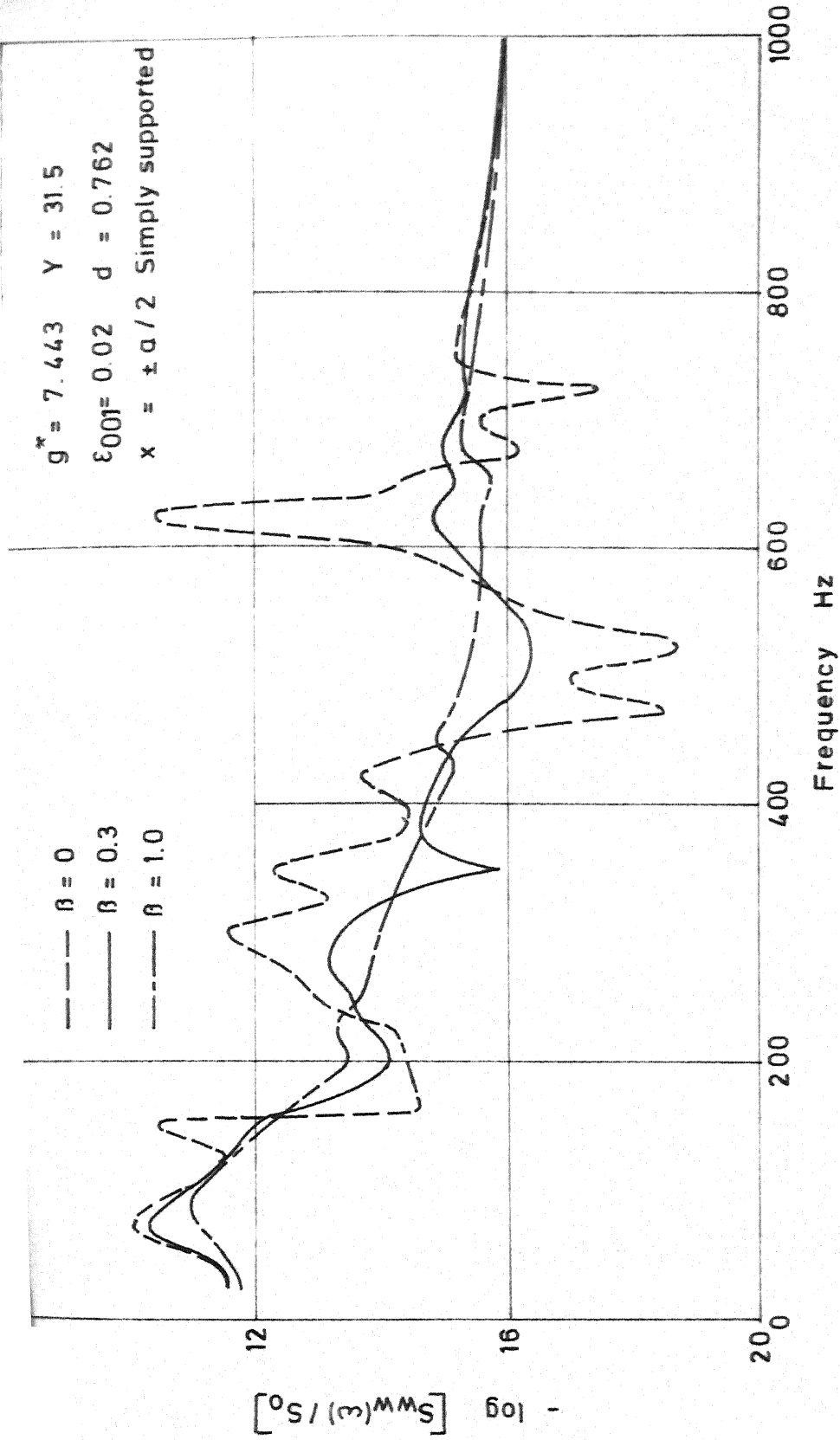


FIG. 4.10 EFFECT OF CORE LOSS FACTOR ON STRUCTURAL RESPONSE

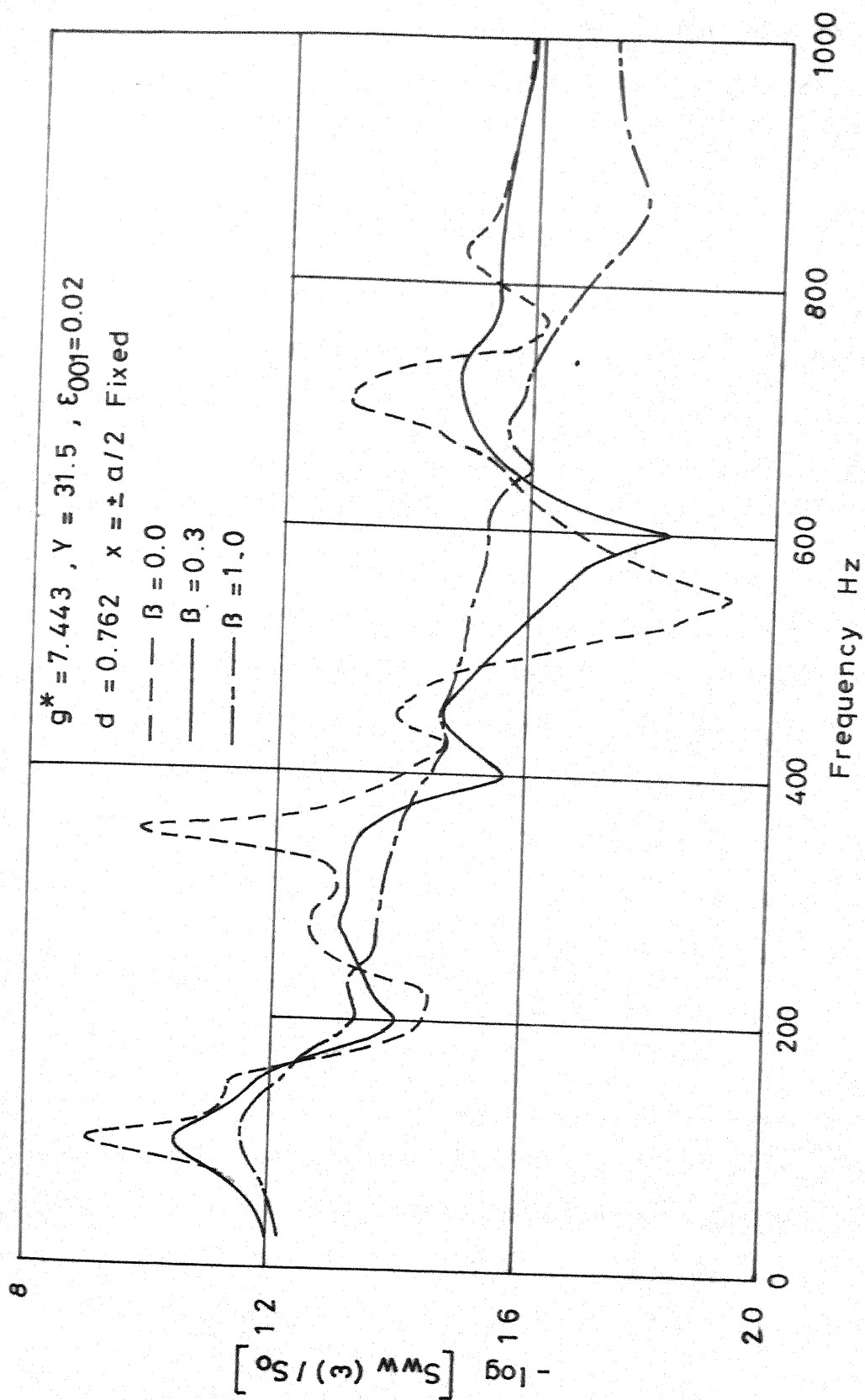


FIG. 4.11 EFFECT OF CORE LOSS FACTOR ON STRUCTURAL RESPONSE

elastic core. With increasing values of  $\beta$  the response at this coupled frequency is considerably reduced as seen from Figure 4.10.

#### 4.5.6 Effect of Shear Parameter

Figures 4.12 and 4.13 present noise reduction curves for different values of the core shear parameter  $g^*$ , respectively for simply supported and fixed edge conditions at  $x = \pm a/2$ . The external excitation is a white noise excitation. For the values of  $g^*$  chosen there are dips in the noise reduction curves corresponding to the first resonant frequency of the structure, in both cases of edge conditions. For  $g^* = 100$  and  $g^* = 1000$ , there are other dips corresponding to structural resonances. This is due to the fact that the modal loss factors corresponding to those values of  $g^*$  are very less. At low frequencies corresponding to  $g^* = 1000$ , negative noise reduction values are obtained around 126 Hz which is the first resonant frequency of the structure. It agrees with the earlier observation in section 4.4 that for low values of  $\eta_{ms}$  and  $\omega_{ms}^{*2}$  the noise reduction could have negative values as seen from equation (4.69). For  $g^* = 1.0$  the noise reduction at 225 Hz is very nearly zero indicating a strong coupling between a structural mode ( $\omega_{33} = 228$  Hz) and a cavity mode ( $\omega_{001} = 216.5$  Hz). For  $g^* = 7.44$  such coupling arises

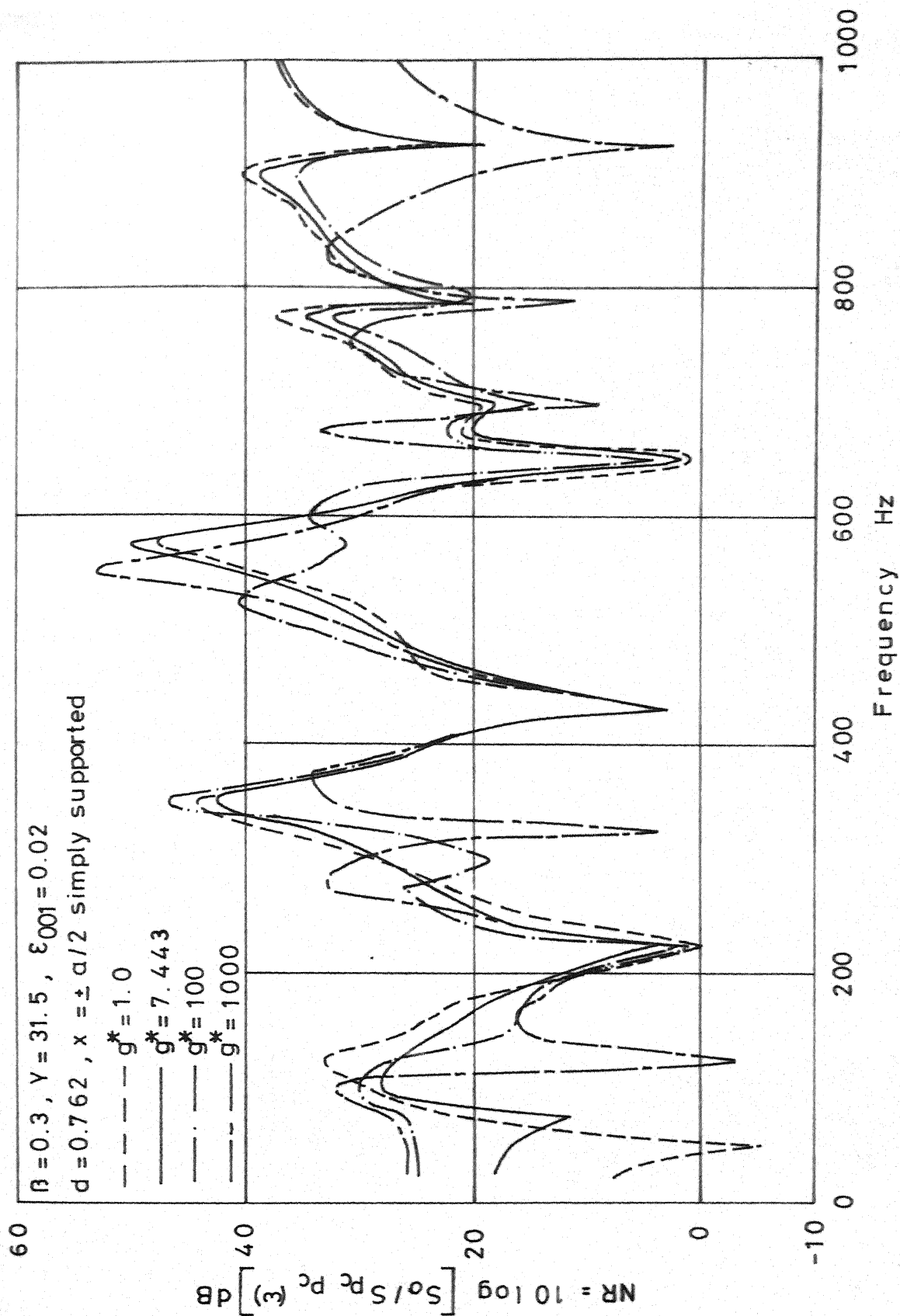


FIG. 4.12 EFFECT OF SHEAR PARAMETER ON NOISE REDUCTION

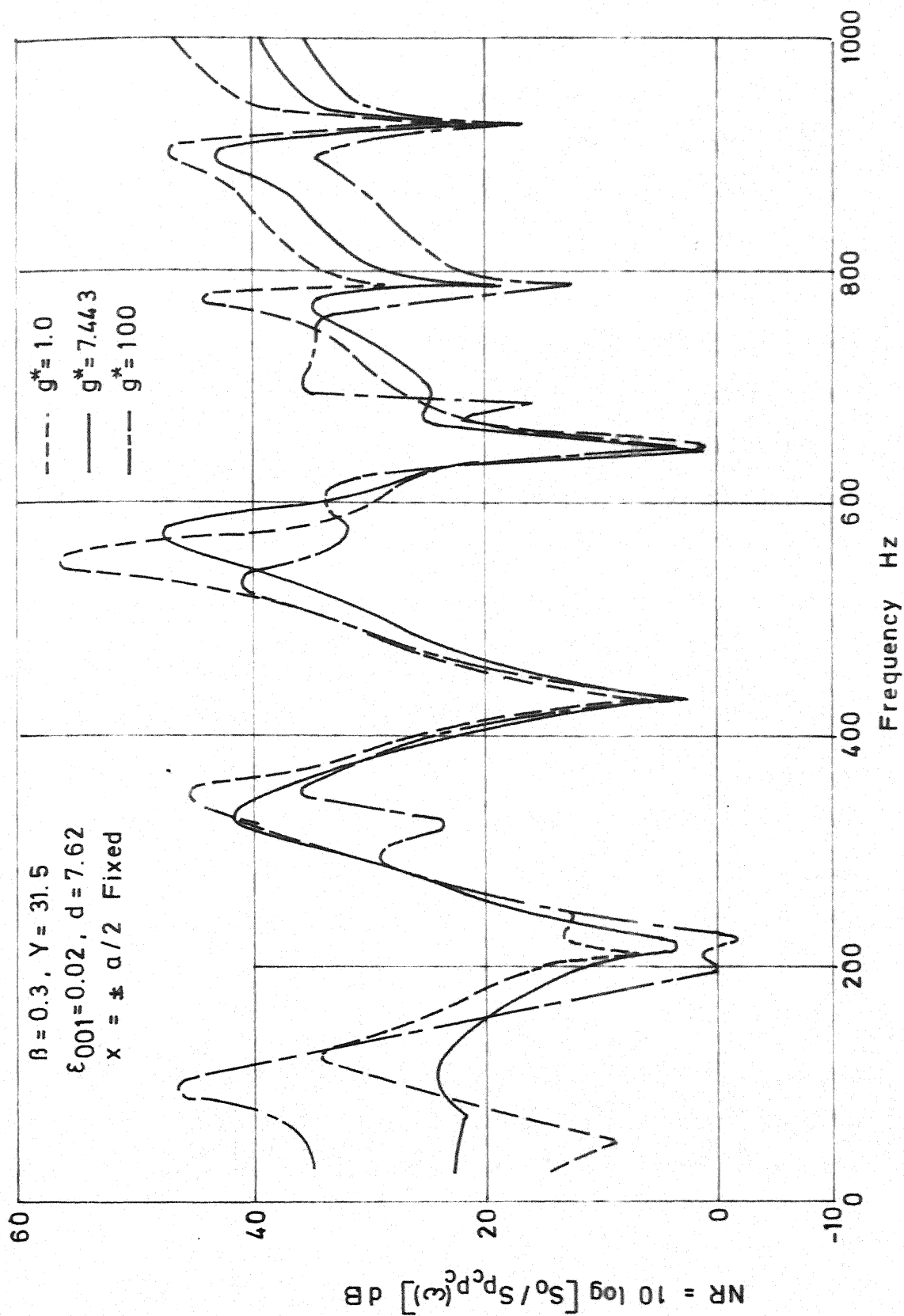


FIG. 4.13 EFFECT OF SHEAR PARAMETER ON NOISE REDUCTION

between structural modes (  $\omega_{51}^* = 627 \text{ Hz}$ ,  $\omega_{53}^* = 665 \text{ Hz}$  ) and the cavity modes (  $\omega_{003} = 649 \text{ Hz}$  and  $\omega_{020} = 660 \text{ Hz}$  ) which is manifested by nearly zero noise reduction corresponding to a frequency of 650 Hz. In almost all cases considered there is a predominant dip around 650 Hz which is due to the coupling between the two proximate acoustic modes of  $\omega_{003} = 649 \text{ Hz}$  and  $\omega_{020} = 660 \text{ Hz}$ . The noise reduction values are considerably higher for higher values of  $g^*$  till about 125 Hz. In the fixed end conditions, there are coupled resonance conditions around frequencies of 200 - 225 Hz and 650 Hz as seen from Figure 4.13.

Figures 4.14 and 4.15 respectively, show the response spectral densities for the above cases. The frequencies at which the response peaks are slightly shifted to the right from the in-vacuo resonant frequencies for the lower order modes. This is because of the proximity of these modes to the rigid cavity mode  $\omega_{000} = 0$ . The closer the structural resonant frequencies are to  $\omega_{000}$ , the greater is the shift to the right. The structural response is generally lower for  $g^* = 7.44$  than for  $g^* = 1$  or 100 because of the relatively higher modal loss factors, in the simply supported conditions. The structural response is the highest for  $g^* = 1000$ .

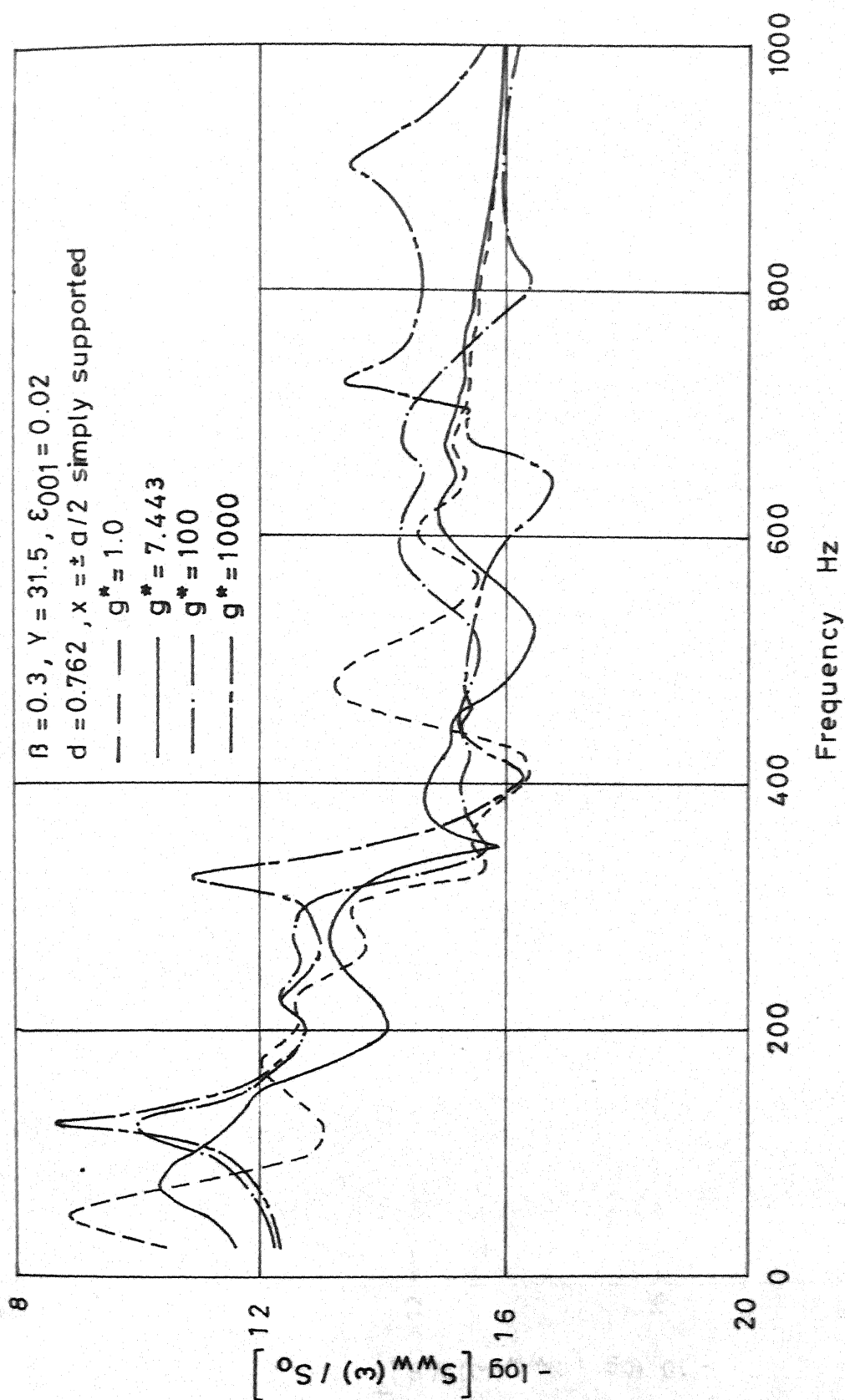


FIG. 4.14 EFFECT OF SHEAR PARAMETER ON STRUCTURAL RESPONSE

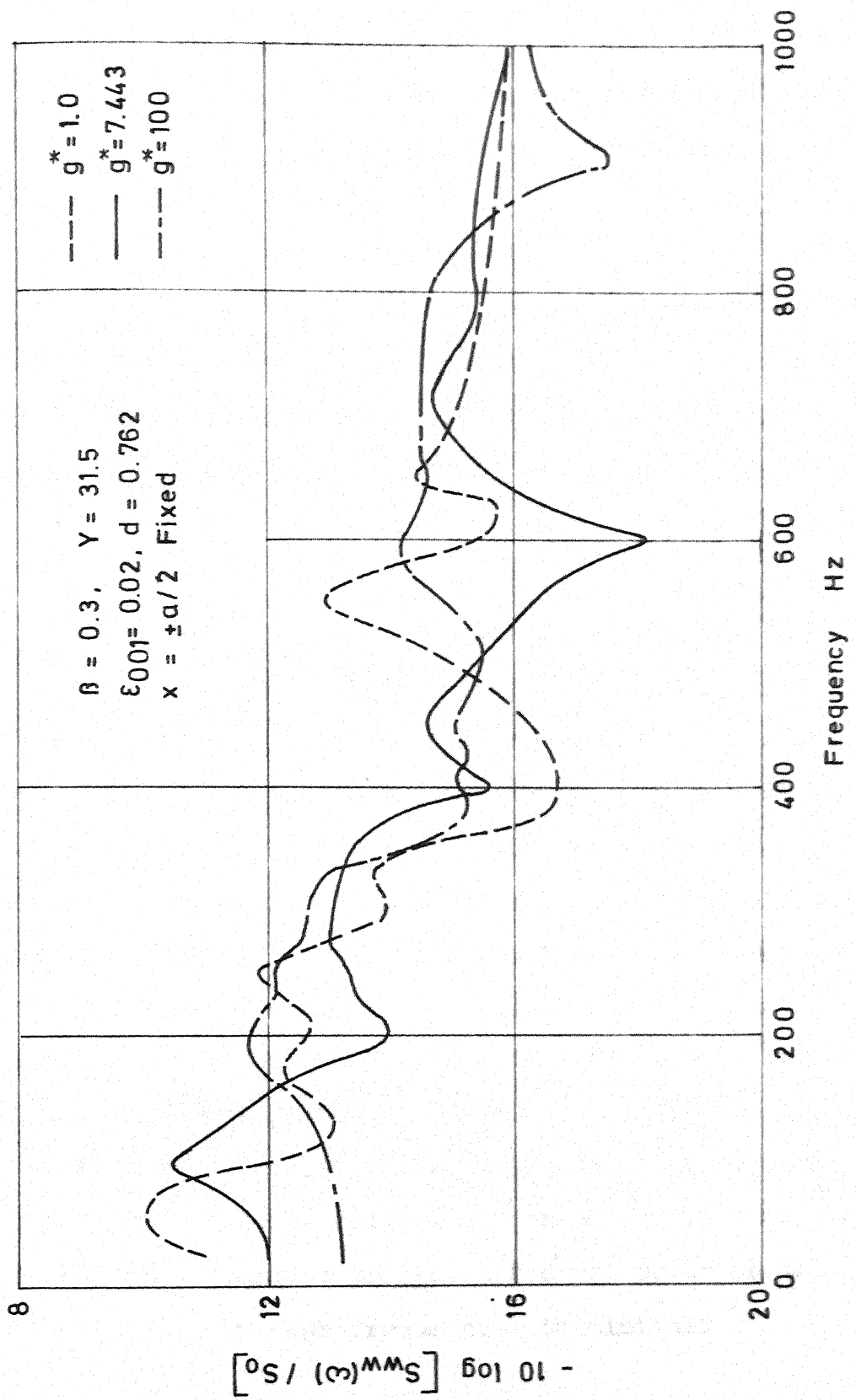


FIG. 4.15 EFFECT OF SHEAR PARAMETER ON STRUCTURAL RESPONSE

#### 4.5.7 Effect of Geometric Parameter

Figures 4.16 and 4.17 show the effect of the core geometric parameter  $Y$  on the noise reduction inside the cavity. Three representative values of  $Y$  corresponding to thin, medium and thick cores are chosen. Figure 4.16 shows for the simply supported conditions, negative or zero noise reduction values for  $Y = 3.63$ , corresponding to frequencies of 45 Hz, 225 Hz and 650 Hz. It is attributed again to the strong coupling between structural resonances and cavity resonances ( $\omega_{11}^* = 38.21$  Hz,  $\omega_{000} = 0$ ); ( $\omega_{31}^* = 206$  Hz and  $\omega_{001} = 216$  Hz) and ( $\omega_{55}^* = 642$  Hz and  $\omega_{003} = 649$  Hz,  $\omega_{200} = 660$  Hz) because of their close proximity. Such coupling exists for the fixed edge conditions because of the close proximity of the structural modes ( $\omega_{51}^* = 624$  Hz,  $\omega_{53}^* = 658$  Hz) and the cavity resonances ( $\omega_{003} = 649$  Hz and  $\omega_{200} = 666$  Hz). In fact, in all the noise reduction curves, a clear dip is shown at a frequency of 650 Hz because of the very strong coupling between the acoustic cavity modes  $\omega_{003} = 649$  Hz and  $\omega_{200} = 666$  Hz which are independent of the plate boundary conditions, damping and stiffness and depend only on the dimensions of the cavity. For very low frequencies below the fundamental resonance of the panel the noise reduction increases with increase in  $Y$ , but the effect of the geometric parameter on the noise reduction at high frequencies is minimal.

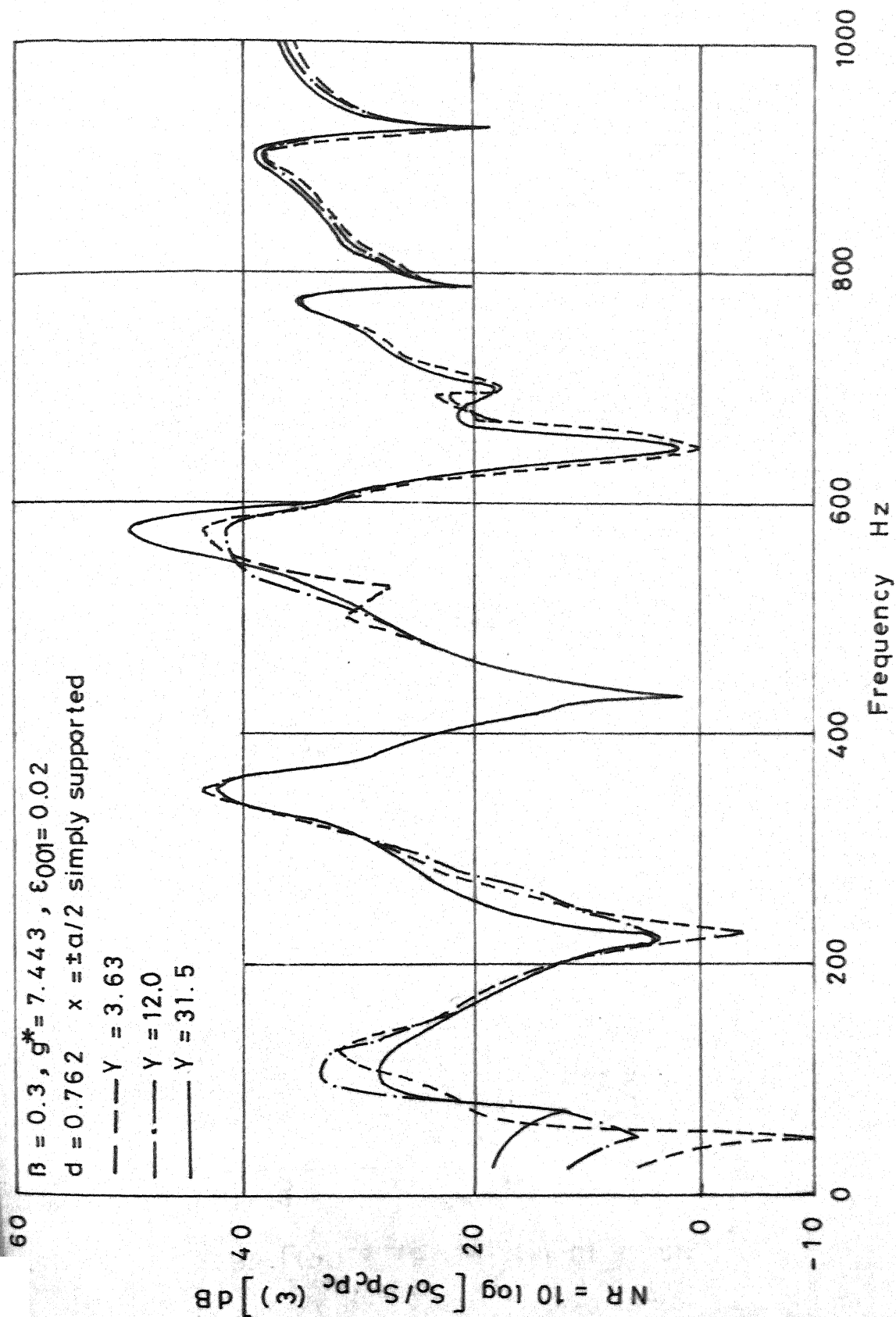


FIG. 4.16 EFFECT OF GEOMETRIC PARAMETER ON NOISE REDUCTION

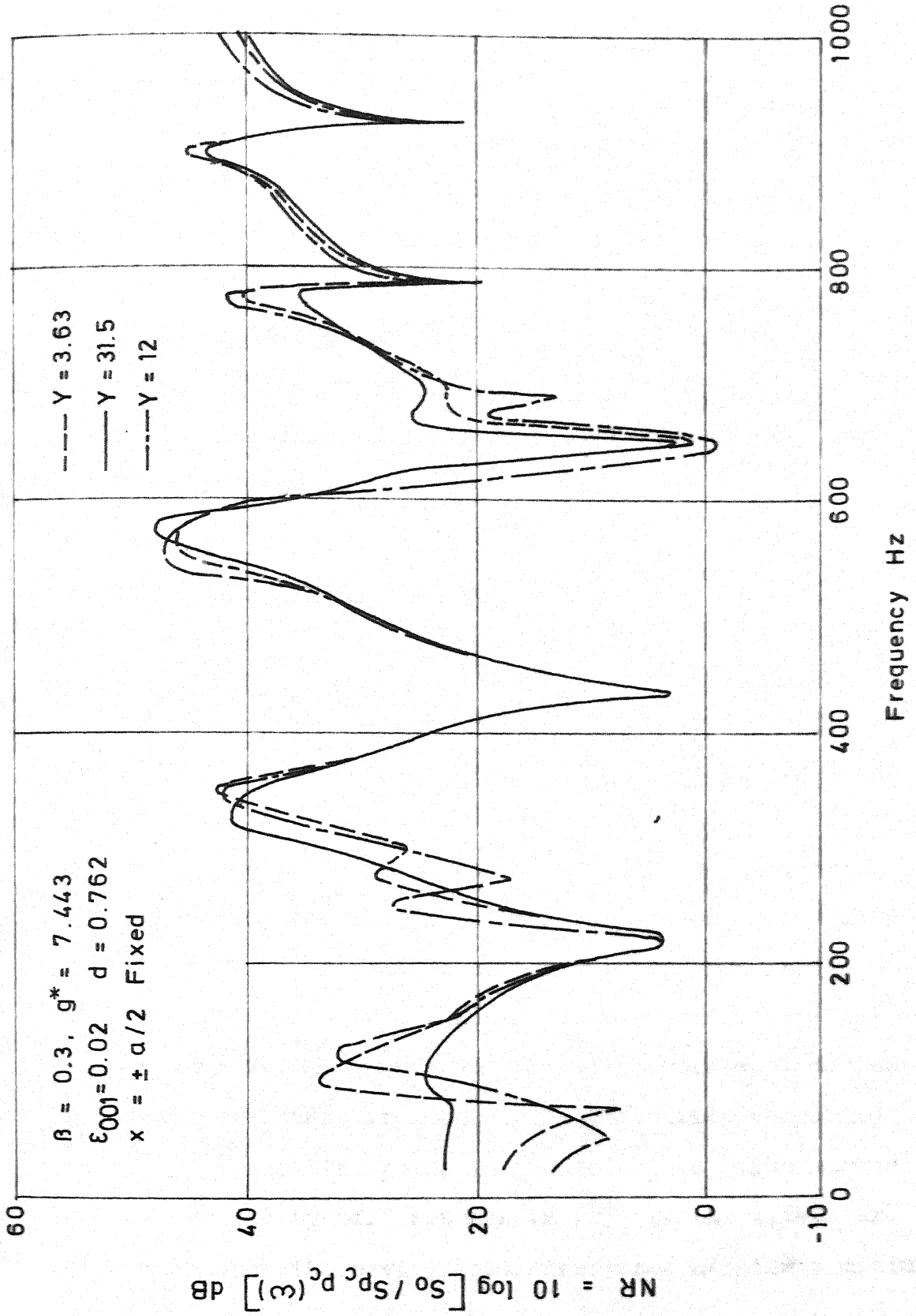


FIG. 4.17 EFFECT OF GEOMETRIC PARAMETER ON NOISE REDUCTION

Figures 4.18 and 4.19 present the structural response variation with  $Y$  for the two boundary conditions. For  $Y = 3.63$  the first peak in the structural response is perceptibly shifted to the right by about 10 Hz both in the simply supported and fixed cases. It is due to the effect of the rigid cavity mode  $\omega_{000} = 0$  which adds to the stiffness of the plate. The coupled structural-cavity natural frequency can be approximately calculated from equation (4.71). The calculations agree well with the frequency of the first structural response peak.

#### 4.5.8 Effect of Cavity Damping

Figures 4.20 to 4.23 show the effect of cavity damping on noise reduction and structural response respectively. The other conditions are shown in the figures. Increase in cavity damping flattens the noise reduction curves at the cavity resonances and increases the noise reduction considerably at the lower order cavity resonances. For higher frequencies, the effect of cavity damping on noise reduction is not appreciable. However, increased cavity damping brings down the maximum noise reduction values as the cavity impedances at these frequencies increase with increased cavity damping. The peaks in the noise reduction curves are termed as 'cavity off' resonances [53] in the literature and occur when the cavity modal impedance attains a minimum

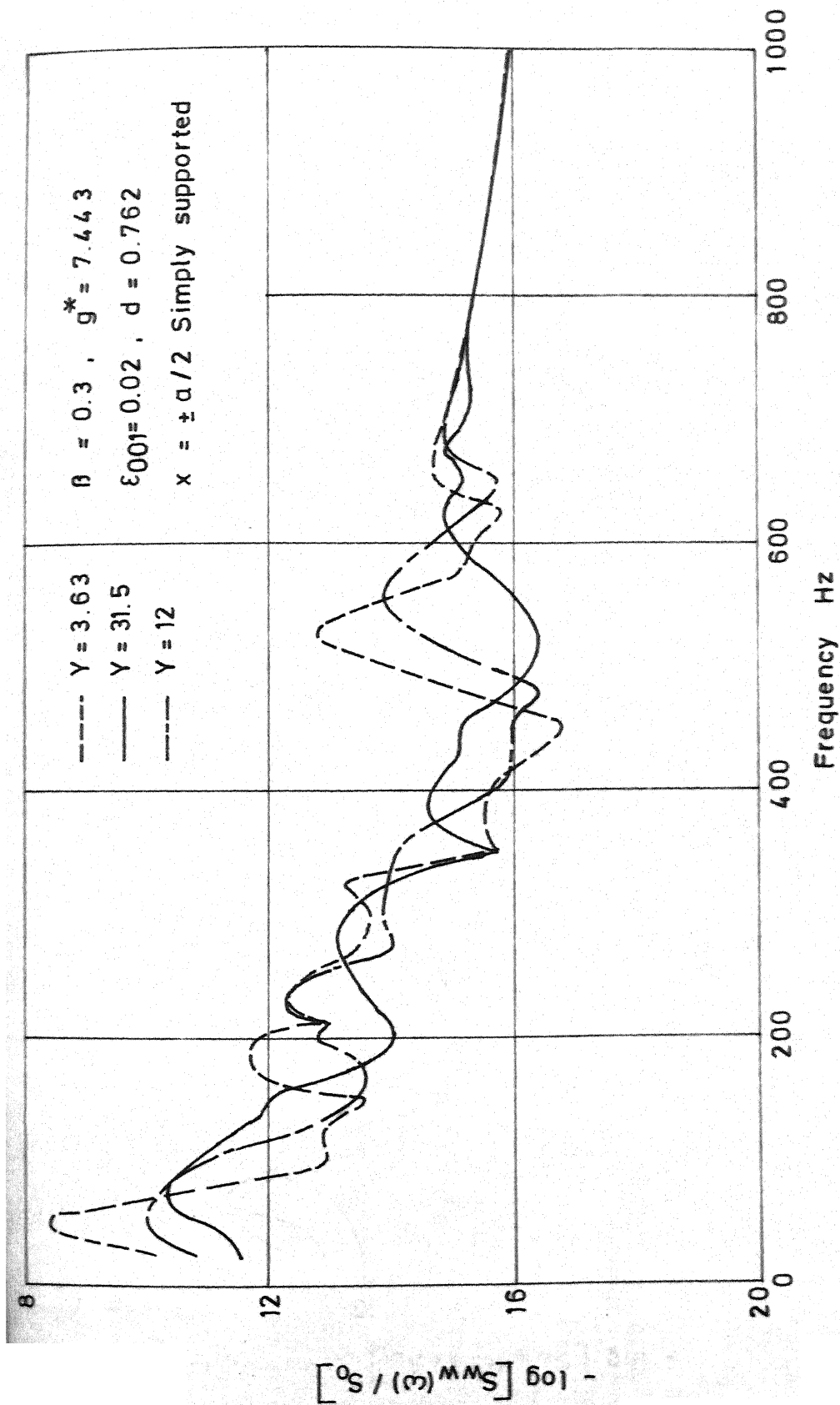


FIG. 4.18 EFFECT OF GEOMETRIC PARAMETER ON STRUCTURAL RESPONSE

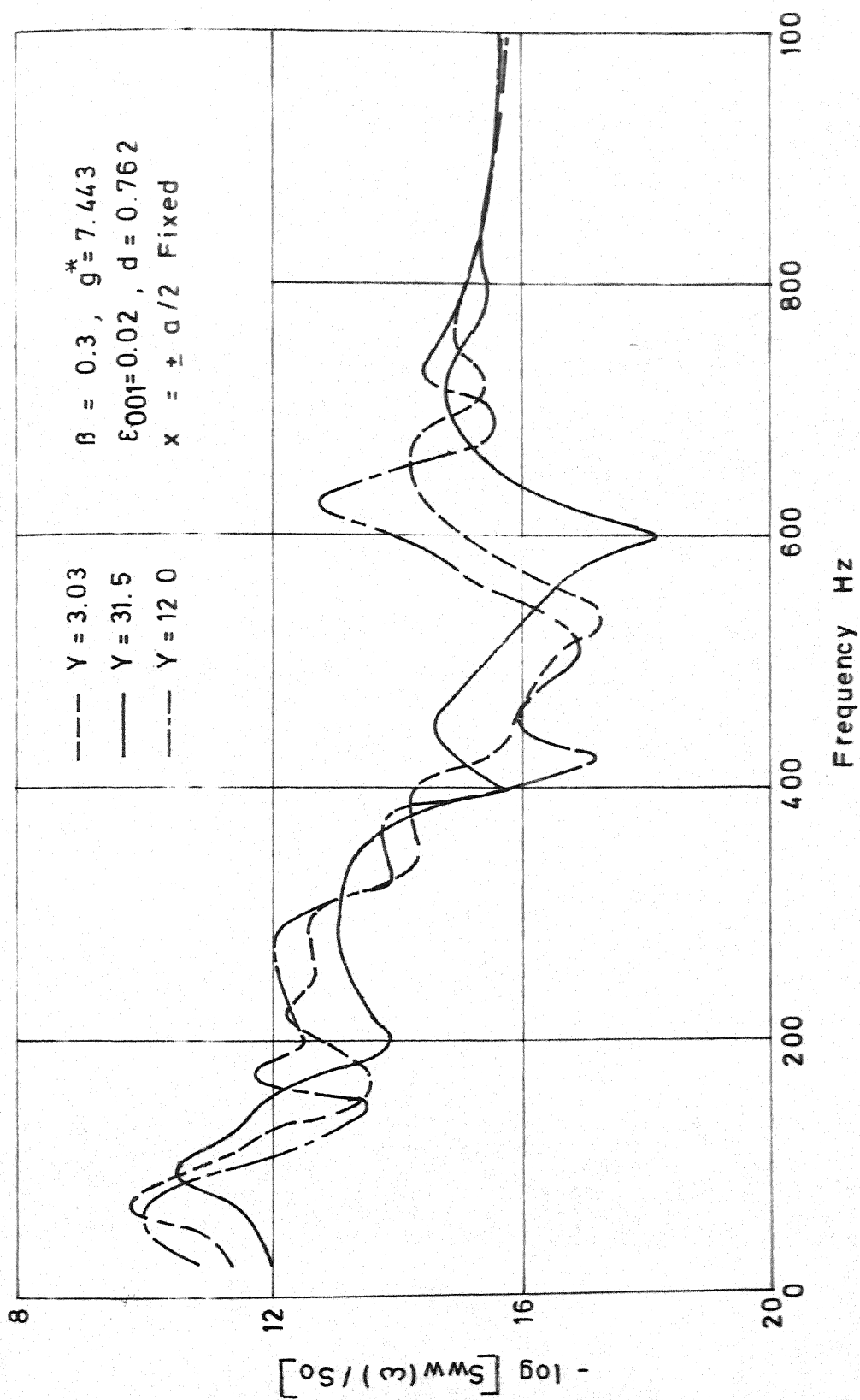


FIG. 4.19 EFFECT OF GEOMETRIC PARAMETER ON STRUCTURAL RESPONSE

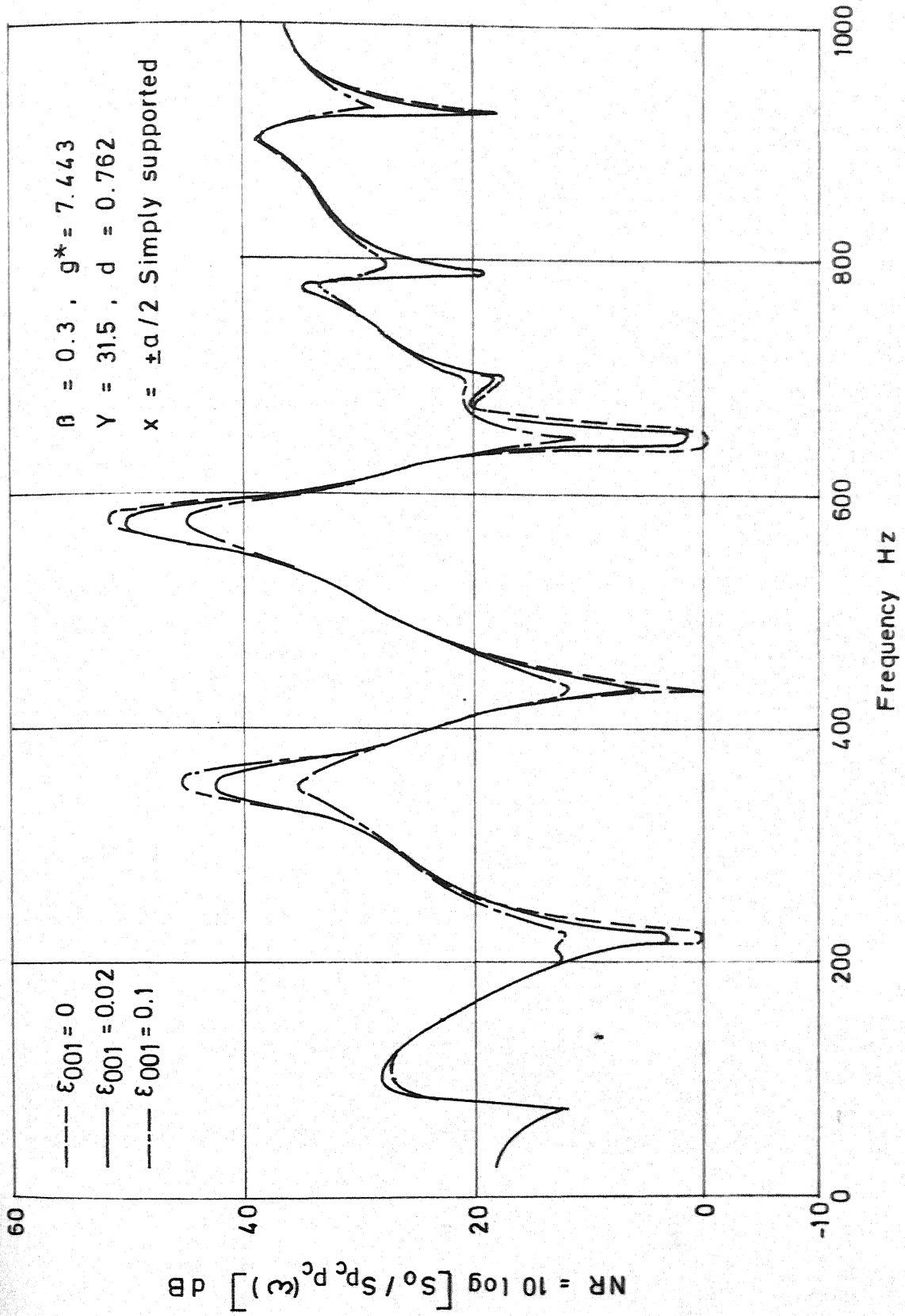


FIG. 4.20 EFFECT OF CAVITY DAMPING ON NOISE REDUCTION

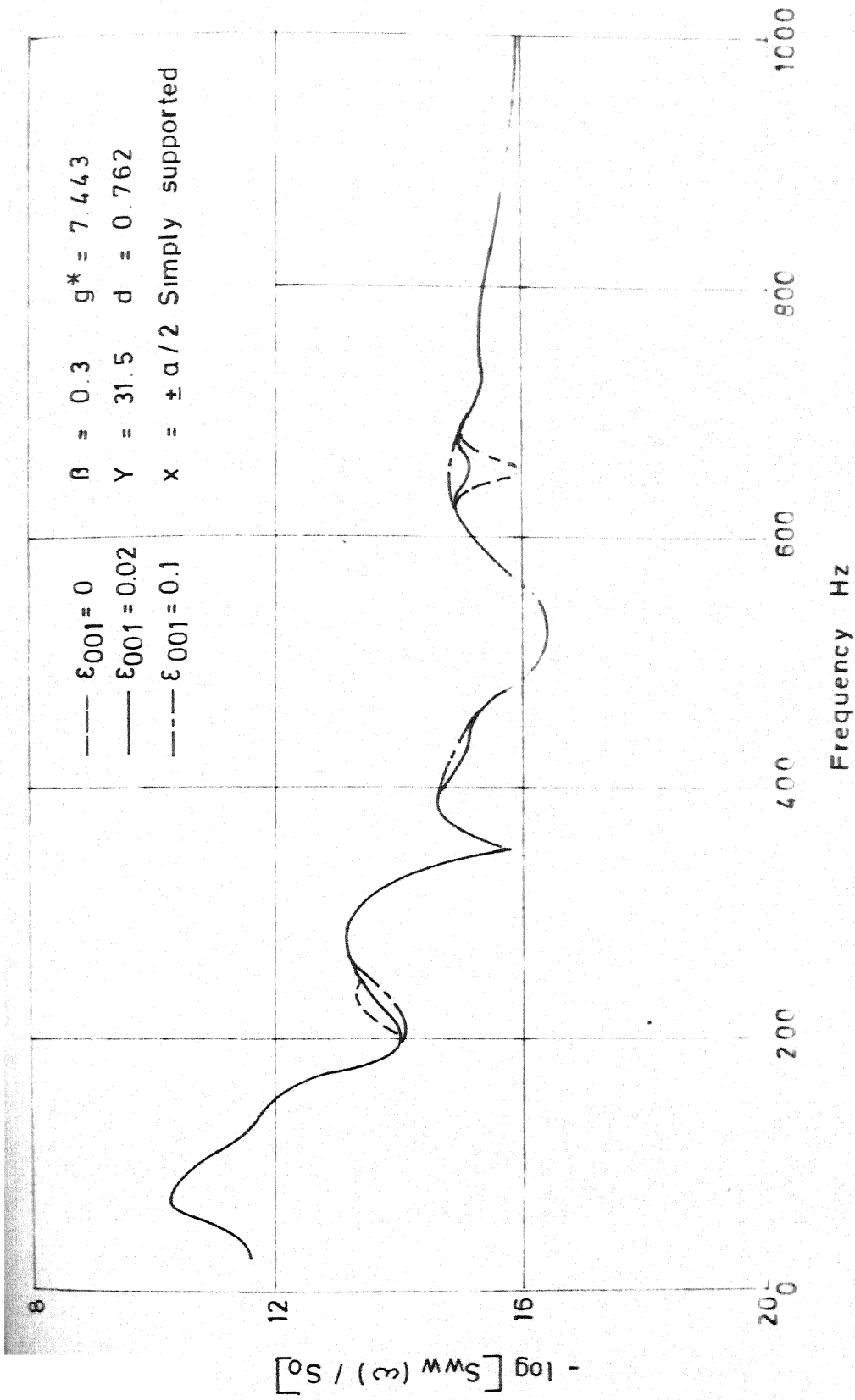


FIG 4.21 EFFECT OF CAVITY DAMPING ON STRUCTURAL RESPONSE

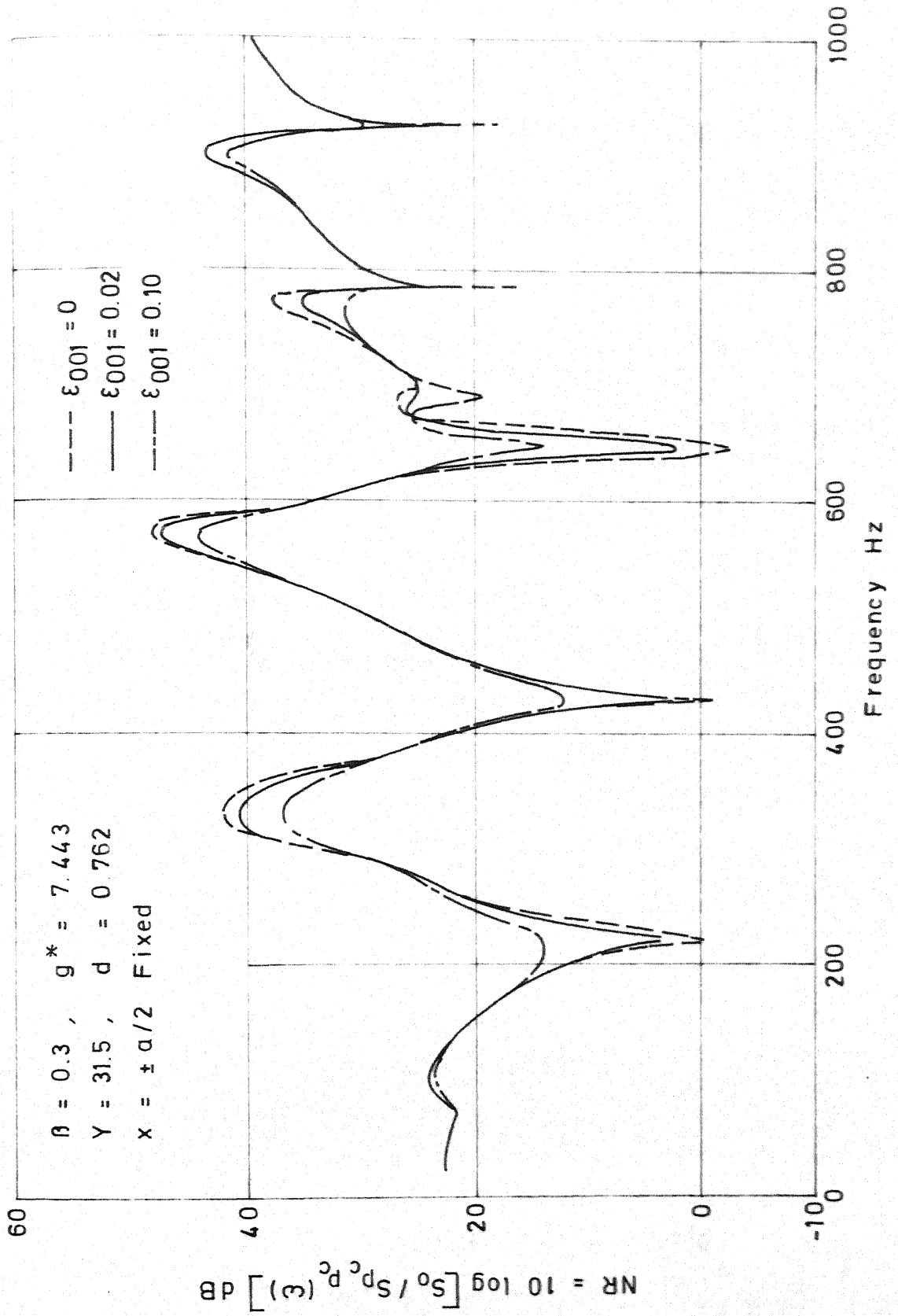


FIG. 4.22 EFFECT OF CAVITY DAMPING ON NOISE REDUCTION

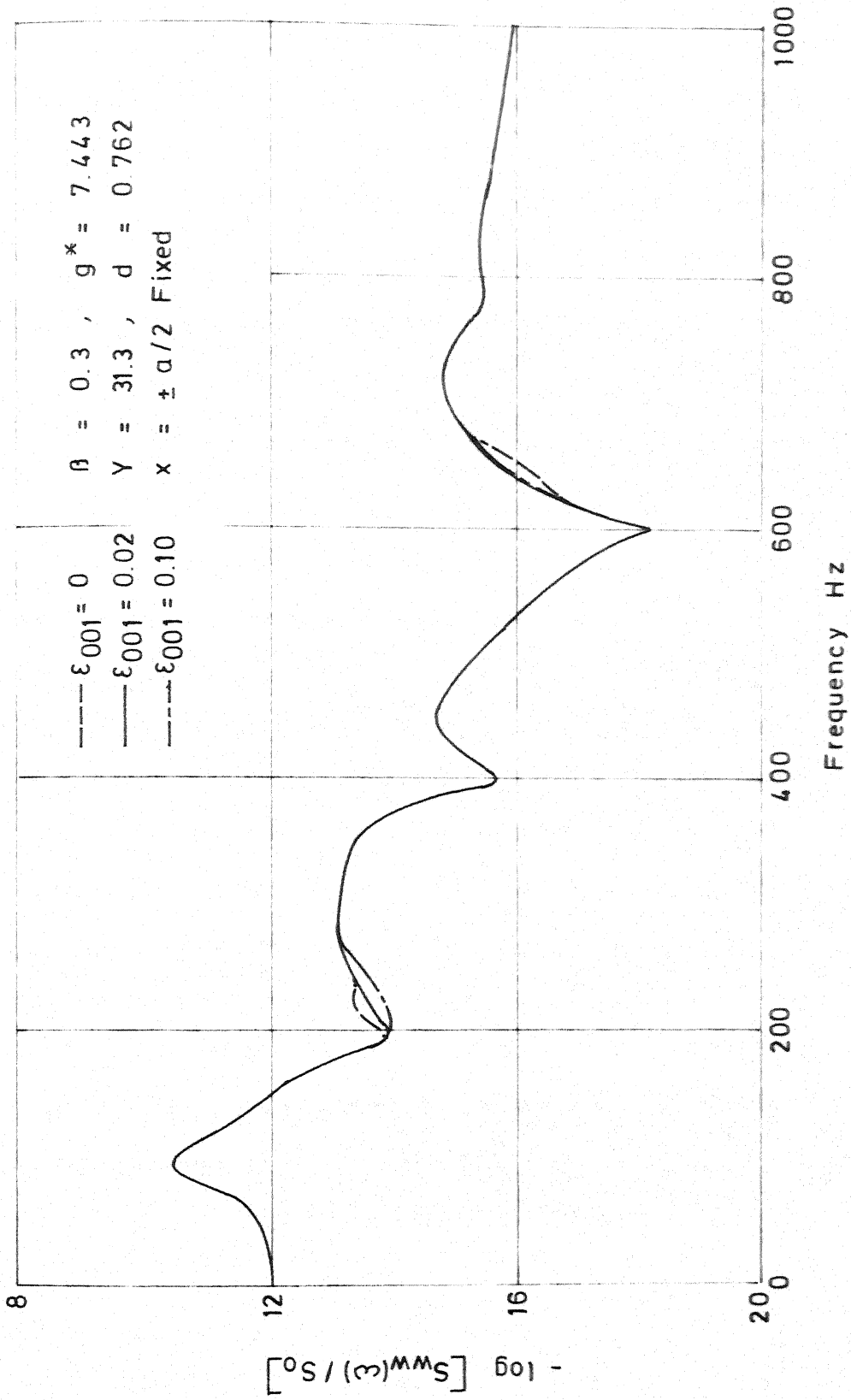
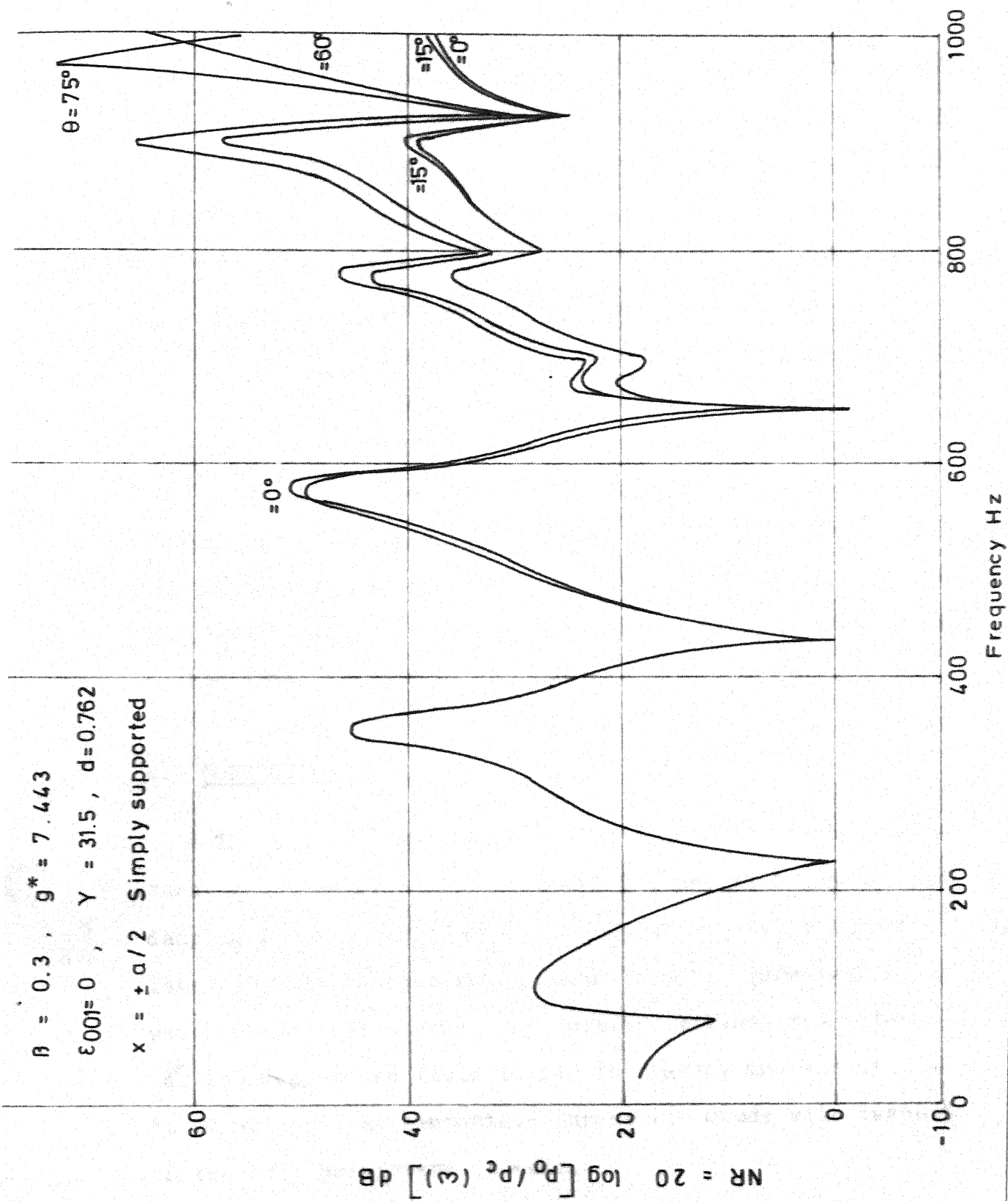


FIG. 4.23 EFFECT OF CAVITY DAMPING ON STRUCTURAL RESPONSE

value. For higher frequencies the cavity damping does not have significant effect on noise reduction, because the modal damping coefficient defined in equation (4.11) varies inversely as the square of the cavity resonant frequency. Cavity damping has little effect on the structural response as depicted by Figure 4.21, which also agrees the result of Guy and Bhattacharya [53].

#### 4.5.9 Effect of Incidence Angle

The noise reduction curves shown for harmonic excitation so far correspond to normal incidence of the external pressure excitation. Figure 4.24 shows the noise reduction curves for different incidence angles. It is observed that the incident angle has practically no effect on the noise reduction upto a frequency of 650 Hz. Above that frequency the noise reduction values increase with increasing angles of incidence which behaviour is quite different from that of the infinite sandwich panel. However the dips in the noise reduction curves which may be likened to the coincidence of finite panels described by Bhattacharya, Guy and Crocker [54] occur at frequencies independent of the incident angle.



#### 4.5.10 Effect of Cavity Depth

The effects of changing the cavity depth on the noise reduction and structural response are shown in Figures 4.25 and 4.26 respectively. Increasing the cavity depth adds to the number of cavity modes and decreasing the cavity depth decreases the number of cavity modes in the frequency range of interest. Accordingly the dips in the noise reduction curves change depending on the coupling between a structural mode and cavity mode. The change in the cavity depth has negligible effect on the structural response for the depths shown. However, for  $d = 1.524$  m the coupled natural frequency of the cavity panel system is shifted to 75 Hz, because the proximate acoustic cavity mode of 108 Hz is greater than the fundamental structural frequency of 81 Hz and hence adds to the total inertia of the panel.

#### 4.6 CONCLUSIONS

The noise transmission characteristics and the structural response of a finite sandwich panel with constrained damping layer, backed by a rectangular cavity is investigated in this chapter in an acoustoelastic formulation which takes into account the coupling between the internal sound pressure field inside the cavity and the structural motion. An exhaustive parametric study with respect to the core parameters is made.

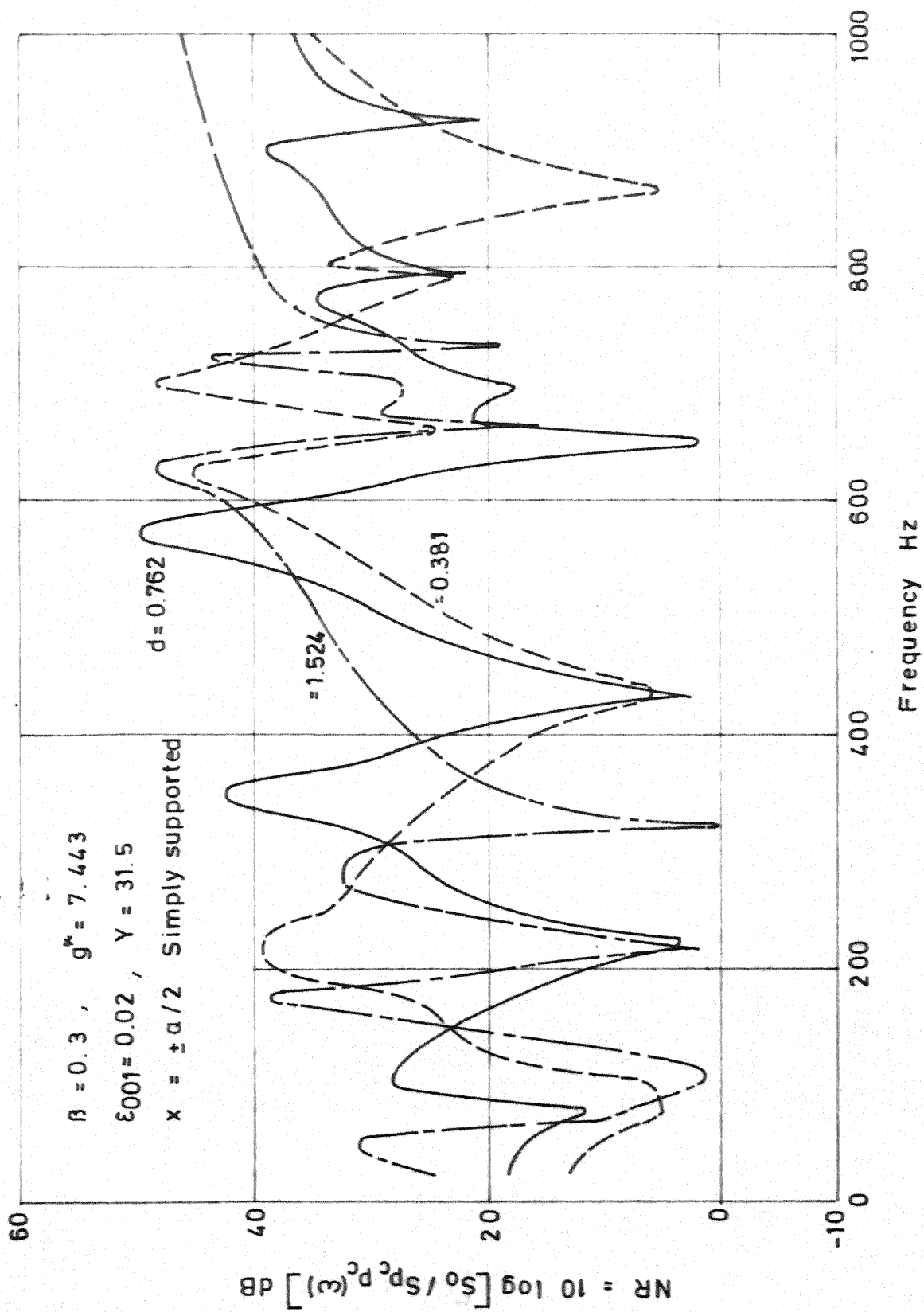


FIG. 4.25 EFFECT OF CAVITY DEPTH ON NOISE REDUCTION

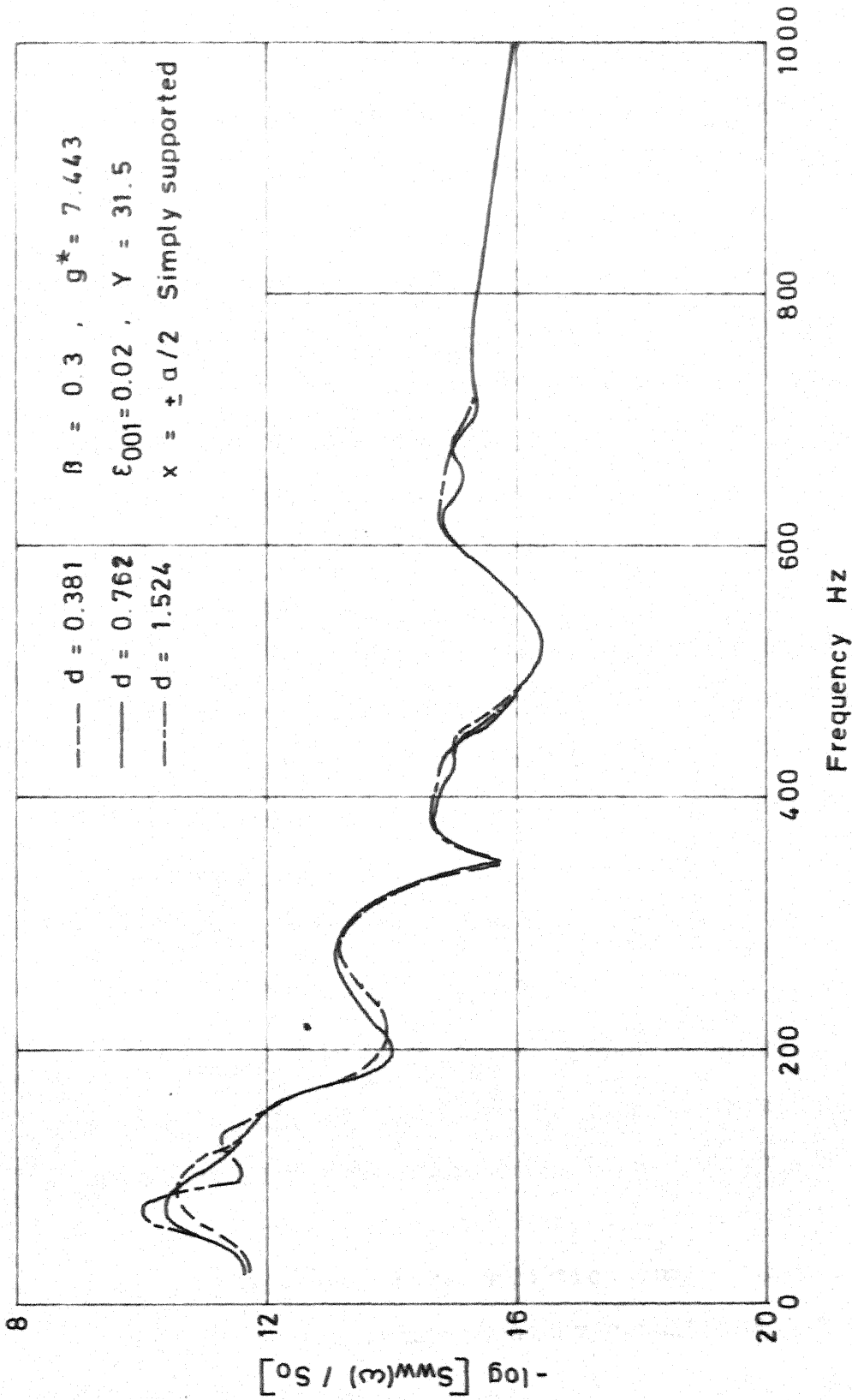


FIG. 4.26 EFFECT OF CAVITY DEPTH ON STRUCTURAL RESPONSE

The noise transmission characteristics of finite sandwich panels backed by a cavity are very similar to those of finite homogeneous panels. But because of the presence of the damping layer the noise transmission characteristics of the sandwich panel are considerably improved at the lower order structural resonant frequencies, especially at the panel's fundamental resonance. A proper choice of the core shear parameter  $g^*$  ensures large modal loss factors which improve the noise transmission characteristics of the sandwich and reduce the structural response at structural resonant frequencies. Thus the analysis presented indicates the existence of an optimum value of  $g^*$  for maximum damping effectiveness corresponding to the different structural modes. Increase in the core loss factor  $\beta$  has only marginal effect on the sound transmission at higher frequencies. But the effect of  $\beta$  is strongly exhibited in the structural response, which is considerably reduced by increase in  $\beta$  at the structural resonant frequencies.

The effect of the plate boundary conditions is noticeable only in the lower frequency ranges and is marginal at higher frequencies. This chapter clearly shows the efficacy of using the damped normal modes in response calculations and noise reduction computations, to take care of the arbitrary boundary conditions and arbitrary damping.

This chapter also presents a simple matrix inversion scheme to solve the coupled acoustoelastic problem, both for harmonic and random excitation which avoids the necessity of carrying out an eigenvalue analysis.

shells by including the effects of external flow, reflection and scattering of incident wave, internal cabin pressurization, cavity resonances and structural damping.

A survey of the literature, reveals that there is no work on the sound transmission characteristics of sandwich shells with additive damping treatments. In continuation of the investigation on the sound transmission through infinite sandwich panels and finite sandwich panels considered in Chapter 3 and Chapter 4, the noise transmission and structural response of finite closed circular cylindrical sandwich shells are analysed in this chapter. In addition to the treatment of the sandwich shell with constrained viscoelastic damping layer, the case of a layered shell with unconstrained damping treatments in different configurations of the damping layers is also considered in this chapter.

Full interaction between the internal cavity pressure field and the structural motion has been taken care of in an acoustoclastic formulation. Only the axisymmetric vibrations of the shell are considered in the analysis as the variation of the external pressure field along the circumference is assumed to be uniform. The shell ends are assumed to be simply supported which facilitates closed form solutions of the natural frequencies and the modal loss factors of the layered shell. There is no restriction on the formulation, if other boundary conditions are specified

at the shell ends, except that it would involve iterative procedures similar to that outlined in Chapter 2, in the determination of the natural frequencies and damped normal modes. Results are presented as noise reduction curves for both harmonic and random excitation. The shell response is also plotted as a function of frequency. The frequency range of interest has been restricted to 1000 Hz.

## 5.2 EQUATIONS OF MOTION FOR LAYERED SHELL WITH UNCONSTRAINED DAMPING LAYER TREATMENT

The layered cylindrical shell considered in this chapter consists of a thin circular elastic shell of finite length  $l$ , to which is applied an unconstrained viscoelastic damping layer. Three different types of layer constructions are considered. 1. Outside coating (OC), the damping treatment being applied on the outside of the elastic shell, (Fig.5.1(a)). 2. Inside coating (IC), the damping treatment being applied on the inside of the elastic shell, (Figure 5.1(b)). 3. Two-side coating (TC), the damping treatment being symmetrically applied both inside and outside of the elastic shell, (Figure 5.1(c)).

The equations of motion of the layered shell in axisymmetric vibration have been adopted from Markus [37], who derived them under the following assumptions.

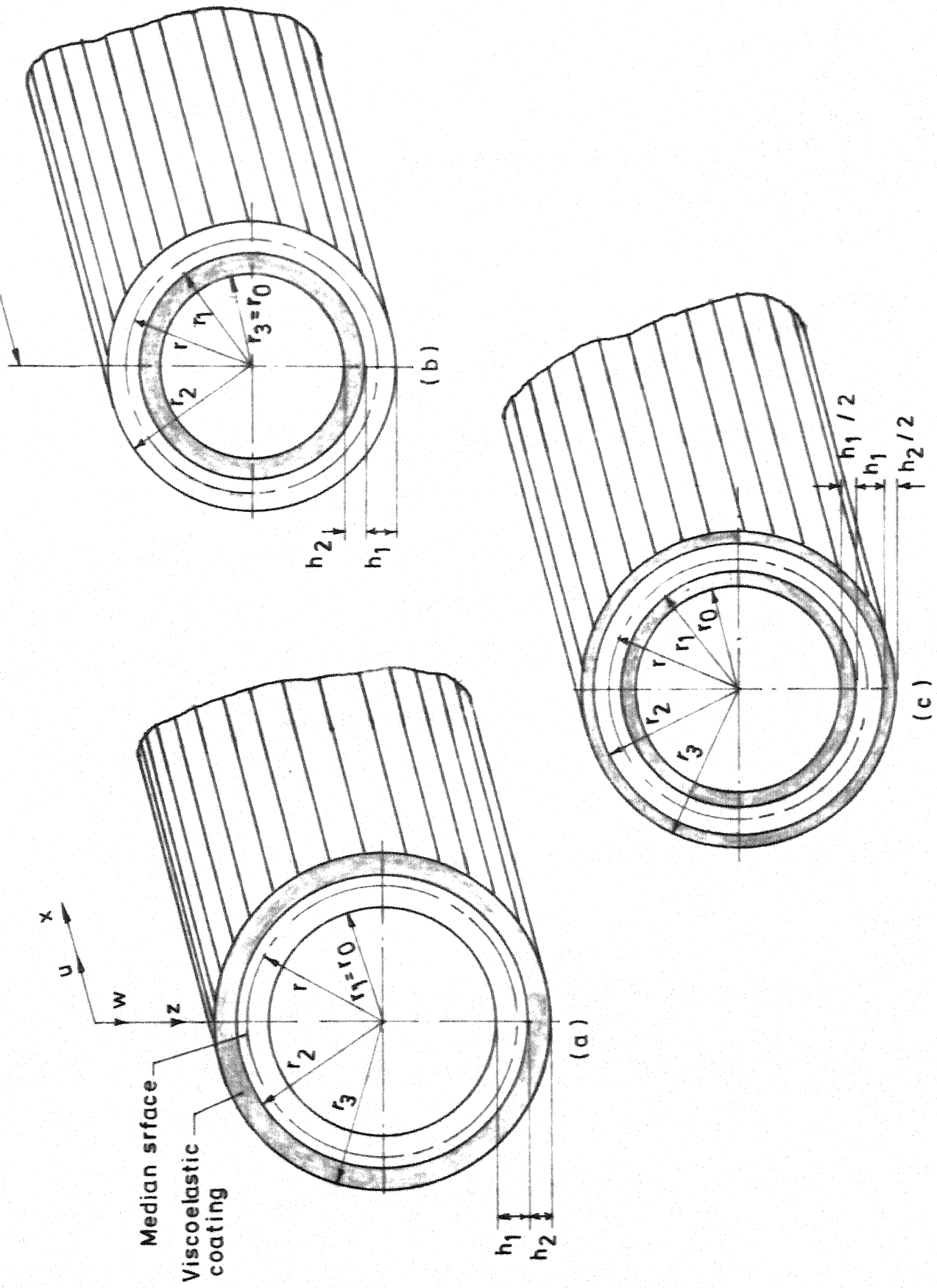


FIG. 5.1 DIMENSIONS AND COORDINATE SYSTEM OF LAYERED SHELL a) OUTSIDE COATING (OC) b) INSIDE COATING (IC) c) TWO SIDE COATING (TC)

- (i) The thickness of the shell  $h_1$  is much smaller than the radius of the median surface  $r$ , that is,  $(h_1/r)^2 \ll 1$ .
- (ii) The viscoelastic material has a complex modulus  $E_2 = E_2^* (1+i\beta)$ , where  $\beta$  is the loss factor of the viscoelastic material and  $E_2^*$  is the storage Young's modulus of the damping material.  
( $E_2^{**}$  and  $\beta$  are assumed to be frequency independent in the analysis).
- (iii) The face layer to which the damping treatment is applied is assumed to be elastic and non-dissipative.
- (iv) The cylinder motion in the transverse direction for all the layers is the same.

Considering the displacement continuity at the interfaces of the layers and the equilibrium of forces and moments, and eliminating the longitudinal displacement the following equations for the shell motion in the transverse direction for the three cases of damping layer configuration OC, IC and TC can be obtained.

$$A w^{IV} - (B/r) w^{II} + (C/r^2) w + \mu \ddot{w} = p(x,t) \quad (5.1) \text{ (OC)}$$

$$A w^{IV} + (B/r) w^{II} + (C/r^2) w + \mu \ddot{w} = p(x,t) \quad (5.2) \text{ (IC)}$$

$$D w^{IV} + (C/r^2) w^{II} + \mu \ddot{w} = p(x,t) \quad (5.3) \text{ (TC)}$$

where, A, B, C and D are constants depending on the extensional

rigidities of the different layers in the composite shell, their Poissons ratios and thicknesses.  $\mu$  is the surface mass density of the composite shell.

The constants A, B, C and D are given by,

$$A = \frac{1}{3} \alpha_1 h_1^2 + \frac{1}{3} \alpha_2 h_2^2 + d^2 (\alpha_1 + \alpha_2) - d(\alpha_1 h_1 - \alpha_2 h_2) \quad (5.5)$$

$$\begin{aligned} B = & \frac{1}{2} \alpha_1 (v_2 - v_1) (\alpha_2^* h_1 + \alpha_2 h_2) / (\alpha_1 + \alpha_2^*) \\ & + \frac{1}{2} (\alpha_2 h_2 v_2 - \alpha_1 h_1 v_1) + d(\alpha_1 v_1 + \alpha_2 v_2) \\ & + d \alpha_1 (v_2 - v_1) (\alpha_2 - \alpha_2^*) / (\alpha_1 + \alpha_2^*) \end{aligned} \quad (5.6)$$

$$C = \alpha_1 + \alpha_2 - (\alpha_1 v_1 + \alpha_2 v_2) (\alpha_1 v_1 + \alpha_2^* v_2) / (\alpha_1 + \alpha_2^*) \quad (5.7)$$

$$D = \frac{1}{12} (\alpha_1 h_1^2 + \alpha_2 h_2^2 + 3 \alpha_2 h_1 (h_1 + h_2)) \quad (5.8)$$

$$\text{where, } d = \frac{1}{2} (\alpha_1 h_1 - \alpha_2^* h_2) / (\alpha_1 + \alpha_2^*)$$

$$\alpha_i = E_i h_i / (1 - v_i^2) \quad (5.9)$$

$$\alpha_2^* = E_2^* h_2 / (1 - v_2^2) \quad (5.10)$$

and  $E_i$  is the Young's modulus,  $v_i$ , the Poisson's ratio and  $h_i$  the thickness of the  $i^{\text{th}}$  layer.

For an external loading of the form  $p(x,t) = -i\eta\mu\ddot{w}$ , it can be shown that the motion of the plate is harmonic and can be expressed in separable form

$$w = W(x) e^{i\omega t} \quad (5.11)$$

Substituting equation (5.11) into equations (5.1) to (5.3), one obtains,

$$A W^{IV} - (B/r) W^{II} + (C/r^2) W - \mu \omega^{*2} (1+i\eta) W = 0 \quad (5.12)$$

$$A W^{IV} + (B/r) W^{II} + (C/r^2) W - \mu \omega^{*2} (1+i\eta) W = 0 \quad (5.13)$$

$$D W^{IV} + (C/r^2) W - \mu \omega^{*2} (1+i\eta) W = 0 \quad (5.14)$$

where  $\omega^{*2}$  is the square of the natural frequency and  $\eta$  the associate loss factor.

The natural frequencies, loss factors and the damped normal modes would depend on the boundary conditions at the ends of the shell. As the main interest pertains to the noise transmission through the shell into the cavity, and as it had been observed in the case of finite plates, that the behaviour of the noise transmission does not vary qualitatively with the plate edge conditions, the analysis is restricted to simply supported end conditions. For such a case, the natural frequencies and the loss factors can be obtained by closed form expressions. It can be shown that for simply supported ends the damped normal modes take the form

$$W_n(x) = a_n \sin \frac{n\pi x}{l} \quad (5.15)$$

for all the three cases of layer constructions OC, IC and TC.

Substituting equation (5.15) into equations (5.12) to (5.14) the natural frequencies and the modal loss factors are given by

$$\omega_m^{*2} (1+i\eta_m) = [A \frac{m^4 \pi^4}{l^4} + (B/r) \frac{m^2 \pi^2}{l^2} + (C/r^2)]/\mu \quad (5.16) \quad (OC)$$

$$\omega_m^{*2} (1+i\eta_m) = [A \frac{m^4 \pi^4}{l^4} + (B/r) \frac{m^2 \pi^2}{l^2} + (C/r^2)]/\mu \quad (5.17) \quad (IC)$$

$$\omega_m^{*2} (1+i\eta_m) = [D \frac{m^4 \pi^4}{l^4} + (C/r^2)] \quad (5.18) \quad (TC)$$

The natural frequencies and associated loss factors for various elastic and geometric properties of the layer materials are given in Tables 5.1 to 5.3 .

### 5.3 EQUATIONS OF MOTION OF DAMPED SANDWICH SHELL

The sandwich shell considered is a thin circular cylindrical shell (Figure 5.2), consisting of three layers, two symmetric face layers of equal thicknesses and same material, with a constrained viscoelastic damping layer. The equations of motion of the sandwich shell in axisymmetric vibrations have been derived by Pan [36] following an analysis of DiTaranto [12] for three layered sandwich beams. The following assumptions were made in the derivation.

- i) The shell is thin and hence the radial displacements

Table 5.1 - Resonant Frequencies and Loss Factors of Layered Shell  
 $(h_1/h_2 = 0.1, \beta = 0.3, E_2^* = 4.14 \times 10^6 \text{ N/m}^2)$

m	OC			IC			TC		
	$f_m$ (Hz)	$\eta_m \times 10^5$	$f_m$ (Hz)	$\eta_m \times 10^5$	$f_m$ (Hz)	$\eta_m \times 10^5$	$f_m$ (Hz)	$\eta_m \times 10^5$	$f_m$ (Hz)
1	461.47	.1607	461.47	.1607	461.47	.1607	461.47	.1607	
3	461.55	.1607	461.55	.1606	461.55	.1606	461.55	.1607	
5	462.09	.1603	462.09	.1603	462.09	.1603	462.09	.1603	
7	463.85	.1591	463.85	.1590	463.85	.1590	463.85	.1591	
9	467.93	.1563	467.93	.1563	467.93	.1563	467.93	.1563	
11	475.76	.1512	475.76	.1512	475.76	.1512	475.76	.1512	
13	488.96	.1432	488.96	.1431	488.96	.1431	488.96	.1431	
15	509.19	.1320	509.19	.1320	509.19	.1320	509.19	.1320	
17	537.93	.1183	537.93	.1182	537.93	.1182	537.93	.1183	
19	576.32	.1030	576.35	.1030	576.35	.1030	576.35	.1030	
21	625.20	.0876	625.20	.0875	625.20	.0875	625.20	.0875	

Table 5.2 - Resonant Frequencies and Loss Factors of Layered Shell

$$(h_2/h_1 = 0.1, \beta = 0.3, E_2^* = 4.14 \times 10^9 \text{ N/m}^2)$$

m	OC			IC			TC	
	$f_m$ (Hz)	$\eta_m \times 10^5$	$f_m$ (Hz)	$f_m$ (Hz)	$\eta_m \times 10^5$	$f_m$ (Hz)	$\eta_m \times 10^5$	
1	462.74	159.9	462.74	462.74	159.87	462.74	159.89	
3	462.81	159.8	462.83	462.83	159.80	462.82	159.84	
5	463.33	159.5	463.40	463.40	159.41	463.36	159.46	
7	465.09	158.3	465.21	465.21	158.21	465.15	158.24	
9	469.20	155.5	469.40	469.40	155.36	469.29	155.46	
11	477.11	150.4	477.41	477.41	150.19	477.24	150.32	
13	490.47	142.3	490.87	490.87	142.07	490.63	142.23	
15	510.95	131.1	511.47	511.47	130.86	511.14	131.05	
17	540.07	117.4	540.69	540.69	117.09	540.27	117.30	
19	579.00	102.1	579.72	579.72	101.86	579.19	102.06	
21	628.47	86.69	629.29	629.29	86.44	628.65	86.63	

Table 5.3 - Resonant Frequencies and Loss Factors of Layered Shell, O.C.

$(h_2/h_1 = 10, \beta = 0.3)$				
m	$E_2^* = 4.14 \times 10^6$		$E_2 = 4.14 \times 10^9$	
	$f_m$ (Hz)	$\eta_m \times 10^3$	$f_m$ (Hz)	$\eta_m \times 10^{-1}$
1	269.17	.1612	333.19	1.0520
3	269.22	.1611	336.82	1.0290
5	269.60	.1607	374.12	0.8344
7	270.86	.1592	483.58	0.4994
9	273.80	.1558	678.27	0.2538
11	279.44	.1496	951.40	0.1290
13	288.91	.1399	1295.15	0.0696
15	303.34	.1269	1704.89	0.0401
17	323.66	.1115	2178.18	0.0246
19	350.56	.0950	2713.66	0.0158
21	384.41	.0790	3310.59	0.0106

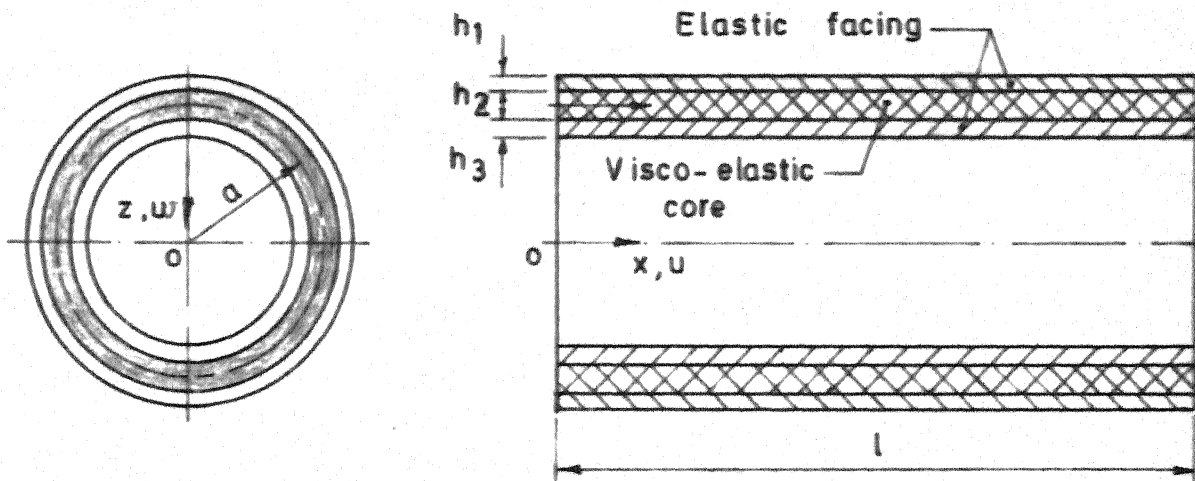
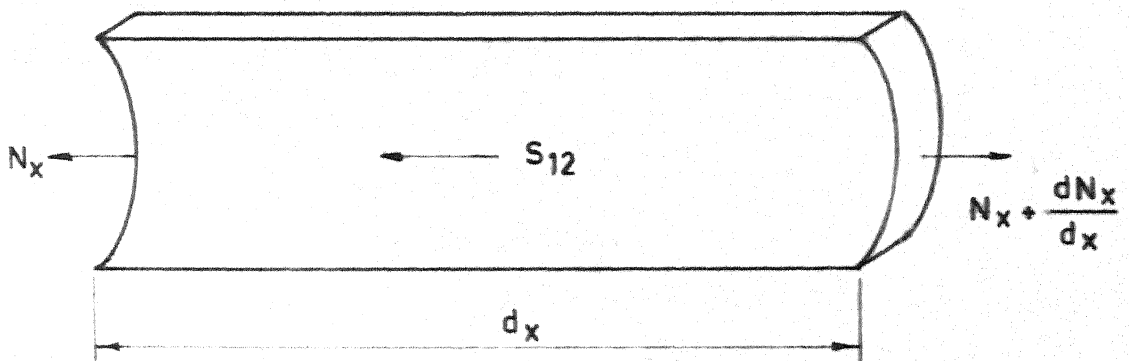


FIG. 5.2 DIMENSIONS AND COORDINATE SYSTEM OF SANDWICH SHELL



$S_{12}$  = Shear force / unit length between core and facing

FIG. 5.3 EQUILIBRIUM OF LONGITUDINAL FORCES OF FACE LAYERED ELEMENT

for all the three layers are assumed to be the same and equal to  $w$ .

ii) The bending stresses in the face layer are much larger compared to the direct bending stresses in the viscoelastic core.

iii) Displacement continuity is maintained at the interfaces of the three layers.

iv) Inertia forces in the longitudinal direction are negligible.

Neglecting the extensional force carried by the viscoelastic layer and neglecting the longitudinal inertia, force equilibrium in the axial direction results in

$$\frac{E_1 h_1}{1 - \nu_1^2} (u_1' - \nu_1 \frac{w}{a}) + \frac{E_3 h_3}{1 - \nu_3^2} (u_3' - \nu_3 \frac{w}{a}) = 0 \quad (5.18)$$

where,  $E_i, h_i$  and  $u_i$  refer respectively to the Young's modulus, thickness and mid-surface displacement of the  $i^{\text{th}}$  layer respectively. A prime indicates differentiation with respect to  $x$  and  $\nu_i$  is the Poisson's ratio of the  $i^{\text{th}}$  layer.  $w$  is the radial displacement of the shell and  $a$  is the radius of the midsurface of the core layer.

The displacement continuity at the interfaces is expressed by the relation

$$(u_1 - \frac{h_1}{2} \varphi) - (u_3 + \frac{h_3}{2} \varphi) = h_2 (\varphi + \Psi) \quad (5.19)$$

where,  $\varphi = \partial w / \partial x$  is the rotation of the section, assumed same for the layer 1 and 3 and  $\Psi$  is the shear strain of the viscoelastic core layer.

Considering the equilibrium of forces in the longitudinal direction of an element of layer 1 it can be shown that (Figure 5.3)

$$\Psi = \frac{1}{G} \frac{E_1 h_1}{1 - \nu_1^2} (u_1' - \nu_1 \frac{w''}{a}) \quad (5.20)$$

where  $G = G^* (1 + i\beta)$  is the complex shear modulus of the viscoelastic core.

Making use of the fact that  $E_1 = E_3 = E$  and  $\nu_1 = \nu_3 = \nu$  and using the continuity condition (5.19) in conjunction with equations (5.18) and (5.20) one gets,

$$\frac{E h_1 h_2}{G(1 - \nu^2)} u_1''' - 2u_1' + 2 \frac{\nu w}{a} + [(h_1 + h_2) - \frac{E h_1 h_2}{G(1 - \nu^2)}] w'' = 0 \quad (5.21)$$

The bending moment  $M_x$  at any section is obtained by taking moments of the axial forces and is given by, (assuming extensional forces in the core damping layer to be zero)

$$M_x = - \frac{E h_1}{1 - \nu_1^2} (h_1 + h_2) (u_1' - \frac{\nu w}{a}) - D_t w'' \quad (5.22)$$

where,

$$D_t = \frac{E h_1^3}{6(1-\nu^2)} \quad (5.23)$$

For the axisymmetric vibration of the shell, the equation of motion can be represented as

$$M_x'' + \frac{1}{a} N_\varphi = \mu \frac{\partial^2 w}{\partial t^2} + p(x, a, t) \quad (5.24)$$

where  $N_\varphi$  is the total circumferential force per unit length of the whole sandwich given by

$$N_\varphi = -2 E h_1 (w/a) \quad (5.25)$$

$\mu$  is the surface mass density of the composite shell and  $p(x, a, t)$  is the external pressure loading on the surface of the shell.

Substituting equations (5.22) and (5.25) in equation (5.24) and using equation (5.21) to eliminate  $u_1$  from the equation, the equation of motion in  $w$  can be written as

$$\begin{aligned} w^{vi} - \frac{2G(1-\nu^2)w^{iv}}{E h_1 h_2} \left[ 1 + \frac{E h_1 (h_1 + h_2)^2}{2D_t(1-\nu^2)} \right] \\ + \frac{E h_1}{2a^2 D_t} w'' - \frac{G(1-\nu^2) h_1}{a^2 h_1 h_2 D_t} w \\ = - \frac{\mu}{D_t} \left[ \frac{\partial^2 w''}{\partial t^2} - \frac{2G(1-\nu^2)}{E h_1 h_2} \frac{\partial^2 w}{\partial t^2} \right] + \frac{1}{D_t} \frac{\partial^2 p}{\partial x^2} \end{aligned} \quad (5.26)$$

Equation (5.26) can be rewritten as

$$\begin{aligned}
 w^{VI} - g'(1+Y)w^{IV} + \frac{12(1-\nu^2)}{a^2 h_1^2} w'' - \frac{12g'(1-\nu^2)}{a^2 h_1^2} w \\
 = -\frac{\mu}{D_t} \left[ \frac{\partial^2 w''}{\partial t^2} - g' \frac{\partial^2 w}{\partial t^2} \right] + \frac{1}{D_t} \frac{\partial^2 p}{\partial x^2}
 \end{aligned} \quad (5.27)$$

where  $g' = \frac{2G(1-\nu^2)}{E h_1 h_2}$  is the shear parameter and

$Y = 3 \left(1 + \frac{h_2}{h_1}\right)^2$  is the geometric parameter which

are the same expressions as for the sandwich plate.

For an external loading of the form  $p(x,t) = i\eta\mu \frac{\partial^2 w}{\partial t^2}$  it can be shown that the plate motion is harmonic and can be expressed in separable form in damped normal modes as,

$$w = W(x) e^{i\omega t} \quad (5.28)$$

Substituting equation (5.28) into equation (5.27) one obtains,

$$w^{VI} - g'(1+Y)w^{IV} - (w^{II} - g'w) \left[ \frac{\mu \omega^{*2}}{D_t} (1+i\eta) - \frac{12(1-\nu^2)}{a^2 h_1^2} \right] = 0 \quad (5.29)$$

where  $\omega^{*2}$  is the square of the natural frequency and  $\eta$  the associated loss factor. Equation (5.29) is of similar form as the equation of motion for sandwich beams with constrained damping layer [13].

The natural frequencies, the loss factors for simply supported end conditions can be obtained in closed form by substituting pure sinusoidal modes of the form

$$W_m(x) = a_m \sin \frac{m\pi x}{l} \quad (5.30)$$

into equation (5.29). The resulting expression for the complex natural frequency in the  $m^{\text{th}}$  mode is given by

$$\omega_m^{*2} (1 + i\eta_m) = \frac{D_t}{\mu} \frac{\left(\frac{m\pi}{l}\right)^6 + g'(1+Y)\left(\frac{m\pi}{l}\right)^4 + \frac{12(1-\nu^2)}{a^2 h_1^2} \left[\left(\frac{m\pi}{l}\right)^2 + g'\right]}{\left(\frac{m\pi}{l}\right)^2 + g'} \quad (5.31)$$

The natural frequencies and the associated loss factors of the sandwich shell for typical values of  $\beta$ ,  $\bar{g}$  and  $Y$  are presented in Tables 5.4 to 5.6.

## 5.4 ACOUSTOELASTIC FORMULATION

### 5.4.1 Acoustic Solution

Consider the closed cylindrical cavity shown in Figure 5.4, occupying the cylindrical volume  $V = \pi a^2 l$ . It is assumed that the wall formed by the layered shell or the sandwich shell is flexible and the two ends of the cylindrical are closed with rigid walls. The pressure  $p_c$  inside the cylindrical cavity is governed by the acoustic wave equation in cylindrical polar coordinates.

Table 5.4 - Resonant Frequencies and Loss Factors for Different Shear Parameters  
(Sandwich Shell)

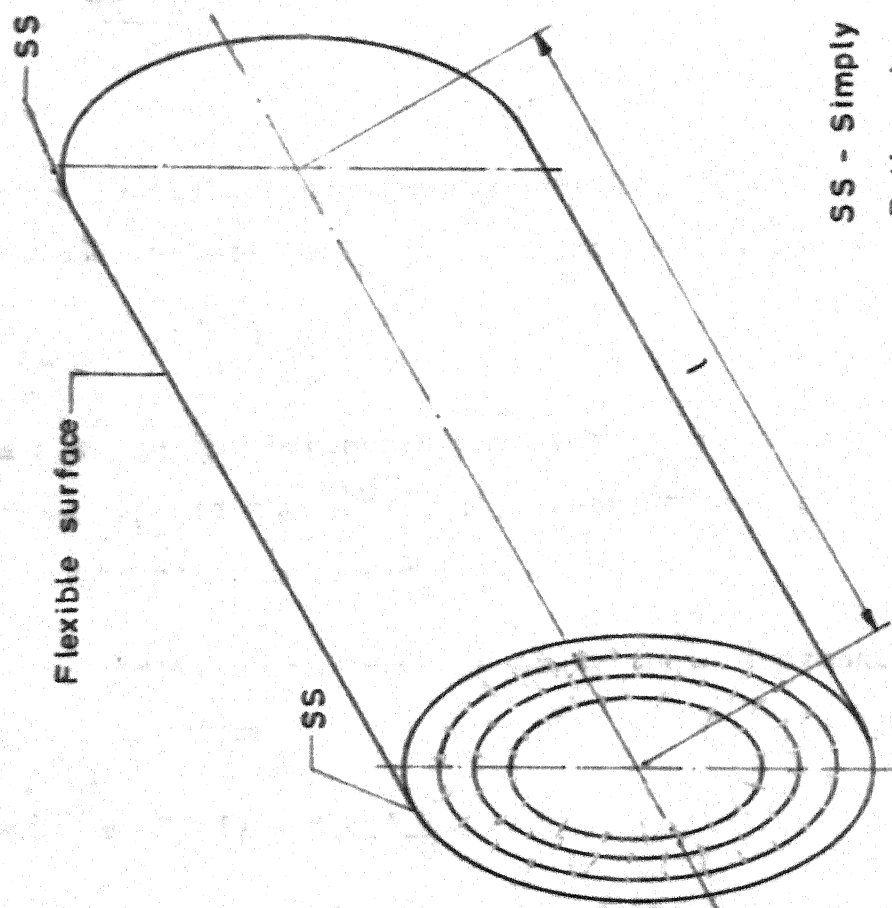
( $\beta = 0.3$ ,  $Y = 31.5$ )

m	10		119		5000	
	$f_m$ (Hz)	$\eta_m$	$f_m$ (Hz)	$\eta_m$	$f_m$ (Hz)	$\eta_m$
1	402.10	$.448 \times 10^{-5}$	402.11	$.120 \times 10^{-5}$	402.11	$.331 \times 10^{-7}$
3	402.23	$.135 \times 10^{-3}$	402.71	$.352 \times 10^{-3}$	403.10	$.233 \times 10^{-4}$
5	402.64	$.428 \times 10^{-3}$	404.88	$.246 \times 10^{-2}$	409.62	$.457 \times 10^{-3}$
7	403.63	$.868 \times 10^{-3}$	408.89	$.673 \times 10^{-2}$	429.22	$.289 \times 10^{-2}$
9	405.64	$.144 \times 10^{-2}$	415.02	$.127 \times 10^{-1}$	469.31	$.984 \times 10^{-2}$
11	409.24	$.213 \times 10^{-2}$	423.68	$.199 \times 10^{-1}$	533.59	$.224 \times 10^{-1}$
13	415.13	$.291 \times 10^{-2}$	435.41	$.277 \times 10^{-1}$	621.19	$.392 \times 10^{-1}$
15	424.06	$.373 \times 10^{-2}$	450.75	$.357 \times 10^{-1}$	728.47	$.577 \times 10^{-1}$
17	436.80	$.452 \times 10^{-2}$	470.25	$.431 \times 10^{-1}$	851.17	$.763 \times 10^{-1}$
19	454.11	$.523 \times 10^{-2}$	494.38	$.495 \times 10^{-1}$	985.50	$.938 \times 10^{-1}$
21	476.62	$.580 \times 10^{-2}$	523.55	$.545 \times 10^{-1}$	1128.50	.109



Table 5.6 - Resonant Frequencies and Loss Factors for Different Geometric Parameters  
(Sandwich Shell)  
( $\bar{g} = 119$ ,  $\beta = 0.3$ )

m	Y = 3.63		Y = 12		Y = 31.5	
	$f_m$ (Hz)	$\eta_m$	$f_m$ (Hz)	$\eta_m$	$f_m$ (Hz)	$\eta_m$
1	442.65	$.138 \times 10^{-6}$	424.16	$.459 \times 10^{-6}$	402.11	$.120 \times 10^{-5}$
3	442.76	$.407 \times 10^{-4}$	424.42	$.134 \times 10^{-3}$	402.71	$.352 \times 10^{-3}$
5	443.24	$.286 \times 10^{-3}$	425.43	$.944 \times 10^{-3}$	404.88	$.246 \times 10^{-2}$
7	444.43	$.796 \times 10^{-3}$	427.51	$.261 \times 10^{-2}$	408.89	$.673 \times 10^{-2}$
9	446.79	$.153 \times 10^{-2}$	431.05	$.500 \times 10^{-2}$	415.02	$.127 \times 10^{-1}$
11	450.95	$.245 \times 10^{-2}$	436.61	$.796 \times 10^{-2}$	423.68	$.109 \times 10^{-1}$
13	457.66	$.351 \times 10^{-2}$	444.87	$.113 \times 10^{-1}$	435.41	$.277 \times 10^{-1}$
15	467.74	$.463 \times 10^{-2}$	456.56	$.147 \times 10^{-1}$	450.75	$.357 \times 10^{-1}$
17	482.04	$.573 \times 10^{-2}$	472.42	$.181 \times 10^{-1}$	470.25	$.431 \times 10^{-1}$
19	501.38	$.672 \times 10^{-2}$	493.13	$.210 \times 10^{-1}$	494.38	$.495 \times 10^{-1}$
21	526.43	$.754 \times 10^{-2}$	519.27	$.235 \times 10^{-1}$	523.55	$.545 \times 10^{-1}$



SS - Simply supported  
Both ends closed by  
rigid surfaces

FIG. 5.4 CYLINDRICAL CAVITY-SHELL SYSTEM

$$\frac{\partial^2 p_c}{\partial r^2} + \frac{1}{r^2} \frac{\partial^2 p_c}{\partial \theta^2} + \frac{1}{r} \frac{\partial p_c}{\partial r} + \frac{\partial^2 p_c}{\partial x^2} = \frac{1}{c^2} \frac{\partial^2 p_c}{\partial t^2} \quad (5.32)$$

with the boundary conditions

$$\begin{aligned} \frac{\partial p_c}{\partial r} &= - \frac{\partial^2 w(x, \theta)}{\partial t^2} \quad \text{at} \quad r = a \\ \frac{\partial p_c}{\partial x} &= 0 \quad \text{at} \quad x = 0, 1 \end{aligned} \quad (5.33)$$

Equation (5.32) for homogeneous boundary conditions has normal mode solutions  $F_n e^{i \omega t}$  which satisfy the equations

$$\nabla^2 F_n = - (\omega_{nA}/c)^2 F_n \quad (5.34)$$

where  $\nabla^2$  is the Laplacian operator in cylindrical coordinates,  $\omega_{nA}$  is the  $n^{\text{th}}$  cavity resonant frequency and  $F_n$  the corresponding cavity mode.

The cavity normal modes satisfy the orthogonality relation of the form

$$\frac{1}{V} \int V F_r F_n dV = M_{nA} \delta_{rn} \quad (5.35)$$

where  $\delta_{rn}$  represents the Kronecker delta.

The acoustic pressure inside the cavity can be expanded similar to the case of the plates in terms of the acoustic normal modes  $F_n$  as

$$p_c = \rho c^2 \sum \frac{P_n F_n}{M_{nA}} \quad (5.36)$$

The pressure coefficients  $P_n$  in the acoustic normal mode expansion are governed by the set of ordinary differential equations

$$\ddot{P}_n + 2\epsilon_{nA} \omega_{nA} \dot{P}_n + \omega_{nA}^2 P_n = - \frac{A_F}{V} \ddot{W}_n \quad (5.37)$$

where,

$$P_n = \frac{1}{\rho c^2 V} \int_V p_c F_n dV \quad (5.38)$$

$$W_n = \frac{1}{A_F} \int_{A_F} w F_n dA_F \quad (5.39)$$

where  $A_F$  is the surface area of the flexible cylindrical wall and  $\epsilon_{nA}$  is the modal damping coefficient.

#### 5.4.2 Structural Solution

The response of the cylindrical shell (layered and sandwich) can be expanded in the damped normal modes as

$$w(x,a,t) = \sum_m q_m(t) \varphi_m \quad (5.40)$$

where,

$$\varphi_m = \sin \frac{m\pi x}{l}$$

The normal coordinates are governed by the set of ordinary differential equations

$$M_{ms} [\ddot{q}_m + \omega_{ms}^{*2} (1 + i\eta_{ms}) q_m] = Q_{mc} + Q_{me} \quad (5.41)$$

where,

$$M_{ms} = \int_{A_F} \mu \varphi_m^2 dA$$

$$Q_{mc} = \int_{A_F} p_c \varphi_m dA$$

$$Q_{me} = - \int_{A_F} p_e \varphi_m dA$$

and  $p_e$  is the external pressure loading on the cylindrical shell. It has also been assumed in the analysis that the radiation loading on the cylindrical surface external to the cavity is negligible compared to the external pressure field. Substituting equation (5.40) in equations (5.38) and (5.39) and equation (5.38) in equation (5.41) the coupled acoustoelastic equation in the pressure coefficients and the damped normal coordinates are obtained as

$$\ddot{P}_n + 2\epsilon_{nA} \omega_{nA} \dot{P}_n + \omega_{nA}^2 P_n = - \frac{A_F}{V} \sum_m L_{nm} \ddot{q}_m \quad (5.42)$$

$$M_{ms} [\ddot{q}_m + \omega_{ms}^{*2} (1 + i\eta_{ms}) q_m] = \rho c^2 A_F \frac{P_n L_{nm}}{M_{nA}} + Q_m^E \quad (5.43)$$

where,

$$L_{nm} = \frac{1}{A_F} \int_{A_F} F_n \varphi_m dA \quad (5.44)$$

are the acousto-structural modal coupling coefficients.

### 5.4.3 Modal Damping Coefficients and Other Modal Parameters

It can be shown that the acoustic normal mode  $F_n$ , for the cylindrical cavity is of the form

$$F_n(x, r, \theta) = \cos \frac{i\pi x}{l} \cos j \theta J_j(\lambda_{jk} r) \quad (5.45)$$

where as seen from the equation, the index  $n$  includes in itself the three indices  $i, j, k$  corresponding to the axial, circumferential and radial directions. In the foregoing equation  $J_j$  represents the Bessel function of first kind of order  $j$  and  $\lambda_{jk} = \alpha_{jk}/a$  where  $\alpha_{jk}$  is the  $k^{\text{th}}$  root of the equation  $dJ_j/dr = 0$ .

Since only the axi-symmetric vibrations of the shell is considered it is sufficient to admit in the acoustic mode only the  $j = 0$  term in equation (5.45) as the contributions from the modes corresponding to  $j = 1, 2$ , etc. to the generalized force or the coupling coefficient will vanish. Then the cavity modes can be expressed as

$$F_n(x, r) = \cos \frac{i\pi x}{l} J_0(\lambda_{0k} r) \quad (5.46)$$

The generalized mass of the structure in all the structural modes is given by

$$M_{ms} = \int_0^{2\pi} \int_0^l \mu a d\theta \sin^2 \frac{\pi x}{l} dx = \pi \mu a l \quad (5.47)$$

The cavity generalized mass from equation (5.35) is,

$$M_{nA} = \frac{1}{\pi a^2 l} \int_0^a \int_0^{2\pi} \int_0^l r J_0^2(\lambda_{ok} r) \cos^2 \frac{i\pi x}{l} dx dr d\theta \quad (5.48)$$

which on integration yields,

$$\begin{aligned} M_{nA} &= \frac{J_0^2(\lambda_{ok} a) + J_1^2(\lambda_{ok} a)}{2} \quad \text{for } i \neq 0 \text{ and } k \neq 0 \\ &= J_0^2(\lambda_{ok} a) + J_1^2(\lambda_{ok} a) \quad \text{for } i = 0 \text{ and } k \neq 0 \\ &= \frac{1}{4} \quad \text{for } i \neq 0 \text{ and } k = 0 \\ &= \frac{1}{2} \quad \text{for } i = 0 \text{ and } k = 0 \end{aligned} \quad (5.49)$$

The cavity frequencies are given by

$$\omega_{nA}^2 = \omega_{ijk}^2 = c^2 \left[ \lambda_{jk}^2 + \left( \frac{i\pi}{l} \right)^2 \right] \quad (5.50)$$

Assuming the external pressure loading to be uniform and harmonic of the form  $p_e(x, a, t) = p_0 e^{i\omega t}$ , the generalized force

$$Q_{mB} = \int_0^{2\pi} \int_0^l p_e(x, a, t) \varphi_m(x) dx d\theta = p_0 (1 - \cos m\pi) \frac{2al}{m} e^{i\omega t} \quad (5.51)$$

The acoustic structural modal coupling coefficients

$L_{nm}$  are given by

$$L_{nm} = \frac{J_0(\lambda_{ok} a)}{A_F} \int_0^l \int_0^{2\pi} \sin \frac{m\pi x}{l} \cos \frac{i\pi x}{l} dx d\theta \quad (5.52)$$

$$L_{nm} = \frac{J_0(\lambda_{ok} a)}{2\pi} \left\{ \frac{1}{m+i} - \frac{\cos(m+i)\pi}{m+i} + \frac{1}{m-i} - \frac{\cos(m-i)\pi}{m-i} \right\} \quad (5.53)$$

The above equation has nonzero values only for the combinations ( $i = \text{even}, m = \text{odd}$ ) or ( $i = \text{odd}, m = \text{even}$ ) for which, equation (5.53) reduces to

$$L_{nm} = \frac{2m J_0(\lambda_{ok} a)}{\pi (m^2 - i^2)} \quad (5.54)$$

From equation (5.51) it is seen that the generalized force  $Q_{mE}$  has contributions only for the odd order structural modes. In the solution of the acoustoelastic problem only the combinations ( $i = \text{even}, m = \text{odd}$ ) cavity and structural modes are considered in the analysis.

#### 5.4.4 Acoustoelastic Problem Solution

Equation (5.40) and (5.43) can be expressed in matrix notation similar to that in Chapter 4 (equation 4.45).

Hence, following the steps adopted in section (4.3.3) for a harmonic external pressure loading the cavity pressure can be determined as

$$p_c = \rho c^2 e^{i\omega t} \sum_n \frac{\bar{P}_n F_n}{M_{nA}} \quad (5.55)$$

and the structural response as

$$w(x, a, \theta, t) = e^{i\omega t} \sum_m \bar{q}_m \varphi_m(x) \quad (5.56)$$

and the noise reduction as,

$$NR = 20 \log \frac{P_o}{|P_c|} \quad (5.57)$$

where  $\bar{P}_n$  and  $\bar{q}_m$  are the complex amplitudes of the harmonic pressure coefficient  $P_n$  and the structural generalized coordinate  $q_m$  respectively.

Similarly for a stationary uniform random external pressures with constant power spectral density function  $S_o$ , the power spectral density of the cavity pressure is given by

$$S_{p_c p_c}(x, r, \theta, \omega) = \rho^2 c^4 \begin{Bmatrix} \alpha \end{Bmatrix}^T [S_{pp}(\omega)] \begin{Bmatrix} \alpha^* \end{Bmatrix} \quad (5.58)$$

(1xn) (nxn) (n x 1)

The structural response power spectral density of the cylindrical shell is given by

$$S_{ww}(x, a, \theta, \omega) = \begin{Bmatrix} \gamma \end{Bmatrix}^T [S_{qq}(\omega)] \begin{Bmatrix} \gamma^* \end{Bmatrix} \quad (5.59)$$

(1+m) (m x m) (m x 1)

where  $\{\alpha\}$  and  $\{\gamma\}$  are vectors of orders  $n$  and  $m$  respectively with elements,

$$\alpha_n = \frac{F_n(x, r, \theta)}{M_{nA}} \quad \text{and} \quad \gamma_m = \varphi_m(x, a, \theta)$$

and the matrices  $[S_{pp}(\omega)]$  and  $[S_{qq}(\omega)]$  are cross spectral density matrices of the pressure coefficients and structural coordinates, whose elements can be obtained from the cross-spectral density matrix of the generalized forces  $[S_{qq}(\omega)]$  in a similar fashion as explained in section (4.3.3).

The corresponding cross acceptance function  $I_{mr}(\omega)$  between the  $m^{\text{th}}$  and  $r^{\text{th}}$  structural mode is given by

$$I_{mr}(\omega) = \int_{A_F} \int_{A_F} r(x_1, \theta_1; x_2, \theta_2; \omega) \varphi_m(x_1, \theta_1) \varphi_r(x_2, \theta_2) dA_1 dA_2 \quad (5.60)$$

where for  $r(x_1, \theta_1; x_2, \theta_2; \omega) = 1.0$

$$I_{mr}(\omega) = \frac{4 a_1^2}{mn} (1 - \cos m\pi)(1 - \cos r\pi) \quad (5.61)$$

which has nonzero values only for  $m = \text{odd}$  and  $r = \text{odd}$ .

The solution of the acoustoelastic problem can be effected by a matrix inversion procedure explained in Chapter 4.

## 5.5 RESULTS AND DISCUSSION

The material and geometric properties of the shell, both layered and sandwich, adopted in the analysis are given below.

### a) Layered Shell (Unconstrained damping treatment)

Young's modulus of face layer	$E = 7.24 \times 10^{10} \text{ N/m}^2$
Density of face layer material	$\rho_p = 2770 \text{ Kg/m}^3$
Thickness of face layer	$h_1 = 0.002 \text{ m}$
Mean radius of the shell	$r = a = 1.83 \text{ m}$
Density of damping layer	$\rho_c = 0.2 \rho_p$
Loss factor of the damping layer material	$\beta = 0.3$
Length of the cylinder	$l = 2.0 \text{ m}$

The other parameters like the thicknesses of the damping layers in the three configurations OC, IC and TC, the storage Young's modulus of the damping layer are varied in the analysis.

### b) Sandwich Shell (Constrained damping treatment)

Young's modulus of face layer	$E = 7.24 \times 10^{10} \text{ N/m}^2$
Density of face layer material	$\rho_p = 2770 \text{ Kg/m}^3$
Thickness of each face layer	$h_1 = .001 \text{ m}$
Mean radius of the shell	$a = 1.83 \text{ m}$
Density of constrained damping layer (core)	$\rho_c = 0.2 \rho_p$
Loss factor of the damping layer material	$\beta = 0.3$
Length of the cylinder	$l = 2.0 \text{ m}$

The shear parameter  $\bar{g}$  and the geometric parameters  $Y$  are varied in the analysis. The core loss factor  $\beta$  is also varied in the analysis.

In both the cases, the cavity modal damping coefficient in most of the numerical investigations is taken to be  $\epsilon_{ool} = 0.02$ . The effect of cavity damping on the noise reduction inside the cylinder is also studied by varying the cavity modal damping coefficient.

#### 5.5.1 Natural Frequencies and Loss Factors

a) Layered Shell: Table 5.1 shows the natural frequencies and associated loss factors of the layered shell in the three configurations of OC, IC and TC of the unconstrained damping layer treatment. In the two sided coating the unconstrained damping layer is assumed to be symmetrically applied to the base layer on either side with damping layer thickness equal to half the thickness of the damping layer in the case of outside and inside coatings. The thickness of the damping layer is one tenth of the thickness of the face layer. The storage Young's modulus of the damping layer is taken as  $E_2^* = 4.14 \times 10^6 \text{ N/m}^2$ .

It is seen from the table that the damping layer configuration does not have any effect on the natural frequencies and loss factors as they remain practically the

same for all the three configurations of OC, IC and TC especially in the lower order modes. It is also observed from the table that the natural frequencies are clustered in the axisymmetric modes of vibration, especially in the lower order modes, because in the equations (5.16), (5.17) and (5.18) the term corresponding to  $C/r^2$  is very much larger compared to the other two terms that depend on the modal number. The loss factors are small and decrease monotonically with modal number.

Table 5.2 shows the resonant frequencies and modal loss factors of the layered shell in the three configurations of the applied damping treatment with the storage modulus of the damping layer changed to  $E_2^* = 4.14 \times 10^9 \text{ N/m}^2$ . The other parameters are the same as that in Table 5.1. In this case also the natural frequencies are clustered near the first fundamental frequency. The modal loss factors decrease monotonically with modal number. The difference between the two results is only in the modal loss factor value, which increases by the same order of magnitude as the increase in  $E_2^*$ .

Table 5.3 shows the natural frequencies and loss factors for two different values of the damping larger Young's modulus and for a thickness of the damping layer ten times the thickness of the base layer, for the outside coating

of the damping treatment. It is clearly observed from the table that with increase in thickness and increase in the storage Young's modulus of the damping layer, the modal loss factors are considerably increased almost in a linear manner both with respect to the damping layer thickness, and its Young's modulus. The clustering of the natural frequencies around its fundamental frequency is somewhat reduced with increased values of  $E_2^*$  and  $h_2$ . The modal loss factors again decrease with modal number.

b) Sandwich Shell: Table 5.4 presents the resonant frequencies and loss factors of the sandwich shell for the three values of the core shear parameter. In this case too, the natural frequencies are closely packed near the first resonant frequency. The predominant term in the frequency equation (5.31) is the term

$$\frac{D_t}{\mu} \frac{12(1-\nu^2)}{a^2 h_1^2}$$

for the first few modal numbers and is independent of modal number. This term corresponds to the square of the ring frequency of a homogeneous shell having flexural rigidity equal to twice the flexural rigidity of a shell of face layer material of thickness  $h_1$ . It is because of the independence of this term with respect to modal number, that the natural frequencies are clustered. The modal loss factors turn out to be extremely

small in the first few modes, essentially due to the same reason, the imaginary part of equation (5.31) being negligibly small compared to the real part. The modal loss factor increases in all cases of  $\bar{g}$  with modal number. As has been the case with the infinite and finite sandwich plates, it is seen from the table that there exists an optimum value  $\bar{g}$  which depends on the modal number for maximum modal loss factor. The natural frequencies increase monotonically with  $\bar{g}$ , the increase being significant only in the higher modes, for reasons mentioned above.

Table 5.5 gives the resonant frequencies and loss factors for different values of the core loss factor  $\beta$ . The resonant frequencies do not change significantly with respect to  $\beta$  for the particular value of  $\bar{g}$  chosen. The modal loss factors increase with  $\beta$ . The increase is very nearly linear for modal numbers greater than 5. Thus even with increase in  $\beta$ , the modal loss factor in the fundamental mode is not improved significantly due to the predominance of the third term in equation (5.31).

Table 5.6 shows the variation of resonant frequencies and loss factors with respect to the geometric parameter  $Y$ . The resonant frequencies decrease with increasing  $Y$ , the increase becoming less for higher modal numbers. The loss

factors increase with increase in  $Y$ , but in the first two modes of the structure the loss factor remains extremely small.

Table 5.7 shows the cavity resonant frequencies for the dimensions of the cavity adopted.

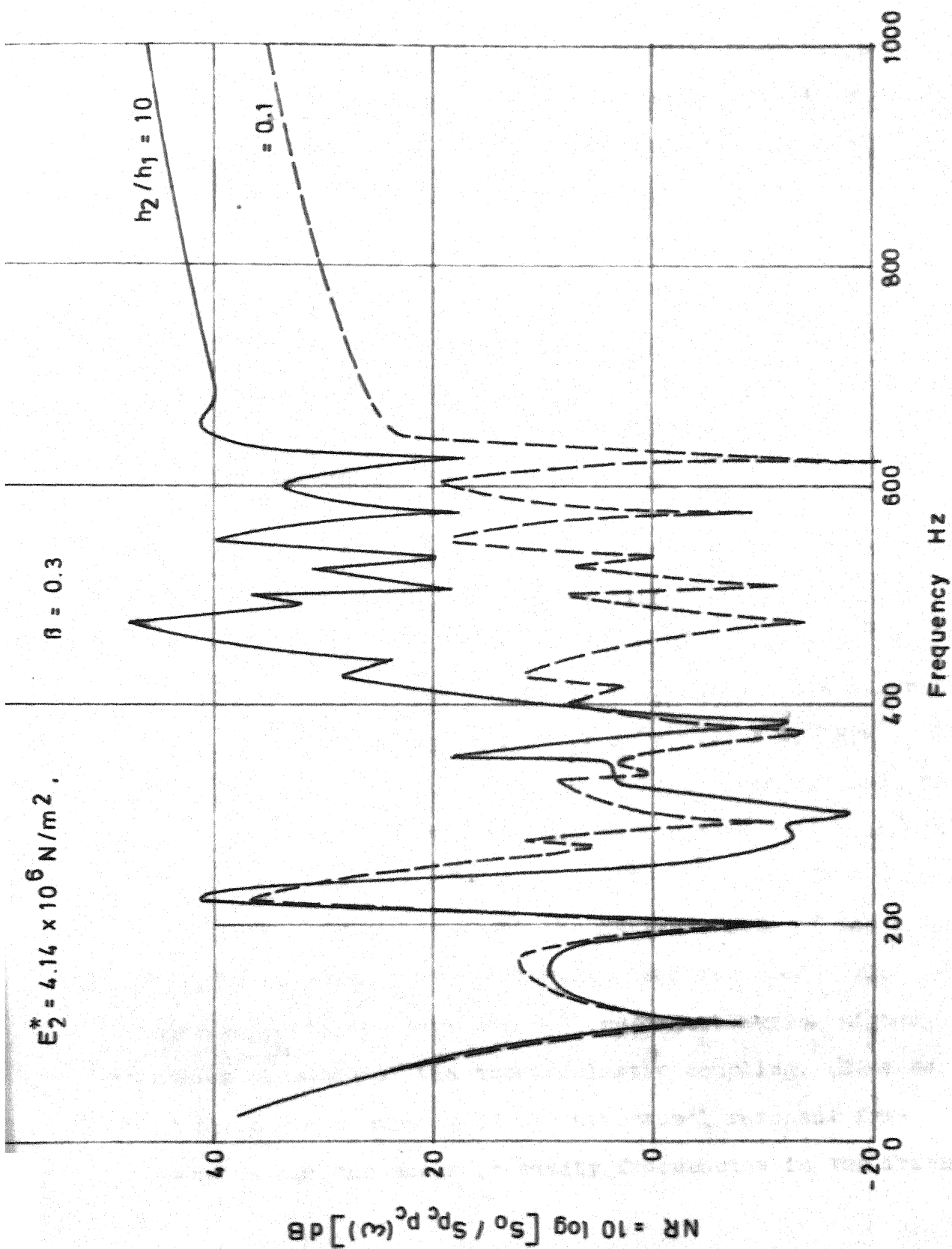
### 5.5.2 Noise Reduction and Structural Response

a) Layered Shell: Figure 5.5 shows the variation of the noise reduction inside the cylindrical enclosure for two different thickness ratios of the damping layer to the face layer, and for a constant value of the damping layer Young's modulus  $E_2^* = 4.14 \times 10^6 \text{ N/m}^2$ . The excitation considered is white noise excitation with spectral density function  $S_0$ . The noise reduction curves show dips of negative values corresponding to most of the cavity resonant frequencies of Table 5.7 in the case of thickness ratio of the damping layer to the elastic face layer equal to 0.1. There are many structural resonant frequencies and cavity resonant frequencies within the range of 650Hz, that it is difficult to describe the coupling action between the structure and the cavity modes. For the case of a higher thickness ratio of 10, the noise reduction improves significantly beyond a frequency of 400 Hz, essentially due to the increased surface mass density of the layered shell. Even though dips occur at the cavity

Table 5.7 - Acoustic Resonant Frequencies of a Circular  
Cylindrical Cavity (Axi-symmetric Modes )

i	k	$f_{i0k}$ (Hz)
0	0	0.0
0	1	109.00
2	0	165.00
2	1	198.29
0	2	201.36
2	2	260.33
0	3	291.99
4	0	330.00
2	3	335.39
4	1	347.84
0	4	382.40
4	2	386.58
2	4	416.48
4	3	440.64
6	0	495.00
4	4	505.00
6	1	507.07
6	2	534.39
6	3	574.70
6	4	625.50

FIG. 5.5 EFFECT OF DAMPING LAYER THICKNESS ON NOISE REDUCTION



resonances in this case, the minimum values of noise reduction are in the positive range. Sometimes the increase in noise reduction value for the higher thickness ratio as compared to the lower thickness ratio is as much as 40 dB (at 625 Hz). Beyond 625 Hz, there are no dips in the noise reduction curves, for the cavity modes beyond 625 Hz have not been included in the analysis. The very low value of the noise reduction for  $h_2/h_1 = 0.1$  at 625 Hz is due to the high degree of coupling between a structural mode and cavity mode.

Figure 5.6 shows the noise reduction curves for the same thickness ratios, but for a different value of the Young's modulus of the damping layer  $E_2^* = 4.14 \times 10^9 \text{ N/m}^2$ . In this case, the dips at cavity resonances are smaller than for the corresponding values for  $E_2^* = 4.14 \times 10^6 \text{ N/m}^2$ . The increased thickness of the damping layer does not help to improve the noise reduction values for  $E_2^* = 4.14 \times 10^9 \text{ N/m}^2$  unlike the case for  $E_2^* = 4.14 \times 10^6 \text{ N/m}^2$ . The fact that at the cavity 'off resonances' the maximum value of the noise reduction values are considerably less for  $E_2^* = 4.14 \times 10^9 \text{ N/m}^2$  may be due to the cavity modal impedances having higher values because of the acoustoelastic coupling. Because of the close proximity of the structural resonant frequencies and the acoustic cavity frequencies in the frequency

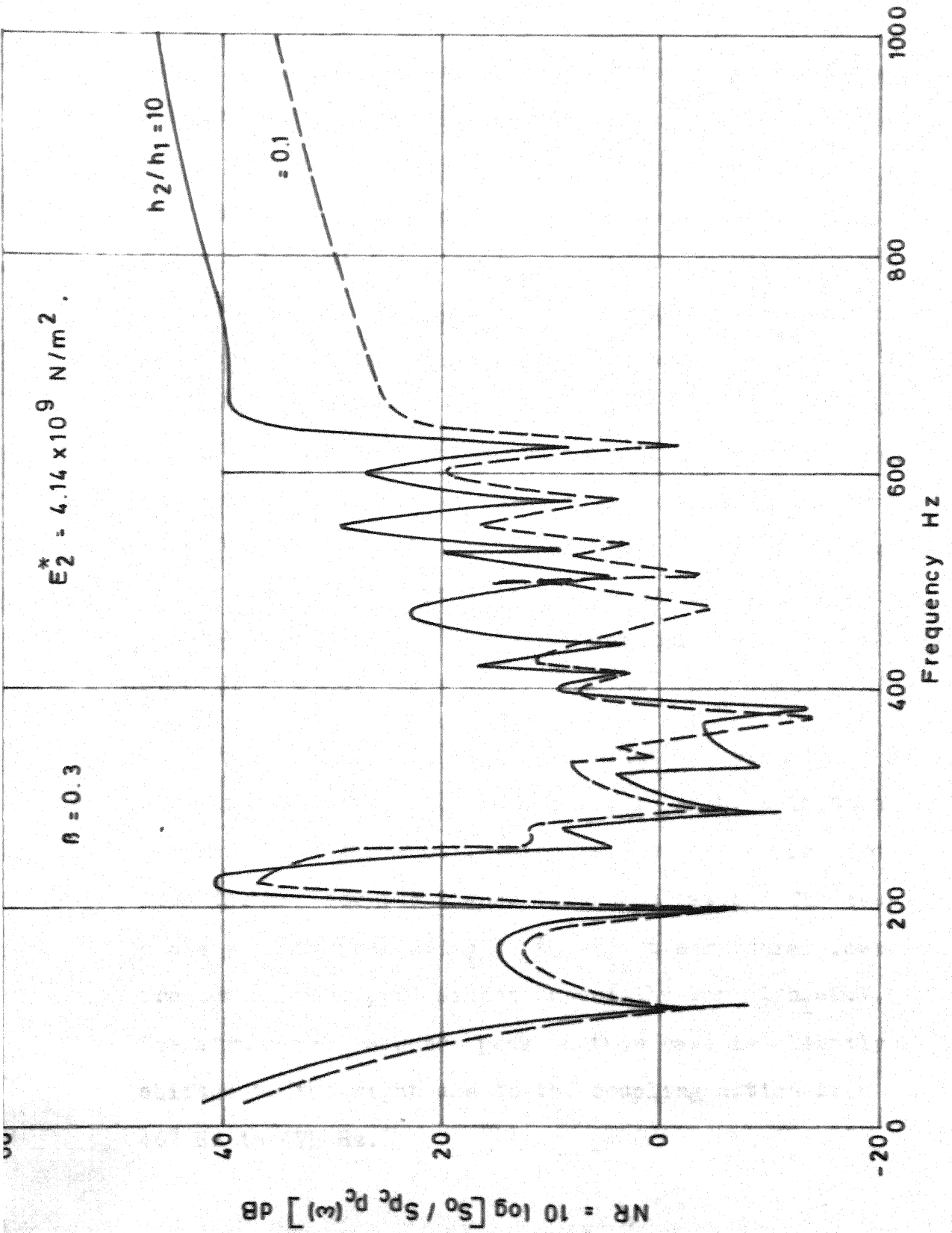


FIG. 5.6 EFFECT OF DAMPING LAYER THICKNESS ON NOISE REDUCTION

range considered, it is very difficult to describe the coupling action between the structural motion and the cavity pressure with respect to the properties of the layer materials. Figures 5.7 and 5.8 respectively show the shell response spectral densities corresponding to Figures 5.5 and 5.6. It is observed from Figure 5.7 that for  $h_2/h_1 = 0.1$  and  $E_2^* = 4.14 \times 10^6 \text{ N/m}^2$ , the structural response peaks at 475 Hz and at 625 Hz. The peak at 625 Hz is predominant due to the strong coupling of the structural mode and cavity mode which coincide at that frequency. For  $h_2/h_1 = 10$ , the response levels are considerably lower than for  $h_2/h_1 = 0.1$  because of high modal loss factors. In this case the response peaks at 300 Hz which is considerably higher than the first natural frequency of the structure of 269 Hz.

From Figure 5.8, it is seen that the structural response has low levels corresponding to  $h_2/h_1 = 10.0$  as compared to  $h_2/h_1 = 0.1$ , which is due to the high modal loss factors for the higher thickness ratio. The response peak corresponding to the first structural resonant frequencies are predominant especially for  $h_2/h_1 = 0.1$ . The structural response peak in this case is slightly shifted to the right due to the coupling action from 462 Hz to 475 Hz.

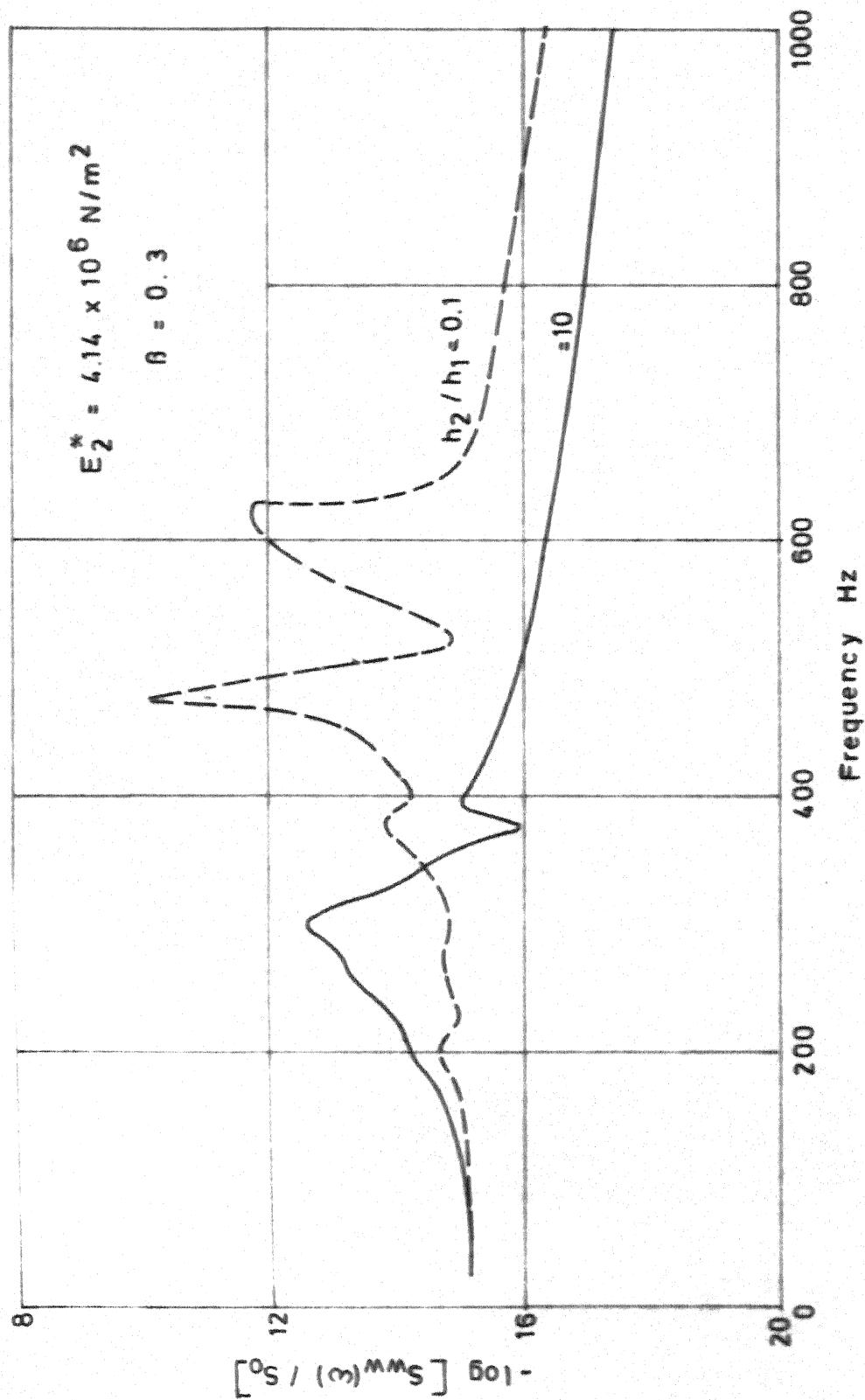


FIG. 5.7 EFFECT OF DAMPING LAYER THICKNESS ON STRUCTURAL RESPONSE

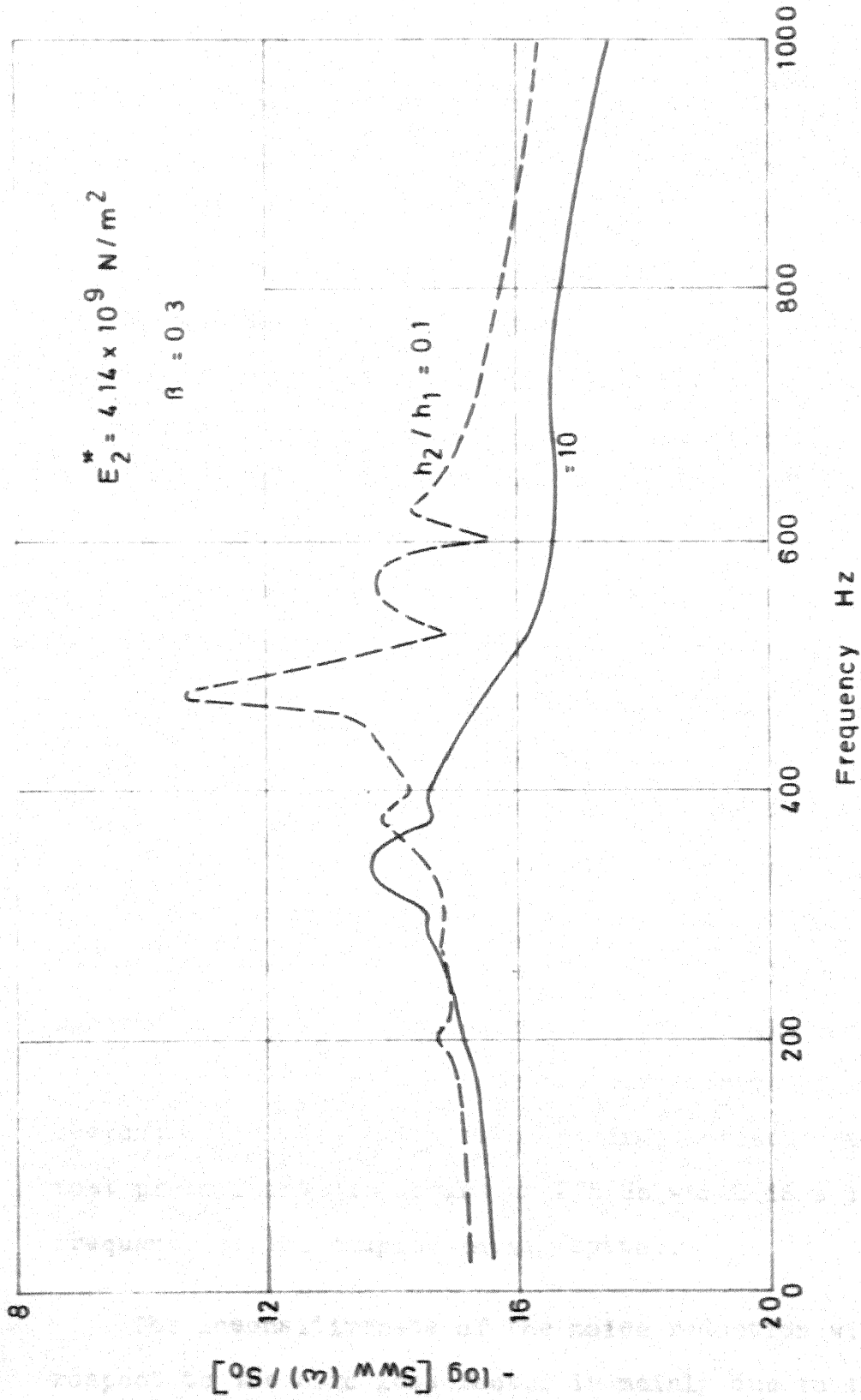


FIG. 5.8 EFFECT OF DAMPING LAYER THICKNESS ON STRUCTURAL RESPONSE

b) Sandwich Shell: Figures 5.9 to 5.11 show the variation of noise reduction respectively with respect to the core shear parameter, loss factor and geometric parameter, for an external white noise excitation. The noise reduction has negative values corresponding to the cavity resonant frequencies for all value of  $\bar{g}$  upto a frequency of 400 Hz as seen from Figure 5.9. The dip at 275 Hz which is neither a cavity frequency nor a structural frequency is a resonant frequency of the coupled cavity-structure system. Corresponding to this frequency the noise reduction value is improved for a higher value of  $\bar{g} = 5000$ . Otherwise, there is no significant difference in the noise reduction values for the different values of  $\bar{g}$ . Even though there are three cavity resonant frequencies in the range 400 - 500 Hz, the noise reduction curves do not have dips in this range due to the coupling action of the cavity and the structural motion. Figure 5.10 shows the variation of noise reduction with respect to the core loss factor  $\beta$ . Again there is no significant variation in the noise reduction curves. The noise reduction curves have dips corresponding to the cavity resonant frequencies. But the most predominant dip occurs at 275 Hz which is a resonant frequency of the coupled cavity system.

The insensitiveness of the noise reduction with respect to the core loss factor is mainly due to the fact

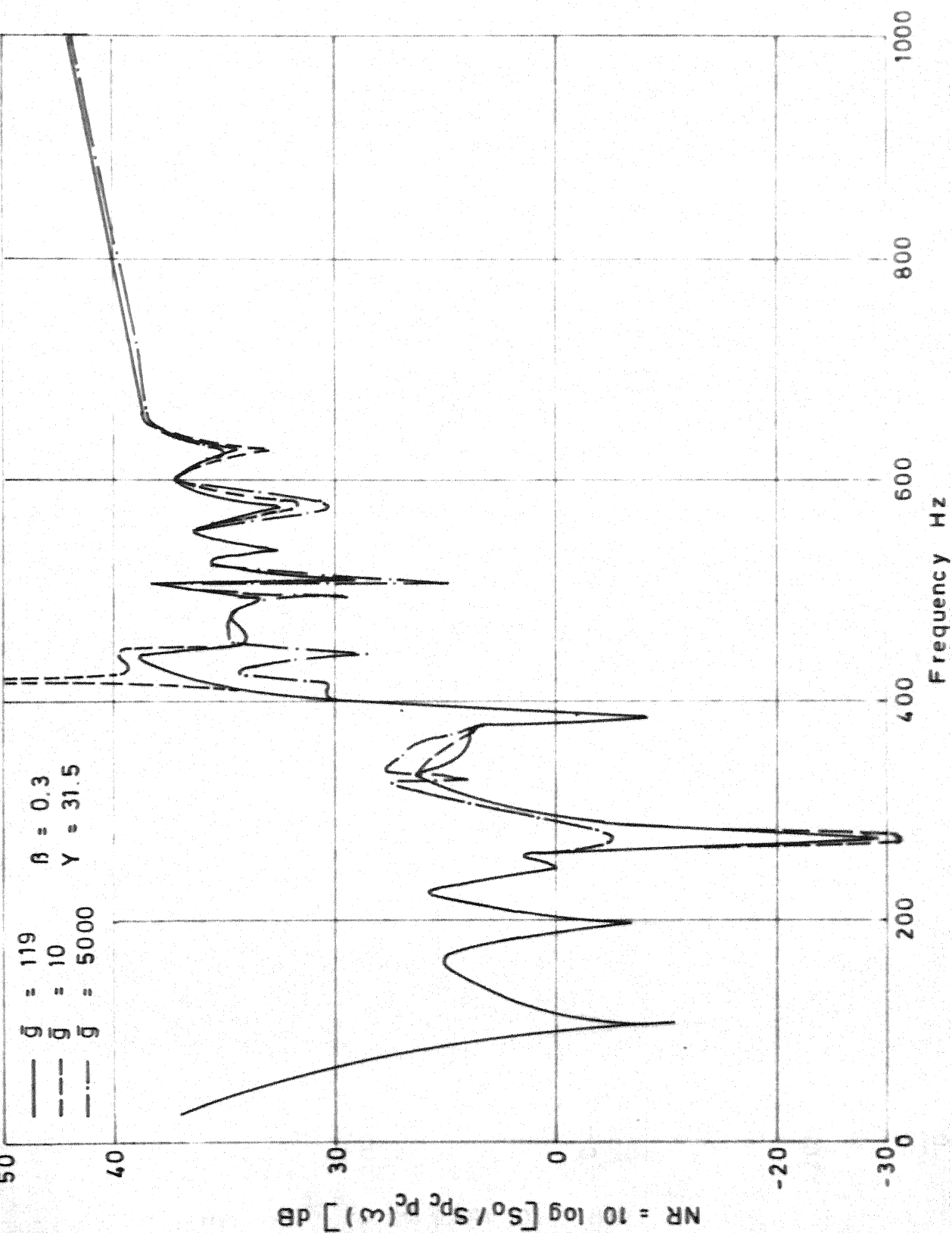


FIG. 5.9 EFFECT OF SHEAR PARAMETER ON NOISE REDUCTION (SANDWICH SHELL)

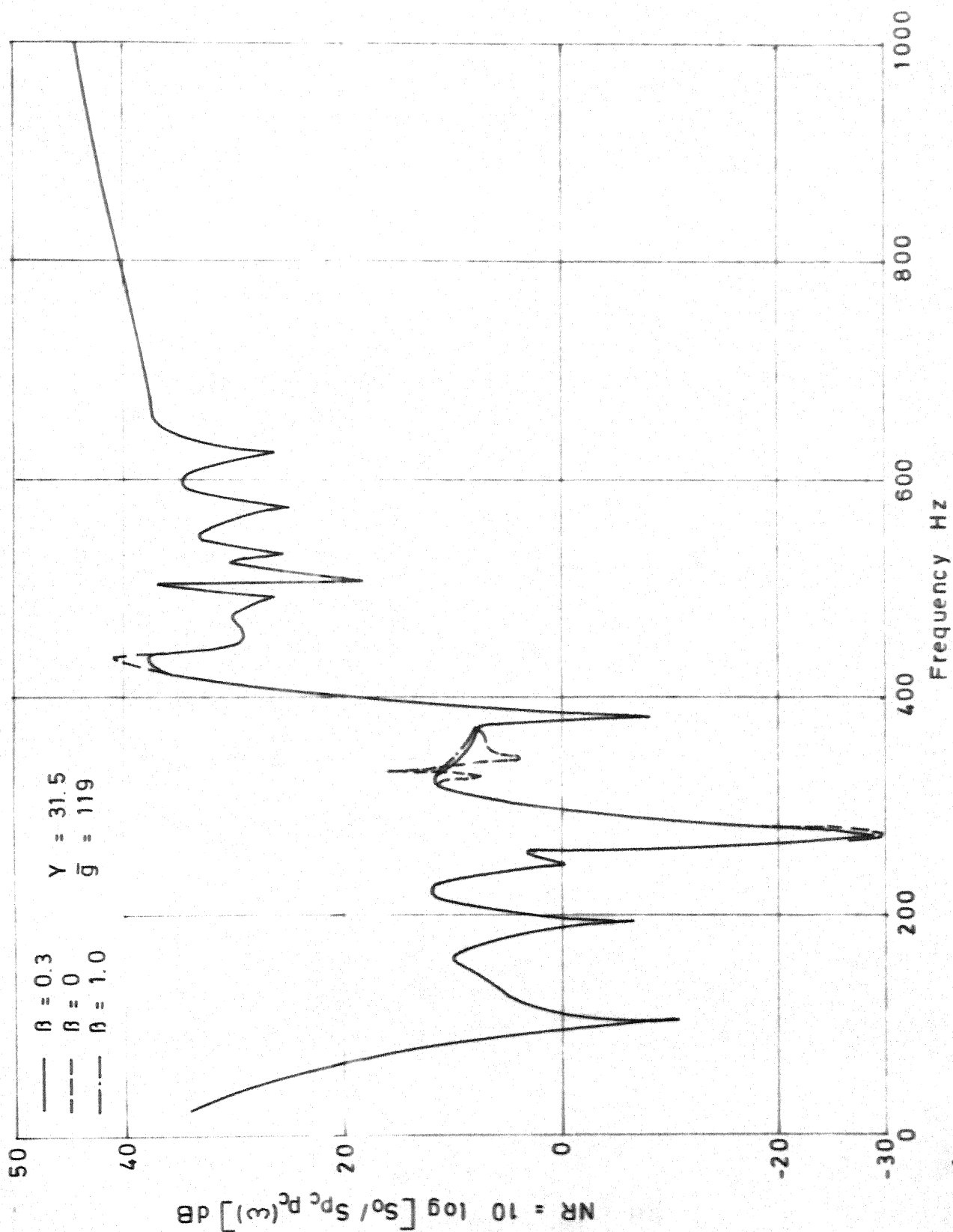


FIG. 5.10 EFFECT OF CORE LOSS FACTOR ON NOISE REDUCTION

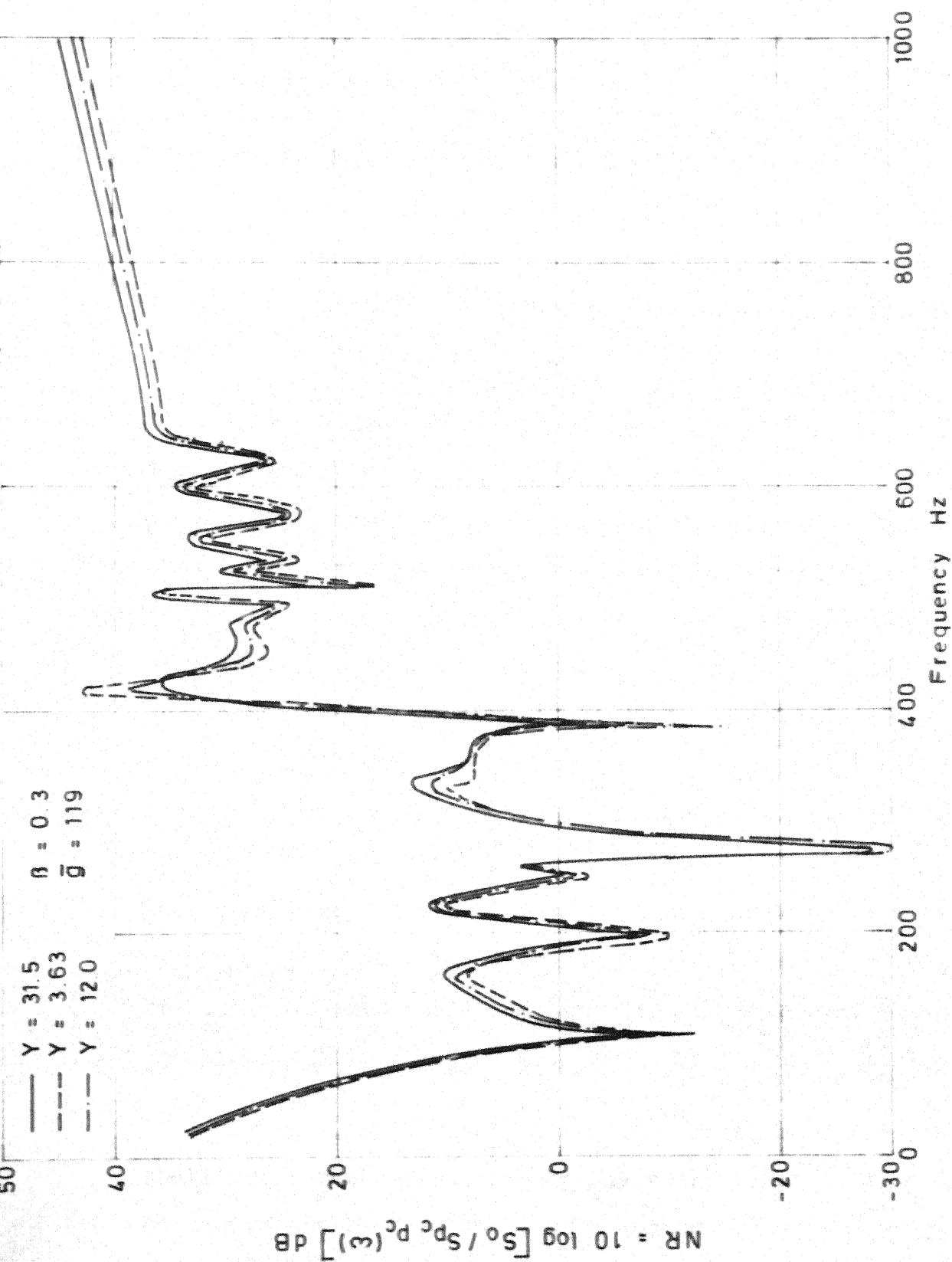


FIG 5.11 EFFECT OF GEOMETRIC PARAMETER ON NOISE REDUCTION  
(SANDWICH SHELL)

that in the low frequency ranges the modal loss factors are very low.

Figure 5.11 shows the variation of the noise reduction inside the cylindrical shell with respect to the geometric parameter. In this case too, the noise reduction is insensitive to the geometric parameter and the differences are only marginal.

Figures 5.12 to 5.14 show the variations in structural response with respect to  $\bar{g}$ ,  $\beta$  and  $Y$  respectively. In all the three cases the predominant structural response peak occurs at a frequency of 275 Hz corresponding to a resonant frequency of the coupled cavity, structure system. Surprisingly, the structural response curves are also not very sensitive to the variations in the sandwich core parameters. It is due to the low values of the modal loss factors obtained in the low frequency ranges because of the predominance of the ring frequency term in the natural frequency expression of equation (5.31). The constrained layer damping treatment in the axisymmetric modes of vibration of the shell in the lower order structural modes is not very effective.

Figure 5.15 compares the noise reduction of a sandwich shell with constrained damping layer treatment to that of an equivalent layered shell with unconstrained damping

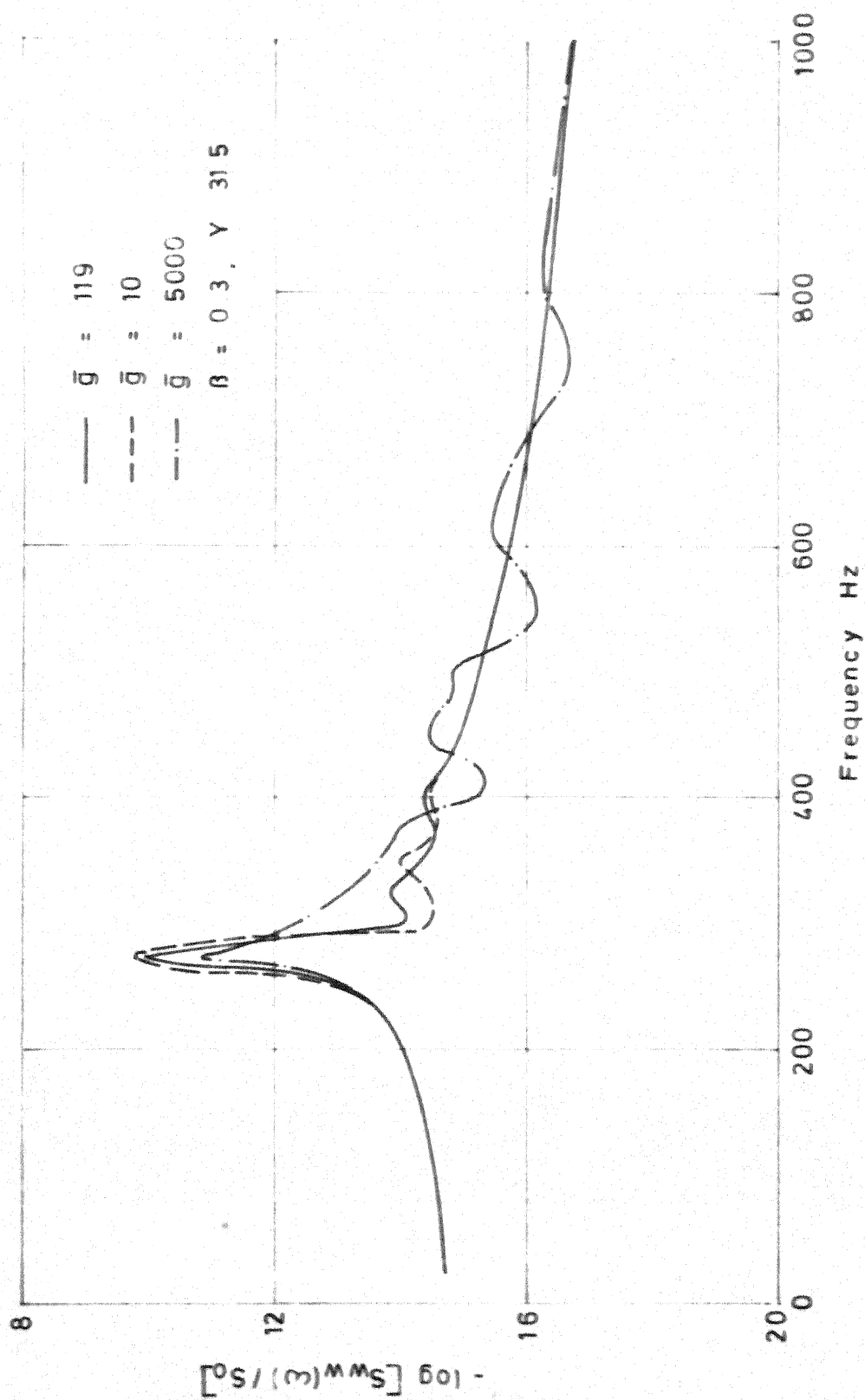


FIG. 5.12 EFFECT OF SHEAR PARAMETER ON STRUCTURAL RESPONSE  
(SANDWICH SHELL)

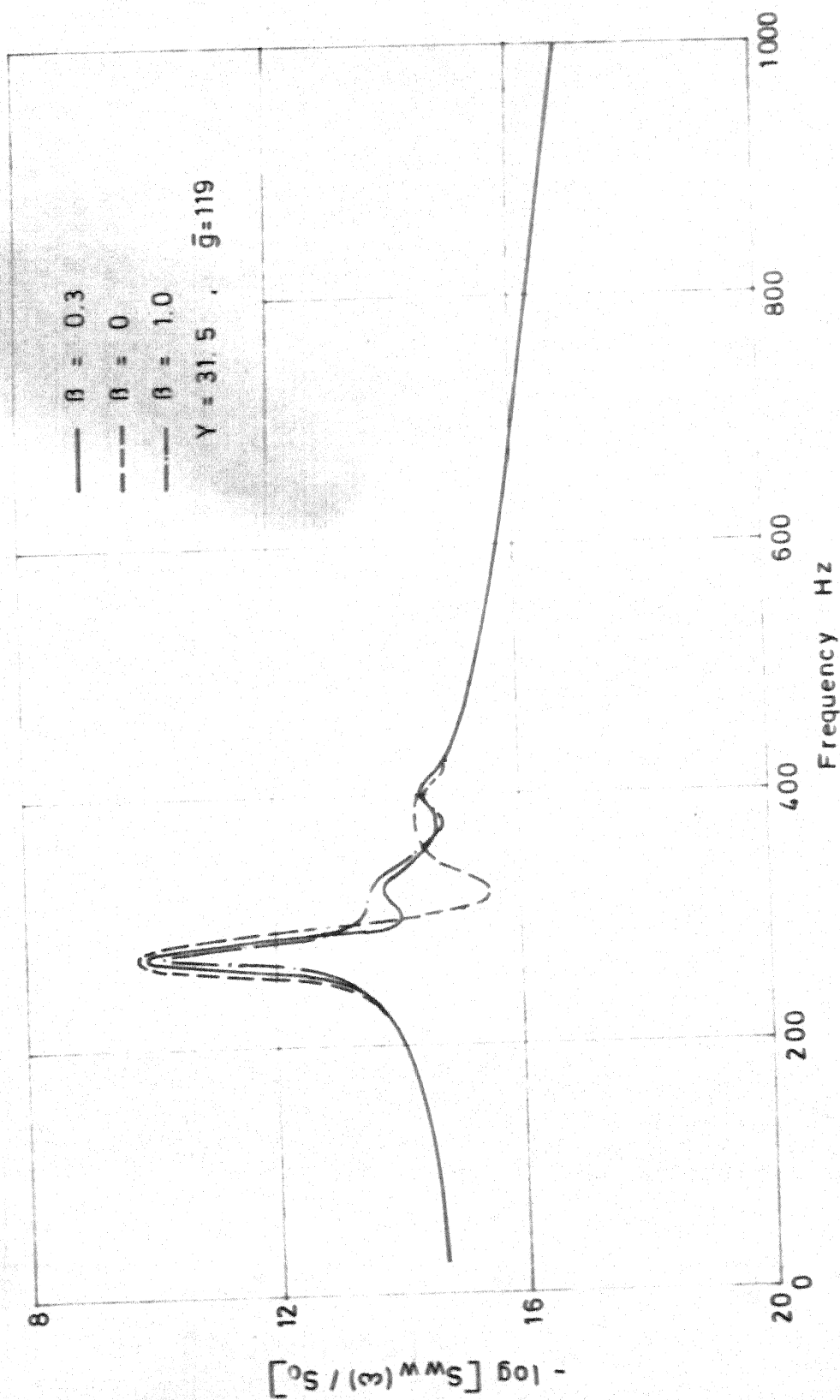


FIG. 5.13 EFFECT OF CORE LOSS FACTOR ON STRUCTURAL RESPONSE  
(SANDWICH SHELL)

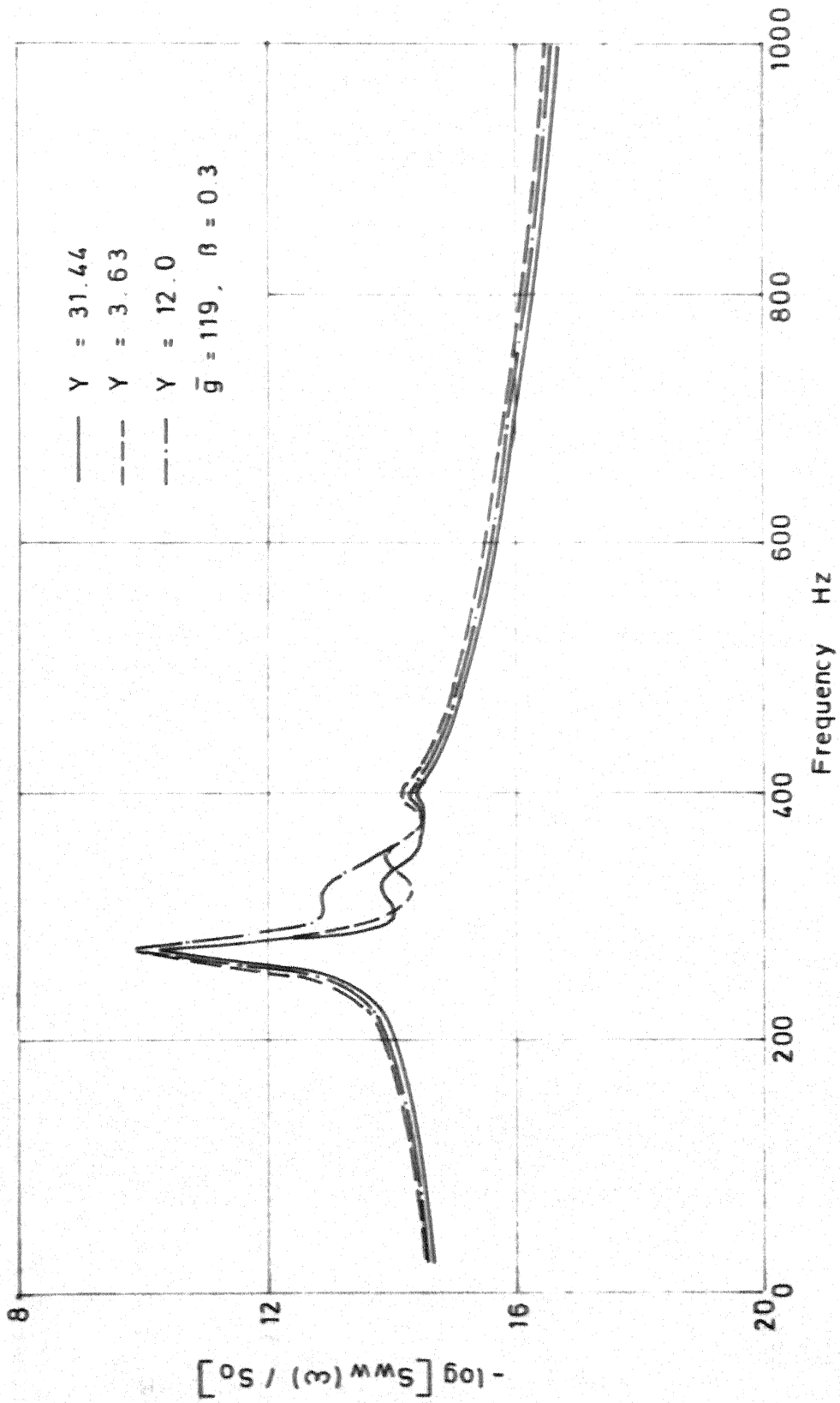


FIG. 5.14 EFFECT OF GEOMETRIC PARAMETER ON STRUCTURAL RESPONSE  
(SANDWICH SHELL)

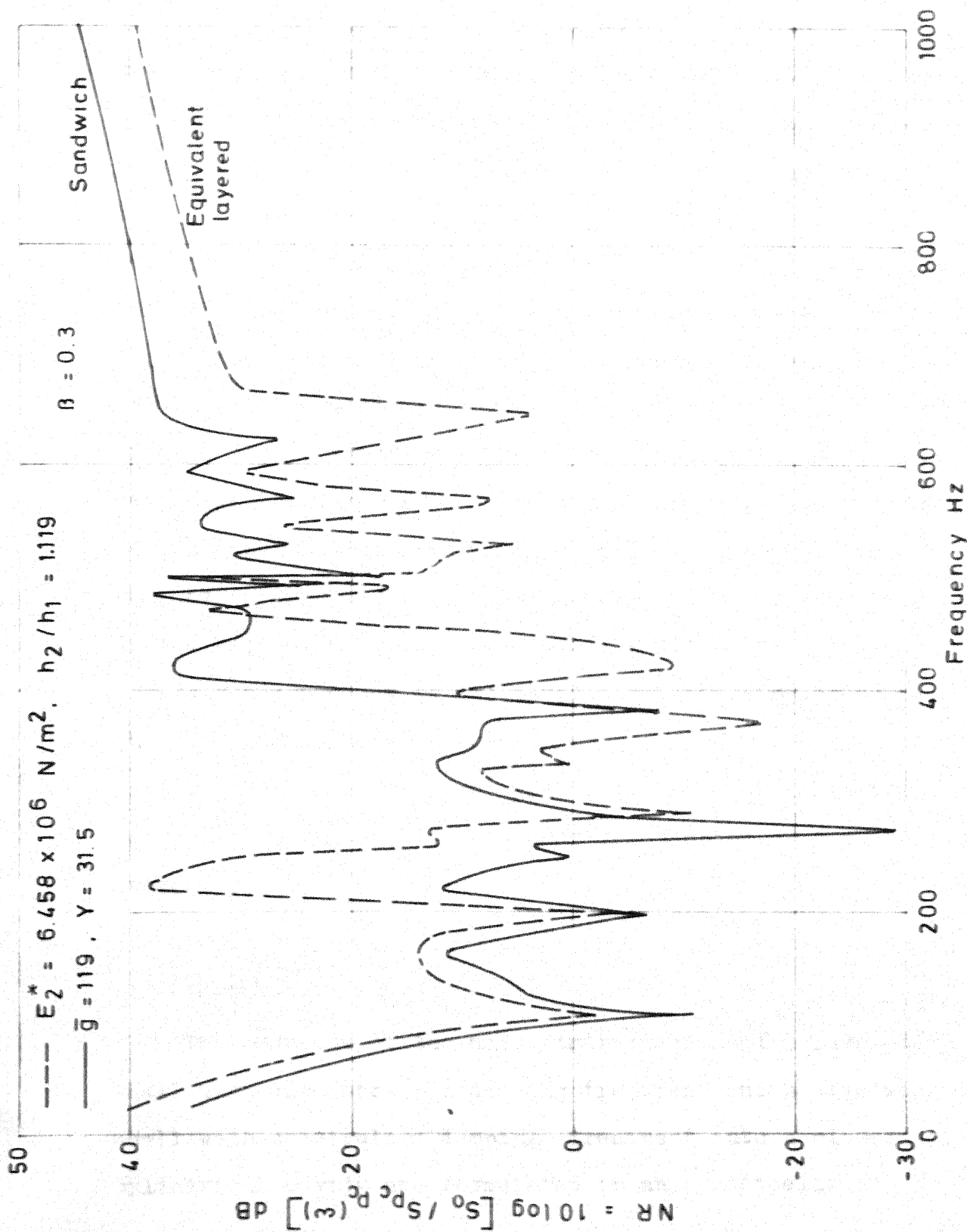


FIG. 5.15 COMPARISON OF NOISE REDUCTION BETWEEN SANDWICH AND

treatment applied as an outside coating. In both the cases the surface mass density is kept constant. The resonant frequencies and modal loss factors of the equivalent layered shell is shown in Table 5.8, along with those of the corresponding sandwich shell. The modal loss factor in the equivalent layered shell is less than that for the sandwich shell in all the modes except the first mode. From Figure 5.15 it is seen that beyond 400 Hz the sandwich shell has slightly improved transmission characteristics. The dips in the noise reduction curves in the case of the sandwich shell are less pronounced, beyond that frequency. Figure 5.16 shows the corresponding structural response in the two cases. While in the case of the sandwich shell the structural peak occurs corresponding to the coupled resonant frequency of the cavity-structure system, in the case of the equivalent layered shell, the response peaks occur by and large with respect to the uncoupled resonant frequencies of the structure.

## 5.6 CONCLUSIONS

The problems of the noise transmission of a layered shell with unconstrained damping treatment and a sandwich shell with constrained damping treatment into a closed cylindrical cavity are formulated in an acoustoelastic

Table 5.8 - Resonant Frequencies and Loss Factors

m	Equivalent layered shell (OC)		Sandwich shell	
	$E_2^* = 6.458 \times 10^6 \text{ N/m}^2$	$(h_1 = 0.001\text{m}, \gamma = 31.5, \bar{g} = 119, \beta = 0.3)$		
	$f_m \text{ (Hz)}$	$\eta_m \times 10^4$	$f_m \text{ (Hz)}$	$\eta_m \times 10^4$
1	421.32	.2808	402.11	.012
3	421.44	.2807	402.71	3.520
5	422.25	.2796	404.88	24.600
7	424.89	.2761	408.89	67.300
9	430.99	.2684	415.02	127.000
11	442.61	.2545	423.68	199.000
13	461.95	.2336	435.41	277.000
15	491.05	.2067	450.75	357.000
17	531.47	.1767	470.25	431.000
19	584.19	.1461	494.38	495.000
21	649.54	.1181	523.55	545.000

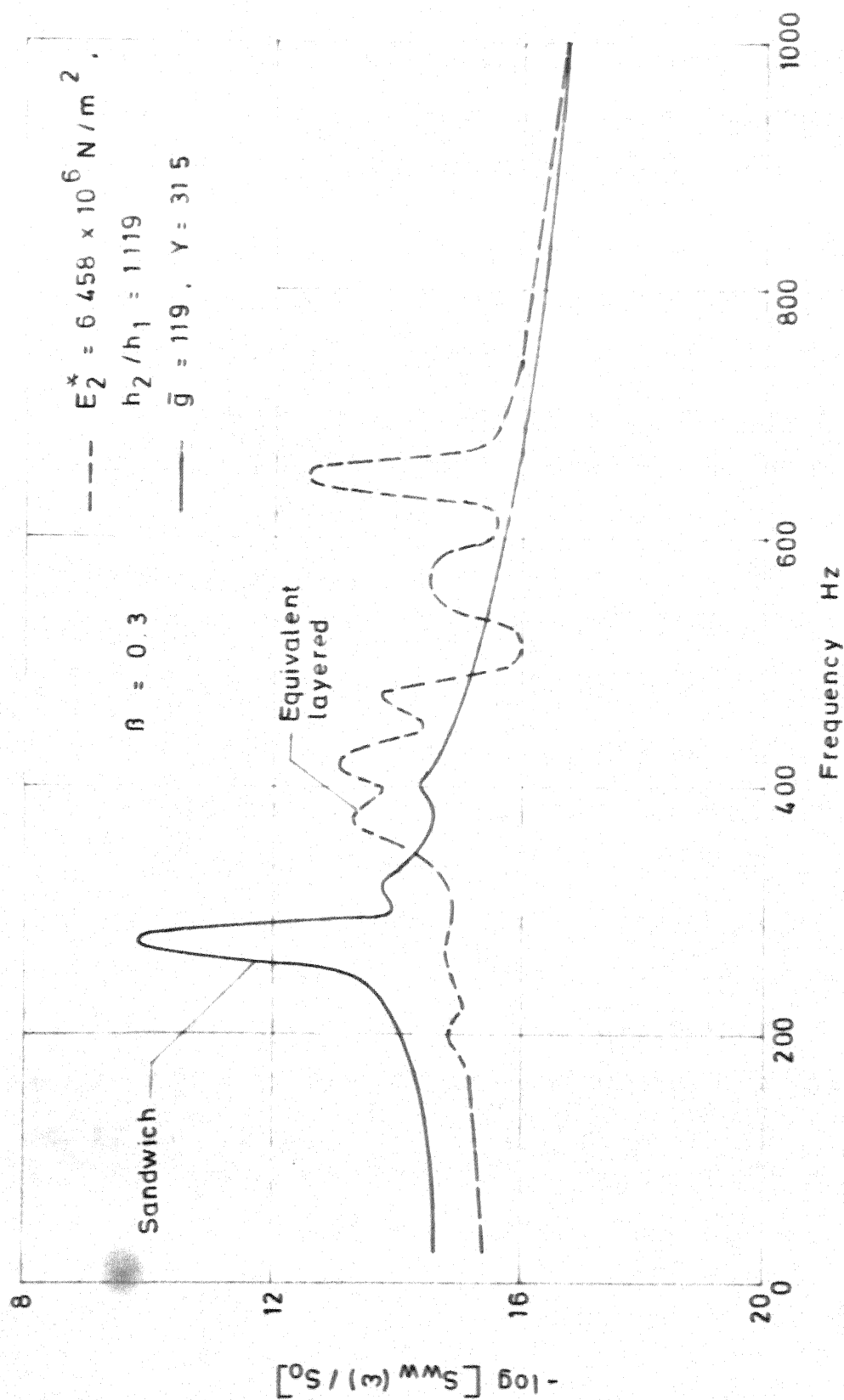


FIG. 5.16 COMPARISON OF STRUCTURAL RESPONSE BETWEEN SANDWICH AND EQUIVALENT LAYERED SHELL

formulation. Only the axisymmetric vibrations of the shell are considered. The coupled cavity-structure equations are solved by a matrix inversion scheme.

The results show that the applied damping treatment is not very effective in the axisymmetric modes of vibration of the sandwich shell because of the predominance of vibration corresponding to the ring frequency of the composite shell. Hence the noise reduction and structural response are insensitive to the changes in the sandwich core parameters. The in-vacuo structural resonant frequency of the sandwich shell is reduced due to the coupling action, as the cavity adds to the inertia of the structure.

In the case of the layered shell significant improvements in the noise transmission characteristics of the shell are possible by increasing the thickness of the damping layer and a suitable choice of the Young's modulus of the damping layer material. The noise transmission characteristics and the structural response do not vary with the three configurations of the layer treatment OC, IC and TC.

## CHAPTER 6

### SUMMARY AND CONCLUSIONS

This thesis presents mainly a theoretical analysis of the noise transmission characteristics of sandwich structures with constrained damping layer treatment. The different problems considered in the analysis are:

1. Sound transmission through an infinite sandwich plate,
2. Noise transmission through an elastically supported finite sandwich plate into a rectangular cavity
3. The noise transmission through finite circular cylindrical sandwich shell into a closed cavity.

The noise transmission through a layered shell with unconstrained damping treatment into a cylindrical enclosure is also studied. The influence of the damping treatments on the structural response of the composite structure is investigated in the analysis. The coupling between the acoustic pressure loading and the structural motion is adequately treated in all the examples.

#### 6.1 INFINITE SANDWICH PLATE

The problem of the sound transmission of a damped sandwich plate of infinite extent is formulated on classical

lines. The formulation takes into account the interaction between the structural motion, and the radiated pressures on either side of the panel, the incident and reflected pressures.

The damping layer consists of a viscoelastic material of relatively low rigidity constrained between two elastic face layers. In the analysis the face plates are assumed to be of the same material and same thickness. The equations of motion of a three layered sandwich plate [6] have been reduced to represent the equation of motion of the infinite sandwich.

Expressions for the sound transmission loss of the sandwich plate and the coincidence frequency have been derived in terms of the sandwich core parameters, the face plate properties and the incidence angle of the external harmonic pressure wave using the dispersion relation between flexural wave number and frequency of the sandwich plate.

Unlike the case of the homogeneous <sup>elastic</sup> sandwich panel, the coincidence frequency for the sandwich panel becomes a complex number as a consequence of the flexural wave motion in the plate being a spatially damped wave. The sound transmission coefficient for the sandwich plate is

derived in terms of the specific transmission impedance of the sandwich panel. The specific transmission impedance of the sandwich panel has both reactive and resistive components, unlike the case of the homogeneous elastic panel, whose specific transmission impedance is wholly reactive. Because of the damping layer, the transmission loss has a positive value at all frequencies.

A parametric study of the sound transmission loss of the sandwich plate is undertaken with respect to the core parameters, namely, the shear parameter, core loss factor and the geometric parameter, and the incidence angle of the incident pressure wave. The following conclusions are drawn as a result of the investigation.

1. The sound transmission loss is very much sensitive to the variations in the core shear parameter  $g'$ . The coincidence frequency decreases with increasing values of  $g'$ . The analysis also shows the existence of an optimum value of  $g'$  for maximum transmission loss at coincidence.
2. The coincidence transmission loss of the sandwich increases with increase in core loss factor. The maximum increase of transmission loss with core loss factor is achieved for the optimum value of the shear parameter  $g'$ .

3. The transmission loss increases marginally with increase in the geometric parameter.
4. The coincidence frequency for the sandwich panel is higher than for an equivalent homogeneous panel of the same surface mass density.
5. The sound transmission loss decreases with increase in incidence angles upto the coincidence frequency. The coincidence frequency decreases with increasing angles of incidence.

The study clearly reveals that significant improvements in the sound insulation characteristics of homogeneous panels can be achieved by constrained layer damping treatments mainly due to two reasons. The coincidence frequency can be shifted to higher ranges of frequency by the sandwich construction. Secondly the coincidence transmission loss can be increased significantly by a proper choice of the core shear parameter and loss factor.

## 6.2 FINITE SANDWICH PLATE

The noise transmission through a finite sandwich plate with constrained damping layer treatment into a rectangular cavity is formulated as an acoustoelastic problem on the lines of Dowell [5], taking into consideration the interaction between the internal sound field

in the cavity and the structural motion. A direct matrix inversion scheme is proposed and used to solve the coupled matrix acoustoelastic equations in the pressure coefficients and the structural generalized coordinates. This method takes advantage of the diagonal nature of some of the matrices in a 'partition' analysis which avoids the use of an eigenvalue analysis which may be a difficult proposition in view of the order of the matrix involved and the elements in the matrix being complex values.

The formulation admits elastic boundary conditions at the longer edges of the plate representing realistic boundary conditions that would obtain in sheet-stringer panel construction. The other two edges are assumed to be simply supported. The presence of the damping layer and the assumption of boundary conditions other than simply supported necessitates a 'forced damped normal mode' analysis for the response and noise transmission calculations. The damped normal mode analysis is systematically applied analogous to the classical normal mode analysis for determining the vibroacoustic response. The natural frequencies, associated loss factors and damped normal modes of the sandwich plate are obtained by an iterative interpolation method. Expressions for the modal parameters, like the generalized mass, generalized force, acousto-structural modal coupling coefficients are derived in terms of the

sandwich properties. Only the symmetric structural modes are considered in the analysis in view of symmetric boundary conditions and uniform loading on the plate. The frequency range of interest in the study has been restricted to 1000 Hz. Both harmonic and stationary random loading are considered in the analysis.

An exhaustive parametric study with respect to the sandwich core parameters is undertaken. The following conclusions are drawn from the parametric study.

1. The effect of the boundary conditions on the noise reduction is mainly felt only at the fundamental structural resonances of the panel.
2. The induced damping improves the noise reduction values at structural resonances especially in the lower order structural modes.
3. Negative noise reduction values inside the enclosure are obtained corresponding to low structural resonant frequencies and loss factors, and whenever the in-vacuo structural resonant frequencies and cavity resonant frequencies occur in close proximity.
4. As in the case of the infinite sandwich plate, by a suitable choice of  $g^*$ , the core shear parameter and the core loss factor  $\beta$ , the modal loss factors can be increased with consequent improvement in the noise transmission characteristics corresponding to structural resonant frequencies.

5. The structural response reduces significantly with increase in the core loss factor  $\beta$ . The structural response has maximum values corresponding to its first resonant frequency which may be slightly altered due to the coupling action of the cavity pressure.
6. The structural response attains higher values also corresponding to a coupled natural frequency of the cavity-structure system due to close proximity of the in-vacuo structural resonant frequency and a cavity resonant frequency.

The results of the vibro-acoustic response study of cavity backed finite sandwich panel are qualitatively similar to those of finite homogeneous panels, but because of the presence of the damping layer the noise transmission of the sandwich panel is improved especially at the lower order structural modes.

### 6.3 FINITE LAYERED AND SANDWICH SHELLS

The problems of noise transmission and structural response of a layered circular cylindrical shell with unconstrained damping layer treatment and a sandwich shell with constrained damping treatment are considered in the analysis in a similar manner as that of a finite

sandwich plate. Only the axi-symmetric vibrations of the shell and simply supported end conditions are investigated.

The acoustoelastic problems are formulated in a matrix format taking into account the interaction of the cavity pressure field and the flexible wall. The cavity pressure is expanded in terms of the cavity normal modes (axi-symmetric), the radial variations in terms of Bessel functions of the first kind and the longitudinal variations in terms of sine functions. The structural motion is expanded in terms of sine functions, resulting in terms of a coupled matrix differential equations in the pressure coefficients and structural generalized coordinates. The problem is solved by a matrix inversion procedure similar to that adopted for the sandwich plate. It may be mentioned here, that, perhaps for the first time in this work, that the noise transmission through layered shells with constrained and unconstrained damping treatments is analysed.

For the case of the finite shell, extensive parametric studies as in the case of the sandwich plate are not carried out. Moreover, because of the close proximity of a number of structural and cavity resonant frequencies in the frequency range of interest, it becomes difficult to explain the coupling action between the cavity pressure and the structural motion precisely.

Damping effectiveness in the case of sandwich shells is small in the lower order axisymmetric modes of vibration. In the natural frequency expressions for the sandwich shell, a term similar to the ring frequency of homogeneous elastic shells, which is independent of the damping layer properties and the modal numbers, predominates over the other terms. Hence, the natural frequencies are clustered near the first resonant frequency and the modal loss factors in the first resonant frequency and for subsequent lower order modes are very small.

In the case of the layered shell the modal loss factor decreases with modal number, while for the sandwich shell the modal loss factor increases with modal number. The modal loss factor for the layered shell can be increased by increasing the elastic modulus of the damping layer and its thickness. However, the modal loss factor associated with the first mode of the sandwich shell cannot be increased sufficiently as explained earlier. Hence, the noise reduction in the case of the sandwich shell is quite insensitive to variations in the sandwich core parameters. The structural response of the sandwich shell is also not affected by the variations in the core parameters. But, the coupled natural frequencies of the structure-cavity system are significantly different from the in-vacuo structural resonant frequencies for the sandwich

shell considered in the analysis. For the layered shell however, the shifts in the natural frequencies from their in-vacuo values are not as much pronounced.

The noise reduction for the layered shell is sensitive to both the thickness and the elastic modulus of the damping layer, especially so for the non-resonant transmission of sound.

#### 6.4 SCOPE FOR FURTHER RESEARCH

The problem of noise transmission of sandwich structures, presented in this thesis can be extended to include irregular geometries of the cavity and arbitrary shapes of the sandwich panel. It can be achieved by considering finite element formulations both for the sandwich panel and the irregular acoustic enclosure. Craggs [68,95,96] has used acoustic finite elements and plate finite elements for the response and noise transmission characteristics of flexible homogeneous panels. The finite elements for the sandwich panel can be adopted from the works of Lu, Killian and Everstine [28,29]. Using a combination of these finite elements the acoustoelastic problem can be solved.

In the problem formulation it has been consistently assumed that the loss factor and the elastic moduli of

the viscoelastic damping layer are frequency and temperature independent. But this restriction on the material properties of the damping layer can be relaxed in the finite element formulation by incorporating the frequency variations of the properties of the viscoelastic layer.

Even though a matrix inversion scheme has been adopted for solving the acoustoelastic problem, better understanding of the precise nature of the coupling between the structural motion and the cavity pressure can be had by performing a matrix eigenvalue analysis which will give the coupled natural frequencies of the cavity-structure system and the corresponding loss factors. The method given by Meirovich [93] can be extended to handle matrices having complex elements.

In the analysis of the sound transmission of finite plates and shells the frequency range of interest has been restricted to 1000 Hz. The frequency range of interest can be extended to higher frequencies. In that case the equations of motion of the sandwich plate and shell adopted have to be modified to include the effects of shear deflection and rotary inertia. For very high frequency ranges the acoustoelasticity analysis presented in the thesis will not be suitable as one may have to contend with a large number of structural and cavity modes. The

statistical energy analysis (SEA) may be used for the prediction of response and noise transmission statistics in such cases. The SEA parameters, like the modal density and the radiation impedance of the sandwich panels can be derived analytically from the appropriate equations of motion of the sandwich structures. However, sufficient care has to be exercised in the energy flow calculations, as the usual assumption of weak coupling between the resonant modes in the frequency bands is not valid, due to the large modal damping induced by the constrained damping layer with significant intermodal coupling. Recently, Chandiramani [97] and Smith [98] have presented SEA models where the transition from weak to strong coupling between the modes are analysed. Making use of these models it may be possible to solve the coupled acoustoelastic problem of damped sandwich structures in the high frequency ranges.

In the case of the layered and sandwich shells, only the axisymmetric vibrations are considered. The formulation can be extended to consider the circumferential lobar modes of the shell.

## REFERENCES

1. Mixson, J.S., Barton, C.K. and Vaicaitis, R., 'Investigation of Interior Noise in a Twin-Engine Light Aircraft', J. of Aircraft, 15, PP 227-233, 1978.
2. Vaicaitis, R., 'Noise Transmission by Viscoelastic Sandwich Panels', NASA-TND-8516, August, 1977.
3. Reddy, C.V.R., 'Some Studies on the Effect of Damping Treatments on the Vibration and Noise Attenuation in Structures', Ph.D. Thesis, I.I.T., Madras, December, 1979.
4. Mead, D.J., 'The Vibration Characteristics of Damped Sandwich Plates with Stiffeners and Various Boundary Conditions', Strojnický časopis, XXII, C.1, PP 53-67, 1971.
5. Dowell, E.H., 'Acoustoelasticity', Department of Aerospace and Mechanical Sciences, Princeton University, AMS Report No. 1280, May, 1976.
6. Mead, D.J., 'The Effect of Certain Damping Treatments on the Response of Idealized Aeroplanes Structures Excited by Noise', U.S.A.F. Report No. AFML-TR-65-284, 1965.
7. Oberst, H., 'On Damping of Bending Vibration of Thin Sheet Metal by Additive Layer of Damping Materials', J. of Acustica, 2, Akustische, 4, PP 181-194, 1952.
8. Kerwin, E.M., 'Damping of Flexural Waves by a Constrained Viscoelastic Layer', J. Acous. Soc. Am. V. 31, PP 952-962, 1959.
9. Ross, D. and Kerwin, E.M., 'Damping of Flexural Vibrations in Plates by Free and Constrained Viscoelastic Layers', BBN Report, 632, 1959.
10. Ross, D., Ungar, E.E. and Kerwin, E.M., 'Damping of Plate Flexural Vibrations by Means of Viscoelastic Laminates', ASME-Colloquium on Structural Damping, PP 49-87, 1959.

11. Yu, Y.Y., 'Viscoelastic Damping of Vibrations of Sandwich Plates and Shells', Proc. IASS, Symp., Warsaw, PP. 551-561, 1967.
12. DiTaranto, R.A., 'Theory of Vibratory Bending of Elastic-Viscoelastic Layered Finite Length Beams', J. Appl. Mech., 32, PP 881-886, 1965.
13. Mead, D.J. and Markus, S., 'The Forced Vibration of a Three Layer Damped Sandwich Beam with Arbitrary Boundary Conditions', J. Sound and Vibration, 10(2), PP 163-175, 1959.
14. Mead, D.J., 'The Existence of Normal Modes of Linear Systems with Arbitrary Damping', Paper No. C-5, Symposium on St. Dynamics, Part 2, Ed. by Johns, D.J., Loughborough University, England, March, 1970.
15. Yan, M.J. and Dowell, E.H., 'Governing Equations for Vibrating Constrained-Layer Damping Sandwich Plates and Beams', Tr. ASME, J. App. Mech. 39(4), PP 1041-1046, 1972.
16. Mead, D.J., 'Governing Equations for Vibrating Constrained-Layer Damping Sandwich Plates and Beams', J. Appl. Mech., 40, PP 639-640, 1973.
17. Mead, D.J. and Markus, S., 'On the Problem of Bending Vibration of Sandwich Cantilevers with Various Boundary Conditions Applied at the Free End', J. Strojnický Casopis, 1970.
18. Mead, D.J. and Markus, S., 'Loss Factors and Resonant Frequencies of Encastre Damped Sandwich Beams', J. Sound and Vibration, 12(1), PP 99-112, 1970.
19. Oravsky, V., Markus, S. and Simkova, O., 'A New Approximate Method of Finding the Loss Factors of a Sandwich Cantilever', J. Sound and Vibration 33(3), PP 335-352, 1974.
20. Yan, M.J. and Dowell, E.H., 'High-Damping Measurements and a Preliminary Evaluation of an Equation for Constrained-layer Damping', AIAA J., 11(3), PP 388-390, 1973.
21. Lu, Y.P. and Douglas, B.E., 'On the Forced Vibration of Three-Layer Damped Sandwich Beams', J. Sound and Vibration, 32, PP 513-516, 1974.

22. Douglas, B.E. and Yang, J.C.S., 'Transverse Compressional Damping in the Vibratory Response of Elastic-Viscoelastic-Elastic Beams', AIAA J., 16(9), PP 925-930, 1978.
23. DiTaranto, R.A. and McGraw Jr., J.R., 'Vibratory Bending of Damped Laminated Plates', Tr. ASME, J. Engg. for Industry, 91(4), PP 1081-1090, 1969.
24. Mead, D.J., 'The Damping Properties of Elastically Supported Sandwich Plates', J. Sound and Vibration, 24(3), PP 275-295, 1972.
25. Rao, Sadasiva, Y.V.K. and Nakra, B.C., 'Vibration of Unsymmetrical Sandwich Beams and Plates with Viscoelastic Cores', J. Sound and Vibration, 32, PP 175-187, 1974.
26. Grootenhuis, P., 'The Control of Vibrations with Viscoelastic Materials', J. Sound and Vibration, 11(4), PP 421-433, 1970.
27. Mead, D.J., 'Loss Factor and Resonant Frequencies of Periodic Damped Sandwich Plates', ASME Publication, Paper No. 75-DET-19, 1975.
28. Lu, Y.P., Killian, J.W. and Everstine, G.C., 'Vibrations of Three Layered Damped Sandwich Plate Composites', J. Sound and Vibration, 64, PP 63-71, 1979.
29. Lu, Y.P. and Everstine, G.C., 'More on Finite Element Modeling of Damped Composite Systems', J. Sound and Vibration, 69(2), PP 199-205, 1980.
30. Yu, Y.Y., 'Vibrations of Elastic Sandwich Cylindrical Shells', J. Appl. Mech., 27, PP 653, 1960.
31. Yu, Y.Y. and Ren, N., 'Damping Parameters of Layered Plates and Shells', Proc. 2nd International Conference on Acoustical Fatigue of Aerospace Structures, Ed. Trapp and Forney, Syracuse University Press, 1965.
32. Jones, I.W. and Salerno, V.L., 'The Effect of Structural Damping on the Forced Vibrations of Cylindrical Sandwich Shell', J. Engg. for Ind., 88, PP 318-324, 1966.

33. DiTaranto, R.A., 'Free and Forced Response of Laminated Ring', J.Acoust.Soc.Am., 53(3), PP 748-757, 1973.
34. DiTaranto, R.A., Lu, Y.P. and Douglas, B.E., 'Forced Response of a Discontinuously Constrained Damped Ring', J.Acoust.Soc.Am., 54(1), PP 74-79, 1973.
35. Lu, Y.P., Douglas, B.E. and Thomas, E.V., 'Mechanical Impedance of Damped Three-Layered Sandwich Rings', AIAA J. 11(3), PP 300-304, 1973.
36. Pan, H.H., 'Axisymmetrical Vibrations of a Circular Sandwich Shell with a Viscoelastic Core Layer', J. Sound and Vibration, 9(2), PP 338-348, 1969.
37. Markus, S., 'Damping Properties of Layered Cylindrical Shells', Vibrating in Axially Symmetric Modes', J. Sound and Vibration, 48(4), PP 511-524, 1976.
38. Cremer, L., Heckl, M. and Ungar, E.E., 'Structure-Borne Sound', Springer Verlag, Heidelberg, N.Y., 1973.
39. Junger, M.C. and Feit, D., 'Sound Structures and Their Interaction', The MIT Press, Cambridge, Massachusetts, and London, England, 1972.
40. Lyon, R.H. and Smith, P.W., 'Sound and Structural Vibration', NASA, CR-160, 1965.
41. Lyon, R.H., 'Statistical Energy Analysis of Dynamical Systems: Theory and Application', The MIT Press, Cambridge, Massachusetts, and London, England, 1975.
42. Beranek, L.L. and Work, G.A., 'Sound Transmission Through Multiple Structures', J.Acoust.Soc.Am., 21, PP 419, 1949.
43. London, A., 'Transmission of Reverberent Sound Through Single Walls.', J. of Research of the National Bureau of Standards, 42, PP 605-615, 1949.
44. Feshbach, H., 'Transmission Loss of Infinite Single Plates for Random Incidence', Bolt Beranek and Newman Inc., Rept.1, PP 1-10, Oct. 1954.
45. Cremer, L., 'Theorie der Schalldämmung dünner Wände bei schrägen Einfall', Akustische, Zeitschrift 7, PP 81-104, 1942.

46. Beranek, L.L., 'The Transmission and Radiation of Acoustic Waves by Structures', J.Inst.Mech.Engrs., 6, PP 162-169, 1959.
47. London, A., 'Transmission of Reverberant Sound Through Double Walls', J.Acous.Soc.Am., 22, PP 270-279, 1950.
48. Mullohand, K.A., Parbrook, H.D. and Cummings, A., 'The Transmission Loss of Double Panels', J.Sound and Vibration, 6(3), PP 324-334, 1967.
49. Pretlove, A.J., 'Forced Vibrations of a Rectangular Plate Backed by a Cavity', J.Sound and Vibration, 3, PP 252-261, 1966.
50. Dowell, E.H., 'Transmission of Noise from a Turbulent Boundary Layer Through a Flexible Plate into a Closed Cavity', J.Acous.Soc.Am., 46(1), Part 2, PP 238-252, 1969.
51. Dowell, E.H. and Voss, H.M., 'The Effect of a Cavity on Panel Vibration', AIAA J, 1, PP 476, 1963.
52. Bhattacharya, M.C. and Crocker, M.J., 'Forced Vibration of a Panel and Radiation of Sound into a Room', Acustica, 18, PP 11-20, 1967.
53. Guy, R.W. and Bhattacharya, M.C., 'The Transmission of Sound Through a Cavity Backed Finite Plate', J.Sound and Vibration, 27(2), PP 201-203, 1973.
54. Guy, R.W., Bhattacharya, M.C. and Crocker, M.J., 'Coincidence Effect with Sound Waves in a Finite Plate', J.Sound and Vibration, 18, PP 157-169, 1971.
55. Dowell, E.H., Gorman, G.F. and Smith, D.A., 'Acousto-elasticity: General Theory, Acoustic Natural Modes and Forced Response to Sinusoidal Excitation, Including Comparisons with Experiment', J.Sound and Vibration, 52(4), PP 519-542, 1977.
56. Guy, R.W., 'The Response of a Cavity Backed Panel to External Airborne Excitation: A General Analysis', J.Acous.Soc.Am., 65(3), PP 719-731, 1979.
57. Lyon, R.H., 'Noise Reduction of Rectangular Enclosures with One Flexible Wall', J.Acous.Soc.Am., 35, PP 1791-1797, 1963.

58. Eichler, E., 'Thermal Circuit Approach to Vibrations in Coupled Systems and the Noise Reduction of a Rectangular Box', J.Acoust.Soc.Am., 37(6), PP 995 - 1007, 1965.
59. White, P.H. and Powell, A., 'Transmission of Random Sound and Vibration Through a Rectangular Double Wall', J.Acoust.Soc.Am., 40, PP 821-832, 1966.
60. Crocker, M.J. and Price, A.J., 'Sound Transmission using Statistical Energy Analysis', J.Sound and Vibration, 9(3), PP 469-486, 1969.
61. Price, A.J. and Crocker, M.J., 'Sound Transmission through Double Panels Using Statistical Energy Analysis', J.Acoust.Soc.Am., V.47(1), PP 683-693, 1970.
62. Maidanik, G., 'Response of Ribbed Panels to Reverberant Acoustic Fields', J.Acoust.Soc.Am., 34, PP 809-826, 1962.
63. Maidanik, G., 'Radiation Efficiency of Panels', J.Acoust.Soc.Am., 35, PP 115, 1963.
64. Pope, L.D., 'On the Transmission of Sound Through Finite Closed Shells: Statistical Energy Analysis, Modal Coupling, and Non-resonant Transmission', J.Acoust.Soc.Am., 50(3), Part 2, PP 1004-1018, 1971.
65. Pope, L.D. and Wilby, J.F., 'Band-limited Power Flow into Enclosures', J.Acoust.Soc.Am., 62(4), PP 906 - 911, 1977.
66. McDonald, W.B., Vaicaitis, R. and Myers, M.K., 'Noise Transmission Through Plates into an Enclosure', NASA Technical Paper 1173, May, 1978.
67. Vaicaitis, R. and Slazak, M., 'Noise Transmission Through Stiffened Panels', J.Sound and Vibration, 70(3), PP 413-426, 1980.
68. Craggs, A., 'Computation of the Response of Coupled Plate-acoustic Systems Using Plate Finite Elements and Acoustic Volume-Displacement Theory', J.Sound and Vibration, 18(2), PP 235-245, 1971.
69. Craggs, A., 'The Transient Response of Coupled Acousto-mechanical Systems', NASA CR-1421, 1969.

70. Kurtze, G. and Watters, B.G., 'New Wall Design for High Transmission Loss or High Damping', J. Acous. Soc. Am., 31(6), PP 739-748, 1959.
71. Ford, R.D., Lord, P. and Walker, A.W., 'Sound Transmission Through Sandwich Constructions', J. Sound and Vibration, 5(1), PP 9-21, 1967.
72. Smolenski, C.P. and Krokosky, E.M., 'Dilational-mode Sound Transmission in Sandwich Panels', J. Acous. Soc. Am., 54(6), 1449-1457, 1973.
73. Dym, C.L., Ventres, C.S. and Lang, M.A., 'Transmission of Sound Through Sandwich Panels: A Reconsideration', J. Acous. Soc. Am., 59, PP 364-367, 1976.
74. Guyader, J.L. and Lesueur, C., 'Acoustic Transmission Through Orthotropic Multilayered Plates, Part II: Transmission Loss', J. Sound and Vibration, 58(1), PP 69-86, 1978.
75. Madigosky, W. and Fiorito, R., 'Modal Resonance Analysis of Acoustic Transmission and Reflection Losses in Viscoelastic Plates', J. Acous. Soc. Am., 65(5), PP 1105-1115, 1979.
76. Junger, M.C. and Smith, Jr. P.W., 'The TL of curved Structures', Acustica, 5, PP 47-48, 1955.
77. Smith Jr. P.W., 'Sound Transmission Through Thin Cylindrical Shells', J. Acous. Soc. Am., 29, PP 721 - 729, 1957.
78. Cremer and Heckl, M., 'Transmission of Acoustic Wave Through an Infinite, Homogeneous Isotropic Cylinder', Acustica, 9, P 200, 1959.
79. White, P.H., 'Sound Transmission Through a Finite Closed, Cylindrical Shell', J. Acous. Soc. Am., 40, PP 1121-1130, 1966.
80. Manning, J.E. and Maidanik, G., 'Radiation Properties of Cylindrical Shells', J. Acous. Soc. Am., 36, PP 1691-1698, 1964.
81. Heckl, M., 'Vibrations of Point Driven Cylindrical Shell', J. Acous. Soc. Am., 34, PP 1553-1557, 1962.

82. Koval, L.R., 'On Sound Transmission into a Thin Cylindrical Shell Under Flight Conditions', J. Sound and Vibration, 48(2), PP 265-275, 1976.
83. Koval, L.R., 'Effect of Cavity Resonances on Sound Transmission into a Thin Cylindrical Shell', J. Sound and Vibration, 59(1), PP 23-33, 1978.
84. Koval, L.R., 'On Sound Transmission into an Orthotropic Shell', J. Sound and Vibration, 63(1), PP 51-59, 1979.
85. Lin, Y.K., 'Free Vibrations of Continuous Skin-Stringer Panels', J. of Appl. Mech., ASME, 27, PP 669-676, 1960.
86. Sengupta, G., 'Natural Frequencies of Periodic Skin Stringer Structures Using a Wave Approach', J. Sound and Vibration, 16(4), PP 567-580, 1971.
87. Lin, Y.K., Brown, I.D. and Deutschle, P.C., 'Free Vibrations of a Finite Row of Continuous Skin-Stringer Panels', J. Sound and Vibration, 1(1), PP 14-27, 1964.
88. Narayanan, S. and Mallik, A.K., 'Free Vibration of Thin Walled Open Section Beams with Constrained Damping Treatment', Accepted for Publication in J. Sound and Vibration, 74(3), 1981.
89. Lin, Y.K., 'Probabilistic Theory of Structural Dynamics', McGraw-Hill Book Co., N.Y., 1967.
90. Richards, E.J. and Mead, D.J., 'Noise and Acoustic Fatigue in Aeronautics', John Wiley and Sons Ltd., London, New York, Sydney, 1968.
91. Ungar, E.E., 'Highly Damped Structures', Machine Design, 35, PP 162-168, 1963.
92. Courant, R. and Hilbert, D., 'Methods of Mathematical Physics, Vol. I', Interscience Publication, Inc., 1953.
93. Meirovitch, L., 'A New Method of Solution of the Eigenvalue Problem for Gyroscopic Systems', AIAA J., 12(10), PP 1337-1342, 1974.
94. Foxwell, J.H. and Franklin, R.E., 'The Vibrations of a Thin-Walled Stiffened Cylinder in an Acoustic Field', The Aeronautical Quarterly, 10, PP 47-64, 1959.

## APPENDIX A

### BOUNDARY CONDITIONS AND DAMPED NORMAL MODES

The symmetric modes are obtained by applying the boundary conditions at one edge only, namely at  $x = a/2$ .

(a) The boundary conditions for edges with elastic rotational restraint and no transverse displacement and unriveted edges are,

$$\sum_{r=1}^3 A_r \cos \frac{\lambda_r}{2} = 0 \quad (A.1)$$

$$\begin{aligned} \sum_{r=1}^3 A_r (\lambda_r^2 + \nu P_n^2) [\lambda_r^2 + P_n^2 + g(1+\nu)/(\lambda_r^2 + P_n^2 + g)] \cos \frac{\lambda_r}{2} \\ + P_n^2 (P_n^2 K_{\Gamma} + K_{sv}) \lambda_r \sin \frac{\lambda_r}{2} = 0 \end{aligned} \quad (A.2)$$

$$\sum_{r=1}^3 A_r [(\lambda_r^2 + P_n^2)/(\lambda_r^2 + P_n^2 + g)] \cos \frac{\lambda_r}{2} = 0 \quad (A.3)$$

The above three boundary conditions are due to zero displacement, moment equilibrium between stiffener and plate and no axial stress in either of the face plates respectively.  $K_{\Gamma} = E_s \Gamma / (D_t a^3)$ , is the torsion bending stiffness parameter and  $K_{sv} = G_s J / (D_t a)$  is the St.Venant torsion stiffness parameter of the stringer cross-section,  $E_s$  and  $G_s$  are the elastic and shear moduli of the stringer material,  $\Gamma$ , the torsion bending constant and  $J$  is St.Venant torsion constant of stiffener cross-section.

(b) The first two boundary conditions for edges with elastic rotational restraint and no transverse displacement, but with riveted edges are the same as given by equations (A.1) and (A.2). The last boundary condition arises because of the prevention of shear strain in the core due to riveting. This is given by

$$\sum_{r=1}^3 \frac{A_r [\lambda_r (\lambda_r^2 + P_n^2)]}{[\lambda_r^2 + P_n^2 + g]} \sin \frac{\lambda_r}{2} = 0 \quad (\text{A.4})$$

(c) The boundary condition for transverse elastic constraint and no rotation are

$$\sum_{r=1}^3 A_r \lambda_r \sin \frac{\lambda_r}{2} = 0 \quad (\text{A.5})$$

$$\sum_{r=1}^3 \frac{A_r [\lambda_r (\lambda_r^2 + P_n^2)]}{[\lambda_r^2 + P_n^2 + g]} \sin \frac{\lambda_r}{2} = 0 \quad (\text{A.4})$$

$$\sum_{r=1}^3 A_r [\lambda_r^2 + (2 - \nu) P_n^2] \cdot \left[ \frac{\lambda_r^2 + P_n^2 + g (1 + \nu)}{\lambda_r^2 + P_n^2 + g} \right] \sin \frac{\lambda_r}{2} - [P_n^4 K_f \cos \frac{\lambda_r}{2}] = 0 \quad (\text{A.6})$$

where  $K_f = (EI)_s / (a D_t)$  is the flexural stiffness parameter. Equation (A.6) represents the equilibrium of shear forces between the stiffener and the plate.

$(EI)_s$  is the flexural rigidity of the stiffener.

(d) The boundary conditions for the fixed-fixed edges at  $x = \pm a/2$ , are

$$\sum_{r=1}^3 \Lambda_r \cos \frac{\lambda_r}{2} = 0 \quad (A.1)$$

$$\sum_{r=1}^3 \Lambda_r \sin \frac{\lambda_r}{2} = 0 \quad (A.5)$$

$$\sum_{r=1}^3 \frac{\Lambda_r [\lambda_r (\lambda_r^2 + P_n^2)]}{[\lambda_r^2 + P_n^2 + g]} \sin \frac{\lambda_r}{2} = 0 \quad (A.4)$$

In each of the above cases the forced damped normal modes can be expressed as

$$W_{mn}(\xi, \psi) = (\cos \lambda_{1mn} \xi + M \cos \lambda_{2mn} \xi + N \cos \lambda_{3mn} \xi) \sin \frac{n\pi a}{b} \psi \quad (A.7)$$

where,  $\lambda_{1mn}$ ,  $\lambda_{2mn}$  and  $\lambda_{3mn}$  are the complex roots of the bicubic equation (2.15) corresponding to the  $mn^{\text{th}}$  mode (The other three roots are just the negative of  $\lambda_{1mn}$ ,  $\lambda_{2mn}$  and  $\lambda_{3mn}$ ). The quantities M and N corresponding to the different edge conditions are obtained as,

(a) No transverse displacement and elastic rotational constraint with no rivets:

$$M = \frac{(R_1 - R_3) \cos \frac{\lambda_{1mn}}{2}}{(R_3 - R_2) \cos \frac{\lambda_{2mn}}{2}}, \quad N = \frac{(R_1 - R_2) \cos \frac{\lambda_{1mn}}{2}}{(R_2 - R_3) \cos \frac{\lambda_{3mn}}{2}} \quad (A.9)$$

(b) No transverse displacement and elastic rotational constraint with rivets,

$$M = \frac{\lambda_{1mn} R_1 \sin \frac{\lambda_{1mn}}{2} - \lambda_{3mn} R_3 \cos \frac{\lambda_{1mn}}{2} \tan \frac{\lambda_{3mn}}{2}}{\lambda_{3mn} R_3 \cos \frac{\lambda_{3mn}}{2} \tan \frac{\lambda_{3mn}}{2} - \lambda_{2mn} R_2 \sin \frac{\lambda_{2mn}}{2}} \quad (A.10)$$

$$N = \frac{\lambda_{1mn} R_1 \sin \frac{\lambda_{1mn}}{2} - \lambda_{2mn} R_2 \cos \frac{\lambda_{1mn}}{2} \tan \frac{\lambda_{2mn}}{2}}{\lambda_{2mn} R_2 \cos \frac{\lambda_{3mn}}{2} \tan \frac{\lambda_{2mn}}{2} - \lambda_{3mn} R_3 \sin \frac{\lambda_{3mn}}{2}} \quad (A.11)$$

(c) Transverse elastic constraint and no rotation

$$M = \frac{\sin \frac{\lambda_{1mn}}{2} (R_1 \lambda_{3mn} - R_3 \lambda_{1mn})}{\sin \frac{\lambda_{2mn}}{2} (R_3 \lambda_{2mn} - R_2 \lambda_{3mn})} \quad (A.12)$$

$$N = \frac{\sin \frac{\lambda_{1mn}}{2} (R_2 \lambda_{1mn} - R_1 \lambda_{2mn})}{\sin \frac{\lambda_{3mn}}{2} (R_3 \lambda_{2mn} - R_2 \lambda_{3mn})} \quad (A.13)$$

(d) Fixed edge conditions

$$M = \frac{\lambda_{1mn} \sin \frac{\lambda_{1mn}}{2} (R_1 - R_3)}{\lambda_{2mn} \sin \frac{\lambda_{2mn}}{2} (R_3 - R_2)} \quad (A.14)$$

$$N = \frac{\lambda_{1mn} \sin \frac{\lambda_{1mn}}{2} (R_1 - R_2)}{\lambda_{3mn} \sin \frac{\lambda_{3mn}}{2} (R_2 - R_3)} \quad (A.15)$$

In the above equations

$$R_r = \frac{\lambda_{rmn}^2 + P_n^2}{\lambda_{rmn}^2 + P_n^2 + g}, \quad r = 1, 2, 3 \quad (A.16)$$

and  $K_t = P_n^2 (P_n^2 K_{\square} + K_{sv})$  is the equivalent torsional stiffness parameter.

It should be noted that the results for the simply supported edge conditions can be obtained by letting  $M = N = 0$  and  $\lambda_{lmn} = m\pi$ , ( $m = 1, 3, 5..$ ) in equation (A.7).

## APPENDIX B

### GENERALIZED MASS , GENERALIZED FORCE, ACCEPTANCE FUNCTIONS AND COUPLING COEFFICIENTS

The expressions for the generalized mass and the generalized force from equations (4.15) (2.31) and (2.32), corresponding to the forced damped normal modes are,

$$\begin{aligned} \mu_{mn} = \frac{\mu_{ab}}{2} \left\{ \frac{(1+M^2+N^2)}{2} + 2M \left[ \frac{\sin\left(\frac{\lambda_{1mn} + \lambda_{2mn}}{2}\right)}{\lambda_{1mn} + \lambda_{2mn}} \right. \right. \\ + \frac{\sin\left(\frac{\lambda_{1mn} - \lambda_{2mn}}{2}\right)}{\lambda_{1mn} - \lambda_{2mn}} \left. \right] + 2N \left[ \frac{\sin\left(\frac{\lambda_{1mn} + \lambda_{3mn}}{2}\right)}{\lambda_{1mn} + \lambda_{3mn}} \right. \\ + \frac{\sin\left(\frac{\lambda_{1mn} - \lambda_{3mn}}{2}\right)}{\lambda_{1mn} - \lambda_{3mn}} \left. \right] + 2MN \left[ \frac{\sin\left(\frac{\lambda_{2mn} + \lambda_{3mn}}{2}\right)}{\lambda_{2mn} + \lambda_{3mn}} \right. \\ + \frac{\sin\left(\frac{\lambda_{2mn} - \lambda_{3mn}}{2}\right)}{\lambda_{2mn} - \lambda_{3mn}} \left. \right] + \frac{\sin \lambda_{1mn}}{2 \lambda_{1mn}} + M^2 \frac{\sin \lambda_{2mn}}{2 \lambda_{2mn}} \\ + N^2 \frac{\sin \lambda_{3mn}}{2 \lambda_{3mn}} \left. \right\} \end{aligned} \quad (B.1)$$

$$p_{mn}(t) = p_0 \exp [i\omega t] \gamma_{mn} \quad (B.2)$$

where,

$$\gamma_{mn} = \frac{2ab}{n\pi} (1 - \cos n\pi) \sum_{r=1}^3 \frac{\sigma_r \left( \lambda_{rmn} \sin \frac{\lambda_{rmn}}{2} \cos \frac{F}{2} - F \cos \frac{\lambda_{rmn}}{2} \sin \frac{F}{2} \right)}{(\lambda_{rmn}^2 - F^2)} \quad (B.3)$$

where,  $\sigma_1 = 1$ ,  $\sigma_2 = M$  and  $\sigma_3 = N$  and  $F = \frac{k'}{a} \sin \theta$

Note for  $n$  even,  $\gamma_{mn} = 0$  and along the  $x$  direction only the symmetric modes are considered.

For  $r_{xy} = 1$ , from equation (2.36), the expression for  $I_{mnrs}(\omega)$  is independent of frequency and is given by

$$I_{mnrs} = \gamma_{mn} \gamma_{rs}^* \quad (B.4)$$

The acoustic structural coupling coefficient given in equation (4.21) is obtained from the damped normal modes as,

$$L_{mnij} = \frac{2abn (1 - \cos n\pi \cos j\pi)}{\pi (n^2 - j^2)} \sum_{r=1}^3 \sigma_r \frac{\lambda_{rmn} \sin \frac{\lambda_{rmn}}{2}}{\lambda_{rmn}^2 - i^2 \pi^2} \cos^2 \left( \frac{i\pi}{2} \right) \quad (B.5)$$

Because only the symmetric structural modes are admissible, the contributions to the acoustic-structural modal coupling coefficients are only from the even order acoustic modes in the  $x$  and  $y$  directions.